Characterization of CAPN15 in mice

Congyao Zha

Integrated program in neuroscience

McGill University

Montreal, Quebec, Canada

August 2023

A thesis submitted to McGill University in partial fulfillment of the requirements of the degree of Doctor of Philosophy

Table of Contents

Acknowledgements

I would like to thank my supervisor Dr. Wayne Sossin for his patience and support along my journey. His skepticism and critical thinking are valuable lessons that not only help me be a better scientist, but also a human being with clearer mind. I would also like to thank my co-supervisor Dr. Oliver Hardt for his help and guidance on my study. His immense knowledge in behavioral neuroscience allowed me, a molecular neuroscientist, to traverse in a new exciting field.

I would like to thank my committee members Dr. Edward Ruthazer and Dr. Jean-François Cloutier for their advice and guidance along the way. Their supportive nature and smiley faces always calm me down and make me realize that I have done a good job.

I would like to thank my lab members Xiaotang Fan, Taylor Dunn, Carole Abi Farah, Magaret Hastings, Larissa Ferguson, Mina Anadolu, Keren Ginzburg, Jessie Langille, Angie Ni and Jewel Li for their advice, company and support. In particular, I would like to thank Xiaotang for her help in genotyping and molecular biology, and Carole as ‘training wheels’. I would like to thank Karine Gamache, Matteo Bernabo from Nader lab, Isabelle Groves and Celia Sciandra from Hardt lab, who patiently helped me and guided me on the rodent behavior project; Jeanne Madranges from Kennedy lab for the chemical LTP project; and Reesha Raja from Cloutier lab for her help and advice on histology and imaging. Big thanks to Anjie Ni who translated the abstract.

I would like to thank my parents Simon and Emily, as well as my wife Jenny, for their unconditional support. I appreciate that you can back me up whenever I need you; I appreciate that none of you stressed me about having kids; I appreciate that you all make me a better and

confident man. I also would like to thank my cats Huituan and Meimei for their fluffy company, so that we overgroom and shed together.

Abstract

Small optic lobe (SOL) calpain is an intracellular protease that belongs to the calpain protease family. It is required for proper optic lobe development in *Drosophila* and the induction of non-associative long-term facilitation, the cellular analog of sensitization behavior in *Aplysia*. This implies that SOL calpain functions in development and plasticity. However, its role in vertebrates is still unknown. In order to study the function of SOL calpain in vertebrates, we knocked out SOL calpain orthologue *Capn15* in mice. We found that CAPN15 expression is the highest in the brain during early development and its expression decreases drastically in adulthood. Histology data suggests that CAPN15 is expressed in the retinal ganglion cell layer of the eye and is ubiquitously expressed in the developing brain. However, in adult brain, CAPN15 expression is restricted to certain brain regions that are linked to plasticity, such as the hippocampus, amygdala, and Purkinje cells, which is consistent with its expression profile assessed by Western blots. Further, using magnetic resonance imaging, we showed that loss of CAPN15 results in a significant reduction in brain volume, with certain brain regions being more affected. Interestingly, *Capn15* KO mice are not born in a mendelian ratio and those that survived are usually accompanied with developmental eye anomalies such as microphthalmia, anophthalmia, and cataract. Human patients with homozygous and heterozygous compound variants in *CAPN15* also displayed microphthalmia/coloboma as well as other development-related phenotypes, suggesting a conserved role of CAPN15 in eye development as well as global development in mammals. In order to investigate how the loss of CAPN15 affects mouse behavior, we used *CaMKII-Cre Capn15* cKO mice, which do not show any developmental deficits. However, we found that loss of CAPN15 in forebrain excitatory neurons results in changes in certain behavior: *Capn15* cKO mice buried significantly fewer marbles, had poorer

performance during accelerating rotarod test, and less fear generalization after auditory fear conditioning with a strong unconditioned stimulus, which might indicate the presence of non-associative memory in vertebrates.

Taken together, our data show that CAPN15 is critical to development, which is supported by the fact that patients with mutations in *CAPN15* have syndromic developmental disorders. We show that removing CAPN15 in excitatory neurons in the forebrain leads to changes in certain behaviors. Thus, this work provides important insights into the function of SOL calpain and brings the protein to spotlights for future research.

Résumé

La calpaïne du Small Optic Lobes (SOL) est une protéase intracellulaire qui appartient à la famille des protéases calpaïnes. Elle est nécessaire au bon développement du lobe optique chez la drosophile et à l'induction de la facilitation non associative à long terme, l'analogue cellulaire du comportement de sensibilisation chez l'aplysie. Cela implique que la calpaïne SOL joue un rôle dans le développement et la plasticité. Cependant, son rôle chez les vertébrés est encore inconnu. Afin d'étudier la fonction de la calpaïne SOL chez les vertébrés, nous avons éliminé l'orthologue de la calpaïne SOL, *Capn15*, chez la souris. Nous avons constaté que l'expression de CAPN15 est la plus élevée dans le cerveau au cours du développement précoce et que son expression diminue considérablement à l'âge adulte. Les données histologiques suggèrent que CAPN15 est exprimée dans la couche des cellules ganglionnaires de la rétine et qu'elle est exprimée de façon ubiquitaire dans le cerveau durant le développement. Cependant, dans le cerveau adulte, l'expression de CAPN15 est limitée à certaines régions cérébrales liées à la plasticité, telles que l'hippocampe, l'amygdale et les cellules de Purkinje, ce qui est cohérent avec son profil d'expression évalué par Western blots. De plus, en utilisant l'imagerie par résonance magnétique, nous avons montré que la perte de CAPN15 entraîne une réduction significative du volume cérébral, avec certaines régions du cerveau étant plus touchées que d'autres. Il est intéressant de noter que les souris *Capn15* KO ne naissent pas dans un rapport mendélien et que celles qui ont survécu sont généralement accompagnées d'anomalies du développement oculaire telles que la microphtalmie, l'anophtalmie et la cataracte. Les patients humains présentant des variantes composées homozygotes et hétérozygotes de *CAPN15* ont également présenté des microphtalmies/colobomes ainsi que d'autres phénotypes liés au développement, ce qui suggère un rôle conservé de CAPN15 dans le développement de l'œil

ainsi que dans le développement global chez les mammifères. Afin d'étudier comment la perte de CAPN15 affecte le comportement de la souris, nous avons utilisé des souris *CaMKII-Cre Capn15* cKO, qui n'ont présenté aucun déficit au niveau du développement. Par contre, nous avons constaté que la perte de CAPN15 dans les neurones excitateurs du cerveau antérieur entraînait des modifications de certains comportements : les souris *Capn15* cKO enterrent significativement moins de billes, ont de moins bonnes performances lors du test du rotarod accéléré, et ont moins de généralisée peur après un conditionnement de peur auditive avec un stimulus inconditionnel fort, ce qui pourrait indiquer la présence d'une mémoire non-associative chez les vertébrés.

Dans l'ensemble, nos données montrent que CAPN15 est essentiel au développement, ce qui est corroboré par le fait que les patients présentant des mutations dans CAPN15 ont des troubles du développement syndromiques. Nous montrons que l'élimination de CAPN15 dans les neurones excitateurs du cerveau antérieur entraîne des modifications de certains comportements. Ainsi, ce travail fournit des informations importantes sur la fonction de la calpaïne SOL et met la protéine sous les yeux des chercheurs pour de futures recherches.

Contribution to original knowledge

The aim of the studies is to expand our knowledge of SOL calpain (CAPN15), the most understudied calpain in the calpain family. The contributions to original knowledge are based on studies described in chapters 2, 3, and 4.

In the first study (Chapter 2), we generated *Capn15* KO mice and documented their general phenotypes. We found that *Capn15* KO mice are not born in a mendelian ratio and those that survived are usually accompanied by developmental eye anomalies such as microphthalmia, anophthalmia, and cataract. Human patients with homozygous or compound heterozygous variations in *CAPN15* also displayed microphthalmia/coloboma as well as other development-related phenotypes, suggesting a conserved role of CAPN15 in eye development as well as global development in mammals.

The second study (Chapter 3) illustrated volumetric changes in the brain of *Capn15* KO mice and CAPN15 expression patterns in the adult brain. By using MRI, we showed that *Capn15* KO brains are around 12% smaller than the control WT brains. In addition, certain brain areas such as the thalamus, CA1, CA2, and dentate gyrus of the hippocampus are significantly smaller while other areas such as the amygdala are bigger. By using histology, we showed that CAPN15 is expressed in brain regions that are heavily related to plasticity, such as the hippocampus, amygdala, cortex as well as Purkinje cells, which does not explain the volumetric changes in those brain regions. These results suggest that CAPN15 might serve different functions in a developing brain and an adult brain. Unfortunately, it is still unclear why *Capn15* KO brains are smaller, as the neuronal density of CA1 pyramidal cells and cerebellar Purkinje cells is not changed in the *Capn15* KO group. This study also showed that *CaMKII-Cre Capn15* cKO mice, in which CAPN15 is only knocked out in excitatory neurons in the forebrain post-

neurodevelopment, do not have any signs of developmental deficits, further suggesting that CAPN15 is important to early development.

The third study (Chapter 4) demonstrated the behavioral characteristics of *CaMKII-Cre Capn15* cKO mice. Loss of CAPN15 in forebrain excitatory neurons alter certain behaviors, such as marble burying, rotarod, and fear generalization in auditory fear conditioning. We showed that *Capn15* cKO mice buried significantly fewer marbles, had poorer performance during the accelerating rotarod test, and less fear generalization after auditory fear conditioning with intense shock intensity, which might indicate the presence of non-associative plasticity in vertebrates.

Contribution of authors

The results of chapter 2 were published as 'Biallelic variants in the small optic lobe calpain CAPN15 are associated with congenital eye anomalies, deafness and other neurodevelopmental deficits' by Congyao Zha, Carole A Farah, Richard J Holt, Fabiola Ceroni, Lama Al-Abdi, Fanny Thuriot, Arif O Khan, Rana Helaby, Sébastien Lévesque, Fowzan S Alkuraya, Alison Kraus, Nicola K Ragge, Wayne S Sossin. Hum Mol Genet. 2020 Nov 4;29(18):3054-3063. doi: 10.1093/hmg/ddaa198. I performed all experiments and data analyses for Figure 3, 4 and 5. Carole A Farah assisted in data analyses. Both Carole and I participated in writing the draft of the manuscript regarding to experiments on mice. Data and manuscript regarding to human patients were collected and written by Richard J Holt, Fabiola Ceroni, Lama Al-Abdi, Fanny Thuriot, Arif O Khan, Rana Helaby, Sébastien Lévesque, Fowzan S Alkuraya, Alison Kraus, Nicola K Ragge. Wayne Sossin provided intellectual guidance and support in experimental design. All participated in giving comments on the draft.

The results of chapter 3 were published as 'MRI of Capn15 Knockout Mice and Analysis of Capn 15 Distribution Reveal Possible Roles in Brain Development and Plasticity' by Congyao Zha, Carole A Farah, Vladimir Fonov, David A Rudko and Wayne S Sossin. Neuroscience 2021 Jun 15;465:128-141. I performed all experiments except for Figure 2 and 3. Vladimir Fonov and David Radko generated and analyzed data from Figure 2 and 3. I performed quantification for Figure 1 and Figure 9; Carole A Farah performed quantification for Nissl staining in CA1; Wayne Sossin performed quantification for immunostaining in cerebellum. Both Carole and I created all figures for the manuscript except Figure 2 and 3, which were created by Vladimir Fonov and David Radko. Both Carole A Farah and I participated in writing the draft of the manuscript except topics related to MRI, which were written by Vladimir Fonov and David

Radko. Wayne Sossin provided intellectual guidance and support in experimental design. All participated in giving comments on the draft.

The results from chapter 4 were published as ‘Behavioral characterization of *Capn15* conditional knockout mice’ by Congyao Zha, Karine Gamache, Oliver M Hardt and Wayne S Sossin. Behav Brain Res. 2023 Oct 2:454:114635. doi: 10.1016/j.bbr.2023.114635. I performed behavior battery experiments on three cohorts of animals and auditory fear conditioning on two cohorts of naïve animals. Karine Gamache performed behavior battery experiments on one cohort of animals. Karine Gamache collected data from grooming, open field, object location and marble burying. I collected data from marble burying, elevated plus maze, rotarod, and auditory fear conditioning and extinction and analyzed all data. I prepared all the figures. I wrote the manuscript. Oliver Hardt and Wayne Sossin provided intellectual guidance and support in experimental design and edited the manuscript. All participated in giving comments on the draft.

List of abbreviations

AMC		Anophthalmia, microphthalmia, and coloboma
AMPA		L-α-amino-3-hydroxy-5-methyl-4-isoxazolepropionic acid
	AMPAR	AMPA receptor
ATP		Adenosine triphosphate
ASD		Autism spectrum disorders
BAF		BRG1/BRM associated factors
	BRG1	Brahma-related gene-1
	BRM	Brahma
BDNF		Brain derived neurotrophic factor
BMP		Bone morphogenetic protein
CaMKII		Calmodulin-dependent kinase II
CDK		Cyclin-dependent kinase
CHD		Chromodomain helicase DNA-binding protein
CREB		cAMP-responsive element binding protein
	cAMP	Cyclic adenosine monophosphate
CS		Conditioned stimulus
	CS+	Paired CS
	CS-	Unpaired CS
DN		Dominant negative
ERK		Extracellular signal-regulated kinases, also referred to MAPK
FGF		Fibroblast growth factor
ICAP		[4-(5-amino-4-carbamoylimidazol-1-yl)-2,3-dihydroxycyclopentyl] methyl dihydrogen
KO		Knockout
	cKO	Conditional knockout
LTF		Long-term facilitation
	A-LTF	Associative long-term facilitation

NA-LTF	Non-associative long-term facilitation
LTP	Long-term potentiation
MAPK	Mitogen-activated protein kinase
MITF	Microphthalmia-associated transcription factor
MRI	Magnetic resonance imaging
mTOR	Mammalian/mechanistic target of rapamycin
mTORC	mTOR complex
NMDA	N-methyl-D-aspartate
NMDAR	NMDA receptor
PAX	Paired box protein
PKA	Protein kinase A
PKC	Protein kinase C
PKM	Protein kinase M
PSD	Postsynaptic density
PTSD	Post-traumatic stress disorder
SCOP	Suprachiasmatic nucleus circadian oscillatory protein
SHH	Sonic hedgehog
SOL calpain	Small optic lobe calpain
SOX	SRY-box protein
SRY	Sex determining region Y
STF	Short-term facilitation
SWI/SNF	Switch/sucrose non-fermentable
VSX	Visual system homeobox protein
WT	Wild type
X-gal	5-bromo-4-chloro-3-indolyl-β-D-galactopyranoside
ZIP	Zeta inhibitory peptide
β-gal	β-galacatosidase

List of figures

Chapter 1 - Introduction

1.1 General introduction

The brain is probably the most complex and sophisticated organ in the human body. Ironically, this statement comes from my brain and is probably well accepted by brains of other fellow humans. An adult human brain contains millions of neurons and each neuron can create connections to other neurons, close or distant, forming trillions of synapses (Silbereis et al., 2016). All of the cells that comprise a brain come from a piece of tissue at the anterior end of the neural tube. Brain development is a series of orchestrated cellular and molecular events mediated by a genetic instruction manual and environmental factors. Errors in the manual may deviate brain development from the correct path. Neurodevelopmental disorders are a class of disorders that affect the development of the central nervous system and lead to abnormal brain functions (Parenti et al., 2020). A combination of many different factors, including but not limited to genetic risk, nutritional factors, environmental factors, and infection, can lead to neurodevelopmental disorders (Nikolich et al., 2015). In this introduction, I will focus on the genetic causes of neurodevelopmental disorders.

After development, the brain remains plastic, as one of the functions of the brain is to learn and remember. Learning induces changes in neuronal circuits, which is reflected in changes in behavior. Memories are formed when those changes in neuronal circuits occur, possibly through an increase in synaptic strength. Therefore, to store a memory for a very long time, persistent changes in synaptic strength are required to maintain long-term memories.

SOL calpain is an interesting protein that is implicated in both neurodevelopment in *Drosophila* and long-term memory in *Aplysia*. The work described in this thesis aims to have a

better understanding of the function of SOL calpain/CAPN15 in vertebrates. Based on the work that is presented in this thesis, the introduction will cover three main topics: neurodevelopment, eye development, and synaptic plasticity.

1.2 Brain development

In this section, I will go over literature reviews regarding to brain development, focusing on neurogenesis and neuronal migration, and critical genes that are involved in the process. I will also talk about disruptions in those processes that are associated to congenital neurodevelopmental disorders, due to mutations in certain genes.

1.2.1 Literature review of brain development

After the formation of the neural tube, neuroepithelial cells line the hollow center of the neural tube, which eventually becomes the ventricles of the brain (Stiles & Jernigan, 2010). The lining along the ventricle that contains neuroepithelial cells is the ventricular zone. The first goal of neuroepithelial cells is to expand their population, through division. Neuroepithelial cells first undergo symmetric cell division to expand their population. After that, neuroepithelial cells differentiate into radial glia cells, which are also referred to as neural progenitor cells, because studies using lineage analysis suggest that the dividing neural progenitor cells are indeed radial glia cells (Anthony et al., 2004; Noctor et al., 2001; Noctor et al., 2002). Hence, in this section, I will use the terms neural progenitor cells and radial glia cells interchangeably, depending on the context and reference. A small portion of neural progenitor cells/radial glia cells undergoes proliferative symmetric division for self-renewal while a majority of them undergo asymmetric

division to produce one self-renewing daughter cell and a post-mitotic neuron or an intermediate precursor cell that will move to subventricular zone. A vast majority of intermediate precursor cells divide symmetrically and terminally to produce two identical neurons while a small portion of them divide symmetrically into two intermediate neural progenitors (Noctor et al., 2004). However, it is unclear how many neurons can be produced by a single intermediate progenitor cell, as various studies have suggested different answers, up to 32 neurons (Mihalas & Hevner, 2018; Noctor et al., 2004; Vasistha et al., 2015). Radial glia cells have very long processes reaching the pia mater, which act as scaffolds for neuronal migration. Neurons migrate into the developing cortex through radial glia cells to form a cortical plate (Noctor et al., 2001). Neuronal migration follows the 'inside out' manner: early-born neurons fill the deepest layer of the cortex while late-born neurons migrate upwards to bypass the layer formed by early born neurons and fill the superficial layers of the cortex. This is accomplished with the help of reelin-expressing Cajal-Retzius cells residing in the uppermost layer, which act as a stop signal of neuronal migration in the cortex (Ogawa et al., 1995; Stiles & Jernigan, 2010).

Cortical inhibitory interneurons are believed to be generated from a separate population of progenitor cells in ganglionic eminences (medial and caudal) and the preoptic area in the ventral forebrain (Llorca & Deogracias, 2022). In addition to progenitor cells in ganglionic eminences, high-throughput clonal lineage tracing experiments showed that human cortical progenitor cells give rise to both excitatory and inhibitory neurons (Delgado et al., 2022). Regardless, radial glia cells residing in the ventricular zone undergo asymmetric division and give rise to either interneurons that migrate away or intermediate progenitor cells that undergo symmetric division in the subventricular zone (Brown et al., 2011). While the generation of inhibitory neurons is similar to that of excitatory neurons, their migration behavior is completely

different. Instead of radial migration as seen in excitatory neurons, tracer labeling studies showed that interneurons born in the ventral forebrain adopted tangential migration to reach the developing cortex (Anderson et al., 1997; Lavdas et al., 1999; Orourke et al., 1995).

Extrinsic cues, such as the Notch pathway, Wnt pathway, Sonic Hedgehog (SHH) pathway, and Fibroblast Growth factors (FGF), all contribute to maintaining the self-renewal of radial glia cells (Tiberi et al., 2012). Late E15 radial glia cells, when transplanted into young E12 embryos, can be respecified and behave like an E12 radial glia cell, through activation of the Wnt signaling pathway. In addition, Wnt expression is higher during early development. These results suggest a role of environmental factors in shaping the behavior of progenitor cells (Oberst et al., 2019). However, radial glia cells will not retain their pluripotency and divide indefinitely. As development progresses, radial glia cells gradually switch from proliferative symmetric division to neurogenic asymmetric division (Gao et al., 2014). Cell cycle regulation is one of the many factors that might contribute to the switch from proliferation to differentiation in neural progenitor cells. A physiological increase in the length of G_1 phase of cell cycle in neural progenitor cells is observed and is believed to reduce proliferation and promote neurogenesis (Liu et al., 2019; Takahashi et al., 1995). In vivo studies in mice showed that overexpression of cdk4/cyclin D1 in cells in the ventricular zone through in utero electroporation shortens the length of G_1 phase of cell cycle, delays neurogenic differentiation, and increases the population of intermediate progenitor cells in the subventricular zone. Conversely, knockdown of cdk4/cyclinD1 using RNAi showed the opposite effects (Lange et al., 2009). Furthermore, experiments in cultured mouse neural progenitor cells showed that cyclin-dependent kinase (CDK) dependent phosphorylation of transcription factor SOX2 inhibits neurogenic differentiation. Upon differentiation, SOX2 is cleaved and dephosphorylated, possibly due to a

reduction in CDK level. The truncated and dephosphorylated version of SOX2 preferably binds to and induces the expression of genes that induce neurogenesis. Overexpression of truncated and dephosphorylated SOX2 leads to a significant upregulation of proneural transcription factor NGN2 in vitro and an increase in neuronal formation in vivo (Lim et al., 2017). Another study showed that a high level of CDK level inhibits neurogenic differentiation through phosphorylation of proneural transcription factor NGN2. NGN2 has multiple phosphorylation sites. Electrophoretic mobility shift assay showed that the DNA binding ability of NGN2 is negatively correlated to the number of sites phosphorylated (Ali et al., 2011). In addition, NGN2 can trigger cell cycle exit by repressing the expression of cyclins D1 and E2, setting up a positive feedback loop to ensure cell cycle exit (Lacomme et al., 2012). Transcription repressor, BCL6, is also found to be critical to the switch. RNA sequencing transcriptome analysis on embryonic stem cell derived cortical progenitors showed that BCL6 is able to repress the expression of genes related to Notch, Wnt, SHH, and FGF signaling pathways that promote proliferation, and upregulate genes related to neuronal differentiation. BCL6 is also found to repress expression of cyclin D, through Sirt1-dependent histone deacetylation (Bonnefont et al., 2019).

1.2.2 Critical genes and proteins involved in brain development and the consequences of mutations in such genes

Thanks to the development in sequencing technology, the ability to sequence genomes of individuals with disorders has been able to identify de novo mutations in known disease-causing genes as well as in genes that are not previously linked to any disorders. While it can be overwhelming that countless mutations in different genes lead to different outcomes in different individuals, fortunately, the products of many of those genes can be classified into four

categories: proteins that are important to transcriptional regulation, cytoskeleton proteins, synaptic proteins, and proteins that are critical to the regulation of protein synthesis (Parenti et al., 2020).

Many biological processes are mediated by precise and stepwise changes in gene expression, especially during development (Ronan et al., 2013). Hence, it is not surprising that a small imbalance in gene expression during early development can have a devastating effect. In this section, I will mainly focus on two of the many transcription regulators: the mammalian SWI/SNF complex and the chromodomain helicase DNA-binding (CHD) proteins.

Chromatin regulators are a group of proteins that dynamically regulate chromatin structure and therefore, gene expression. The mammalian SWI/SNF complex, also known as BRG1/BRM-associated factor (BAF) complex, is an ATP-dependent chromatin remodeling complex that promotes DNA accessibility and gene expression (Bogershausen & Wollnik, 2018). It is a polymorphic complex with 15 subunits that is composed of products of at least 29 genes (Kadoch & Crabtree, 2015). This allows the presence of many distinct BAF complexes due to combinatorial assembly, with distinct functions in different tissues. Indeed, studies in mouse embryonic stem cells showed that the BAF complex with a specific combination of subunits is critical to the renewal and pluripotency of embryonic cells (Ho et al., 2009). Similarly, in the nervous system, a specific composition of the BAF complex is required for neural progenitor proliferation. A switch of BAF subunits in postmitotic neurons is required for neuronal differentiation (Lessard et al., 2007).

CHD proteins are another group of ATP-dependent chromatin remodeling proteins. In humans, there are nine CHD proteins in total and can be further divided into three groups, with CHD1-2 in group I, CHD 3-5 in group II, and CHD 6-9 in group III, based on their structures

(Mills, 2017). All CHD proteins have a conserved helicase-ATPase domain and two tandem chromodomains that bind to methylated histone residues (Liu et al., 2021). Despite CHD proteins in the same group share similar structures, they play non-redundant roles in cells. Studies on CHD3, CHD4, and CHD5 showed that each of them has distinct and mostly non-overlapping tasks during cortical development. Deletion of CHD4 in the nervous system during early development leads to smaller brains in mice and is lethal. Deletion of CHD4 causes premature cell cycle exit of neural progenitor cells and depletion of intermediate progenitor cells. Depletion of CHD5 in the brain disrupts early neural radial migration while depletion of CHD3 disrupts late neural radial migration and layer specification (Nitarska et al., 2016).

Mutations in chromatin regulators in humans have been implicated in multiple developmental disorders. For example, heterozygous mutations affecting subunits of BAF complexes lead to Coffin-Siris syndrome (CSS: a multiple malformation syndrome characterized by developmental and cognitive delay, coarse craniofacial features, and hypoplastic or absent fifth digit and nails), except for BRM (SMARCA2), which leads to Nicolaides-Baraitser syndrome (NBS: characterized by development/cognitive delay, coarse craniofacial features, early-onset seizures, and sometimes swelling in inter-phalangeal joints) (Santen et al., 2012; Sekiguchi et al., 2019; Sousa et al., 2009; Tsurusaki et al., 2012; Van Houdt et al., 2012; Wolff et al., 2011). To date, mutations in the gene encoding the core component of BAF complex, *ARID1B,* are the leading cause of CSS (Sekiguchi et al., 2019). De novo mutations in BAF subunits are also found in autism spectrum disorders (ASD) (Neale et al., 2012; O'Roak et al., 2012). In animal studies, deletion of *Brg1 (Smarca4),* the catalytic component of BAF complexes, in neural stem/progenitor cells in mice leads to smaller brains without cerebellum and is lethal. In vitro experiments investigating neurosphere formation and BrdU incorporation

showed that BRG1 is critical to the self-renewal and proliferation of neural stem/progenitor cells, possibly through the Notch pathway (Lessard et al., 2007). Deletion of *Brg1* in mouse embryonic stem cells has been shown to disrupt the binding of pluripotency transcription factor OCT4, SOX2, and NANOG to their targets (King & Klose, 2017). Mutations in proteins from CHD family can lead to developmental disorders, intellectual disability, and autism spectrum disorders (Goodman & Bonni, 2019). Heterozygous mutations in *CHD7* are responsible for CHARGE syndrome, characterized by ocular coloboma, congenital heart defects, choanal atresia (difficult breathing due to narrowing of the nasal passage), developmental retardation, genital anomalies, and ear anomalies, and accounts for possibly more than 65% of cases (Jongmans et al., 2006; Lalani et al., 2006; Legendre et al., 2017; Pagon et al., 1981; Vissers et al., 2004). Microarray analysis in mouse neural stem cells with either SOX2 or CHD7 knockdown showed that CHD7 is a transcriptional cofactor of SOX2. Together, CHD7 and SOX2 regulate genes of the Notch and SHH pathways in a cooperative manner, which might contribute to the overlap of symptoms found in various diseases caused by mutations in *CHD7*, *SOX2*, and genes in the Notch or SHH pathways (Engelen et al., 2011). Studies in neural progenitor cells derived from mouse embryonic stem cells showed that CHD7 is not required for the maintenance and survival of mouse embryonic stem cells and neural progenitor cells, but is essential to neuronal differentiation of neural progenitor cells (Yao et al., 2020). In addition, in vitro experiments using neural crest cells induced from human embryonic stem cells showed that CHD7 is required for the formation of neural crest cells. In vivo experiments using *Xenopus* embryo showed that Chd7 is required for the expression of transcription factors that are important to the formation of neural crest cells, such as Sox9, and neural crest cell migration (Bajpai et al., 2010). Patients with CHARGE syndrome due to mutation in *CHD7* also showed cerebellar vermis hypoplasia,

suggesting that CHD7 is also implicated in cerebellum development (Yu et al., 2013). In mice, knocking out *CHD7* in cerebellar granule cells results in cerebellar hypoplasia, due to failed differentiation and enhanced cell death of cerebellar granule cells (Feng et al., 2017).

Cytoskeleton proteins are critical to neurodevelopment at different stages. Microtubule, for example, is important to neuronal generation, migration, and differentiation (Breuss et al., 2017). Mice with heterozygous mutation in *Tuba1a* that disrupt GTP binding and heterodimer formation showed abnormal cortical and hippocampal architecture, due to impaired neuronal migration (Keays et al., 2007). Mutations in human *TUBA1A* were found in humans with lissencephaly (characterized by the absence of convolutions in the cerebral cortex), sometimes accompanied by abnormalities in hippocampus, cerebellum, corpus callosum, and brainstem (Keays et al., 2007; Kumar et al., 2010; Poirier et al., 2007). Heterozygous mutations in *TUBB2B* are found in patients with polymicrogyria (characterized by multiple small gyri with abnormal cortical lamination). In utero knockdown of *Tubb2b* in rats disrupted neuronal migration (Jaglin et al., 2009). Mutations in microtubule interacting proteins such as DCX and LIS1 also disrupt neuronal migration, leading to lissencephaly (Reiner, 2013). In fact, mutations in *LIS1* and *DCX* account for 85% of classic lissencephaly (Kumar et al., 2010). Indeed, knockdown of DCX in developing rodent brains showed stall radial migration within the subventricular zone and intermediate zone (Bai et al., 2003). Other than tubulins, mutations in genes encoding actin isoforms, *ACTB* and *ACTG1*, has been linked to Baraitser-Winter syndrome, characterized by dysmorphic craniofacial features, developmental and cognitive delay, coloboma and/or hearing impairment, and brain malformations (Baumann et al., 2020; Cuvertino et al., 2017; Nie et al., 2022; Rainger et al., 2017; Sandestig et al., 2018).

Synaptic proteins, such as synaptic receptors, ion channels, cell adhesion molecules, and scaffold proteins, are important to proper formation and maintenance of neuronal connectivity. It has been suggested that mutations in synaptic proteins or proteins that are critical to their regulation lead to a distortion in neuronal connectivity, and hence ASD (Bourgeron, 2015; Zoghbi & Bear, 2012). Shank proteins are a class of scaffolding proteins found in postsynaptic density. They are important to the maturation and growth of dendritic spines through their interactions with other synaptic proteins, such as glutamate receptors, PSD95, Homer, and actin regulatory protein cortactin (Naisbitt et al., 1999; Sala et al., 2001; Tu et al., 1999). Experiments in rodents showed that knockdown of Shank3 in cultured hippocampal neurons leads to reduced spine density, while expression of Shank3 in cultured aspiny cerebellar granule cells induces de novo formation of dendritic spines (Roussignol et al., 2005). Deletion of *Shank3* (complete removal of $Shank3_{\alpha}$ and $Shank3_{\beta}$, significant reduction of $Shank3_{\gamma}$) in mice showed excessive overgrooming, social deficits, and anxiety-like behavior. Biochemical and electrophysiological studies showed that *Shank3* deletion leads to reduced level of postsynaptic density (PSD) scaffolding proteins and glutamate receptor subunits in striatal neurons, altered medium spiny neuron morphology, and reduced corticostriatal synaptic transmission (Peca et al., 2011). Similarly, deletion of *Shank1* or *Shank2* also leads to altered PSD composition, synapse morphology, synaptic transmission, and ASD-type behavior (Hung et al., 2008; Schmeisser et al., 2012; Silverman et al., 2011). In humans, mutations in Shank proteins are linked to neurodevelopmental disorders, including autism, intellectual disability, and schizophrenia (Wan et al., 2022). *SHANK3* is the causative gene of Phelan-McDermid syndrome, a microdeletion syndrome of chromosome 22q13 characterized by neonatal hypotonia, global developmental delay, intellectual disability, delayed speech, and minor dysmorphic features (Bonaglia et al.,

2001; Phelan & McDermid, 2012). Other heterozygous mutations in *SHANK3* are also found in patients diagnosed with ASD later on (Wan et al., 2022). Interestingly, duplications of *SHANK3* or chromosome 22q13 are also discovered in patients with ASD and developmental delay, further suggesting that changes in *SHANK3* dosage are linked to neurodevelopmental disorders (Chen et al., 2017; Durand et al., 2007; Okamoto et al., 2007).

One well-known pathway that is involved in the regulation of protein synthesis and protein homeostasis is the mTOR (mammalian target of rapamycin) signaling pathway. mTOR signaling pathway is a vital signaling hub that organizes cell growth by mediating protein synthesis, gene expression, catabolism, and anabolism (Liu & Sabatini, 2020). mTOR is the catalytic subunit of two big complexes, mTORC1 and mTORC2, defined by their distinctive subunits, RAPTOR and RICTOR, respectively. mTORC1 controls the balance of anabolism and catabolism depending on upstream signals and environmental conditions while mTORC2 is involved in proliferation and survival (Saxton & Sabatini, 2017). Given its essential role in cell growth and proliferation, it is not surprising that the mTOR signaling pathway is important to different stages of neurodevelopment, including neurogenesis, neuronal migration, and neuronal differentiation. Mice with loss of function mutation in the *mTOR* gene showed severe deficits in forebrain development due to deficits in cell proliferation and died mid-gestation (Hentges et al., 2001). Inactivation of mTORC1 or mTORC2 through the removal of either RAPTOR or RICTOR in the nervous system during development results in microcephaly, due to a reduction of cell number and size (Cloetta et al., 2013; Thomanetz et al., 2013). Decreasing mTORC activity through deletion of *Lin28a/Lin28b* in neural progenitor cells results in mice with smaller brains, due to reduced proliferation of neural progenitor cells, whereas ectopic expression of *Lin28a* leads to increased neural progenitor cell proliferation and brain size (Yang et al., 2015).

While downregulated mTORC activity is usually associated with reduced cell proliferation and impaired neuronal differentiation, upregulation of mTORC activity leads to abnormal cell growth, aberrant neuronal migration, and premature neuronal differentiation (Lee, 2015). Upregulation of mTORC1 pathway due to deletion of upstream protein TSC1 during embryonic development results in cortical hypertrophy and defects in cortical lamination (Carson et al., 2012; Magri et al., 2011). In humans, constitutively active mTORC1 due to loss of function of TSC1 or TSC2 leads to tuberous sclerosis complex, characterized by the growth of benign tumors in multiple organs, which is usually accompanied by ASD (Ehninger & Silva, 2011). De novo mTOR activating mutations in *PIK3CA*, *AKT3*, and *MTOR* are also identified in humans diagnosed with a spectrum of brain overgrowth phenotypes including focal cortical dysplasia (cortical dyslamination and large dysmorphic neurons), hemimegalencephaly (one side of the brain is abnormally larger), and megalencephaly (abnormally large brain) (Lee et al., 2012; Mirzaa et al., 2016).

1.3 Eye development

In this section, I will first go over literature reviews regarding to eye development, focusing on ocular morphogenesis, and critical genes/proteins that are involved in the process. I will also talk about relevant eye disorders.

1.3.1 Literature review of eye development

At the beginning of eye development, an eye field is formed at the anterior part of the neural plate. Cells in the eye field express a network of transcription factors known as eye field transcription factors including *Pax6*, *Rax*, *Six3*, and *Lhx2*. Expression of a cocktail of eye field

transcription factors is able to induce ectopic eye formation in developing *Xenopus* embryos (Zuber et al., 2003). Afterward, the eye field is separated along the midline through the Shh signaling pathway, produced from the ventral midline of the developing forebrain (Chiang et al., 1996; Echelard et al., 1993). Shh is also involved in the spatial distribution of Pax2 and Pax6 in eye primordia. Studies in zebrafish showed that loss of Shh leads to ectopic development of retina and absence of optic stalk due to a lack of Pax2 while overexpression of Shh leads to overdevelopment of optic stalk and reduced retina and retinal pigment epithelia due to a lack of Pax6, suggesting a role of those molecules in eye patterning (Macdonald et al., 1995). Each eye field evaginates laterally into two optic vesicles, which eventually touch the surface ectoderm. Similar to Pax2 expression in prospective optic stalk tissue, retinal stem cells in optic vesicles are patterned such that cells in different compartments of optic vesicles express distinct sets of transcription factors. The presumptive retinal pigment epithelium expresses MITF, and the future neural retina expresses VSX2, due to the repression of MITF by FGF-expressing surface ectoderm (Liu et al., 1994; Nguyen & Arnheiter, 2000). BMP and Wnt-β-catenin signaling pathways respectively mediate maintenance of VSX2 expression in neural retina and MITF expression in retinal pigment epithelium (Murali et al., 2005; Westenskow et al., 2009). After interacting with the surface ectoderm, each optic vesicle invaginates and forms the bilayered optic cup and optic stalk. The inner layer and the outer layer will differentiate into neural retina and retinal pigment epithelium respectively (Heavner & Pevny, 2012). The surface ectoderm invaginates and forms the lens pit, which is surrounded by the optic cup. At the same time, optic fissure is formed at the ventral edge of optic vesicles and optic stalk through invagination of the optic stalk and eventually, the fissure is sealed. Fissure closure is initiated at the midpoint and

zips up in both directions and requires signals secreted by periocular mesenchyme cells. Proper apoptosis at the optic fissure is also critical to fissure closure (Patel & Sowden, 2019).

1.3.2 Critical genes and proteins involved in eye development and the consequences of mutations in such genes

Eye development is tightly regulated by gene expression. Disruption of such event at different developmental stages will lead to different types of eye anomalies. For example, mutations in genes that are critical during eye field formation can lead to anophthalmia or microphthalmia (Voronina et al., 2004); disruption during optic fissure formation or closure can lead to coloboma (Chang et al., 2006). Although scientists have identified a series of genes involved in eye development, the genetic causes of those disorders in a majority of patients remain undetermined. For instance, the genetic cause of anophthalmia, microphthalmia, and coloboma (AMC) is only determined in around 20–30% of patients, depending on the severity of the disorder (Chassaing et al., 2014; Gerth-Kahlert et al., 2013).

So far, candidate genes involved in AMC encode a variety of proteins, including, but not limited to, transcription factors, gene expression regulators, proteins involved in BMP signaling pathways, and proteins involved in retinoic acid metabolism. Heterozygous mutation in *SOX2* is the most common cause of AMC in humans (Plaisancie et al., 2019). SOX2 is a transcription factor that is expressed during the beginning of eye development. Studies in mice showed that the severity of eye anomalies is correlated to SOX2 expression level. Conditional knockout mice of *Sox2* in neural retina showed that SOX2 is important to the proliferation and differentiation of retinal progenitor cells (Taranova et al., 2006). Mutations in other transcription factors that are

critical during early eye development, such as *OTX2, PAX6, PAX2, RAX, VSX2,* and *MITF* are identified in AMC patients as well (Plaisancie et al., 2019).

As mentioned earlier in section 1.2.2, individuals diagnosed with CHARGE syndrome, mainly caused by heterozygous mutations in *CHD7,* also showed ocular anomalies such as coloboma, microphthalmia, and cataract (Krueger & Morris, 2022). Studies in mice showed that CHD7 is expressed in surface ectoderm throughout lens placode induction and lens vesicle formation. It is also found in neural ectoderm-derived optic vesicle, optic cup, optic stalk and inner and outer layers of optic cup. While deletion of *Chd7* in surface ectoderm only showed some minor effects in early eye development, deletion of *Chd7* in neural ectoderm results in malformed or even complete absence of optic cups, small or not apparent lens, and defects in optic fissure closure (Gage et al., 2015). In addition, CHD7 has been shown to bind to the promotor of tumor suppressor gene *p53* and negatively regulate its expression. Knock-in mice that express increased level and activity of p53 dies around E14.5 and exhibit CHARGE-like phenotypes, suggesting a role of dysregulated p53 in developmental disorders (Van Nostrand et al., 2014). Likewise, individuals with CSS sometimes also showed ophthalmological anomalies, including coloboma and microphthalmia (Errichiello et al., 2017; Santen et al., 2013).

Coloboma is caused by complete or partial failure of optic fissure closure, although it is often associated with microphthalmia, anophthalmia, and systemic congenital deficits (Gregory-Evans et al., 2004). Other than mutations in transcription factors and signaling molecules that globally disrupt eye development, mutations in proteins that disrupt the very process of optic fissure fusion can interrupt eye development as well. Recently, a homozygous frameshift mutation in *FAT1*, encoding the FAT atypical cadherin 1, was found in patients with syndromic colobomatous microphthalmia. Deletion of *Fat1* in mice leads to coloboma and microphthalmia.

Furthermore, experiments using cultured retinal pigment epithelium cells showed that FAT1 is important in mediating cell-cell junctions during optic fissure fusion (Lahrouchi et al., 2019).

1.4 Calpains

In this section, I will talk about the structure and functions of different families of calpains, focusing on their role in development, and plasticity, if any.

1.4.1 General introduction to calpains

Calpains were first discovered in 1964 as a calcium-dependent protease extracted from rat brains (Guroff, 1964). Later on, multiple labs reported and confirmed the presence of calpains in their experiments (Busch et al., 1972; Ishiura et al., 1978; Meyer et al., 1964). While the protein was named differently by different labs, it was eventually settled as calpain in 1991 (Suzuki, 1991). The name ‘calpain’ was the combination of two words, ‘calcium’ and ‘papain’, due to its calcium-dependent nature and the cysteine residue involved in catalytic activity similar to the previously characterized protease, papain (Murachi et al., 1980).

1.4.2 Structure and functions of different calpains

There are four conserved families of calpains in metazoans: Classical, PalB, Tra, and SOL. The most ancient family of these calpains is PalB which is expressed in fungi, followed by SOL which is found in pre-metazoans such as choanoflagellates, while Tra and classical calpains diverged from PalB in early metazoans (Hastings et al., 2017).

The classical calpain subfamily is the most thoroughly characterized among all the calpain families. Classical calpain is characterized by the N-terminal anchor α-helical domain, the conserved protease domain, the C2-like domain, and the penta EF-hand domain. The N-terminal helical domain can be autolyzed upon activation by calcium, lowering the calcium requirement for activation (Inomata et al., 1988; Suzuki et al., 1981). The C2-like domain is named after the C2 domain, due to the resemblance in their tertiary structures. C2 domains are found in hundreds of proteins and can act as a protein-protein interaction domain, a protein-lipid domain, and in some cases bind calcium in a phospholipid-dependent manner (Farah & Sossin, 2012). In spite of the similarity in structures, C2L domain serves different functions in calpain. Crystal structure of CAPN2 and endogenous inhibitor calpastatin showed that C2L domain does not bind calcium, but is important to stabilize the catalytic domain of calpain and maximize its catalytic activity (Moldoveanu et al., 2008). The classical calpain penta EF-hand domain is involved in calcium binding (EF-hands motif 1-4) and dimerization (EF-hands motif 5) (Campbell & Davies, 2012). Dimerization is observed in heterodimers of CAPN1 or CAPN2 and the regulatory small subunit CAPNS1 (Sorimachi et al., 2011), heterodimers of gastrointestinal tracts specific CAPN8 and CAPN9 (Hata et al., 2016), and homodimers of CAPN3 (Ravulapalli et al., 2005). Calcium binding to penta EF-hand domain lowers the calcium requirement for activation of rat classical calpain CAPN2, but is not necessary for calpain activation since mutations in penta EF-hand domain affect neither calpain activation nor maximum catalytic activity (Dutt et al., 2000). Interestingly, mini calpain containing only the catalytic domain of CAPN1 can be activated by calcium. Structures of classical calpains demonstrate that there are two calcium binding sites located in the catalytic domain of classical calpain. Calcium binding on these two sites induces a conformational change involving a salt bridge that aligns the triad

and enables calpain activity (Moldoveanu et al., 2002; Moldoveanu et al., 2004). Although calpain catalytic domain alone can be activated by calcium, it requires facilitation from other domains to reach maximum catalytic activity (Moldoveanu et al., 2008; Moldoveanu et al., 2002).

Classical calpains are important to development and mutations in genes encoding classical calpain isoforms are usually associated with different disorders. *CAPNS1* encodes the small regulatory subunit of calpain 1 and calpain 2 that might stabilize the catalytic subunit of CAPN1 and CAPN2 for proper folding (Ono & Sorimachi, 2012; Yoshizawa et al., 1995). Deletion of *Capns1* in mice abolishes both CAPN1 and CAPN2 activity and leads to embryonic lethality at pre-implantation stage (Arthur et al., 2000; Zimmerman et al., 2000). Deletion of *Capn2* in mice leads to lethality before the implantation stage (Dutt et al., 2006). Interestingly, deletion of *Capn1* results in viable animals, suggesting that CAPN2 is critical during early embryogenesis and can not be compensated by CAPN1 (Azam et al., 2001; Dutt et al., 2006). Inhibition of both CAPN1 and CAPN2 using either calpain inhibitors or siRNA to reduce calpain-dependent LIS1 breakdown is able to partially rescue lissencephaly phenotype in *Lis1* heterozygous mice (Yamada et al., 2009). CAPN3 is expressed predominantly in skeletal muscle (Sorimachi et al., 2011). Mutations in CAPN3 cause limb-girdle muscular dystrophy in humans (Piluso et al., 2005; Richard et al., 1995). CAPN8 and CAPN9 are gastrointestinal tract-specific classical calpains. Mice without either CAPN8 or CAPN9 have no developmental abnormalities, but they are susceptible to gastric mucosal injury induced by ethanol. Single nucleotide polymorphisms in *CAPN8* and *CAPN9*, including those resulting in missense variations in conserved residues and frameshift, are observed in the population but none of them are linked to any diseases (Hata et al., 2010). CAPN12 can be found in the cortex of hair follicles (Dear et al.,

2000). Two heterozygous mutations in *CAPN12* were identified in a patient with congenital erythroderma, hypotrichosis, severe nail dystrophy, and poor growth (Bochner et al., 2017). CAPN14 is highly expressed in the esophagus and single nucleotide polymorphisms in *CAPN14* are associated with eosinophilic esophagitis (Kottyan et al., 2014).

CAPN1 and CAPN2, the two most studied calpains, are implicated not only in development but also in synaptic plasticity. Studies using calpain inhibitors (inhibit both CAPN1 and CAPN2) showed that suprachiasmatic nucleus circadian oscillatory protein (SCOP) is degraded by calpains after novel object recognition training. The decrease in SCOP was also accompanied by an increase in phospho-ERK2 level, which is critical for hippocampus-dependent memory formation (Giovannini, 2006; Shimizu et al., 2007). Activation of calpain by BDNF also promotes activation of the mTOR pathway through the degradation of negative mTOR regulators: PTEN, TSC1, and TSC2 (Briz et al., 2013). Using calpain inhibitors, calpains are also shown to degrade translational repressor poly(A)-binding protein (PABP)-interacting protein 2A (PAIP2A) following contextual fear conditioning (Khoutorsky et al., 2013). PAIP2A binds to PABP and inhibits its translation-inducing activity (Derry et al., 2006; Karim et al., 2006). Activity-dependent degradation of PAIP2A by calpains releases PABP and allows its binding to memory related mRNAs, such as *CaMKIIα* mRNA (Khoutorsky et al., 2013). Furthermore, deletion of *Capsn1* in *Nestin-Cre* mice has reduced dendritic branching and spine density in the apical dendrites of CA1 pyramidal neurons, impaired hippocampal LTP induction, and impaired spatial memory (Amini et al., 2013).

PalB calpain is composed of a conserved protease domain, surrounded by an N-terminal microtubule interacting and transport (MIT) motif and two C-terminal C2L domains in tandem (Sorimachi et al., 2011). It was first discovered in fungus *E. nidulans* as a protease that is critical

to pH adaptation (Denison et al., 1995). In an acidic environment, transcription factor PacC is held in the closed conformation through intramolecular interactions (Espeso et al., 2000). However, in an alkaline environment, PacC is essential to activate the transcription of alkaline-expressed genes and at the same time repress the transcription of acid-expressed genes (Tilburn et al., 1995). Changes in environment pH from acidic to alkaline induce a signal transduction pathway, which recruits PalB calpain and PalA to the endosomal membrane complex (Penalva et al., 2008). Transcription factor PacC is also recruited to the complex by PalA (Vincent et al., 2003; Xu & Mitchell, 2001). With PacC being in close proximity to PalB, PalB is able to remove the C-terminal of the transcription factor PacC, which allows further processing of PacC by proteasomes for activation (Diez et al., 2002; Hervas-Aguilar et al., 2007). CAPN7 is the mammalian orthologue of PalB calpain (Futai et al., 2001). Biochemical analysis on human CAPN7 showed that the MIT domain permits protein-protein interaction with a subset of proteins from ESCRT-III (endosomal sorting complex required for transport) complex (Yorikawa et al., 2008). Both the MIT domain and the C-terminal C2L domain are required for catalytic activity, as deletion of either MIT domain or C2L domain reduces and abolishes catalytic activity respectively (Maemoto et al., 2013). Purified CAPN7 also showed autolysis activity in vitro and its activity is enhanced by binding of ESCRT-III family member IST-1 at the MIT domain. Interestingly, the autolysis activity was observed regardless of calcium (Osako et al., 2010). Further studies proposed that CAPN7 activation might require ESCRT-III family member, CHMP4, to recruit both CAPN7 and CAPN7 substrate recruiter ALIX, the mammalian PalA orthologue (Maemoto et al., 2013). Unfortunately, physiological substrates and roles of CAPN7 in vertebrates are still unknown, probably because *CAPN7* is not identified as a causative gene to any human diseases (Sorimachi et al., 2011; Spinozzi et al., 2021).

TRA-3 isoform of calpain is composed of a conserved protease domain, a C2L domain, and a C2 domain at C-terminus (Sorimachi et al., 2011). CAPN5 is the mammalian orthologue of TRA3 calpain and can be activated in vitro by calcium, as suggested by its autolysis activity (Velez et al., 2018; Waghray et al., 2004). TRA-3 calpain was first discovered as a sex-determination gene in nematode *C. elegans* (Barnes & Hodgkin, 1996). During hermaphrodite development, TRA-3 cleaves membrane-bound TRA-2A, freeing up the intracellular domain of TRA-2A (TRA-2ic) (Sokol & Kuwabara, 2000). This allows the interaction between the N-terminus of TRA-2ic and FEM-3 to inhibit male development as well as the interaction between the C-terminus of TRA-2ic and transcription factor TRA-1 to promote female development (Kuwabara et al., 1998; Mehra et al., 1999; Wang & Kimble, 2001). In humans, heterozygous mutations in *CAPN5* lead to adult-onset autosomal dominant neovascular inflammatory vitreoretinopathy (ADNIV) (Bassuk et al., 2015; Mahajan et al., 2012), due to hyperactivation of its activity (Velez et al., 2020; Wert et al., 2015). It is speculated that those mutations, all located in the G1 loop in the protease core 2 domain, disrupt the regulatory function of the loop, resulting in reduced calcium requirement for activation (Bassuk et al., 2015; Mahajan et al., 2012). Moreover, heterozygous mutation in CAPN5 that lead to stronger hyperactivation result in a more severe phenotype, with earlier onset NIV, as well as hearing loss and developmental delay, suggesting a correlation between disease severity and proteolytic activity (Velez et al., 2018). Crystal structure of the protease core domain of CAPN5 revealed 3 distinct elongated loops compared to classical calpains. Heterozygous mutation in the third loop also results in early-onset severe NIV, suggesting that the third loop can remotely regulate catalytic activity (Randazzo et al., 2019; Velez et al., 2020). Interestingly, removal of CAPN5 in photoreceptors in mice does not have any ocular abnormalities. Similarly, in humans, heterozygous loss of function

variants in *CAPN5* due to mutations in highly conserved residues actually can be non-pathogenic (Wert et al., 2019). Recently, the gain of function theory of CAPN5 in NIV has been challenged. The study proposed a dominant negative mechanism for some of the variants of CAPN5 in NIV. They showed that many reported NIV mutants disrupt membrane association of CAPN5 and impair autolysis activity. Co-immunoprecipitation of WT CAPN5 and CAPN5 mutants showed possible dimerization or multimerization of CAPN5. The lack of autolysis in a mixture of co-pulled WT CAPN5 and CAPN5 mutants suggests that CAPN5 mutants might act as dominant negatives (Geddes et al., 2023).

SOL calpain consists of a conserved protease domain, flanked by a N-terminal zinc finger domain and a C-terminal SOL homology domain (Sorimachi et al., 2011). The N-terminal zinc finger domain binds polyubiquitin, while the function of the SOL homology domain remains unknown. Neither calcium nor polyubiquitin is able to activate SOL calpain in vitro, probably due to a lack of conservation in residues that are critical to induce conformational change upon binding of calcium in classical calpain (Hastings et al., 2018). SOL calpain was first identified in *Drosophila*, in which mutations in SOL gene resulted in a 50% reduction in cell numbers in optic lobes due to degeneration (Delaney et al., 1991; Fischbach & Heisenberg, 1981). Other than its role in proper optic lobe development in *Drosophila*, it is also implicated in synaptic plasticity in *Aplysia*. It was shown to be critical to the induction of non-associative long-term facilitation in *Aplysia* sensory and motor neurons (Hu, Adler, et al., 2017; Hu, Ferguson, et al., 2017) (details in section 1.5.2). CAPN15 is the mammalian orthologue of SOL calpain and is detected in olfactory bulbs in mouse and rat brains (Kamei et al., 2000; Kamei et al., 1998). However, little is known about this protein in vertebrates.

1.5 Synaptic plasticity

In this section, I will talk about synaptic plasticity and protein kinase C/M, and how calpains are related.

1.5.1 General introduction to protein kinase C/M

Memories are believed to be maintained by persistent changes in synaptic connections (Kandel & Schwartz, 1982). However, it is still unknown how those persistent changes are maintained over a long time. Decades of research showed that memories in fact can be specifically erased without affecting general synaptic connectivity, suggesting the presence of distinct molecular complexes in those synapses dedicated to memory (Sossin, 2018). One of the well-studied candidates is protein kinase M (PKM), which is the persistent active form of protein kinase C (PKC).

PKM was first discovered in 1977 by Dr. Nishizuka's lab as the proteolytic product of the proenzyme PKC (Inoue et al., 1977; Takai et al., 1977). Three families of PKC isoforms were present in the common ancestor of vertebrates and mollusks: classical PKCs (Apl I in *Aplysia*), novel PKCs (Apl II in *Aplysia*), and atypical PKCs (Apl III in *Aplysia*) (Sossin, 2007). Subsequent studies confirmed that calpains, specifically CAPN1 and CAPN2, are responsible for the cleavage of classical PKCs into PKMs (Kishimoto et al., 1983; Kishimoto et al., 1989).

All PKCs share conserved domains including a pseudosubstrate in the regulatory domain that inhibits kinase activity. If the regulatory domain is separated from the catalytic domain, the isolated catalytic domain forms a persistently active kinase called PKM. In vertebrates, PKM zeta is generated by an alternative transcript, which excludes the regulatory domain of PKC zeta, and is expressed exclusively in the brain (Hernandez et al., 2003). Outside of vertebrates, no

alternative transcription start sites for PKMs were found (Bougie et al., 2009). In fact, they are formed through proteolytic cleavage, by calpains (Kishimoto et al., 1983; Kishimoto et al., 1989; Takai et al., 1977).

1.5.2 PKMs and synaptic plasticity

The constitutively active nature of PKM zeta makes it a key candidate in memory maintenance (Sacktor et al., 1993). Many evidence supporting the role of PKMs in memory maintenance comes from experiments using pharmacological agents to inhibit PKMs. Zeta inhibitory peptide (ZIP) has been widely used to inhibit PKM zeta in vertebrates and atypical PKM in *Aplysia* in order to study the role of PKMs in learning and memory. It is designed to mimic the sequence of the pseudosubstrate domain of PKC zeta so as to inhibit the catalytic activity of PKC/PKM zeta. However, we and others have shown that ZIP can inhibit PKMs and other kinases at high concentrations (Farah et al., 2017; Ling et al., 2002; Lisman, 2012). Regardless, electrophysiology experiments showed that ZIP is able to disrupt LTP five hours after induction in hippocampal slices (Serrano et al., 2005). Behavior experiments using ZIP in vivo showed that PKM zeta is important to memory maintenance in vertebrates. Acute injection of ZIP into nucleus accumbens core after training impaired drug-associated memory tested 30 minutes after injection (Crespo et al., 2012). Blocking PKM zeta with ZIP in dorsal hippocampus at least 22 hours after training disrupts spatial memory, tested by object location, and Morris water maze (Hardt et al., 2010; Serrano et al., 2008); Blocking PKM zeta in amygdala with ZIP 1 day after auditory or contextual fear conditioning abolishes the fear response to tone or context (Serrano et al., 2008). Blocking PKM zeta with ZIP in insular cortex days after training disrupts taste aversion memory (Shema et al., 2007). In addition, ZIP injected three days after training

can still block memory tested one month later, when ZIP is probably no longer in the system, further suggesting the role of PKM zeta in memory maintenance (Shema et al., 2007). In *Aplysia*, it was shown that ZIP can erase long-term facilitation in culture induced by 5 spaced pulses of serotonin as well as long-term sensitization behavior in living *Aplysia* measured by siphon withdrawal response (Cai et al., 2011). However, two studies showed that PKM zeta is not critical to memory maintenance at all because PKM zeta null mice have normal LTP and learning ability, which can still be impaired by ZIP, indicating the presence of another target of ZIP that is also vital to learning and memory (Lee et al., 2013; Volk et al., 2013). Subsequent research showed that the normal learning ability found in PKM zeta null mice was possibly due to compensation, by the other atypical PKC in vertebrates, PKC iota. By using the PKC iota specific inhibitor ICAP, they showed that ICAP is able to impair memory maintenance only in PKM zeta null mice, but not in WT mice (Tsokas et al., 2016). Experiments using more specific methods to knock down PKMs, such as shRNA and dominant negatives, still support the role of PKMs in memory maintenance (Dong et al., 2015; Hu, Adler, et al., 2017; Hu, Ferguson, et al., 2017; Wang et al., 2016).

1.5.3 Synaptic plasticity in *Aplysia*: roles of PKMs and calpains

Aplysia is a reductionist model organism in order to study the physical manifestation of memory storage. One of the simple but classic behaviors studied in *Aplysia* is sensitization. When an *Aplysia* experiences a noxious stimulus, it forms a memory that can be measured by an increased defensive reflex in response to touch. The duration of sensitization memory is correlated to the strength and repetition of the noxious stimulus. A short-term memory that lasts for minutes is formed after a single tail shock while a long-term memory that lasts for days is

formed after repeated spaced tail shocks (Frost et al., 1985). On a cellular level, sensitization in *Aplysia* is caused by an increase in synaptic strength between presynaptic sensory neurons and postsynaptic motor neurons, mediated by serotonergic interneurons (Brunelli et al., 1976; Marinesco & Carew, 2002). Short-term sensitization is accomplished by enhanced neurotransmitter availability and release. It involves activation of the cAMP-PKA pathway by serotonin, which results in increased excitability and action potential broadening in presynaptic sensory neurons, due to a reduction in potassium current (Castellucci et al., 1980; Siegelbaum et al., 1982). Long-term sensitization, on the other hand, requires protein synthesis and transcription (Castellucci et al., 1989; Montarolo et al., 1986). In addition to modifying pre-existing proteins, activated PKA recruits MAPK and phosphorylates transcription factor CREB-1, which activates transcription and eventually results in the growth of new synapses between presynaptic and postsynaptic neurons (Bailey & Chen, 1988; Bartsch et al., 1998). An advantage of using *Aplysia* as the model organism is that the circuit involved in sensitization behavior can be recapitulated in culture (Kandel & Schwartz, 1982). In sensorimotor coculture, a single pulse of serotonin and repeated spaced pulses of serotonin can mimic the effect of tail shocks in living animals, leading to short-term facilitation (STF) and long-term facilitation (LTF) between the interconnected sensory neuron and motor neuron (Montarolo et al., 1986).

There are both associative (classical conditioning) and non-associative (sensitization) forms of the increased defensive reflex in *Aplysia*. Classical conditioning in the increased defensive reflex requires specific temporal pairing of a conditioned stimulus (a light tactile stimulus to the siphon) and an unconditioned stimulus (strong electric shock to the tail) while sensitization does not require such pairing (Carew et al., 1981). These forms are supported by associative long-term facilitation (A-LTF) induced in culture by pairing one pulse of serotonin

and induction of action potential in the sensory neuron through tetanization, and non-associative long-term facilitation (NA-LTF) induced in culture by five spaced pulses of serotonin. Studies showed that the maintenance of different forms of LTFs requires different isoforms of PKMs: dominant negative (dn)-PKM Apl I expressed in motor neuron two days after LTF induction erased NA-LTF, but not A-LTF, while dn-PKM Apl III expressed in motor neuron two days after LTF induction erased A-LTF, but not NA-LTF. Similarly, induction of A-LTF and NA-LTF are mediated by different calpain isoforms: dn-SOL calpain expressed in motor neurons 4-5 hours after LTF induction blocked the induction of NA-LTF, but not A-LTF, while dn-classical calpain expressed in motor neurons 4-5 hours after LTF induction blocked the induction A-LTF, but not NA-LTF (Hu, Adler, et al., 2017).

Furthermore, in cultures where one motor neuron is innervated by two sensory neurons, with one sensory neuron expressing A-LTF and the other, NA-LTF, overexpression of dn-PKM Apl I in postsynaptic neurons two days after induction erased NA-LTF between the presynaptic and postsynaptic neurons, while overexpression of dn-PKM Apl III in postsynaptic neurons two days after induction erased A-LTF between the presynaptic and postsynaptic neurons. Likewise, blocking SOL calpain activity in the postsynaptic motor neuron only affected the induction of NA-LTF, but not the A-LTF. Blocking classical calpain activity in the postsynaptic neuron would affect the induction of both A-LTF and NA-LTF, as NA-LTF is induced through heterosynaptic facilitation, which is dependent on the induction of A-LTF (Hu, Ferguson, et al., 2017). Together, these results suggest that a single postsynaptic neuron is able to express multiple forms of plasticity that require different molecular mechanisms. More importantly, each form of plasticity can be erased/blocked without affecting the other form of plasticity.

1.6 Rationale and objectives

In *Drosophila*, mutations in SOL gene lead to a 50% reduction in the volume of *Drosophila* optic lobes (Fischbach & Heisenberg, 1981). However, how SOL calpain is involved in the proper development of *Drosophila* optic lobe development is lacking and its function in vertebrates is completely unknown. Hence, we generated *Capn15* KO mice as well as *CaMKII-Cre Capn15* conditional KO mice to have a better understanding of the role of CAPN15 in development in vertebrates.

Other than its mysterious role in development, SOL calpain is also implicated in learning and memory. In *Aplysia*, we learned that SOL calpain is important to the induction of non-associative long-term facilitation (Hu, Adler, et al., 2017; Hu, Ferguson, et al., 2017). Mechanisms underlying the induction of facilitation require conserved molecules, which were shown to be important for memory formation in all organisms (Kandel, 2001). Hence, it is possible that vertebrates use a similar strategy to store memories. If true, certain affiliated or derivative 'non-associative memories' in vertebrates can be specifically erased as well, without affecting the original associative memory, as seen in *Aplysia*. Since post-traumatic stress disorder (PTSD) is associated with strong non-associative memories, such as generalized fear (Lissek & van Meurs, 2015), this suggests possible therapeutic potential for specific erasure of non-associative memories. Therefore, we generated *Capn15* KO mice as well as *CaMKII-Cre Capn15* conditional KO mice in order to study the role of CAPN15 in learning and memory in vertebrates.

Chapter 2 - Biallelic variants in the small optic lobe calpain CAPN15 are associated with congenital eye anomalies, deafness and other neurodevelopmental deficits

2.1 Abstract

Microphthalmia, coloboma and cataract are part of a spectrum of developmental eye disorders in humans affecting ~12 per 100 000 live births. Currently, variants in over 100 genes are known to underlie these conditions. However, at least 40% of affected individuals remain without a clinical genetic diagnosis, suggesting variants in additional genes may be responsible. Calpain 15 (CAPN15) is an intracellular cysteine protease belonging to the non-classical small optic lobe (SOL) family of calpains, an important class of developmental proteins, as yet uncharacterized in vertebrates. We identified five individuals with microphthalmia and/or coloboma from four independent families carrying homozygous or compound heterozygous predicted damaging variants in *CAPN15*. Several individuals had additional phenotypes including growth deficits, developmental delay and hearing loss. We generated *Capn15* knockout mice that exhibited similar severe developmental eye defects, including anophthalmia, microphthalmia and cataract, and diminished growth. We demonstrate widespread *Capn15* expression throughout the brain and central nervous system, strongest during early development, and decreasing postnatally. Together, these findings demonstrate a critical role of *CAPN15* in vertebrate developmental eye disorders, and may signify a new developmental pathway.

2.2 Introduction

Developmental eye anomalies, including anophthalmia (absent eye), microphthalmia (small eye) and coloboma (disruption of the optic fissure closure), collectively known as AMC, are a genetically heterogeneous group of disorders affecting between 11.9 and 30 per 100 000 live births (1). Single gene alterations can underlie these conditions, the most frequent being in *SOX2* (2). To date, ~100 genes have been consistently associated with these phenotypes and are included in standard structural eye disorders diagnostic panels (https://panelapp.genomicsengland.co.uk/panels/509/). Data for congenital cataract are similar, with an estimated prevalence of 1.91–4.24 per 10 000 children (3) and nearly 100 genes considered diagnostic (https://panelapp.genomicsengland.co.uk/panels/230/). There is a degree of genetic overlap in the underlying causes of AMC and cataract, as seen with variants in *GJA8* (4). However, at least 40% of individuals with AMC (depending on phenotype) remain without a genetic diagnosis (2,5), indicating that additional unidentified genetic factors contribute to these conditions.

Calpains are intracellular cysteine proteases (6) with important roles in development. There are four conserved families: Classical, PalB, Transformer (Tra) and small optic lobe (SOL), with ‘classical’ being the best characterized. All calpain isoforms have a conserved catalytic domain and each family is characterized by unique domains: a C-terminal penta-EF hand domain in classical calpains; a C-terminal C2 domain in Tra calpains; an N-terminal MIT domain and an additional C-terminal C2-like domain in PalB calpains, and an N-terminal zinc finger domain that binds polyubiquitin (7) and a C-terminal SOL homology domain (SOLH) in SOL calpains (8,9).

Embryonic mice with a homozygous disruption of the murine classical calpain small subunit gene *Capn4* (causing disruption of the activities of classical calpains Capn1 and Capn2) die midgestation, displaying defects in the cardiovascular system, hemorrhage and accumulation of erythroid progenitors (10). Furthermore, pre-implantation embryonic lethality between the morula and blastocyst stage is observed in mice with a homozygous *Capn2* deletion (11). Transformer 3 (Tra-3) calpain was first discovered in the nematode *Caenorhabditis elegans*, as a sex determination gene (12). Later, studies suggested that Tra-3 cleaves Tra-2, which then interacts with transcription factor Tra-1 both directly and indirectly to promote female development (13,14). In addition, *C. elegans* with a single nucleotide polymorphism in Tra-3 displayed a smaller body size when animals were grown at low temperature (15). In humans, variants in the orthologue of the Tra calpain (*CAPN5*) that hyperactivate its protease activity are associated with inflammatory vitreoretinopathy, hearing loss and developmental delay (16).

An atypical calpain, *CAPN15* (also known as *SOLH or SOL calpain*) is located on chromosome 16p13.3 (17), a region previously implicated in inherited cataracts with microphthalmia (18). It was first characterized in the fruit fly *Drosophila* (19,20), where loss of SOL calpain leads to a 50% reduction in the volume of the optic lobes due to degeneration and absence of certain classes of columnar neurons (20). In *Aplysia*, the orthologue of CAPN15 is required for the induction of long-term plasticity implicated in non-associative memory, but not the long-term plasticity implicated in associative memory (21,22).

Using whole exome sequencing (WES), we identified five individuals from four independent families with likely pathogenic homozygous or compound heterozygous variants in *CAPN15*, displaying microphthalmia and/or coloboma plus additional phenotypes including growth delay. To characterize the role of CAPN15 in vertebrates, we generated a *Capn15*

knockout mouse. *Capn15*$^{(-/-)}$ mice displayed developmental eye anomalies including anophthalmia, microphthalmia and cataract, as well as reduced body weight similar to our affected individuals. Our data show that *CAPN15* plays a critical role in eye development and growth in vertebrates. It is the first intracellular protease linked to AMC, indicating a new pathway and is an important gene to include on diagnostic gene panels for developmental eye disorders and cataract.

2.3 Materials and methods

2.3.1 Ethics approval and consent to participate

The UK cohort of 316 individuals with ocular anomalies was recruited as part of a national 'Genetics of Eye and Brain anomalies' study (REC 04/Q0104/129). Informed consent was obtained according to the tenets of the Declaration of Helsinki. Individual 2 was recruited into the DDD Study, which has UK Research Ethics Committee approval (10/H0305/83, granted by the Cambridge South REC, and GEN/284/12 granted by the Republic of Ireland REC). For individual 3, informed written consent was obtained from all participants under an IRB approved protocol (KFSHRC RAC# 2070023).

Individuals 4 and 5 are members of a Canadian study approved by the institutional ethics review board of Université de Sherbrooke (project 12-167). All participants or their legal guardians provided written consent. All studies on mice were approved by the Montreal Neurological Institute/McGill University Animal care and use committee protocol 2009-5784.

2.3.2 Capn15 antibody

Polyclonal antibodies were raised in rabbits against the carboxy terminal of Capn15 using the following epitope: CDVAGLHGPRPL. A cysteine residue was added to the N-terminal of the peptide to enhance coupling. Peptides were coupled to KLH-maleimide and SulfoLink coupling resin (Thermo Fisher Scientific) according to manufacturer's instruction. After conjugation to KLH-maleimide, rabbits were injected and after four boosts the final serum was affinity purified on SulfoLink columns as previously described (36).

2.3.3 Generation of a *Capn15* KO mouse

We obtained embryonic stem cells with a *lacZ*-Neo cassette inserted into the mouse *Capn15* locus from the IMPC (31). The strategy used by the consortium was to insert a cassette that provides a strong exon entry site coupled with a stop codon, with *lacZ* produced from internal ribosome entry site translation (31,37). To remove this cassette, these mice were bred with mice that contain flippase (FLP) recombinase that recognizes a pair of FLP recombinase target sequences that flank the genomic region containing this cassette leaving lox sites surrounding the calpain catalytic domain exons 4–6 (based on NCBI reference sequence NM_001347334.1). These mice were then bred against mice expressing germline Cre recombinase to remove the floxed exons and generate a KO line (Supplementary Material, Fig. S1).

2.3.4 Dissections

Adult mice were transcardially perfused with ice-cold phosphate-buffered saline (PBS) followed by 4% (wt/vol) ice-cold paraformaldehyde (PFA) in PBS. Brains were post-fixed in 4% PFA for 45 min at 4°C, rinsed in PBS and cryoprotected in 30% sucrose/PBS overnight at 4°C. The following day, brains were embedded in Tissue-Plus™ O.C.T. compound (Fisher Healthcare) and flash frozen in 2-methylbutane chilled in dry ice. The brains were kept at −80°C until further use.

2.3.5 X-gal staining

Sections of 20 μm were incubated overnight at 37°C in solution containing 80 mm Na_2HPO_4, 20 mm NaH_2PO_4, 2 mm $MgSO_4$, 5 mm $K_3[Fe(CN)_6]$, 5 mm $K_4[Fe(CN)_6]$, 0.2% NP-40, 0.1% sodium deoxycholate and 1.5 mg/ml X-gal. Sections were rinsed in PBS, washed in ethanol (50% for 1 min, 70% for 1 min, 95% for 1 min and 100% for 2× 1 min), cleared in xylene, and mounted with Permount (Thermo Fisher Scientific).

2.3.6 Western blotting

Embryonic brains were homogenized manually in lysis buffer containing 25 mm Tris–HCl (pH 7.4), 150 mm NaCl, 6 mm $MgCl_2$, 2 mm EDTA, 1.25% NP-40, 0.125% SDS, 25 mm NaF, 2 mm $Na_4P_2O_7$, 1 mm dithiothreitol (DTT), 1 mm phenylmethylsulfonyl fluoride, 20 mg/ml leupeptin and 4 mg/ml aprotinin. Before loading, 5× sample buffer was added to the lysate and samples were incubated at 95°C for 5 min. Proteins were resolved by SDS–PAGE on Bis-Tris gel and transferred to nitrocellulose membrane (Bio-Rad). The blots were blocked in TBST (Tris-buffered saline + 0.1% Tween) containing 4% skim milk for 30 min at room temperature

and then incubated with primary antibodies overnight at 4°C. After washing three times with TBST, the blots were incubated with horseradish peroxidase (HRP)-conjugated secondary antibodies for 1 h at RT, and washed again three times in TBST. The Western Lightning Plus-ECL kit (NEL103001EA; PerkinElmer LLC Waltham, MA, USA) was used as per manufacturer's instructions to detect protein bands. The primary antibody used was homemade rabbit anti-Capn15 antibody (1:1000) raised against the C-terminus of Capn15. The secondary antibody was HRP-conjugated goat anti-rabbit secondary antibody (1:5000). Antibodies were diluted in Tris buffered saline with Tween containing 4% skim milk powder.

2.3.7 Eye phenotype quantification

Mice eyes were examined and grouped as follows: seems normal, obvious cataract, small eye and no eye. This categorization was performed for both eyes of each mouse. The analysis was performed without the knowledge of the genotype of the mice.

2.3.8 Quantification of immunoblotting

Immunoblots were scanned and imaged using the public domain Image J program developed at the U.S. National Institute of Health (https://imagej.nih.gov/ij/). We calibrated our data with the uncalibrated optical density feature of NIH image, which transforms the data using the formula $\log_{10} \frac{225}{225-x}$, where x is the pixel value (0–254). We used the Ponceau image for each gel to normalize the amount of SOL calpain in brains at different ages to the amount of SOL calpain in E12–E14 brains run on the same gel.

2.3.9 Whole Exome Sequencing

A UK cohort of 316 individuals with ocular anomalies, principally AMC, was recruited as part of a national ‘Genetics of Eye and Brain anomalies’ study (REC 04/Q0104/129). Informed consent was obtained according to the tenets of the Declaration of Helsinki. Patients were screened by indication in known AMC genes. Fifty-five individuals from the cohort were screened by WES as described previously (38,39). Individual 2 was recruited into the DDD Study, which has UK Research Ethics Committee approval (10/H0305/83, granted by the Cambridge South REC, and GEN/284/12 granted by the Republic of Ireland REC).

For individual 3, WES was performed as previously described (40). Sanger sequencing and segregation analysis were completed. Informed written consent was obtained from all participants under an IRB approved protocol (KFSHRC RAC# 2070023).

Individuals 4 and 5 are siblings who were identified through whole-exome sequencing of a Canadian cohort of 51 patients presenting dysmorphisms with or without neurodevelopmental disorders (24).

The following primers were used for sequencing: For individual 1: forward primer CCATCATCCTGCTCACCGA and reverse primer GGCACGCTATCCTGGGTAC; for individual 2 exon 8: forward primer GCAACATGAAGGTGGACGAT and reverse primer AGCTGCCGTTCCAGGAGAAA; for individual 2 exon 10: forward primer GGAGGGCTTCCTATTATAGG and reverse primer AACACCAGGATGCACAGGTC and for individual 3: forward primer GCAGGGGTCCCGAGA and reverse primer CAGACCGGCGACCTCT.

2.3.10 cDNA and splicing studies

Blood samples were collected from individual 1 and her parents, RNA was extracted using a RNeasy Mini kit (Qiagen) and cDNA generated using a high capacity reverse transcriptase kit (Applied Biosystems). To examine the impact of the variant on splicing, forward and reverse PCR primers were designed mapping to exons 11 and 14, respectively (forward: GTCAAGAAGTTCGTCAGCTG, reverse: CTGTCCAGTCACTGAGGAAG).

2.4 Results

2.4.1 Identification of five individuals with CAPN15 mutations and eye anomalies

WES of 55 individuals with developmental eye disorders from a UK cohort (Supplementary Material, Methods) identified one individual with unilateral microphthalmia and bilateral coloboma with a previously unreported homozygous missense variant in *CAPN15* exon 13 (NM_005632.2:c.2905G>A; NP_005623.1:p.(Gly969Ser); chr16:602863 [hg19]) (individual 1) (Fig. 1A). Subsequently, four additional individuals with AMC spectrum disorders and biallelic *CAPN15* variants from three independent families were identified by WES. Individual 2, recruited to the Deciphering Developmental Disorders (DDD) project, was identified with compound heterozygous *CAPN15* variants. The first variant was a paternally inherited missense variant in exon 8 (NM_005632:c.2159C>T; NP_005623.1:p.(Ser720Phe); chr16:601394 [hg19]), absent from the gnomAD database (http://gnomad.broadinstitute.org/) (23). The second variant was a rare maternally inherited missense variant in exon 10 (rs762523863; NM_005632:c.2398C>T; NP_005623.1:p.(Arg800Trp); gnomAD minor allele frequency =

0.00001986) (chr16:602103 [hg19]) (Fig. 1B). Individual 3 carries a homozygous missense variant in *CAPN15* exon 13 (NM_005632.3:c.3083G>A; p.(Arg1028Lys); chr16: 603041 [hg19]) absent from the gnomAD database (23) (Fig. 1C). Finally, individuals 4 and 5, siblings and offspring of distantly related parents, were ascertained through a Canadian cohort of 51 patients presenting with anomalies, with or without neurodevelopmental disorders (24). They harbor a homozygous missense variant in *CAPN15* exon 6 (NM_005632.3:c.1838C>T; NP_005623.1:p.(Ser613Leu); chr16:599467 [hg19]) (Fig. 1D). This variant is extremely rare, reported in only three individuals on the gnomAD database (minor allele frequency 0.00001421), with no individuals with homozygosity for this variant observed. All five variants are predicted damaging by SIFT (25) and PolyPhen-2 (26) and were validated by Sanger sequencing. In each case, the identified variants were inherited from asymptomatic heterozygous parents with no family history of eye anomalies. The siblings of individual 1 were found to be asymptomatic heterozygous carriers. No genotyping data are available for the unaffected sibling of individuals 4 and 5. The segregation of disease with biallelic *CAPN15* variants in these five families confirms a recessive pattern of inheritance. No other likely pathogenic variants in known AMC genes were identified in these individuals by WES.

Detailed phenotypic descriptions of each individual are provided in Table 1, Figure 2 and the Supplementary Material, Results. All five affected individuals presented with AMC spectrum disorders; two individuals (1 and 2) had microphthalmia, four had coloboma (1, 3, 4, and 5), and individual 1 also had a unilateral lens opacity (cataract). Interestingly, some individuals showed additional delay in growth and development. Three individuals showed delayed growth, including short stature (1, 2, and 4), low weight (1 and 2), reduced head circumference (1 and 2) and clinical microcephaly affecting individual 4. Furthermore, individuals 2, 4 and 5 presented

with developmental delay, in addition to cognitive delay (2) and autism (2 and 5). Finally, three individuals (2, 4 and 5) were diagnosed with hearing loss and both individuals 2 and 4 had simple external ear features. It is also interesting to note the presence of multiple miscarriages in family 1.

As the c.2905G>A (individual 1) and c.3083G>A (individual 3) variants affect the first and last nucleotides of *CAPN15* exon 13, respectively, we investigated their impact on splicing. For c.2905G>A, we generated cDNA from blood samples from individual 1 and their parents. However, PCR and Sanger sequencing across exons 11–14 revealed no alteration in splicing (data available on request). Similarly, for individual 3, we observed no impact on splicing after performing RTPCR on RNA extracted from lymphoid cell lines derived from this patient (data available on request).

Within *CAPN15,* all five variants are located within the C-terminal portion of the protein and affect amino acids conserved across multiple vertebrate species (Fig. 3). However, only p.(Ser613Leu) (individuals 4 and 5) and p.(Ser720Phe) (individual 2) are located within an annotated region of the protein, both lying within the Calpain catalytic domain. As no 3D structure for CAPN15 is available, we used I-TASSER (27–29) to generate a predicted structure. Site-directed mutator (SDM; http://marid.bioc.cam.ac.uk/sdm2/prediction) was applied to this model to predict the impact of the variants on CAPN15 stability (Table 2). This indicated that p.(Gly969Ser) and p.(Arg1028Lys) may decrease protein stability ($\Delta\Delta G = -3.27$ and -1.15, respectively), whereas p.(Ser613Leu) is predicted to increase stability ($\Delta\Delta G = 1.85$). Interestingly, both of the mutations predicted to decrease CAPN15 stability are in the highly conserved SOLH domain that is present only in SOL calpains and whose structure and function is unknown.

2.4.2 Capn15$^{(-/-)}$ mice have anophthalmia, microphthalmia and cataract

The protein encoded by the human CAPN15 gene (NP_005623.1) has 87.4% identity/90.9% similarity to the mouse orthologue NP_001334263 using EMBOSS Needle (30). Mouse embryonic stem cells with a *lacZ*-Neo cassette inserted into the *Capn15* locus were obtained from the International Mouse Phenotyping Consortium (IMPC) (31) and used to generate *Capn15* knockout mice (Supplementary Material, Fig. S1A). Disruption of *Capn15* was confirmed by western blotting of brain homogenates using an antibody raised against the C-terminal of the protein (Supplementary Material, Fig. S1B).

In a cross of *Capn15* heterozygous mice, the incidence of *Capn15*$^{(-/-)}$ pups was 12%, significantly lower than the expected 25% (12%, $P = 1.28e^{-5}$, Chi Square test; WT $n = 52$, *Capn15*$^{+/-}$ $n = 155$, *Capn15*$^{-/-}$ $n = 29$). This indicates that homozygous loss of the gene results in decreased viability, and is of further interest given the presence of multiple miscarriages in family 1. Furthermore, *Capn15*$^{(-/-)}$ mice that were successfully weaned weighed 11% (±3% SEM) less than their littermate WT or heterozygous mice ($P = 0.003$ and $P = 0.0006$, respectively. Student's *t*-test; WT $n = 45$, *Capn15*$^{+/-}$ $n = 71$, *Capn15*$^{-/-}$ $n = 18$), recapitulating the delayed growth and development in several of our affected individuals (Fig. 4A). Most significantly, homozygous *Capn15* KO mice displayed a range of developmental eye disorders overlapping those observed in the five affected individuals with biallelic *CAPN15* variants. These included anophthalmia (18%), microphthalmia (26%) and cataract (31%) (Fig. 4B–E). Less than 6% of heterozygous mice overall displayed developmental eye disorders (anophthalmia 1%, microphthalmia 2%, and cataract in 2%). No significant difference was observed between the left and right eyes of adult *Capn15* KO mice (>12 weeks of age) ($P = 0.15$)

and there was no preference for bilateral or unilateral presentation. Therefore, after pooling left and right eyes, the presence of these phenotypes was significantly increased in *Capn15* KO mice compared with heterozygous or WT mice ($^{***}P < 0.0001$; WT $n = 30$, *Capn15*$^{+/-}$ $n = 160$, *Capn15*$^{-/-}$ $n = 90$ including offspring from parents who were both *Capn15*$^{-/-}$; Fig. 4F). This difference in eye phenotype was present in mice at 6 and 12 weeks of age, suggesting that these anomalies were the result of aberrant development.

2.4.3 Capn15 is highly expressed in the brain and eye

To investigate the role of *Capn15* in the brain during development, *lacZ* expression was examined in *Capn15*$^{(lacZ\text{-}Neo)}$ heterozygous mice. X-gal staining of sagittal sections of E12 embryos showed that *Capn15* was primarily expressed in the outer layer of the central nervous system, in particular the mantle zone of the pallium and subpallium (forebrain), and the mantle zone of the rhombomere (hindbrain) (Fig. 5A). At E18, *Capn15* was expressed widely in the nervous system with high levels in the subventricular zone, immediately next to the ventricular zone. Expression was strongest in the deep cortical layer of the cerebral cortex, and neuroepithelium layer in the hippocampus, but not the pyramidal layer. By P3, *Capn15* was ubiquitously expressed in the brain from the olfactory bulb to the cerebellum and also within the retina, particularly in the ganglion cell layer (Fig. 5C and D). To further explore the pattern of expression over time, *Capn15* protein expression in the rat brain was examined over time using immunoblotting. Here, expression was found to be highest during embryonic development (E14–E18 brains), decreasing significantly after birth (P0-adult) (Fig. 5E and F).

2.5 Discussion

Our data demonstrate the importance of the protease *CAPN15* in mammalian eye and brain development. We identified likely pathogenic recessively inherited variants in five individuals with AMC and/or cataract and additional phenotypes including delayed growth and development. These phenotypes were recapitulated in a mouse model, with further data supporting expression of the gene during brain development.

Our cases showed microphthalmia and/or coloboma, while 18% of knockout mice had the more severe anophthalmia. The milder phenotypic range displayed in the humans may be explained by all five variants being missense. These variants could impact protein function by destabilizing protein structure, affecting the calpain catalytic activity, or its regulation by the SOLH domain. This is likely to be less damaging to overall function than the total loss of the gene in the mouse knockout. This may also account for the presence of AMC phenotypes at low frequency in heterozygous mice, which were not detected in humans heterozygous for the missense variants. Alternatively, it may reflect the small sample group of humans or interspecies variation. However, given the lack of a functional assay for CAPN15, it is difficult to determine whether the variability between mouse and human phenotypes and/or amongst the individuals carrying distinct missense changes is due to different effects of these variants on the protein. The penetrance of the eye phenotype in the mouse was also variable, even with a complete knockout, suggesting a complex relationship between the loss of CAPN15 and the eye phenotype. Therefore, screening of additional individuals with AMC would help to determine both the full phenotypic range associated with variants in this gene, as well as potential genotype–phenotype correlations. Furthermore, only individual 1 had cataract, while 31% of mice had this phenotype. This may reflect ascertainment bias, as none of the participants or cohorts included in this study

was recruited on the basis of this phenotype. However, recent reports show that variants in *GJA8*, a gene associated with isolated cataract, are also a significant cause of microphthalmia, accounting for over 1% of cases of AMC in large cohorts (4).

Developmental delay and hearing loss were present in three individuals with *CAPN15* variants. Our data show strong embryonic expression of *Capn15* in the brain, suggesting that it is important in neurodevelopment. Therefore, the *CAPN15* variants may underlie these phenotypes as well as eye anomalies. Similarly, growth delay was observed in three individuals and the *Capn15*$^{-/-}$ mice also exhibited a significant growth deficit.

There is little known about the function of the SOL calpain family, of which CAPN15 is the sole human member. This family diverged from other calpain families before the origin of metazoans and is conserved in all metazoans, suggesting a fundamental role for the protein (9). Two of the identified variants are in conserved residues in the calpain catalytic domain present in all members of the calpain family, while a third variant lies adjacent to it. However, while the N-terminal of the SOL calpain has been shown to bind to poly-ubiquitin (7), there have been no functional studies on the calpain or *SOLH* domain of this family of genes. In *Drosophila*, the large loss of neurons in the optic lobe was thought to be due to degeneration (20), but a role for Capn15 in early differentiation during development was not excluded. In *Aplysia*, SOL calpain is important for the induction of plasticity associated with non-associative learning (21), perhaps due to cleavage of protein kinase Cs (PKCs) into persistently active protein kinase Ms (PKMs) (7,32). Further investigation of how Capn15 performs these functions may also shed light on its role during eye development. Furthermore, as other calpains function to regulate transcription through regulated cleavage of transcription factors (33), and since many genes underlying ocular

anomalies are transcription factors (2), investigation of the role CAPN15 plays in early developmental transcriptional pathways may also prove a valuable avenue of research.

Together, our data meet criteria for inclusion of *CAPN15* in clinical genetic diagnostic testing for AMC according to both the Clinical Genome Resource (ClinGen) (www.clinicalgenome.org) (34,35) and Genomics England PanelApp (https://panelapp.genomicsengland.co.uk/#!Guidelines). Therefore, these data will contribute to improved care for AMC patients and their families.

2.6 Conclusion

We demonstrate for the first time the importance of *CAPN15* in mammalian eye development, identifying likely pathogenic variants in five individuals with AMC from four families, supported by a mouse KO model and embryonic expression studies. These findings translate to clinical benefit by adding a new gene to clinical diagnostic testing, and potentially a new pathway in the increasingly complex network involved in human eye development.

2.7 Acknowledgement

We would like to thank the families for their participation in our study. The authors would also like to thank Mireille Bouchard-Levasseur for excellent technical assistance in quantification of the transgenic mice eye phenotype, Dr Len Levine for advice concerning the eye phenotype, Dr Zvi Gan-Or for initial assistance in human genomics, the West Midlands Regional Clinical Genetics Service for their help with sample processing and clinical genetic testing of UK families with AMC conditions, Dr Dorine Bax, Oxford Brookes University,

Oxford for research coordination, the Sequencing and Genotyping Core Facilities at KFSRHC for their technical help, the support of the Saudi Human Genome Program, Niema Ibrahim for her help as a clinical coordinator and Annabelle Pratte, genetic counselor, for her help with clinical information of individuals 4 and 5. The DDD study presents independent research commissioned by the Health Innovation Challenge Fund (grant number HICF-1009-003). This study makes use of DECIPHER (http://decipher.sanger.ac.uk/), which is funded by Wellcome. See Nature PMID: 25533962 (https://urldefense.proofpoint.com/v2/url?u=https-3A__www.ncbi.nlm.nih.gov_pubmed_-3Fterm-3D25533962&d=DwIF-g&c=D7ByGjS34AllFgecYw0iC6Zq7qlm8uclZFI0SqQnqBo&r=4KNgiByx5ZDuuQKe7_F5cAmmY9GaslfHYZ8UCyouNzY&m=3qfQbvTNwcqZG71zAHbbAJmPgTH7167rrFR5RarH7e0&s=vT_eWJBaUeCuN2e1yYLyBVP9xBuUJbqAtscisWeG0ns&e=) or http://www.ddduk.org/access.html (http://www.ddduk.org/access.html) for full acknowledgement.

Conflicts of Interest statement. The authors state no conflicts of interest in this study.

2.8 Funding

CIHR (grant MOP 340328 to WSS); Baillie Gifford; Microphthalmia; Anophthalmia; Coloboma Support (MACS) (www.macs.org.uk); Health Innovation Fund, Oxford Brookes University (HEIF); King Salman Center for Disability Research (FSA); Researchers Supporting Project number (RSP-2020/181); King Saud University, Riyadh, Saudi Arabia; institutional funds of the Université de Sherbrooke; La Fondation du Grand Défi Pierre Lavoie; La Fondation

des Étoiles; the DDD study presents independent research commissioned by the Health Innovation Challenge Fund (grant number HICF-1009-003). This study makes use of DECIPHER (http://decipher.sanger.ac.uk/), which is funded by Wellcome.

2.9 Figures and legends

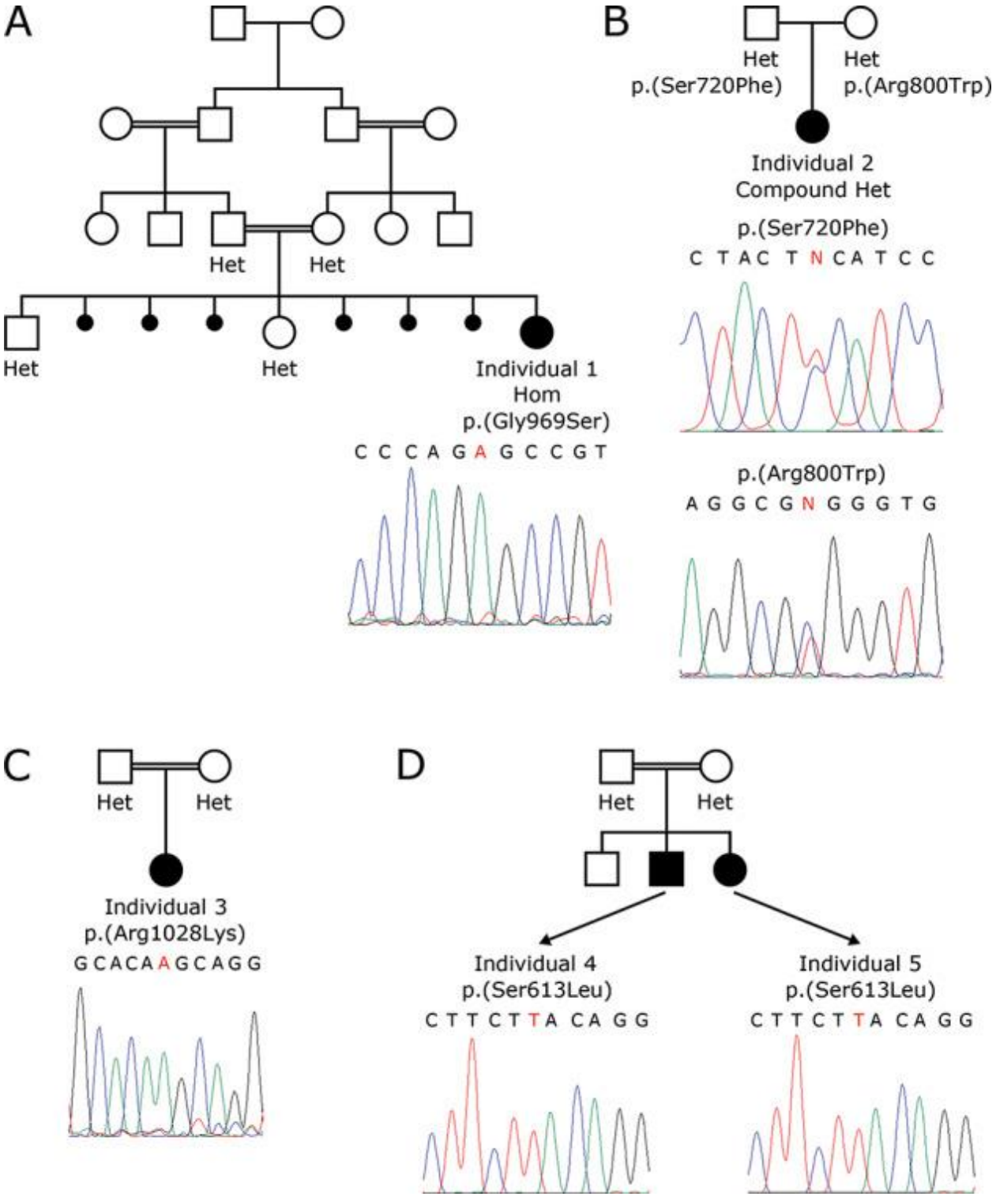

Figure 2.1. Pedigrees of the five individuals with *CAPN15* variants. Chromatograms of Sanger sequencing validation of the variants in affected individuals shown. Position of variant indicated in red. Note that sequencing for individual 3 was performed from cDNA. (**A**) Individual 1, (**B**) individual 2, (**C**) individual 3 and (**D**) individuals 4 and 5.

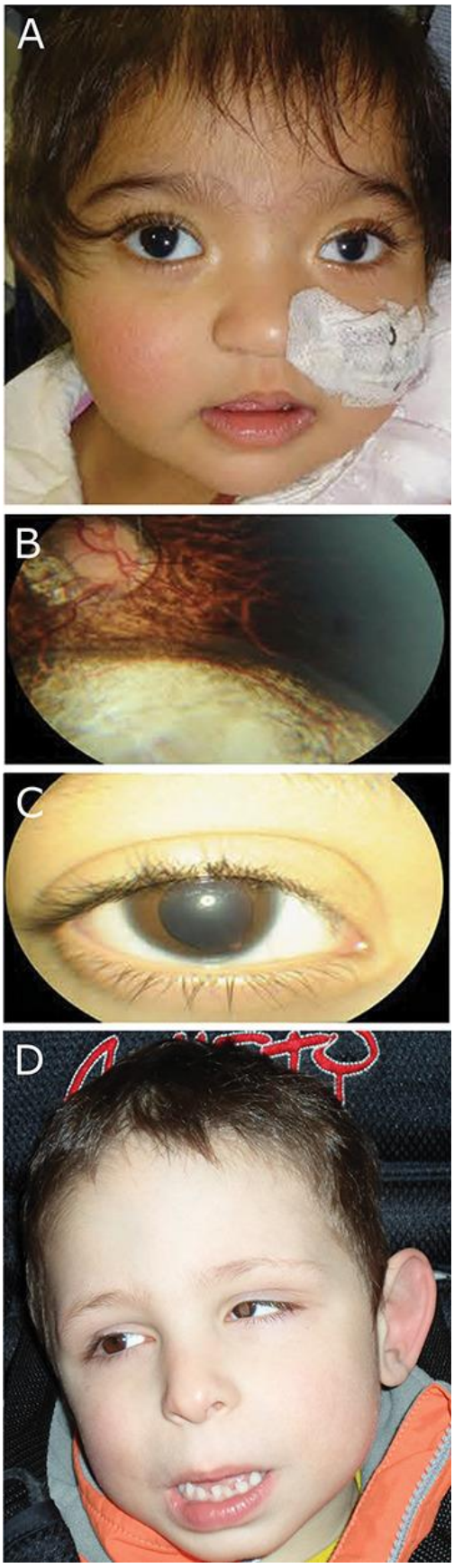
A
B
C
D

Figure 2.2. Phenotypes of individuals 1, 3 and 4. (**A**) Right iris and chorioretinal coloboma, and left mild microphthalmia with an iris and chorioretinal coloboma involving the disk in individual 1. (**B**, **C**) Inferonasal chorioretinal coloboma (B) and iris coloboma of the right eye (C) in individual 3. (**D**) Bilateral iris and chorioretinal coloboma (more prominent in the left eye), and dysmorphic features including left ptosis, left simple ear and prominent columella in individual 4.

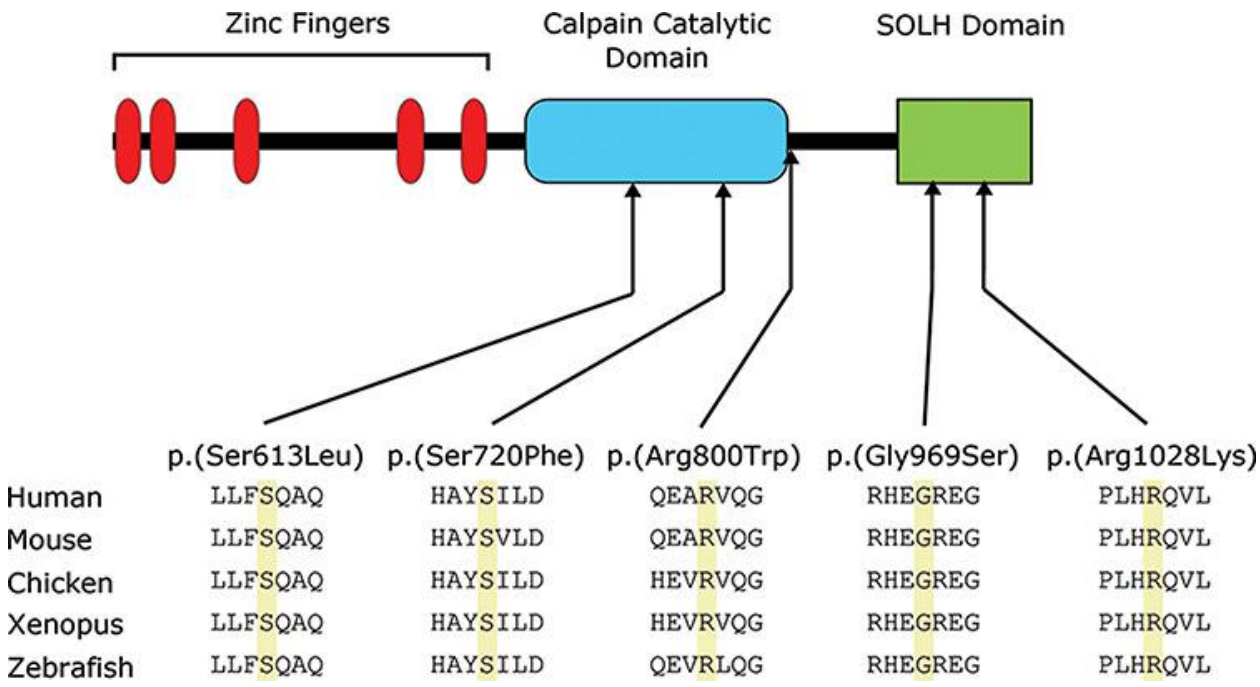

Figure 2.3. Schematic of CAPN15 showing the location of the variants identified in individuals 1–5. Zinc fingers shown in red, the calpain catalytic domain in blue and the SOLH domain in green. The conservation of the affected amino acids in human, mouse, chicken, *Xenopus* and zebrafish is indicated.

A

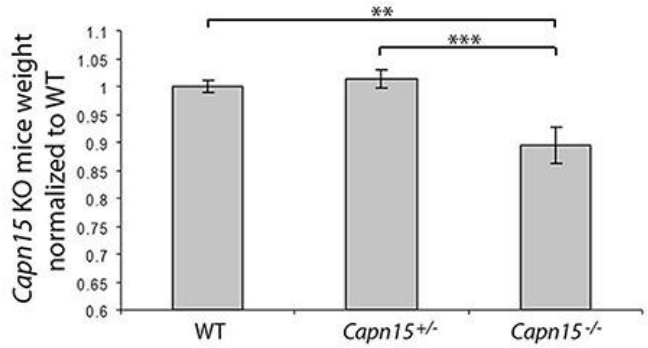
**
***
Capn15 KO mice weight normalized to WT
1.1
1.05
1
0.95
0.9
0.85
0.8
0.75
0.7
0.65
0.6
WT
Capn15+/-
Capn15-/-

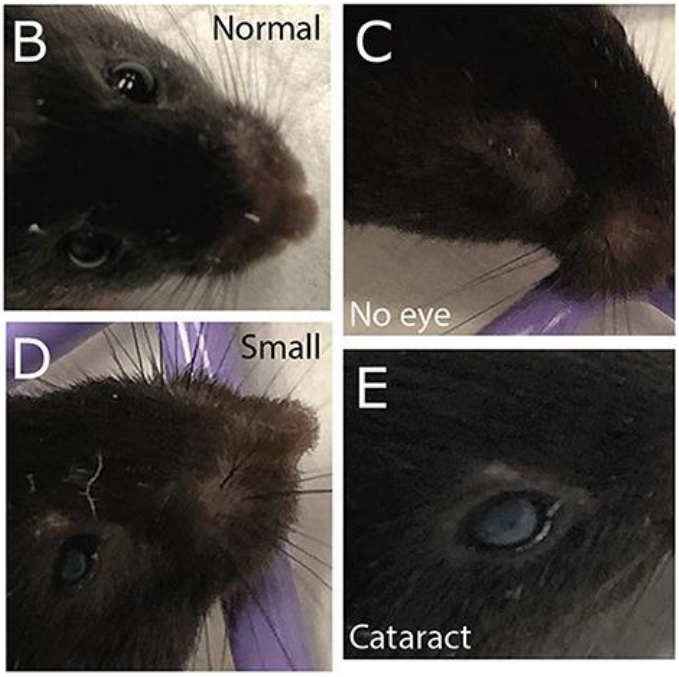
B
Normal
C
No eye
D
Small
E
Cataract

F

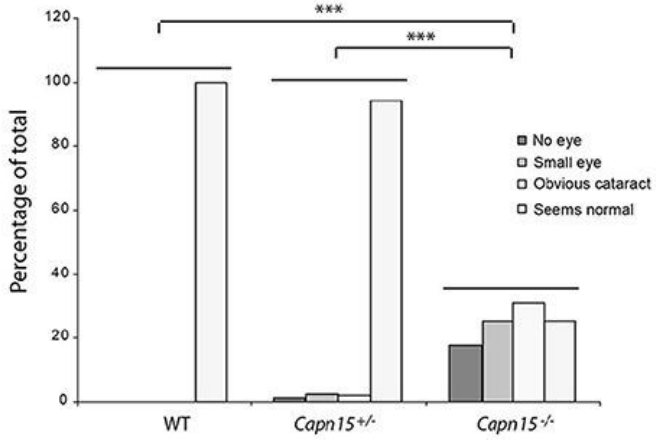
***
***
Percentage of total
120
100
80
60
40
20
0
No eye
Small eye
Obvious cataract
Seems normal
WT
Capn15+/-
Capn15-/-

Figure 2.4. *Capn15* KO mice display growth and eye anomalies. (**A**) Mean weights of *Capn15* KO and *Capn15* heterozygous mice after weaning normalized to the mean weight of WT mice. Error bars represent SEM. (**B**–**E**) Representative photographs of the eye phenotypes of *Capn15* KO mice; normal (B), anophthalmia (C), microphthalmia (D) and cataract (E). (**F**) Comparison of the percentage of eye anomalies in WT, *Capn15* heterozygous and *Capn15* KO mice at more than 12 weeks of age. $^{**}P = 0.003$, $^{***}P = 0.0006$.

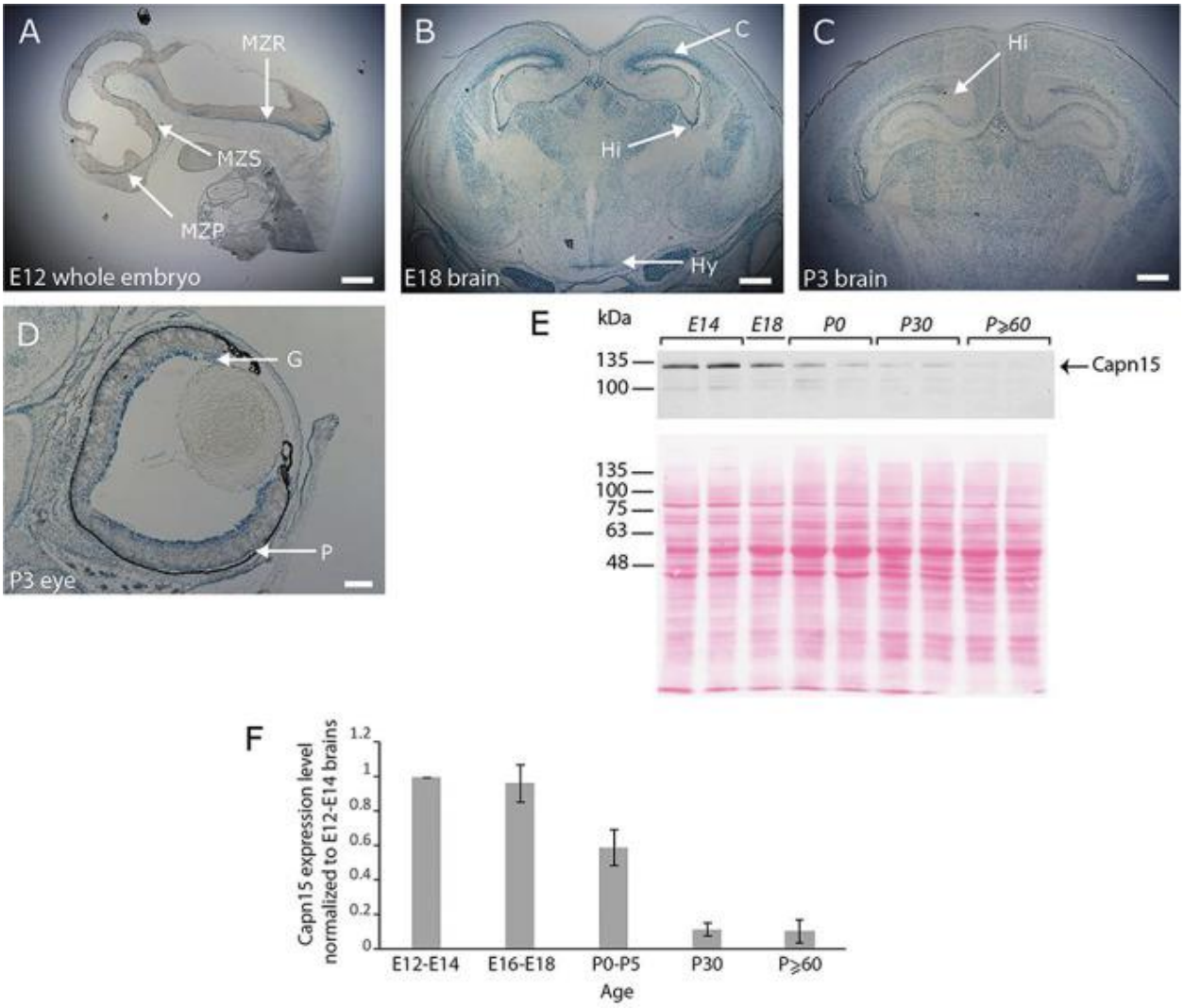

Figure 2.5. Capn15 is enriched in rodent brain and eyes during early development. (**A**–**D**) X-gal staining of sections from E12, E18 and P3 *Capn15*$^{(lacZ\text{-}Neo)}$ heterozygous mice. Scale bar is 200 μm. (A) Sagittal section of whole embryo at E12 showing *Capn15* expression in the mantle zones of the pallium, subpallium and rhombomere. (B) Coronal section of the brain at E18 showing expression in the cerebral cortex, hippocampus. (C) Coronal section of the brain at P3 showing generalized expression, including the hippocampus. (D) Sagittal section of the eye at P3, highlighting expression in the ganglion cells of the retina. (**E**) Western blots using protein

extracts from rat brains at E14, E18, P0, P30 and $P \geq 60$ showing decreasing Capn15 expression with increasing age. Experiment was performed in triplicate. (**F**) Quantification of *Capn15* expression in rat brain. Capn15 expression was normalized to E12–E14 brains; E12–E14 $n = 3$, E16–E18 $n = 4$, P0–P5 $n = 4$, P30 $n = 2$, and $P \geq 60$ $n = 3$. Error bars represent SEM. Abbreviations: C (cortex), G (ganglion cell layer), Hi (hippocampus), Hy (hypothalamus), MZP (mantle zone of pallium), MZR (mantle zone of rhombomere), MZS (mantle zone of subpallium) and P (photoreceptor cell layer).

Table 1

Phenotypes of the five human individuals identified carrying homozygous or compound heterozygous *CAPN15* variants

Individual	**1**	**2**	**3**	**4**	**5**
Variant	p.(Gly969Ser)	p.(Ser720Phe) p.(Arg800Trp)	p.(Arg1028Lys)	p.(Ser613Leu)	p.(Ser613Leu)
Eye	Unilateral microphthalmia, bilateral coloboma, unilateral lens opacity	Bilateral microphthalmia, iridio-corneal adhesions	Bilateral myopia, unilateral coloboma	Bilateral coloboma, unilateral ptosis	Unilateral coloboma
Growth	Poor weight gain	Delayed	Normal	Short stature	Normal
Developmental delay	Normal	Cognitive delay, autism	Normal	Global delay	Developmental delay, autism spectrum disorder
Head circumference	19th % (3.5 y)	5th % (14 y)	Normal	Microcephaly	Normal
Hearing	Normal	Hearing loss	Normal	Deaf	Deaf
Other	Laryngeal cleft, dysphonia, hirsute, sacral dimple	Bicuspid aortic valve, horseshoe kidney, simple ears, unusually shaped small pituitary	–	Facial dysmorphism, imperforate anus, unilateral simple ear, prominent columella	Imperforate anus with vaginal fistula, hemivertebrae

Individuals 4 and 5 are siblings. y, years

Table 2

SDM (http://marid.bioc.cam.ac.uk/sdm2/prediction) analysis of the impact of CAPN15 variants on protein stability

Variant	$\Delta\Delta G$	Stability
p.S613L	1.85	Increased
p.S720F	0.52	Increased
p.R800W	0.24	Increased
p.G969S	−3.27	Reduced
p.R1028K	−1.15	Reduced

2.10 Supplementary materials

Supplemental Data

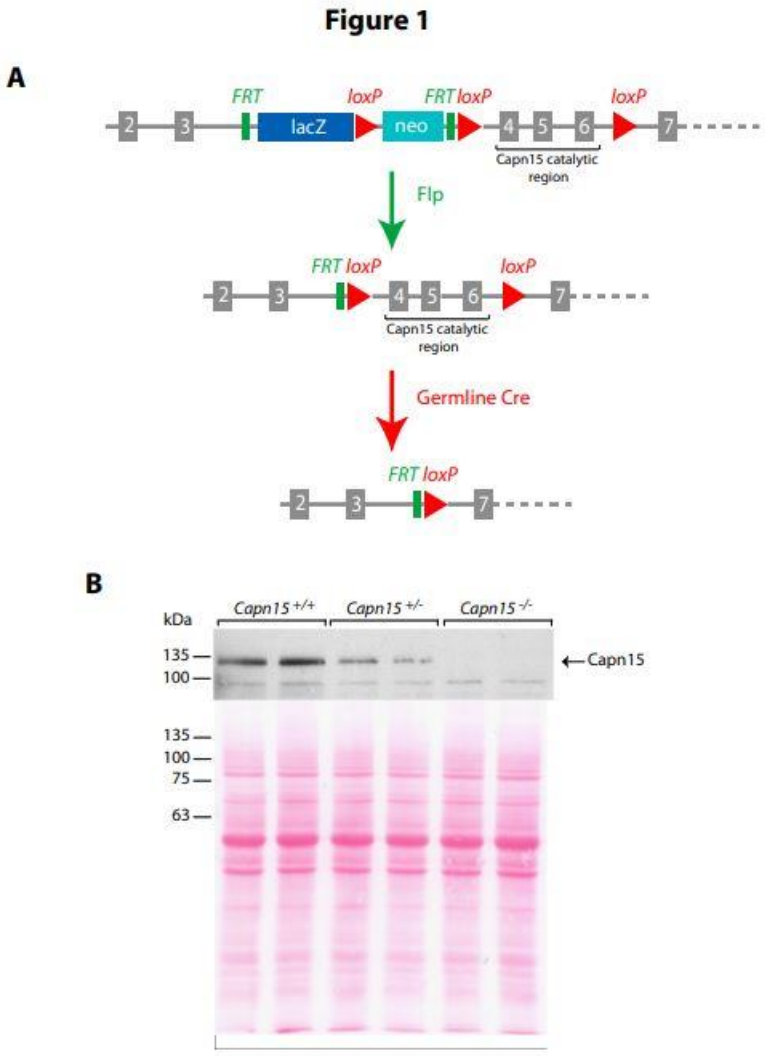

Supplemental Figure 2.1. Validation of the disruption of Capn15. (A) Breeding schematic to generate *Capn15* KO mice. The figure represents isoform NM_001347334.1, which includes 12 exons. Mice with *lacZ* and neo cassette are crossed to mice expressing FLP. The offspring are crossed to mice expressing germline Cre recombinase to remove the exons flanked by two loxP sites encoding the catalytic domain of Capn15. (B) Brains were homogenized and SDS PAGE

and western blotting performed. Capn15 was probed using a rabbit anti-mouse Capn15 antibody. A band of ~130kDa corresponding to the expected molecular weight of Capn15 was detected in brain homogenates from wild type mice (*Capn15*$^{+/+}$), but was undetectable in *Capn15* KO mice (*Capn15*$^{-/-}$). A Ponceau stain of the gel is shown on the bottom.

Supplemental results

Case Reports

Individual 1

Individual 1 was identified through whole exome sequencing (WES) screening of 55 individuals selected from a UK cohort of 316 individuals with ocular anomalies (Supplemental Methods). She is a girl of Pakistani ethnicity with right iris and chorioretinal coloboma involving the disc and a mild lens opacity, and left mild microphthalmia with an iris and chorioretinal coloboma involving the disc. She is slightly hirsute with a low hairline at the front. She was born at 41 weeks' gestation following an uneventful pregnancy with a birth weight of 2.72 kg (0.4-2 nd %) to consanguineous parents. Her mother had experienced multiple miscarriages and stillbirths. Postnatally, Individual 1 was noted to have a sacral dimple, laryngeal cleft and dysphonia. She developed pneumonia in the neonatal period treated with intravenous antibiotics, and had a nasogastric tube inserted for tube feeding due to an unsafe swallow. She had poor weight gain since birth. Her head circumference was 37.5 cm (3 rd %) at 3 months of age. At 4 months of age, her weight was 4.7 kg (almost 0.4 th %), with length 59.2 cm (19th %) and head circumference 39.6 cm (15 th %). She has two siblings, a brother with renal reflux and a congenital heart defect, and a sister with myopia and tachycardia. There was no family history of AMC. The mother was noted to have bilateral cupped discs, but normal intraocular pressures on ocular examination. There is a family history of glaucoma in the maternal grandfather and aunt. At 3 1/2 years, she was doing well except for pains in her arms and legs. She had a head circumference of 47.6 cm (19th %) and her height was 94 cm (24 th %), weight 12.1 kg (4 th %).

In addition to the CAPN15 variant, Individual 1 has trisomy X, identified using BlueGnome 8 x 60k aCGH (Illumina), which was considered to be unrelated to their eye phenotype. No other potential pathogenic variants were identified.

Individual 2

Individual 2 is a 26-year-old male who was born to non-consanguineous parents at 39 weeks' gestation by emergency Caesarean section (foetal distress) weighing 2.6 kg (2-9 th %), after a pregnancy complicated by oligohydramnios. He had bilateral microphthalmia with irido-corneal adhesions, prominent simple ears and a hearing loss of 80-100 db, and a bicuspid aortic valve. Renal ultrasound demonstrated a horseshoe kidney, which has been asymptomatic. Developmental delay was noted in the first year of life; he sat at around 18 months and walked at 4 years of age. At age 14y he had severe developmental and cognitive delay and autism. He had no speech, but communicated using sign language. His growth was delayed; at 14y his height was 139 cm (<1st % [-3SD]), his weight was 33kg (1st % [-2.4SD]) and his head circumference was 52.5 cm (5th %). A brain MRI scan demonstrated an unusually shaped and small pituitary, but pituitary function tests were normal. Individual 2 was previously tested for Branchio-Oto-Renal syndrome. This identified a maternally inherited missense variant in *EYA1* (rs369822742, NM_000503:c.923G>A; NP_000494.2:p.(Arg308Gln); chr8:72184036 [hg19]). This variant is reported in gnomeAD (minor allele frequency = 0.0002028), and classified as likely benign in ClinVar (VCV000363652.1).

Individual 3

Individual 3 is a 7-year-old girl of Arab ethnicity born to consanguineous parents. Both eyes were extremely myopic (right eye -26 D, left eye -19 D). There was right eye inferonasal coloboma of both the iris and the retina. There was no coloboma in the left eye. The extreme myopia was primarily related to increased axial length (Right eye 27.58 mm, and left eye 26.81 mm at age 7 years). There was no history of developmental delay or other anomalies.

Individual 4

Individual 4 is a 11-year-old male and brother of Individual 5. He was born at $39^{4/7}$ weeks from a French-Canadian couple with distant consanguinity. Amniocentesis was performed during pregnancy for increased nuchal translucency, and karyotype was normal. Birth weight, length and head circumference were within normal limits. He showed bilateral iris and chorioretinal coloboma (more prominent in the left eye), bilateral sensorineural deafness, and anal imperforation. He was referred to genetics at $3^{10/12}$ years for a CHARGE-like phenotype and he showed severe global developmental delay, post-natal microcephaly and short stature (between 0.1st - 3rd percentile), severe eczema and dysmorphic features including left ptosis, left simple ear, and prominent columella. Chromosomal microarray, CHD7 and SALL1 sequencing and deletion/duplication analysis were normal. Cerebral MRI, cardiac echogram and abdominal ultrasound yielded normal results.

Individual 5

Individual 5 is a 6-year-old female and sister of Individual 4. She presented at birth with iris and chorioretinal coloboma of the left eye, congenital cardiopathy (VSD, ASD), anal

imperforation with vaginal fistula, hemivertebrae and bilateral sensorineural deafness. She has been diagnosed with developmental delay and autism spectrum disorder.

2.11 References

1. Campbell, H., Holmes, E., MacDonald, S., Morrison, D. and Jones, I. (2002) A capture-recapture model to estimate prevalence of children born in Scotland with developmental eye defects. J. Cancer Epidemiol. Prev., 7, 21–28.

2. Plaisancie, J., Ceroni, F., Holt, R., Zazo Seco, C., Calvas, P., Chassaing, N. and Ragge, N.K. (2019) Genetics of anophthalmia and microphthalmia. Part 1: non-syndromic anophthalmia/microphthalmia. Hum. Genet., 138, 799–830.

3. Wu, X., Long, E., Lin, H. and Liu, Y. (2016) Prevalence and epidemiological characteristics of congenital cataract: a systematic review and meta-analysis. Sci. Rep., 6, 28564.

4. Ceroni, F., Aguilera-Garcia, D., Chassaing, N., Bax, D.A., Blanco-Kelly, F., Ramos, P., Tarilonte, M., Villaverde, C., da Silva, L.R.J., Ballesta-Martinez, M.J. et al. (2019) New GJA8 variants and phenotypes highlight its critical role in a broad spectrum of eye anomalies. Hum. Genet., 138, 1027–1042.

5. Patel, N., Khan, A.O., Alsahli, S., Abdel-Salam, G., Nowilaty, S.R., Mansour, A.M., Nabil, A., Al-Owain, M., Sogati, S., Salih, M.A. et al. (2018) Genetic investigation of 93 families with microphthalmia or posterior microphthalmos. Clin. Genet., 93, 1210–1222.

6. Guroff, G. (1964) A neutral, calcium-activated proteinase from the soluble fraction of rat brain. J. Biol. Chem., 239, 149–155.

7. Hastings, M.H., Qiu, A., Zha, C., Farah, C.A., Mahdid, Y., Ferguson, L. and Sossin, W.S. (2018) The zinc fingers of the small optic lobes calpain bind polyubiquitin. J. Neurochem., 146, 429–445.

8. Zhao, S., Liang, Z., Demko, V., Wilson, R., Johansen, W., Olsen, O.A. and Shalchian-Tabrizi, K. (2012) Massive expansion of the calpain gene family in unicellular eukaryotes. BMC Evol. Biol., 12, 193.

9. Hastings, M.H., Gong, K., Freibauer, A., Courchesne, C., Fan, X. and Sossin, W.S. (2017) Novel calpain families and novel mechanisms for calpain regulation in Aplysia. PLoS One, 12, e0186646.

10. Arthur, J.S. and Elce, J.S. (2000) Fluorescence measurements of Ca2+ binding to domain VI of calpain. Methods Mol. Biol., 144, 121–127.

11. Dutt, P., Croall, D.E., Arthur, J.S., Veyra, T.D., Williams, K., Elce, J.S. and Greer, P.A. (2006) m-Calpain is required for preimplantation embryonic development in mice. BMC Dev. Biol., 6, 3.

12. Hodgkin, J.A. and Brenner, S. (1977) Mutations causing transformation of sexual phenotype in the nematode Caenorhabditis elegans. Genetics, 86, 275–287.

13. Sokol, S.B. and Kuwabara, P.E. (2000) Proteolysis in Caenorhabditis elegans sex determination: cleavage of TRA-2A by TRA-3. Genes Dev., 14, 901–906.

14. Wang, S. and Kimble, J. (2001) The TRA-1 transcription factor binds TRA-2 to regulate sexual fates in Caenorhabditis elegans. EMBO J., 20, 1363–1372.

15. Kammenga, J.E., Doroszuk, A., Riksen, J.A., Hazendonk, E., Spiridon, L., Petrescu, A.J., Tijsterman, M., Plasterk, R.H. and Bakker, J. (2007) A Caenorhabditis elegans wild type defies the temperature-size rule owing to a single nucleotide polymorphism in tra-3. PLoS Genet., 3, e34.

16. Velez, G., Bassuk, A.G., Schaefer, K.A., Brooks, B., Gakhar, L., Mahajan, M., Kahn, P., Tsang, S.H., Ferguson, P.J. and Mahajan, V.B. (2018) A novel de novo CAPN5 mutation in a patient with inflammatory vitreoretinopathy, hearing loss, and developmental delay. Cold Spring Harb Mol. Case Stud., 4, a002519.

17. Kamei, M., Webb, G.C., Young, I.G. and Campbell, H.D. (1998) SOLH, a human homologue of the Drosophila melanogaster small optic lobes gene is a member of the calpain and zinc-finger gene families and maps to human chromosome 16p13.3 near CATM (cataract with microphthalmia). Genomics, 51, 197–206.

18. Yokoyama, Y., Narahara, K., Tsuji, K., Ninomiya, S. and Seino, Y. (1992) Autosomal dominant congenital cataract and microphthalmia associated with a familial t(2;16) translocation. Hum. Genet., 90, 177–178.

19. Delaney, S.J., Hayward, D.C., Barleben, F., Fischbach, K.F. and Miklos, G.L. (1991) Molecular cloning and analysis of small optic lobes, a structural brain gene of Drosophila melanogaster. Proc. Natl. Acad. Sci. USA., 88, 7214–7218.

20. Fischbach, K.F. and Heisenberg, M. (1981) Structural brain mutant of Drosophila melanogaster with reduced cell number in the medulla cortex and with normal optomotor yaw response. Proc. Natl. Acad. Sci. USA., 78, 1105–1109.

21. Hu, J., Adler, K., Farah, C.A., Hastings, M.H., Sossin, W.S. and Schacher, S. (2017) Cell-specific PKM isoforms contribute to the maintenance of different forms of persistent long-term synaptic plasticity. J. Neurosci., 37, 2746–2763.

22. Hu, J., Ferguson, L., Adler, K., Farah, C.A., Hastings, M.H., Sossin, W.S. and Schacher, S. (2017) Selective erasure of distinct forms of Long-term synaptic plasticity underlying different forms of memory in the same postsynaptic neuron. Curr. Biol., 27, 1888–1899 e1884.

23. Lek, M., Karczewski, K.J., Minikel, E.V., Samocha, K.E., Banks, E., Fennell, T., O'Donnell-Luria, A.H., Ware, J.S., Hill, A.J., Cummings, B.B. et al. (2016) Analysis of protein-coding genetic variation in 60,706 humans. Nature, 536, 285–291.

24. Thuriot, F., Buote, C., Gravel, E., Chenier, S., Desilets, V., Maranda, B., Waters, P.J., Jacques, P.E. and Levesque, S. (2018) Clinical validity of phenotype-driven analysis software PhenoVar as a diagnostic aid for clinical geneticists in the interpretation of whole-exome sequencing data. Genet. Med., 20, 942–949.

25. Ng, P.C. and Henikoff, S. (2003) SIFT: predicting amino acid changes that affect protein function. Nucleic Acids Res., 31, 3812–3814.

26. Adzhubei, I.A., Schmidt, S., Peshkin, L., Ramensky, V.E., Gerasimova, A., Bork, P., Kondrashov, A.S. and Sunyaev, S.R. (2010) A method and server for predicting damaging missense mutations. Nat. Methods, 7, 248–249.

27. Roy, A., Kucukural, A. and Zhang, Y. (2010) I-TASSER: a unified platform for automated protein structure and function prediction. Nat. Protoc., 5, 725–738.

28. Yang, J., Yan, R., Roy, A., Xu, D., Poisson, J. and Zhang, Y. (2015) The I-TASSER suite: protein structure and function prediction. Nat. Methods, 12, 7–8.

29. Yang, J. and Zhang, Y. (2015) I-TASSER server: new development for protein structure and function predictions. Nucleic Acids Res., 43, W174–W181.

30. Needleman, S.B. and Wunsch, C.D. (1970) A general method applicable to the search for similarities in the amino acid sequence of two proteins. J. Mol. Biol., 48, 443–453.

31. Brown, S.D. and Moore, M.W. (2012) The international mouse phenotyping consortium: past and future perspectives on mouse phenotyping. Mamm. Genome, 23, 632–640.

32. Farah, C.A., Hastings, M.H., Dunn, T.W., Gong, K., Baker-Andresen, D. and Sossin, W.S. (2017) A PKM generated by calpain cleavage of a classical PKC is required for activity-dependent intermediate-term facilitation in the presynaptic sensory neuron of Aplysia. Learn. Mem., 24, 1–13.

33. Ono, Y. and Sorimachi, H. (2012) Calpains: an elaborate proteolytic system. Biochim. Biophys. Acta, 1824, 224–236.

34. Bean, L.J.H., Funke, B., Carlston, C.M., Gannon, J.L., Kantarci, S., Krock, B.L., Zhang, S., Bayrak-Toydemir, P. and on behalf of the, A.L.Q.A.C (2020) Diagnostic gene sequencing panels: from design to report-a technical standard of the American College of Medical Genetics and Genomics (ACMG). Genet. Med., 22, 453–461.

35. Strande, N.T., Riggs, E.R., Buchanan, A.H., Ceyhan-Birsoy, O., DiStefano, M., Dwight, S.S., Goldstein, J., Ghosh, R., Seifert, B.A., Sneddon, T.P. et al. (2017) Evaluating the clinical validity of gene-disease associations: an evidence-based framework developed by the clinical genome resource. Am. J. Hum. Genet., 100, 895–906.

36. Sossin, W.S. (2003) Phosphopeptide-specific antibodies to protein kinase C. Methods Mol. Biol., 233, 233–244.

37. Skarnes, W.C., Rosen, B., West, A.P., Koutsourakis, M., Bushell, W., Iyer, V., Mujica, A.O., Thomas, M., Harrow, J., Cox, T. et al. (2011) A conditional knockout resource for the genome-wide study of mouse gene function. Nature, 474, 337–342.

38. Holt, R.J., Young, R.M., Crespo, B., Ceroni, F., Curry, C.J., Bellacchio, E., Bax, D.A., Ciolfi, A., Simon, M., Fagerberg, C.R. et al. (2019) De novo missense variants in FBXW11

cause diverse developmental phenotypes including brain, eye, and digit anomalies. Am. J. Hum. Genet., 105, 640–657.

39. Ragge, N., Isidor, B., Bitoun, P., Odent, S., Giurgea, I., Cogne, B., Deb, W., Vincent, M., Le Gall, J., Morton, J. et al. (2019) Expanding the phenotype of the X-linked BCOR microphthalmia syndromes. Hum. Genet., 138, 1051–1069.

40. Saudi Mendeliome, G. (2015) Comprehensive gene panels provide advantages over clinical exome sequencing for Mendelian diseases. Genome Biol., 16, 134.

Chapter 3 - MRI of Capn15 Knockout Mice and Analysis of Capn 15 Distribution Reveal Possible Roles in Brain Development and Plasticity

3.1 Preface

Loss of SOL calpain leads to developmental deficits in *Drosophila* optic lobe (Fischbach & Heisenberg, 1981). However, what it does in vertebrates is unknown. In chapter 2, we generated *Capn15* KO mice and found clear evidence that CAPN15 is important to development: CAPN15 expression is the highest during early development; *Capn15* KO mice have low mendelion ratio, reduced weight, and striking eye anomalies. Moreover, abnormalities in eye development in *Capn15* KO mice are also confirmed in humans with *CAPN15* variants, further demonstrating the importance of CAPN15 in early development.

Other than eye anomalies, patients with *CAPN15* variants also showed various neurological symptoms, such as microcephaly, cognitive delay, and ASD, suggesting deficits during neurodevelopment as well. In this chapter, we looked at how CAPN15 affects brain development using magnetic resonance imaging (MRI). Given that SOL calpain is also implicated in learning and memory, we also investigated CAPN15 expression in adult animals.

3.2 Abstract

The Small Optic Lobe (SOL) family of calpains are intracellular cysteine proteases that are expressed in the nervous system and play an important role in neuronal development in both *Drosophila*, where loss of this calpain leads to the eponymous small optic lobes, and in mouse and human, where loss of this calpain leads to eye anomalies. Some human individuals with biallelic variants in CAPN15 also have developmental delay and autism. However, neither the specific effect of the loss of the Capn15 protein on brain development nor the brain regions where this calpain is expressed in the adult is known. Here we show using small animal MRI that mice with the complete loss of Capn15 have smaller brains overall with larger decreases in the thalamus and subregions of the hippocampus. These losses are not seen in *Capn15* conditional knockout (KO) mice where Capn15 is knocked out only in excitatory neurons in the adult. Based on β-galactosidase expression in an insert strain where lacZ is expressed under the control of the *Capn15* promoter, we show that Capn15 is expressed in adult mice, particularly in neurons involved in plasticity such as the hippocampus, lateral amygdala and Purkinje neurons, and partially in other non-characterized cell types. The regions of the brain in the adult where Capn15 is expressed do not correspond well to the regions of the brain most affected by the complete knockout suggesting distinct roles of Capn15 in brain development and adult brain function.

3.3 Introduction

Calpains are intracellular cysteine proteases that were first discovered in rat brain (Guroff, 1964). There are four conserved families of calpains: Classical, PalB (phosphatase mutants: loss in activity at alkaline pH, but normal or increased activity at acidic pH),

Transformer (Tra), and Small Optic Lobe (SOL) with the classical being the best characterized family. All calpain isoforms have a conserved catalytic domain and each calpain family has unique domains. Of interest to the present study, SOL calpains (Capn15 in vertebrates) have an N-terminal zinc finger domain that binds polyubiquitin (Hastings et al., 2018) and a C-terminal SOL homology domain (Zhao et al., 2012, Hastings et al., 2017). The most ancient family of calpains is PalB which is expressed in Fungi, followed by SOL which is expressed in the earliest metazoans, while Tra and classical calpains diverged from PalB in early pre-bilaterians (Hastings et al., 2017). Thus, of the four families of calpains present throughout animals, SOL is the most diverged (Hastings et al., 2017).

Calpains play diverse roles in cellular physiology (Bertipaglia and Carafoli, 2007, Ono and Sorimachi, 2012). In the nervous system, degradation of repressors of plasticity by classical calpain, Capn1, in the hippocampus is important for the induction of synaptic plasticity associated with memory (Shimizu et al., 2007, Khoutorsky et al., 2013, Briz and Baudry, 2017). Another distinct classical calpain, Capn2, plays an opposite role in limiting plasticity (Wang et al., 2014, Liu et al., 2016). Furthermore, *Capn2* deletion from birth results in embryonic lethality (Dutt et al., 2006) demonstrating multiple distinct roles for this specific calpain isoform in development and in the adult. However, while the role of the classical calpains has been well characterized, the role of the other calpain family members in vertebrates is less clear.

SOL calpain was first identified in the fruit fly *Drosophila* (Fischbach and Heisenberg, 1981, Delaney et al., 1991) where loss of the SOL calpain lead to a 50% reduction in the volume of *Drosophila* optic lobes (Fischbach and Heisenberg, 1981). In *Aplysia*, expression of a dominant negative catalytically inactive SOL calpain specifically prevented a form of non-

associative long-term facilitation (Hu et al., 2017a). However, how SOL calpain is activated and the identity of its substrates remains unknown (Hastings et al., 2018).

We have recently generated *Capn15* knockout (KO) mice and showed that loss of *Capn15* leads to a lower Mendelian ratio, a smaller weight of weaned *Capn15* KO mice and developmental eye anomalies (Zha et al., 2020). Human individuals with biallelic variants in CAPN15 also have developmental eye anomalies (Zha et al., 2020), and a subset of these individuals have developmental delays and autism. However, how loss of Capn15 affects brain development and where Capn15 is expressed in the adult are not known.

In the present study, using 7 T pre-clinical MR imaging, we reveal a decrease in whole brain volume of adult *Capn15* KO mice, as well as in specific regions, such as the thalamus and certain hippocampal subregions. We generate a *Capn15* conditional KO mouse (cKO) in which Capn15 is only removed from a subset of excitatory neurons in the forebrain after early brain development. Unlike *Capn15* KO mice, *Capn15* cKO mice have normal brain volumes as determined using 7 T MR imaging, as well as normal weight and lack eye anomalies. We also characterize the distribution of Capn15 in the brain of adult *Capn15* KO mice and show that Capn15 is expressed in adult hippocampal CA1 and CA3 neurons and in Purkinje cells in the cerebellum, neurons particularly implicated in synaptic plasticity.

3.4 Materials and methods

3.4.1 Generation of the *Capn15* conditional KO mouse

The generation of the *Capn15*$^{(lacZ\text{-}Neo)}$ mouse, the FLOXed *Capn15* mouse and the complete *Capn15* KO mouse has been described (Zha et al., 2020). To generate a conditional KO

line (cKO), the mice were bred with the CaMKIIα-Cre-CRE T29-1 (Tsien et al., 1996) that should only delete exons of *Capn15* after development in forebrain excitatory neurons. The initial breeding was flox/flox × CaMKIIα-CRE T29-1/WT flox/WT. Only a small number of cKO mice were generated from this cross due to the apparent presence of CRE and *Capn15* on the same chromosome (*Capn15* is on chromosome 17 in mouse, the location of the CRE T29-1 has not been described). These cKO mice were used in subsequential breeding as they had presumably recombined the CRE and the floxed *Capn15* allele on the same chromosome. Specifically, we generated cKO mice by breeding cKO mice flox/flox CaMKIIα-Cre-CRE T29-1/WT with flox/flox mice. The CRE- littermates were used as controls.

3.4.2 Dissections

Adult mice (3–6 months) were transcardially perfused with ice-cold phosphate-buffered saline (PBS) followed by 4% (wt/vol) ice-cold paraformaldehyde (PFA) in PBS. Brains were post-fixed in 4%PFA for 45 min at 4 °C, rinsed in PBS, and cryoprotected in 30% sucrose/PBS overnight at 4 °C. The following day, brains were embedded in Tissue-Plus™ O.C.T. compound (Fisher Healthcare) and flash frozen in 2-methylbutane chilled in dry ice. The brains were kept at −80 °C until further use. For amygdala dissection, mouse brains were removed and frozen on dry ice and kept at −80 °C until further use. The amygdala was dissected from each frozen brain in the cryostat using a neuro punch (0.5 mm; Fine Science Tools). For MRI analysis, adult mice were transcardially perfused with ice-cold PBS followed by 4% (wt/vol) ice-cold PFA in PBS. Brains were then post-fixed in 4% PFA overnight at 4 °C, rinsed in 1XPBS, and stored in 1× PBS + 0.05% sodium azide. For brain weight measurement, olfactory bulbs and brain stem were removed before weighing the brains.

3.4.3 X-gal staining

Sections of 20 μm were incubated overnight at 37 °C in solution containing 80 mM Na_2HPO_4, 20 mM NaH_2PO_4, 2 mM $MgSO_4$, 5 mM $K_3[Fe(CN)_6]$, 5 mM $K_4[Fe(CN)_6]$, 0.2% NP-40, 0.1% sodium deoxycholate, and 1.5 mg/ml X-gal. Sections were rinsed in PBS, washed in ethanol (50% for 1 min, 70% for 1 min, 95% for 1 min and 100% for 2X1min), cleared in xylene, and mounted with Permount (Fisher Scientific). 9 adult *Capn15*$^{(lacZ\text{-}Neo)}$ mice (4M and 5F) and 2 WT mice were used for X-Gal staining and results were similar for all mice examined.

3.4.4 Immunohistochemistry

Adult mouse brains were fixed with 2% PLP solution (PBS containing 2% PFA, 10 mM sodium periodate, and 70 mM l-lysine) for 3 h at 4 °C and P3 mouse brains were fixed with 2% PLP solution for 1 h at 4 °C. Brains were cryoprotected in 30% (wt/vol) sucrose in PBS and embedded in OCT (Fisher Healthcare). Brains were frozen on dry ice and cryosectioned (14-μm-thick coronal sections). Sections were first incubated in blocking solution containing 5% (vol/vol) goat serum (or donkey serum for goat antibodies), 0.1% (vol/vol) Triton-X, and 0.5 mg/ml BSA in PBS for 1.5 h. Brain sections and eye sections were incubated with primary antibodies in the blocking solution overnight at 4 °C. After rinsing five times with the blocking solution for 5 min, sections were incubated with secondary antibodies in the blocking solution for 1 h at room temperature. DNA was labeled with Hoechst (1:2000) for 3 min and the sections were mounted using fluorescence mounting media (Dako, S3023). All images were taken using a Zeiss Observer Z1 fluorescent microscope using a 10× objective. For the primary antibody, we used chicken polyclonal antibody directed against β-galactosidase (β-gal; abcam, dilution

1:1000), rabbit polyclonal antibody directed against Purkinje cell protein 4 (PCP4; Sigma, dilution 1:400), rabbit polyclonal antibody raised to Capn15 (Zha et al., 2020), goat polyclonal antibody directed against Brn3a (Santa Cruz, dilution 1:500), goat polyclonal antibody directed against ChAT (Millipore Sigma, dilution 1:100), rabbit polyclonal antibody directed against GFAP (Abcam, dilution 1:500), rabbit polyclonal antibody directed against Iba-1 (FUJIFILM Wako, dilution 1:500) and mouse monoclonal antibody directed against GAD67 (Millipore Sigma, dilution 1:500). For the secondary antibody, we used goat anti-chicken secondary antibody conjugated to Alexa Fluor 488, goat anti-chicken secondary antibody conjugated to Alexa Fluor 594, donkey anti-goat IgG secondary antibody conjugated to Alexa Fluor 488, goat anti-rabbit IgG secondary antibody conjugated to Alexa Fluor 488, goat anti-rabbit IgG secondary antibody conjugated to Alexa Fluor 568 and goat anti-mouse IgG secondary antibody conjugated to Alexa Fluor 568 (Invitrogen, dilution 1:500). Overall, experiments were performed on 9 *Capn15*$^{(lacZ\text{-}Neo)}$ brains and 2 WT brains. All staining were repeated from at least three separate *Capn15*$^{(lacZ\text{-}Neo)}$ mice with the exception of Iba-I staining from two separate animals and GFAP staining which used only one animal.

3.4.5 Quantification of cell number

Neurons in the CA1 area of the hippocampus were counted manually in 2–7 Nissl-stained sections from 3 WT and 3 *Capn15* KO mice that were previously used for MRI imaging. The hand free tool was used to draw an area in the CA1 region of the hippocampus, and the number of neurons was quantitated per mm^2 for each section and then averaged for each mouse by an observer blind to the genotype of the animal. The number of cells in PCP4-labeled cerebellar sections were counted manually in 8–10 Nissl sections through the cerebellum. Density was

calculated as the number of cells per 100 µM as Purkinje cells are mainly contained in a single row of cells. The density of cells was calculated for WT and *Capn15* KO animals by an observer blind to the genetic status of the animal.

3.4.6 Western blotting

Brains were homogenized manually in lysis buffer containing 25 mM Tris-HCl (pH 7.4), 150 mM NaCl, 6 mM $MgCl_2$, 2 mM EDTA, 1.25% NP-40, 0.125% SDS, 25 mM NaF, 2 mM $Na_4P_2O_7$, 1 mM dithiothreitol (DTT), 1 mM phenylmethylsulfonyl fluoride (PMSF), 20 mg/ml leupeptin, and 4 mg/ml aprotinin. Before loading, 5× sample buffer was added to the lysate and samples were incubated at 95 °C for 5 min. Proteins were resolved by SDS–PAGE on Bis-Tris gel and transferred to nitrocellulose membrane (Bio-Rad). The blots were blocked in TBST (TBS + 0.1% Tween) containing 4% skim milk for 30 min at room temperature and then incubated with primary antibodies overnight at 4 °C. After washing three times with TBST, the blots were incubated with HRP-conjugated secondary antibodies for 1 h at RT and washed again 3 times in TBST. The Western Lightning Plus-ECL kit (NEL103001EA; PerkinElmer LLC Waltham, MA USA) was used as per manufacturer's instructions to detect protein bands. The primary antibody used was a homemade rabbit anti-Capn15 antibody (1:1000) raised against the C-terminus of Capn15 (Zha et al., 2020). The secondary antibody was horseradish peroxidase-conjugated goat anti-rabbit secondary antibody (1:5000). Antibodies were diluted in Tris buffered saline with Tween containing 4% skim milk powder.

3.4.7 Eye phenotype quantification

Mice eyes were examined and grouped as follows: seems normal, obvious cataract, small eye and no eye. This categorization was performed for both eyes of each mouse. The analysis was performed without the knowledge of the genotype of the mice.

3.4.8 Quantification of immunoblotting

Immunoblots were scanned and imaged using the public domain Image J program developed at the U.S. National Institute of Health (https://imagej.nih.gov/ij/). We calibrated our data with the uncalibrated optical density feature of NIH image, which transforms the data using the formula $\log_{10} \frac{225}{225-x}$, where *x* is the pixel value (0–254). We find that with this correction and including the entire band (which expands near saturation), values are linear with respect to amount of protein over a wide range of values (Nakhost et al., 1998). We used the Ponceau image for each gel to normalize the amount of SOL calpain to total protein loaded.

3.4.9 Image acquisition

Magnetic resonance imaging was performed using the 7 T Bruker Pharmascan (Bruker Biosciences, Billerica, MA) ultra-high field MRI system of the McConnell Brain Imaging Centre. For imaging, brains were housed in a cylindrical container and immersed in an MR-invisible fluorinated solution, FC-40 (Sigma Aldrich, St. Louis, Missouri), to remove the background MRI signal. For MRI radiofrequency excitation and reception, a 2.3 cm inner diameter volume resonator was utilized. The imaging protocol included a sagittal orientation, 3D steady-state free precession MRI sequence with an echo time (TE) of 5 milliseconds, repetition

time (TR) of 10 milliseconds, receiver bandwidth of 50 kHz and excitation pulse flip angle of 30 degrees. The image acquisition matrix was selected to achieve an isotropic voxel resolution of 100 μm^3. The specific sagittal orientation imaging field of view was $2.3 \times 1.7 \times 1.7$ cm^3. Thirty-one signal averages were collected to improve image signal-to-noise ratio, leading to a total scan time of approximately six hours and 60 s for the full MRI histology scan. For image reconstruction, a trapezoidal filter was applied to the complex image data along the first phase encode direction to reduce subtle effects of Gibbs ringing.

3.4.10 Image processing and statistical analysis

We employed an image registration-based method to investigate anatomical brain volume differences between WT, cKO and KO mice. Specifically, an automated, image intensity-based, affine registration using Elastix tool (Klein et al., 2010) was applied to align all mouse brains to a common coordinate system. During this registration step, it was determined that the KO mouse brains were, on average, 14% smaller than the WT mouse brains. For this reason, scans of all animals were linearly scaled to match the average size of the population. To avoid registration bias caused by differences between our studied population and the mouse template (Kovačević et al., 2005), a population-specific average was constructed using an algorithm described in Fonov et al. (Fonov et al., 2011). This step yielded an average image of all the samples included in our cohort. A mouse brain atlas (Kovačević et al., 2005) containing reference regions of interest (ROIs) for the thalamus, amygdala, parieto-temporal cortex and whole hippocampus was next used to provide suitable ROIs for volumetric measurement. More specifically, a non-linear registration (ANTs (Avants et al., 2008)) between the atlas space (Kovačević et al., 2005) and our population average was conducted to create an anatomical atlas specific to our mouse

population. The deformation fields from the non-linear registration were inverted. The Jacobian determinants of the inverted deformation fields were then calculated to yield estimates of local expansion or contraction at both the ROI and voxel level relative to the population average. We smoothed the Jacobian determinant fields using a Gaussian smoothing kernel with a full width half maximum (FHWM) of 0.2 mm. The choice of the FWHM was based on both image signal-to-noise ratio and the size of the smallest features of interest in the image. We decided to use a FWHM of 0.2 mm as a tradeoff between localization accuracy and noise reduction.

Since we also had a specific interest in volumetric changes in KO mice in the hippocampal sub-fields, a mouse hippocampal sub-field atlas (Badhwar et al., 2013) was non-linearly registered (Avants et al., 2008) and warped to the population average to measure volumes of the Cornu Ammonis 1 (CA1), CA2, CA3, stratum granulosum and dentate gyrus in the mouse brain images.

We next used a linear model in the R software package (Chambers, 1992, Team RC, 2020) to measure the main effect of volume differences (i) in individual ROIs in KO and cKO mice compared to WT mice and (ii) at the voxel-level in KO and cKO mice compared to WT mice. All statistical analyses were corrected for multiple comparisons, utilizing the false discovery rate technique (Genovese et al., 2002) with a 5% threshold. Voxel-based analysis and generation of figures was performed using RMINC package (Lerch et al., 2017). Measurements from the left and right hemisphere were always averaged for volume measurements.

3.5 Results

3.5.1 Generation of a conditional *Capn15* KO mouse

To assess the role of *Capn15* in the adult, we generated *Capn15* conditional KO mice (cKOs) as described in the methods and a CaMKIIα-Cre line was used to this end. CaMKIIα-Cre transgenic mice have the mouse calcium/calmodulin-dependent protein kinase II alpha promoter driving Cre recombinase expression in a subset of excitatory neurons in the forebrain including the hippocampus and the amygdala and CRE is not expressed until after P14 (Sonner et al., 2005). As shown in Fig. 1A–D, Capn15 protein levels are significantly decreased in homogenates from *Capn15* cKO adult mice amygdala (**p = 0.002, Student's t-test; n = 4 cKO, 3 WT) and hippocampus (*p = 0.01, Student's t-test; n = 4 cKO, 4 WT) indicating successful disruption of the *Capn15* gene in cKO mice. Complete *Capn15* KO mice have reduced weight and eye anomalies (Zha et al., 2020). In contrast, *Capn15* cKO mice showed no weight difference compared to WT mice (p = 0.16, Student's t-test; n = 26 for the WT group composed of *Capn15* cKO Cre- littermates and n = 15 for the *Capn15* cKO group; Fig. 1E) and no eye deficits (Fig. 1F, n = 20 *Capn15* cKO, n = 20 WT).

3.5.2 *Capn15 KO* mice have smaller brains

In *Drosophila*, loss of the SOL calpain was mainly reported to cause deficits in the optic lobe (Fischbach and Heisenberg, 1981). However, it is not clear how extensively other brain regions were analyzed. To use a non-biased screen to determine which brain regions are affected by the loss of *Capn15*, we applied whole brain 7 T MRI on 14 WT (9M, 5F), 8 *Capn15* KO (4M, 4F) animals and 5 *Capn15* cKO (5 M). There was no difference in whole brain volume between male and female mice for either the WT (p = 0.97) or the *Capn15* KO groups (p = 0.83).

Accordingly, males and females were grouped together for statistical analysis. There was a highly significant, 14% decrease in whole brain volume in the *Capn15* KO animals (p = 7.32e−87) compared to the WT and cKO animals (Fig. 2A). Measurement of the brain weight of WT and *Capn15* KO animals confirmed that the brains of *Capn15* KO mice were significantly lighter than WT brains, similar to the amount measured by 7 T MRI (0.389 g ± 0.002 for the WT group composed of *Capn15* KO littermates, n = 14; 0.334 g ± 0.002 for the *Capn15* KO group, n = 12; p = 7.28e−14, Student's t-test, SEM).

3.5.3 *Capn15* KO brains have specific decreases in thalamic and hippocampal region volumes

We next examined decrease in volume in specific brain regions in *Capn15* KO, *Capn15* cKO and WT mice after first compensating for the overall decrease in brain size of *Capn15* KO animals (See Methods). The most significant decrease in volume were observed in the hemisphere-averaged thalamic volumes of *Capn15* KO animals compared to the corresponding WT animals (p = 1.28e−5; Fig. 2B, C). There was no difference in thalamic volume between *Capn15* cKO and WT animals (p = 0.35; Fig. 2B, C). Atlas-based region of interest analysis revealed an increase in the amygdala volume of *Capn15* KO mice compared to WT mice (p = 0.003, Fig. 2B, C). However, there was no corresponding difference between *Capn15* cKO and WT mice (p = 0.42). As well, there were no differences in volume of the parieto-temporal cortex between either *Capn15* KO or cKO mice and corresponding WT mice (Fig. 2B, C). We also used voxel-based morphometry to measure local differences in volume between *Capn15* KO and WT mice. This was specifically performed to leverage the high spatial resolution (100 micron isotropic voxels) of the anatomical mouse brain images to carry out an unbiased test of local, voxel-specific volume differences between KO, cKO and WT mice. In essence, unlike ROI-

based analysis where the mean volume difference between genotypes is calculated inside an anatomically defined regions, voxel-based morphometry evaluates volume differences at a very small scale without predefined brain structural boundaries. Twelve representative slices having locally decreased volume of *Capn15* KO brain compared to WT brain (blue colours) and the corresponding locally increased volume (yellow/orange colours) are presented in Fig. 2D. Volume decreases in *Capn15* KO mouse brain are notable (light blue colours) in the hippocampus, superior parietal cortex and thalamus.

Additional attention in our high resolution, MRI-based volumetric analysis was given to the hippocampus due to the possible role of Capn15 in synaptic plasticity (Hu et al., 2017a, Hu et al., 2017b). An image of the hippocampal sub-field atlas we employed for sub-field volumetry is shown in Fig. 3A. We did not observe differences in overall hippocampal volume between either *Capn15* KO or *Capn15* cKO mice and the corresponding WT animals. However, voxel-level differences in hippocampal volume were observed between *Capn15* KO and WT mice when we restricted our linear model statistical analysis to regions inside the hippocampal sub-fields (Fig. 3A, B). In particular, there were voxel decreases in hippocampal volume for mid-line slices of the *Capn15* KO mice brain compared to the WT mice. Examination of the hippocampal sub-fields using region of interest-based analysis identified decreases in the CA1 ($p = 0.001$), the CA2 ($p = 0.002$), the dentate gyrus ($p = 0.05$) and the stratum granulosum ($p = 0.03$) volume of *Capn15* KO mice when compared to WT mice (Fig. 3A, B). Notably, such volumetric differences were not observed in CA3. It is possible that localized significant changes in volume are taking place in sub-regions of the CA3 area but the hippocampal atlas label includes both regions that increase and regions that decrease in volume. Therefore, the box plot does not show statistically significant aggregate volume change in the CA3 label. As well, no differences in

hippocampal sub-field volume were observed between *Capn15* cKO and WT mice. We further performed a voxel-level statistical analysis of contraction/expansion inside the hippocampus to test the hypothesis that within the sub-fields of the mouse hippocampus volume differences exist between KO, cKO and cKO mice. As shown in Fig. 3C, volume decreases in *Capn15* KO mouse brain are notable (light blue colours) in the CA1, CA2, dentate gyrus and stratum granulosum whereas increases (orange) are noted in the CA3 area.

3.5.4 Capn15 is expressed in areas important for brain plasticity in the adult mouse

We have previously described *Capn15* KO mice (Zha et al., 2020) and took advantage of the initial mouse strain with a reporter gene *lacZ* that is under the control of the *Capn15* promoter to characterize distribution of Capn15 in developing brain (the *lacZ* reporter is deleted in the generation of the Floxed Capn15 mouse (Zha et al., 2020)). Capn15 was mainly enriched in the mantle zone in E12 embryos, in the subventricular zone, immediately next to the ventricular zone in E18 embryos and was ubiquitously expressed in the brain in P3 mice (Zha et al., 2020). We also noted that levels of Capn15, measured using immunoblots of whole brains, notably decreased in the adult, but the areas in the brain that retained Capn15 expression were not determined (Zha et al., 2020). To expand on these results, we examined Capn15 distribution in adult *Capn15*$^{(lacZ\text{-}Neo)}$ heterozygous mice using X-gal staining. As shown in Fig. 4, Capn15 is still expressed in specific sets of neurons in the mature brain, including the hippocampus, amygdala, Purkinje neurons, and cortex. A closer look at the hippocampal region shows an unequal distribution of staining. Excitatory pyramidal neurons in CA1 and CA3 and some cells located in stratum radiatum are stained. However, a gap near the expected position of CA2 was seen and in the dentate gyrus, Capn15 is expressed at low levels in the subgranular zone and

showed the strongest signal in the molecular layer. This region contains mainly interneurons such as molecular layer perforant pathway cells (MOPP) (Li et al., 2013) and neurogliaform cells (Armstrong et al., 2011) as well as astrocytes (Pilegaard and Ladefoged, 1996).

To confirm the result obtained with X-gal staining, we stained sections from adult WT and *Capn15* KO mice brains with our home-made antibody to Capn15 (Zha et al., 2020). Unfortunately, this antibody lacked specificity in immunohistochemistry as staining showed no difference between WT and KO animals and thus, could not be used to this end. Thus, we took advantage of the *lacZ* reporter and stained sections from adult *Capn15-lacZ* mice with an anti β-galactosidase (β-gal) antibody as well as an antibody directed against the CA2 marker PCP4 (Lein et al., 2005) to confirm the lack of Capn15 in CA2 seen with X-gal. DNA was labeled with Hoechst. The β-gal immunoreactivity appeared as punctate spots (Fig. 5), perhaps due to aggregation or specific sub-cellular localization of the enzyme in neurons. To confirm β-gal antibody specificity, we co-stained sections from WT mouse brain with the β-gal antibody and Hoechst. As shown in Fig. 5 (top), a weak diffuse signal was observed in WT mice with no punctate spots indicating specificity of the punctate staining in *Capn15-lacZ* mice. Moreover, our result confirmed the absence of Capn15 from the CA2 area (Fig. 5 bottom).

When examining the staining with the β-gal antibody, we noted a striking difference between the punctate spots in the pyramidal neurons and in the molecular layer. This was most obvious comparing staining in CA3 neurons and the molecular layer in the same sections (Fig. 6A). The punctate spots in the molecular layer appeared smaller, more numerous and less associated with nuclei (Fig. 6A). Notably, if the X-gal reaction was ended at earlier time points, the molecular layer staining was less intense (Fig. 6B), suggesting a lower, but broader level of expression in this area that took longer to saturate. The lower expression of Capn15 in the

molecular layer is consistent with the large decrease in overall Capn15 protein observed from immunoblots of adult hippocampal tissue, as the CamKII Cre should not be expressed outside the excitatory neurons in the hippocampus.

We next investigated if β-gal staining in the molecular layer corresponded to astroyctes, microglia, or GABAergic neurons. As shown in Fig. 7, β-gal staining did not colocalize with that of the glial marker GFAP (top) or that of the microglia marker Iba-1 (middle) or with the GABAergic marker GAD67 (bottom). At this point, it is not clear what the basis for this staining is, although it was not seen in WT animals (Fig. 6A), and thus requires lacZ expression from the *Capn15* locus.

There was a poor correlation between the volume loss in the MRI in the CA2 and CA3 areas of the hippocampus in *Capn15* KO mice and Capn15 expression in these areas in adult *Capn15*$^{(lacZ\text{-}Neo)}$ heterozygous mice. The CA2 area showed a significant decrease in volume by MRI but did not express Capn15 in the adult, while the CA3 area was relatively larger, but did express Capn15 in the adult. We began to examine whether the loss of volume was correlated with a loss of Nissl-stained cell bodies in the CA1 region. An initial experiment did not detect a difference (2.6 ± 0.3 thousand cells per mm^2 for the WT group; n = 3 and 2.7 ± 0.3 thousand cells per mm^2 for the *Capn15* KO group; n = 3; SEM, one sample Student's t-test). However, given the large variance (20%) in the counts in the WT group, we performed a power analysis which suggested that 50 animals would be required to have an 80% chance of detecting a 10% change in cell number and this was not feasible. As these were examined from the same animals on which 7 T MRI was performed, we also determined if there was a correlation between CA1 volume (in mm^3) and CA1 neuronal density derived from cell counting, but no correlation was observed (WT, n = 3, KO, n = 3, $p > 0.5$).

Staining in the Purkinje neurons was confirmed by staining sections from adult *Capn15-lacZ* mice with the anti-β-gal antibody as well as an antibody directed against PCP4, which was originally described as a Purkinje cell marker (Ziai et al., 1988). DNA was labeled with Hoechst. As shown in Fig. 8, Capn15 was enriched in Purkinje cells in the cerebellum. As loss of *Capn15* was linked to neurodegeneration in *Drosophila*, we determined whether the loss of *Capn15* led to a loss of Purkinje cell neurons. We did not detect a difference in the number of Purkinje cells in initial experiments examining *Capn15* KO animals and their WT littermates (3.2 ± 0.4 cells/100 μm for the WT group, $n = 5$ compared to 3.2 ± 0.5 cells/100 μm for the KO group, $n = 5$; SEM, $p > 0.5$, Student's *t*-test). Again, given the large variation in the number of cells per animal, power analysis suggested over 50 animals would be required to have an 80% chance of detecting a 10% change and this was not feasible.

As homozygous disruption of *Capn15* leads to abnormal eye development (Zha et al., 2020), we examined Capn15 staining in the eye, although in this case we focused on an earlier stage of development, P3. At this stage, X-gal staining is mainly restricted to the retinal ganglion cell layer (Zha et al., 2020). To confirm expression of Capn15 in retinal ganglion cells, we examined co-localization of β-gal with a marker for retinal ganglion cells, Brn3a (Nadal-Nicolas et al., 2009). As shown in Fig. 9, the two markers co-localized (79 ± 5 of β-gal cells colocalized with Brn3a) but only about half of the retinal ganglion cells contained β-gal (44 ± 2 Brn3a neurons co-localized with β-gal). We also examined co-localization of β-gal with ChAT as a fraction of retinal ganglion cells that do not contain Brn3a are displaced cholinergic amacrine cells (Jeon et al., 1998). Similar to Brn3a staining, about half of the ChAT labelled neurons co-localized with β-gal (62 ± 5). Thus, Capn15 is expressed mainly in the retinal ganglion cell layer in a subset of Brn3a+ and ChAT+ cells.

3.6 Discussion

We have previously described *Capn15* KO mice and found that they had a lower body weight and striking ocular anomalies when compared to their WT littermates (Zha et al., 2020). In this paper, we further characterize these mice using MR imaging and localization of Capn15 expression in the adult. The loss of Capn15 protein leads to smaller brains and specific changes in the thalamus, amygdala and hippocampal subfields. Capn15 is expressed in a variety of brain regions in the adult including excitatory neurons linked to plasticity changes involved in learning and memory.

The average weight of a whole *Capn15* KO mouse was 11% smaller compared to its WT littermate (Zha et al., 2020). MRI results showed that the *Capn15* KO brain was 14% smaller in volume compared to the WT animals and the weight of the brain was similarly reduced. One human individual with a biallelic variant CAPN15 had clinical microencephaly (Zha et al., 2020) as did a patient with a likely loss of function of CAPN15 (Mor-Shaked et al., 2021), consistent with the mouse recapitulating a loss of brain volume also seen in humans. The total change in brain volume was similar to the 11% weight loss, although there is no correlation between body and brain weight in mice (Spring et al., 2007). The brain makes up only a small fraction of the weight of the mouse, so the decrease in brain volume cannot explain the overall weight difference. The loss of whole animal weight and brain volume are likely to be two independent aspects of the *Capn15* KO phenotype.

Certain brain areas such as subfields of the hippocampus and thalamus were still significantly smaller in the *Capn15* KO mice, even when taking the 14% global brain volume

change into account. On the other hand, the amygdala was significantly larger in *Capn15* KO mice after scaling. This indicates that either this region is relatively spared or that amygdala volume increases in the KO mouse. It should be noted that only viable *Capn15* KOs were examined and, based on Mendelian ratios, only 50% of *Capn15* KO animals survive to weaning. Thus, it is possible that the mice that did not survive to weaning had more severe decreases in brain structure volume.

We were not able to associate decreases in brain volume with a decreased neuronal number (using Nissl staining) in Purkinje neurons or CA1 neurons, although we did not have the power to detect changes in cell number in the same range as the decrease in brain volume. Brain volume derived from MRI measurement can also be due to many factors other than cell number. In particular, neuronal cell size, astrocyte size and number, as well as synaptic and axonal density and axonal volume fraction can mediate volume changes (Lerch et al., 2011). It will be interesting in the future to determine more precisely the cause of the overall volume change in these mice.

There does not appear to be a relationship between where Capn15 is expressed in the mature brain and the regions mostly affected by Capn15 loss during development. Thus, our results are consistent with an important role for Capn15 early in brain development that leads to lasting deficits in brain volume in the adult, as opposed to an ongoing requirement for Capn15 for survival. The continued expression of Capn15 in brain areas involved in plasticity is consistent with a possible later role in plasticity, as has been seen in *Aplysia* (Hu et al., 2017a). This may be similar to Capn2 that plays an important role in early development and a later role in plasticity in the adult (Dutt et al., 2006, Liu et al., 2016).

A major unresolved issue is the localization of Capn15 in the dentate gyrus molecular layer. This diffuse staining was not seen in other brain regions, such as the cortex or amygdala. The immunostaining showed much smaller puncta with the antibody to β-gal and the X-gal staining took much longer to saturate, suggesting lower expression in this region. However, the staining did not seem to colocalize with astrocytes, microglia, inhibitory neurons or Hoechst nuclear staining. We do not know the source of this staining.

Removal of *Capn15* in mice results in smaller brains with larger changes in the thalamus and sub-regions of the hippocampus, although the reasons underlying the change in the size of the brain are still unresolved. In the adult mice, Capn15 expression remains in a subset of excitatory neurons, particularly neurons implicated in plastic changes. The *Capn15* cKO mouse should be a good model for exploring the role of Capn15 in plasticity since its brain is of normal size and lacks the eye anomalies present in the complete KO mouse.

3.7 Acknowledgement

This work was supported by CIHR grant MOP 340328 to WSS. The authors would like to thank Mireille Bouchard-Levasseur for excellent technical assistance in quantification of the transgenic mice eye phenotype and Dr. Len Levine for advice concerning the eye phenotype.

Conflict of Interest

The authors state that they have no conflicts of interest.

3.8 Figures and legends

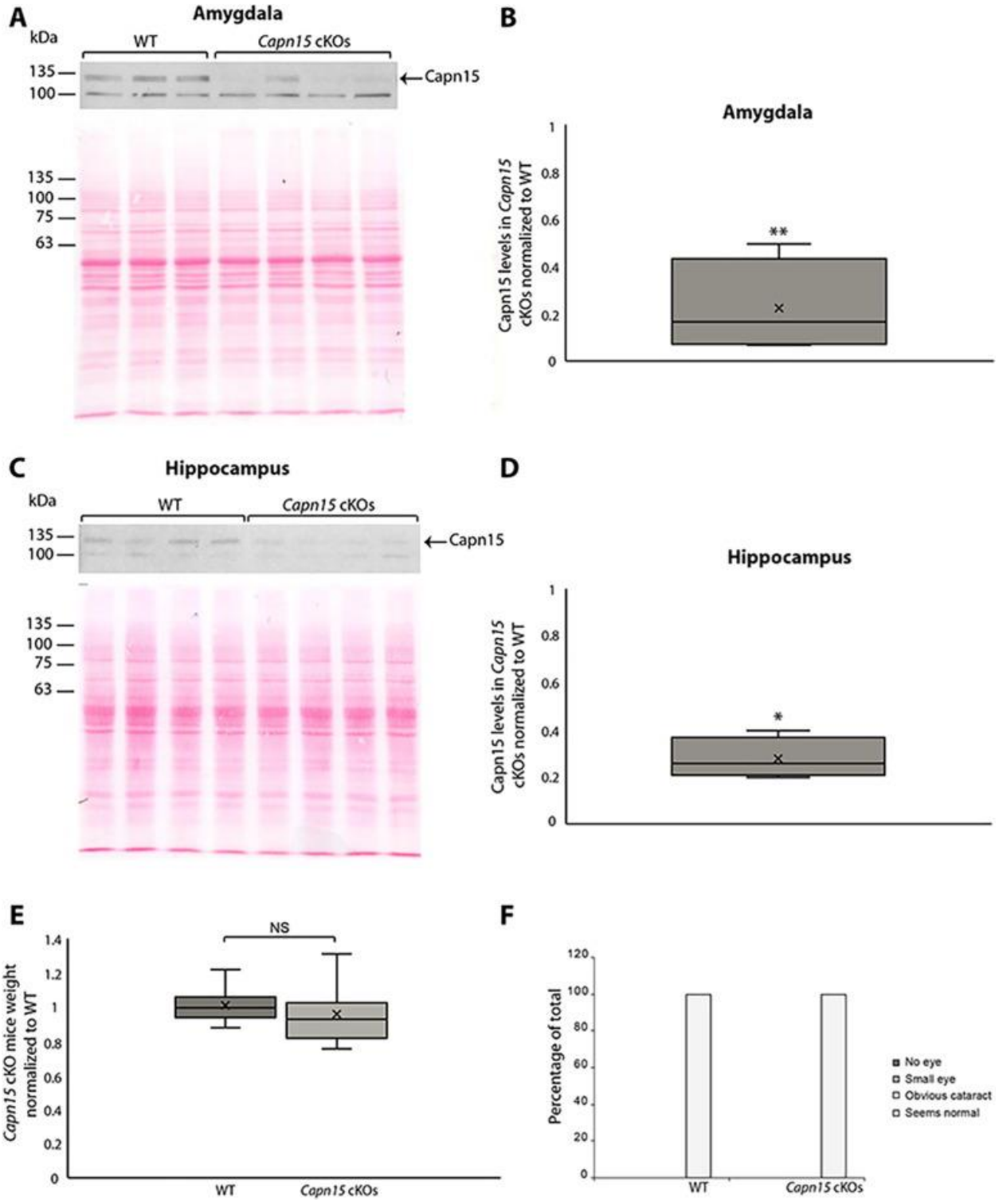

Figure 3.1. *Capn15* cKO mice have reduced Capn 15 levels, but normal weight and eyes. Amygdala **(A)** and hippocampus **(C)** were dissected and homogenized and SDS–PAGE and western blotting were performed as described in Methods. **(B)** Box and whisker plot showing that Capn15 protein levels are significantly decreased in *Capn15* cKO adult mice amygdala, **(D)** Box and whisker plot showing that Capn15 protein levels are significantly decreased in *Capn15* cKO adult mice hippocampus. **(E)** Animals were weighed after weaning. Average weight of *Capn15* cKO was normalized to average weight of the WT mice. **(F)** The percentage of mice having eye deficits between WT and *Capn15* cKO mice. Mice were grouped in 4 categories: Seems normal, obvious cataract, small eye and no eye and this scoring was performed on both left and right eye for each mouse. All of WT and *Capn15* cKO mice eyes scored normal.

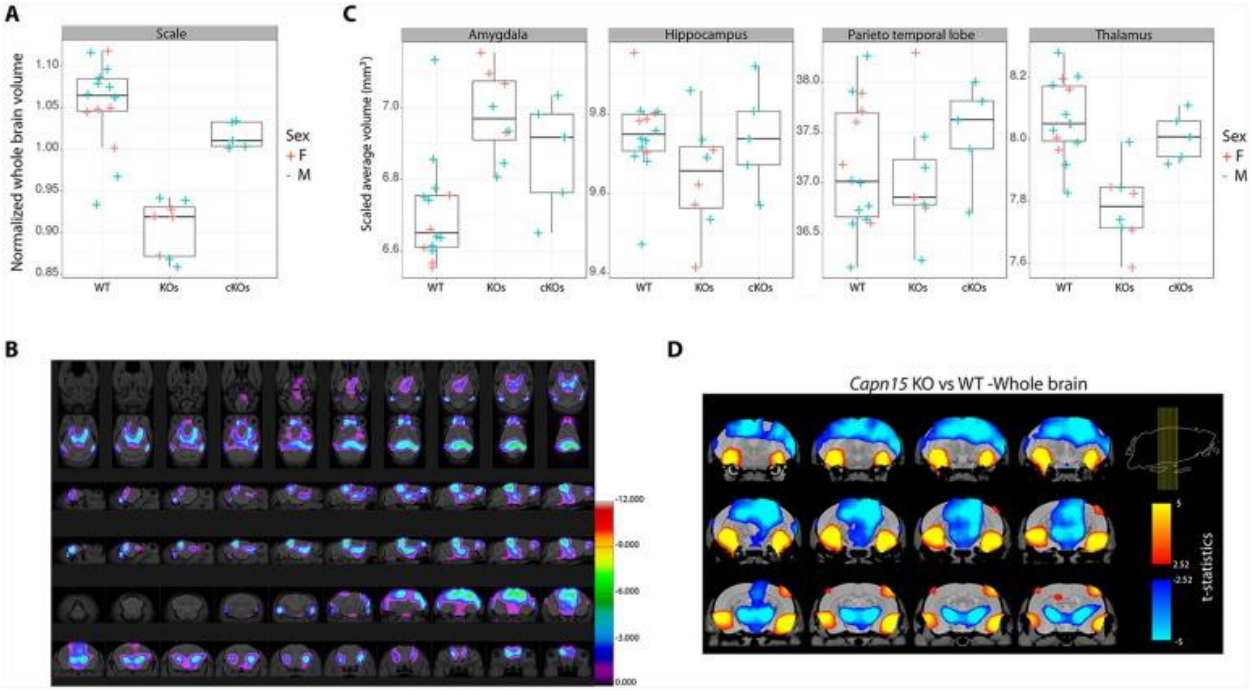

Figure 3.2. Whole-brain visualization of significant decreases in brain structure volume in *Capn15* KO mice relative to cKO and WT mice. **(A)** Box and whisker plots showing scaling factor (see Methods, Fonov et al, 2011) used for each animal to compensate for differences in overall brain size. This scaling factor was applied to all structures shown in Fig. 2, Fig. 3. **(B)**. The top two rows correspond to 20 axial sections through the mouse brain, the middle two rows correspond to 20 sagittal sections through the brain and the bottom two rows correspond to 20 coronal sections. Each section has a thickness of 100 micrometers. Purple/blue/green colour maps overlaid on the mouse brain images identify $\log_{10}(p)$ values at the voxel-level. The colour maps specifically show regions where a significant brain volume decrease was observed for KO mice relative to WT mice. All the $\log_{10}(p)$ values were calculated with a general linear model. Multiple comparisons correction was carried out using the false discovery rate method with a *q*-threshold of 0.05. **(C)** Structure-specific brain volume differences among WT, KO and cKO

mice Box and whisker plots showing volume differences of different brain regions among WT, KO and cKO mice. All anatomical regions in each brain were scaled based on scaling factor shown in **(A)**) to compensate for the overall brain size differences (See methods) **(D)** Magnified coronal views through the mouse mid-brain displaying regional volume decrease (blue colours) and increase (orange) for KO mice compared to WT mice. Each slice through the mid-brain has a thickness of 100 micrometers. The specific position of each slice along the anterior-posterior axis of the mouse brain is shown, overlaid on a sagittal brain slice, in the top right-hand corner of the figure. The colours represent *t*-statistical values calculated with a general linear model. Multiple comparisons correction was carried out using the false discovery rate method with a *q*-threshold of 0.05.

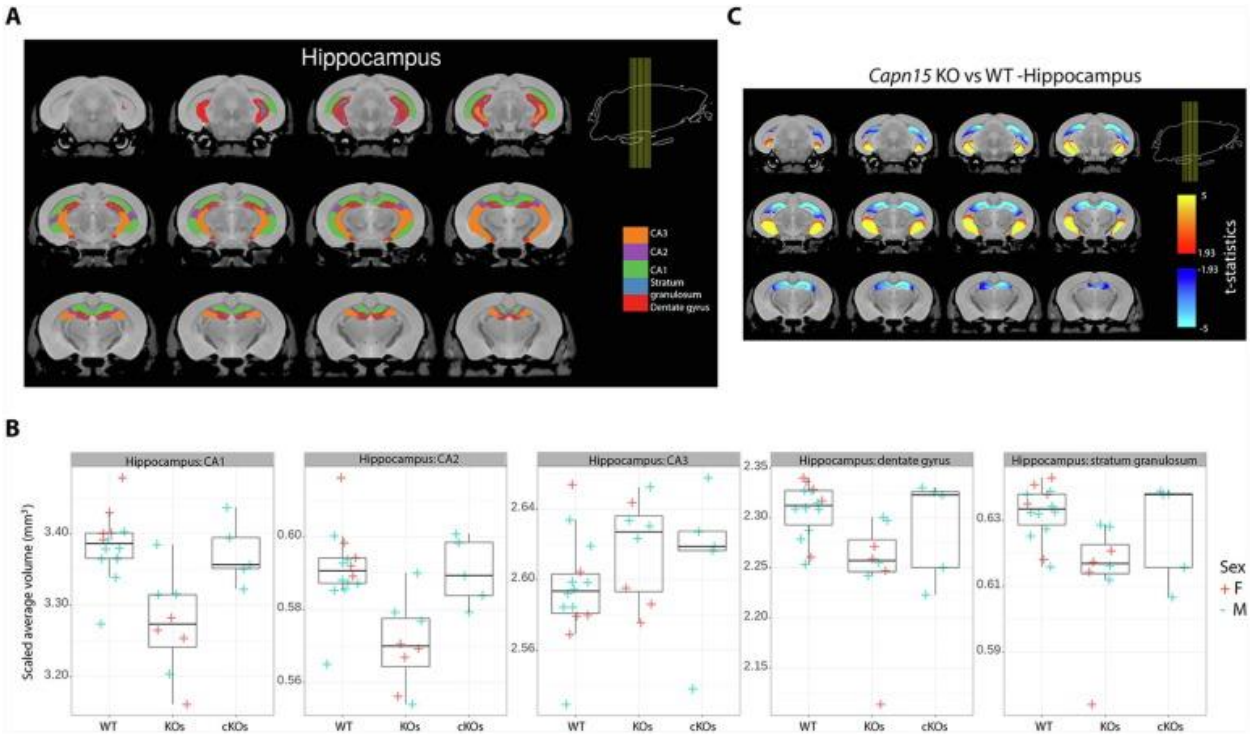

Figure 3.3. Hippocampal subfield-specific volume changes in *Capn15* KO compared to cKO and WT mice. (A) A hippocampal sub-field atlas (Badhwar et al., 2013) was applied to evaluate volumetric changes in the hippocampal subfields. The sub-field atlas includes region of interest labels demarcating the dentate gyrus (red), stratum granulosum (blue), CA1 (green), CA2 (purple) and CA3 (orange). (B) Box and whisker plots showing hippocampal subfield-specific volume differences between WT, KO and cKO mice. All anatomical regions in each brain were scaled based on scaling factor shown in A) to compensate for the overall brain size differences (See methods) (C) Voxel-level *t*-statistical parametric maps showing areas of volumetric contraction (blue colours) or expansion (orange colours) for *Capn15* KO mice compared to WT mice inside the body of the hippocampus. The t-statistical values were calculated with a general linear model. The false discovery rate method was applied for multiple comparisons correction with a *q*-threshold of 0.05. Each slice through the mid-brain has a thickness of 100 micrometers.

The specific position of each slice along the anterior-posterior axis of the mouse brain is shown, overlaid on a sagittal brain slice, in the top right-hand corner of the figure.

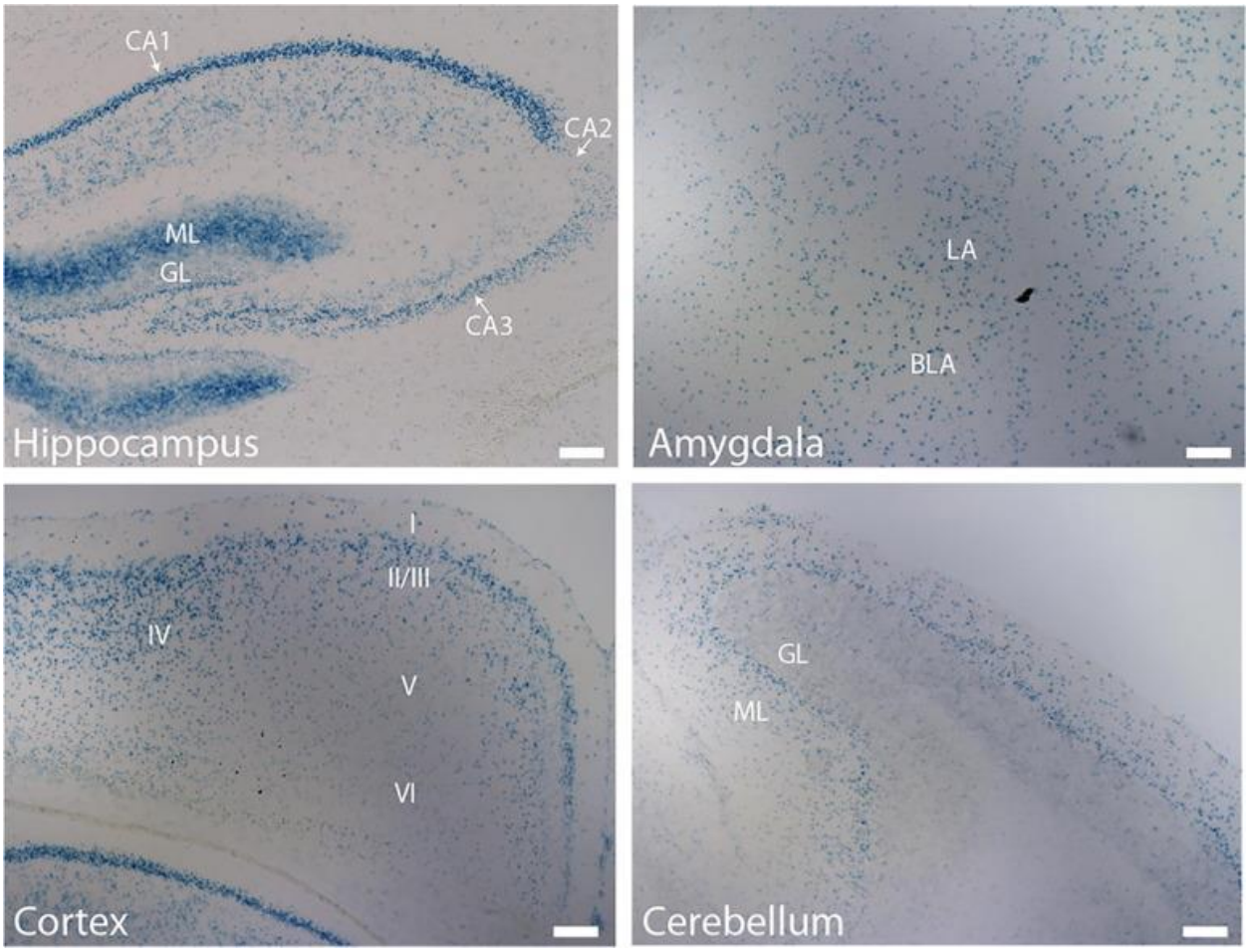

Figure 3.4. Capn15 distribution in *Capn15*$^{(lacZ\text{-}Neo)}$ heterozygous mice brain. X-gal staining of coronal sections from adult *Capn15*$^{(lacZ\text{-}Neo)}$ heterozygous mice hippocampus, amygdala, cortex and cerebellum are shown. Scale bar = 100 μm. LA, lateral amygdala; BLA, basal lateral amygdala; GL, granular layer; ML, molecular layer.

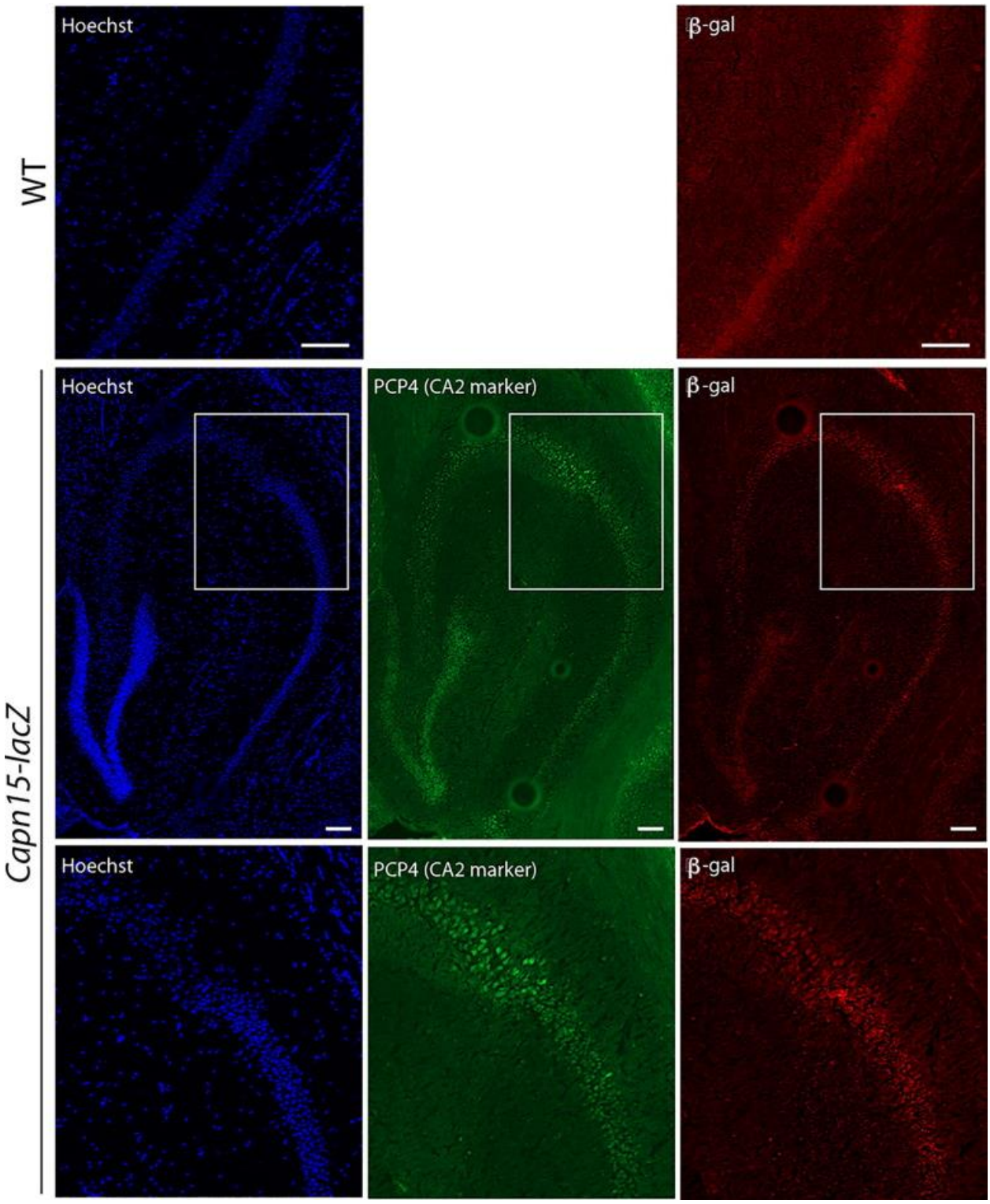
WT
Hoechst
β-gal
Capn15-lacZ
Hoechst
PCP4 (CA2 marker)
β-gal
Hoechst
PCP4 (CA2 marker)
β-gal

Figure 3.5. Capn15 distribution in the hippocampus. The top panel shows the lack of punctate β-gal staining in WT mice. The middle panel shows distribution of a CA2 marker (PCP4) and that of β-gal in a section from the hippocampus from an adult *Capn15-lacZ* brain. The rabbit polyclonal anti-PCP4 and the chicken polyclonal anti-β-gal antibodies were revealed using a secondary anti-rabbit conjugated to Alexa Fluor 488 and a secondary anti-chicken conjugated to Alexa Fluor 594 respectively. DNA was labeled with Hoechst. Capn15 seems to be enriched in all hippocampal areas except in CA2 as illustrated in the magnified inset (boxed region in middle panel) shown in the bottom panel. Scale bars = 100 μm.

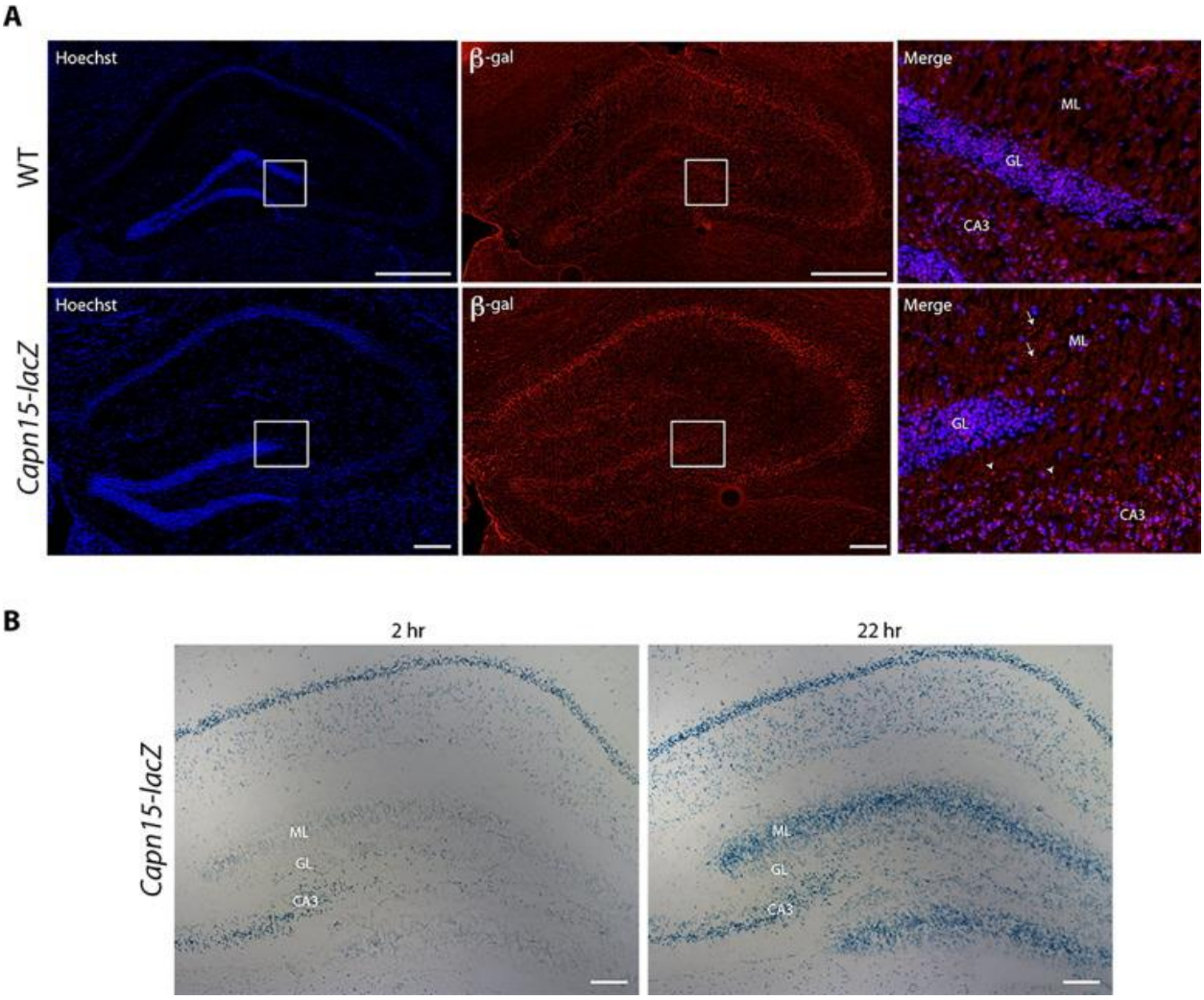

Figure 3.6. Distinct staining of β-galacatosidase (β-gal) in the CA3 region and the molecular layer. (A) The distribution of β-galacatosidase (β-gal) is shown in hippocampal sections from adult *Capn15-lacZ* brains. The chicken polyclonal anti-β-gal antibody was revealed by using a secondary anti-rabbit conjugated to Alexa Fluor 488. DNA was labeled with Hoechst. Capn15 appears to have a distinct expression pattern in the CA3 area and the molecular layer of the hippocampus. Scale bars for top and bottom images = 500 μm and 100 μm, respectively. Experiments were done on 5 *Capn15-lacZ* brains and 2 WT brains with similar results. (B) X-gal

staining of coronal sections from adult *Capn15*$^{(lacZ\text{-}Neo)}$ heterozygous mice hippocampus is shown. The X-gal reaction was ended at 2 or 22 h. Scale bar = 100 μm. GL, granular layer; ML, molecular layer.

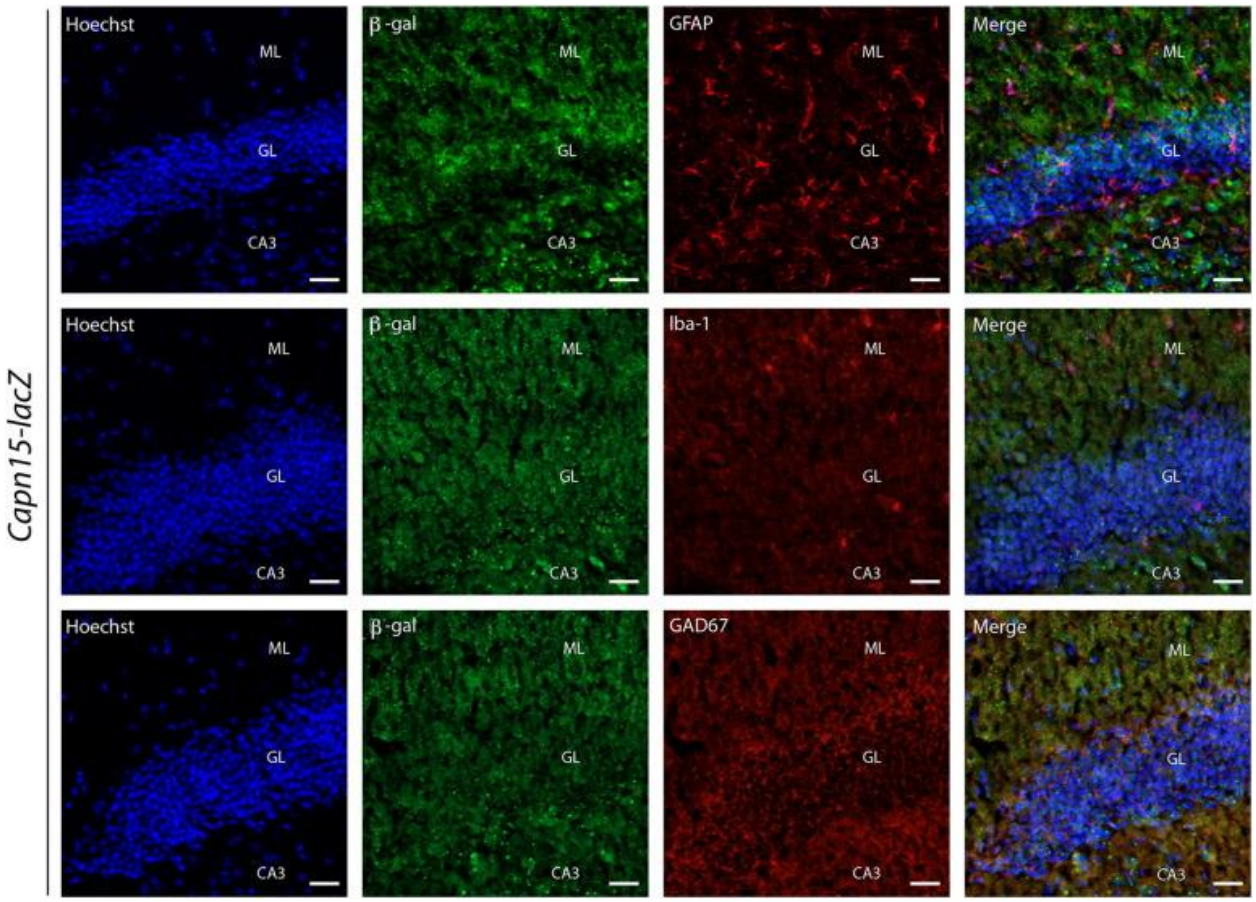

Figure 3.7. The distribution of β-galacatosidase (β-gal) is shown in hippocampal sections from adult *Capn15-lacZ* brains. From left to right are Hoechst staining, β-gal immunoreactivity, cell-type markers and merged images. From top to bottom the cell-type markers are GFAP to label astrocytes, Iba-1 to label microglia and GAD67 to label GABAergic neurons. Scale bar = 25 μm. GL, granular layer; ML, molecular layer.

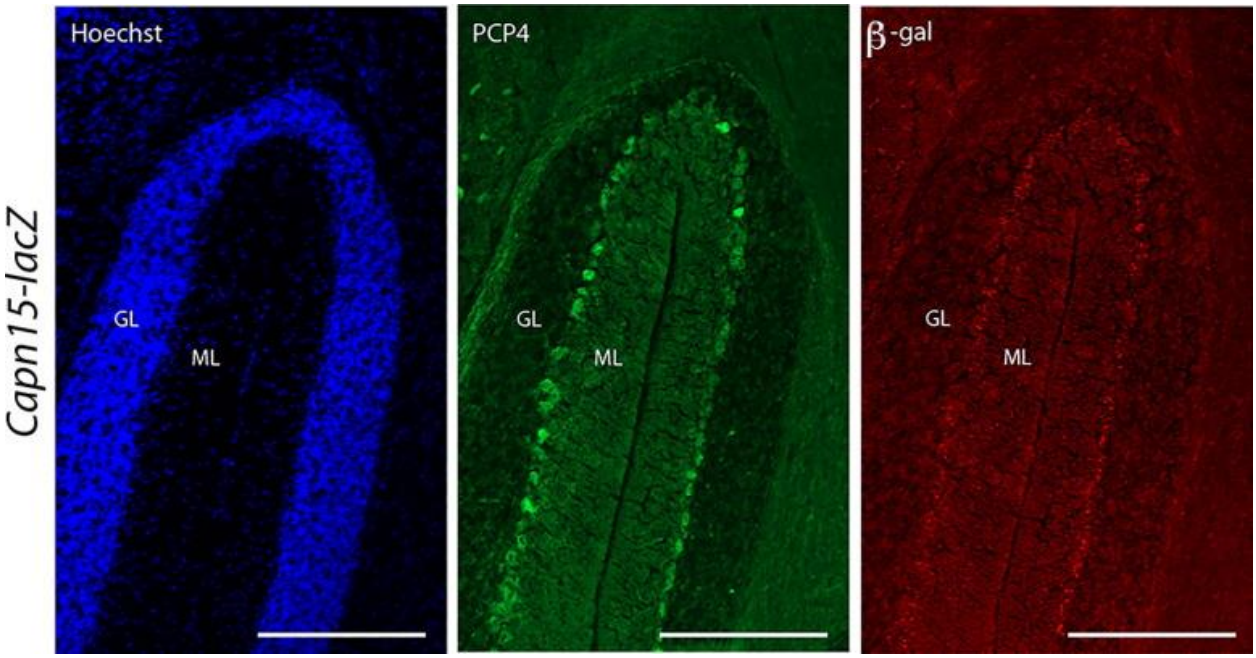

Figure 3.8. Capn15 distribution in the cerebellum. The distribution of a Purkinje cell marker (PCP4) and β-galacatosidase (β-gal) is shown in sections from adult *Capn15-lacZ* brains. The rabbit polyclonal anti-PCP4 and the chicken polyclonal anti-β-gal antibodies were revealed by using a secondary anti-rabbit conjugated to Alexa Fluor 488 and a secondary anti-chicken conjugated to Alexa Fluor 594 respectively. DNA was labeled with Hoechst. Capn15 seems to be enriched in Purkinje cells in the cerebellum. Scale bar = 100 μm. GL, granular layer; ML, molecular layer.

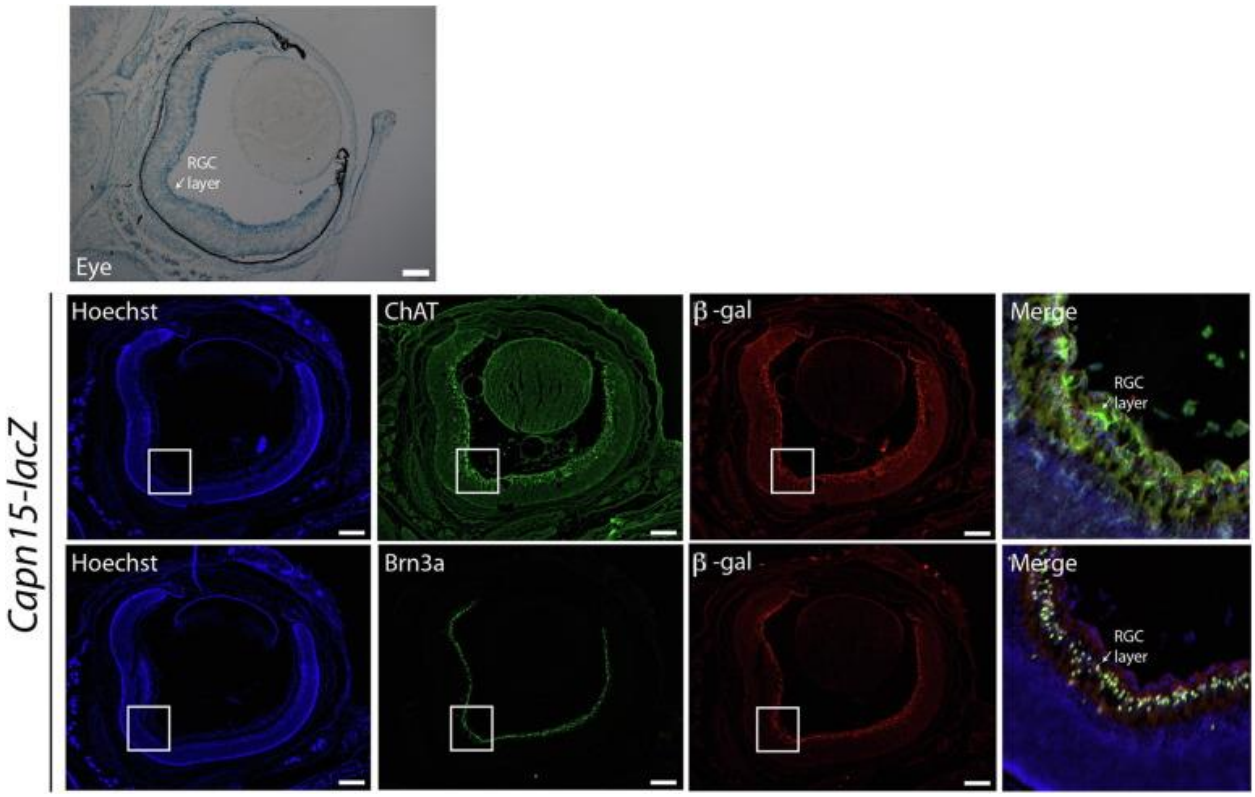

Figure 3.9. Capn15 distribution in the eye. Top, X-gal staining of coronal sections from P3 *Capn15*$^{(lacZ\text{-}Neo)}$ heterozygous mice eyes are shown. Scale bar is 200 μm. RGC, retinal ganglion cells. Bottom, The distribution of a retinal ganglion cell marker (Brn3a) or that of cholinergic amacrine cell marker (ChAT) is shown along with that of β-galacatosidase (β-gal) in sections from adult *Capn15-lacZ* brains. The chicken polyclonal antibody directed against β-gal and either the goat polyclonal antibody directed against Brn3a or the goat polyclonal antibody directed against ChAT were revealed by using a goat anti-chicken secondary antibody conjugated to Alexa Fluor 594 and a donkey anti-goat IgG secondary antibody conjugated to Alexa Fluor 488 respectively. Capn15 is expressed in the retinal ganglion cell layer in a subset of Brn3a+ and ChAT+ cells. Scale bar = 200 μm.

3.9 References

Armstrong C, Szabadics J, Tamas G, Soltesz I (2011) Neurogliaform cells in the molecular layer of the dentate gyrus as feed-forward gamma-aminobutyric acidergic modulators of entorhinalhippocampal interplay. J Comp Neurol 519:1476–1491.

Avants B, Epstein C, Grossman M, Gee J (2008) Symmetric diffeomorphic image registration with cross-correlation: evaluating automated labeling of elderly and neurodegenerative brain. Med Image Anal 12:26–41.

Badhwar A, Lerch JP, Hamel E, Sled JG (2013) Impaired structural correlates of memory in Alzheimer's disease mice. Neuroimage Clin 3:290–300.

Bertipaglia I, Carafoli E (2007) Calpains and human disease. Subcell Biochem 45:29–53.

Briz V, Baudry M (2017) Calpains: master regulators of synaptic plasticity. Neuroscientist 23(3):221–231.

Chambers JM (1992) Linear Models. In: Statistical Models in S, vol. (M CJ, J. HT, eds). Wadsworth and Brooks/Cole.

Delaney SJ, Hayward DC, Barleben F, Fischbach KF, Miklos GL (1991) Molecular cloning and analysis of small optic lobes, a structural brain gene of Drosophila melanogaster. Proc Natl Acad Sci U S A 88(16):7214–7218.

Dutt P, Croall DE, Arthur JS, Veyra TD, Williams K, Elce JS, Greer PA (2006) m-Calpain is required for preimplantation embryonic development in mice. BMC Dev Biol 6:3.

Fischbach KF, Heisenberg M (1981) Structural brain mutant of Drosophila melanogaster with reduced cell number in the medulla cortex and with normal optomotor yaw response. Proc Natl Acad Sci U S A 78(2):1105–1109.

Fonov V, Evans AC, Botteron K, Almli CR, McKinstry RC, Collins DL, Brain Development Cooperative G (2011) Unbiased average age appropriate atlases for pediatric studies. Neuroimage 54:313–327.

Genovese CR, Lazar NA, Nichols T (2002) Thresholding of statistical maps in functional neuroimaging using the false discovery rate. Neuroimage 15(4):870–878.

Guroff G (1964) A neutral, calcium-activated proteinase from the soluble fraction of rat brain. J Biol Chem 239(1):149–155.

Hastings MH, Gong K, Freibauer A, Courchesne C, Fan X, Sossin WS, Permyakov EA (2017) Novel calpain families and novel mechanisms for calpain regulation in Aplysia. PLoS One 12:

e0186646.

Hastings MH, Qiu A, Zha C, Farah CA, Mahdid Y, Ferguson L, Sossin WS (2018) The zinc fingers of the small optic lobes calpain bind polyubiquitin. J Neurochem 146:429–445.

Hu J, Adler K, Farah CA, Hastings MH, Sossin WS, Schacher S (2017a) Cell-specific PKM isoforms contribute to the maintenance of different forms of persistent long-term synaptic plasticity. J Neurosci 37:2746–2763.

Hu J, Ferguson L, Adler K, Farah CA, Hastings MH, Sossin WS, Schacher S (2017b) Selective erasure of distinct forms of long-term synaptic plasticity underlying different forms of memory in the same postsynaptic neuron. Curr Biol 27:1888–1899.e4.

Jeon C-J, Strettoi E, Masland RH (1998) The major cell populations of the mouse retina. J Neurosci 18:8936–8946.

Khoutorsky A, Yanagiya A, Gkogkas CG, Fabian M, Prager-Khoutorsky M, Cao R, Gamache K, Bouthiette F, Parsyan A, Sorge R, Mogil J, Nader K, Lacaille J-C, Sonenberg N (2013) Control of synaptic plasticity and memory via suppression of poly (A)-binding protein. Neuron 78(2):298–311.

Klein S, Staring M, Murphy K, Viergever MA, Pluim J (2010) elastix: a toolbox for intensity-based medical image registration. IEEE Trans Med Imaging 29(1):196–205.

Kovacevic N, Henderson JT, Chan E, Lifshitz N, Bishop J, Evans AC, Henkelman RM, Chen XJ (2005), A three-dimensional MRI atlas of the mouse brain with estimates of the average and variability. Cereb Cortex 15:639-645.

Lein ES, Callaway EM, Albright TD, Gage FH (2005) Redefining the boundaries of the hippocampal CA2 subfield in the mouse using gene expression and 3-dimensional reconstruction. J Comp Neurol 485(1):1–10.

Lerch J, Hammill C, van Eed M, Cassel D, RMINC: Statistical Tools for Medical Imaging NetCDF (MINC) Files. R package version 1.5.2.1, 2017.

Lerch JP, Yiu AP, Martinez-Canabal A, Pekar T, Bohbot VD, Frankland PW, Henkelman RM, Josselyn SA, Sled JG (2011) Maze training in mice induces MRI-detectable brain shape changes specific to the type of learning. Neuroimage 54:2086–2095.

Li Y, Stam FJ, Aimone JB, Goulding M, Callaway EM, Gage FH (2013) Molecular layer perforant path-associated cells contribute to feed-forward inhibition in the adult dentate gyrus. Proc Natl Acad Sci U S A 110(22):9106–9111.

Liu Y, Wang Y, Zhu G, Sun J, Bi X, Baudry M (2016) A calpain-2 selective inhibitor enhances learning & memory by prolonging ERK activation. Neuropharmacology 105:471–477.

Mor-Shaked H, Salah S, Yanovsky-Dagan S, Meiner V, Atawneh OM, Abu-Libdeh B, Elpeleg O, Harel T (2021) Biallelic deletion in a minimal CAPN15 intron in siblings with a recognizable syndrome of congenital malformations and developmental delay. Clin Genet. https://doi.org/10.1111/cge.13920.

Nadal-Nicolas FM, Jimenez-Lopez M, Sobrado-Calvo P, Nieto-Lopez L, Canovas-Martinez I, Salinas-Navarro M, Vidal-Sanz M, Agudo M (2009) Brn3a as a marker of retinal ganglion cells: qualitative and quantitative time course studies in naive and optic nerve-injured retinas. Invest Ophthalmol Vis Sci 50:3860–3868.

Nakhost A, Forscher P, Sossin WS (1998) Binding of protein kinase C isoforms to actin in Aplysia. J Neurochem 71(3):1221–1231.

Ono Y, Sorimachi H (2012) Calpains: an elaborate proteolytic system. Biochim Biophys Acta 1824:224–236.

Pilegaard K, Ladefoged O (1996) Total number of astrocytes in the molecular layer of the dentate gyrus of rats at different ages. Anal Quant Cytol Histol 18:279–285.

Shimizu K, Phan T, Mansuy IM, Storm DR (2007) Proteolytic degradation of SCOP in the hippocampus contributes to activation of MAP kinase and memory. Cell 128:1219–1229.

Sonner JM, Cascio M, Xing Y, Fanselow MS, Kralic JE, Morrow AL, Korpi ER, Hardy S, et al. (2005) Alpha 1 subunit-containing GABA type A receptors in forebrain contribute to the effect of inhaled anesthetics on conditioned fear. Mol Pharmacol 68:61–68.

Spring S, Lerch JP, Henkelman RM (2007) Sexual dimorphism revealed in the structure of the mouse brain using three-dimensional magnetic resonance imaging. Neuroimage 35:1424–1433.

Team RC, R: A language and environment for statistical computing. , R Foundation For Statistical Computing, 2020.

Tsien JZ, Chen DF, Gerber D, Tom C, Mercer EH, Anderson DJ, Mayford M, Kandel ER, Tonegawa S (1996) Subregion- and cell type-restricted gene knockout in mouse brain. Cell 87(7):1317–1326.

Wang Y, Zhu G, Briz V, Hsu YT, Bi X, Baudry M (2014) A molecular brake controls the magnitude of long-term potentiation. Nat Commun 5:3051.

Zha C, Farah CA, Holt RJ, Ceroni F, AlAbdi L, Thuriot F, Khan AO, Helaby R, et al. (2020), Biallelic variants in the small optic lobe calpain CAPN15 are associated with congenital eye anomalies, deafness and other neurodevelopmental deficits. Hum Mol Genet.

Zhao S, Liang Z, Demko V, Wilson R, Johansen W, Olsen OA, Shalchian-Tabrizi K (2012), Massive expansion of the calpain gene family in unicellular eukaryotes. BMC evolutionary biology 12(1):1-12.

Ziai MR, Sangameswaran L, Hempstead JL, Danho W, Morgan JI (1988) An immunochemical analysis of the distribution of a brain-specific polypeptide, PEP-19. J Neurochem 51:1771–1776.

Chapter 4 - Behavioral characterization of Capn15 conditional knockout mice

4.1 Preface

In chapter 3, we used MRI to look at regional volumetric changes in adult WT and *Capn15 KO* brains. We found that *Capn15* KO mice have significantly smaller brains, with even more changes in certain brain areas, such as thalamus, hippocampal CA1, CA2, and dentate gyrus. In adult animals, we found that CAPN15 is expressed primarily in hippocampus, cortex, amygdala, and Purkinje cells, suggesting that CAPN15 might have distinct functions at different life stages. We also generated *CaMKII-Cre Capn15* cKO mice, which deletes *Capn15* in excitatory forebrain neurons after development, and showed that they do not have any signs of developmental deficits.

However, the role of CAPN15 in learning and memory in vertebrates, especially non-associative memory, is not determined. In chapter 4, we used *CaMKII-Cre Capn15* cKO and did a series of behavioral tests, in order to understand the behavioral characteristics of *Capn15* cKO mice and determine whether CAPN15 is involved in putative non-associative memory in vertebrates.

4.2 Abstract

Calpain 15 (CAPN15) is an intracellular cysteine protease belonging to the non-classical small optic lobe (SOL) family of calpains, which has an important role in development. Loss of Capn15 in mice leads to developmental eye anomalies and volumetric changes in the brain. Human individuals with biallelic variants in *CAPN15* have developmental delay, neurodevelopmental disorders, as well as congenital malformations. In *Aplysia*, a reductionist model to study learning and memory, SOL calpain is important for non-associative long-term facilitation, the cellular analog of sensitization behavior. However, how Capn15 is involved in adult behavior or learning and memory in vertebrates is unknown. Here, using *CAPN15* conditional knockout mice, we show that loss of the Capn 15 protein in excitatory forebrain neurons reduces self-grooming and marble burying, decreases performance in the accelerated roto-rod and reduces pre-tone freezing after strong fear conditioning. Thus, Capn 15 plays a role in regulating behavior in the adult mouse.

Key words: calpains; behavior; fear generalization; non-associative plasticity

4.3 Introduction

Calpains are intracellular cysteine proteases that were first discovered in the rat brain (Guroff, 1964). There are four conserved families of calpains in metazoans that are distinguished by conserved domains that are specific for each family outside the catalytic domain: Classical, PalB (named after the screen for acid-sensitive phosphatase mutants in the fungi, Aspergillus), Transformer (Tra), and Small Optic Lobe (SOL) (Hastings et al., 2017). The most ancient family of these calpains is PalB which is expressed in Fungi, followed by SOL which is found in pre-

metazoans such as choanoflagellates, while Tra and classical calpains diverged from PalB in early metazoans (Hastings et al., 2017).

SOL calpains have an N-terminal zinc finger domain that binds polyubiquitin (Hastings et al., 2018) and a C-terminal SOL homology domain (Hastings et al., 2017; Zhao et al., 2012). It was first identified in the fruit fly *Drosophila* (Delaney, Hayward, Barleben, Fischbach, & Miklos, 1991; Fischbach & Heisenberg, 1981) where loss of the SOL calpain leads to smaller optic lobes (Fischbach & Heisenberg, 1981). Recently, we found that CAPN15, which is the only orthologue of SOL calpain in vertebrates, is critical to general development, brain development and eye development, as loss of CAPN15 in mice leads to a smaller mendelian ratio, lighter weights, smaller brains as well as eye anomalies including cataract, microphthalmia and anophthalmia (Zha, Farah, Fonov, Rudko, & Sossin, 2021; Zha et al., 2020). Humans carrying homozygous variants of CAPN15 also showed various degrees of eye disorders and developmental anomalies (Beaman et al., 2022; Marino et al., 2023; Mor-Shaked et al., 2021; Zha et al., 2020) including two with diagnosed autism and an additional 10 with global developmental delay, out of 13 individuals over 3 years old. In addition, patients with biallelic loss of function variants of *CAPN15* seem more likely to suffer from more severe phenotypes (Beaman et al., 2022; Mor-Shaked et al., 2021).

Besides its role in development, SOL calpain is also important for synaptic plasticity underlying memory in the marine mollusc *Aplysia*, particularly the synaptic plasticity thought to underlie non-associative memories such as sensitization (Hu, Adler, et al., 2017; Hu, Ferguson, et al., 2017). Unlike associative fear learning, in which a conditioned stimulus (CS) is paired to an unconditioned stimulus (US), non-associative fear learning does not require such pairing. Sensitization, for example, is a classic model of non-associative fear learning and it is heavily

studied in *Aplysia*. Sensitization in *Aplysia* is demonstrated as an increase in siphon/gill withdrawal response after a noxious stimulus has been applied to the tail (Kandel, 2001). The circuit involved in sensitization behavior can be recapitulated in culture and studies using *Aplysia* sensorimotor cocultures revealed that the molecular mechanism underlying long-term sensitization involves an increase in synaptic strength between siphon sensory neurons and gill motor neurons induced by repeated release of serotonin from interneurons sensitive to noxious stimulus (Kandel & Schwartz, 1982; Marinesco & Carew, 2002). In *Aplysia*, expression of a dominant-negative catalytically inactive SOL calpain in either the sensory neuron or the motor neuron prevented the induction of a long-term form of non-associative long-term facilitation underlying sensitization (Hu, Adler, et al., 2017). Furthermore, in cultures where two sensory neurons are innervated by one motor neuron, with one sensory neuron expressing associative plasticity and the other, non-associative plasticity, blocking SOL calpain activity in the postsynaptic motor neuron affected the induction of non-associative plasticity, but not associative plasticity (Hu, Ferguson, et al., 2017). These results suggest that SOL calpain is important for forms of plasticity associated with non-associative memory in *Aplysia*, but not with forms of plasticity associated with associative memories. However, the role of CAPN15 in adult behavior or in learning and memory paradigms in vertebrates has not been studied.

Here, we used *CaMKII-Cre Capn15* conditional knockout (cKO) mice, which do not present any signs of developmental deficits (Zha et al., 2021), to examine the behavioral characteristics of *Capn15* cKO animals. We showed that *CaMKII-Cre Capn15* cKO buried fewer marbles in marble burying test; showed poorer motor performance in rotarod tests; and showed less fear generalization towards the context after strong auditory fear conditioning.

4.4 Materials and methods

4.4.1 Animals

All animal experiments were carried out in compliance with protocols approved by the Montreal Neurologic Institute animal committee (Protocol MNI-5784). C57BL/6J mice were used to generate our mouse lines. The generation of the *Capn15*$^{(lacZ\text{-}Neo)}$ mouse and the FLOXed *Capn15* mouse has been described elsewhere (Zha et al., 2020). To generate a conditional KO line, the mice were bred with the CaMKIIa-Cre-CRE T29-1 (Tsien et al., 1996) that should only delete exons of *Capn15* after development in forebrain excitatory neurons (Sciolino et al., 2016; Sonner et al., 2005). The initial breeding was flox/flox X CaMKIIa-CRE T29-1/WT flox/WT. Only a small number of cKO mice were generated from this cross due to the apparent presence of CRE and Capn15 on the same chromosome (*Capn15* is on chromosome 17 in mouse, the location of the CRE T29-1 has not been described). These cKO mice were used in subsequential breeding as they had presumably recombined the CRE and the floxed *Capn15* allele on the same chromosome. Specifically, we generated cKO mice by breeding cKO mice flox/flox CaMKIIa-Cre-CRE T29-1/WT with flox/flox mice. The CRE- littermates were used as controls. Mice were bred at the Montreal Neurological Institute and were transported to Stewart biology building for behavior testing. All mice were at least 12 weeks old to ensure maximun loss of CAPN15 protein after knock out of the *Capn15* gene (Zha et al., 2021). All mice were acclimated to the colony room for at least 7 days before experiments began. All mice were group housed (2–4 mice per cage) on a 12 h light/dark cycle (lights on at 7AM and lights off at 7PM) with food and water available ad libitum. All behavioural experiments were conducted during the light cycle were conducted by a male experimenter.

4.4.2 Behavioral procedures

Adult mice of both sexes (12-16 weeks of age) were used for experiments. Mice were handled once per day for 4-5 days before behavioral testing. Mice were transported from their colony room to the behavior testing room 30 min before the beginning of any behavioral experiment. All experiments started at 9AM local time, except afternoon training and testing in the novel object location task, which started at 1PM local time. The experimenter left the room right after the beginning of each experiment except during the rotarod test. We used a series of tests to characterize the behavior of *Capn15* cKO mice, that included (in order) grooming, open field, object location, marble burying, elevated plus maze, rotarod, and auditory fear conditioning, as well as extinction (number of cohorts = 4), although one cohort was not tested in the Rotarod task. Auditory fear conditioning and extinction using "strong shock" training protocols and the accompanying "standard shock" control (number of cohorts = 2) were not part of the battery and were conducted separately with different animals. Data from "standard shock" were combined with data from the battery. Pre-CS freezing was not measured in the first cohort of the animals used in the battery. The experimenter was blind to genotype for all phases of the experiments, including scoring behaviour. Mice were run by cages and cage orders alternated between males and females. Cages had mixed genotypes.

4.4.2.1 Grooming

Mice were individually placed in a novel cage that only contained about 1 cm of fresh bedding material also used in their home cage (corncob). Behavior was recorded for 20 min using a high-resolution video camera placed in front of the cage. Only the last 10 min of the video were

considered. Total grooming time and the number of grooming bouts were manually scored using a stopwatch.

4.4.2.2 Open Field

Mice were placed individually in the center of an open field arena made of white laminated particle board (51.5 cm wide, 51.5 cm deep, 31 cm high). Four animals were run simultaneously in four arenas arranged in a 2 * 2 grid. Mice were allowed to move freely for 10 min. Behavior was recorded with a video camera mounted about 2.5 m above the ground. Open fields were cleaned with paper towel and bio-clean after each trial. The locomotive activity of mice was tracked using the Noldus EthoVision XT video tracking software, which calculated total distance travelled and time spent in the center/corners. The arena was evenly divided into 9 zones in a 3 * 3 grid (17.17 cm wide * 17.17 cm long per zone), which defined center area and the four corners.

4.4.2.3 Object location

We used the four open field arenas described above, arranged in a 2 * 2 fashion as before to run 4 animals at the same time. A yellow star shaped sticker was glued onto a wall about 20 cm above the floor of each open field for orientation. Our behavior protocol consisted of a habituation trial, four training trials, and a test trial. Behavior was recorded with a video camera mounted about 2.5 m above the ground. Arenas and objects were cleaned with paper towel and bio-clean after each trial. Habituation session was scheduled four hours after the beginning of open field experiment. During habituation, mice were placed individually in the center of an empty open field and were allowed to freely explore it for 10 minutes. Mice were then returned to their home cages. During the next two consecutive days, animals were trained. Each day consisted of two training sessions that were four hours apart from each other. During each session, two identical 50 ml falcon tubes, spaced by 30 cm, were securely placed along the mid-

line of the open field, parallel to the wall with the visual cue. Animals were allowed to freely explore the open field for 10 minutes, then were returned to their home cages. Twenty-four hours after the beginning of the last training sessions, novel object location recognition was tested by moving one tube to a corner (10 cm away from the two adjacent walls). We counterbalanced the location of the displaced object and sex of the animal. Animals were placed in the center of the arenas and were allowed to explore the arena for 10 minutes, then they returned to their home cages. Their locomotive and explorative activity were tracked using the Noldus EthoVision XT video tracking software. Exploration of an object was defined when the nose of an animal was inside a circle with a diameter of 10 cm centered around the object. To calculate their novel object location recognition, we used the discrimination index d, with $d = \frac{\text{time (object at new location)} - \text{time (object at old location)}}{\text{time (object at new location)} + \text{time (object at old location)}}$. Values significantly above zero indicate that animals spent more time exploring the object moved to the novel location than the object that remained at the original location, suggesting expression of object location memory. Values equal to zero indicate that animals explore both objects the same, suggesting the absence of object location memory. Animals that spent less than 50 s in total exploring objects during training and/or 20 s in total during testing were removed from the analysis.

4.4.2.4 Marble Burying

We used the same open field arenas as before. Two animals were run simultaneously in two arenas side by side. Mice were placed individually in the center of an open field containing sawdust bedding (5 cm deep) and 20 clean marbles (1.5 cm in diameter; dark green) spaced evenly in a 5 * 4 array. Mice remained in the arena for 20 min. After the test period, buried marbles were counted manually. A marble was considered buried if at least 2/3 of it was covered with sawdust. Behavior was recorded with a video camera mounted about 50 cm above the floor

of the arena. Locomotive activity was tracked using the Noldus EthoVision XT video tracking software, although locomotive activity was not tracked in the first cohort examined. Marbles were cleaned with bio-clean and rinsed with water and feces in the bedding were removed between each trial. Bedding was reused in this experiment. Fecal matters were removed and the bedding was redistributed (mixed) after each animal to disperse possible odour cues, as in previous studies (Augereau, Migues, & Hardt, 2022; Wiebe et al., 2019).

4.4.2.5 Elevated plus maze

The maze is 50 cm above the floor and consists of two open and two closed arms at opposite directions. Each arm was 45 cm long and 10 cm wide. Each arm was connected to the central open platform, which was 10 cm long and 10 cm wide. Sawdust was scattered on the surface to cover the black surface underneath. Mice were placed individually in the central platform and were allowed to move freely for 5 min. Behavior was recorded with a video camera about 2.5 m above the ground. Feces were removed and additional sawdust was added to cover the surface before the introduction of new animals. Time spent in open/close arms was scored manually using a stopwatch. Bedding was reused in this experiment. Fecal matters were removed and the bedding was mixed up after each animal to disperse possible odour cues.

4.4.2.6 Rotarod

The IITC Life Science Rotarod apparatus (CA, USA) was used to assess motor function and learning. The test consisted of two baseline trials (ITI: 2 min) with a constant rotation speed of 4 rpm and four test trials (ITI: 2 min) with an accelerating rotation speed of 4 to 40 rpm over 90 sec. Mice were individually placed on a rod facing away from the direction of rotation. Mice from the same cage were run side by side at the same time. During baseline trials, mice were trained to stay on the rod at a constant rotation speed. Mice that fell were placed back on the

rotarod until the end of the 90-second training period. Then, mice were tested on a gradually accelerating rotarod for 90 seconds. The latency to fall off the rotarod was recorded. Mice that fell during test were returned to their home cages. The apparatus was cleaned with bio-clean and paper towel between each trial.

4.4.2.7 Auditory fear conditioning and extinction

The fear conditioning chamber (17 cm wide, 17 cm deep, 30 cm high) was inside a soundproof isolation cubicle (Coulbourn Habitest, Coulbourn Instruments). Mice were first habituated to the test context (context A: laminated orange plastic floor, built-in low light illumination, transparent plexiglass walls) for 20 min for two consecutive days. The whole chamber was cleaned with bio-clean before the introduction of new animals. On the training day, two minutes after placement in the training context (context B: stainless steel grid floor with 1 cm spacing, white LED illumination, a strip-patterned wall and a dot-patterned curved wall), a tone (CS, 2.8 kHz, 80-85 dB pure tone, 30 s) co-terminated with a foot shock (US). Mice were run at different training intensity. For the “standard shock” group, mice received two pairings of CS and US (0.7 mA, 1s); for the “strong shock” group, mice received four pairings of CS and US (1 mA, 1s). All tone shock pairings were separated with an inter-trial interval of 60 s. Thirty seconds after the last foot shock, mice were returned to the home cage. The chamber and waste collection trays were cleaned with bio-clean before the introduction of new animals. Mice were tested 24h later in Context A. Two minutes after placement in Context A, the first of 12 CS was presented for 30 sec. Tones were separated by 60 s. Thirty seconds after the end of the last tone, mice were returned to their home cage. The whole chamber was cleaned with bio-clean before the introduction of new animals. The behavior of the mice in the fear conditioning chamber was recorded using a camera at the ceiling of the chamber. The percentage of time spent freezing

before the first CS and during the CS was used as a proxy for memory recall. Freezing was defined as immobility, with the exception of respiratory movements, and was scored manually from the videos. The freezing towards two adjacent tones were averaged into a bin. Animals in the 0.7 mA group that froze over 30% during the pre-CS period were removed from the dataset.

4.4.3 Statistics

We analysed data that were normally distributed (Shapiro-Wilk) with t-tests, ANOVA or repeated-measures ANOVA, as appropriate; otherwise, we used Mann-Whitney U-tests, Kruskal-Wallis, or Friedman test. Statistical outliers (Grubb's test, alpha = 0.05) were removed. We used jamovi for our analyses (jamovi, 2022). We rejected the null hypothesis if $p < 0.05$.

4.5 Results

We characterized the behaviour of *Capn15* cKO mice using the open field test, elevated plus maze, grooming analysis, marble burying task, Rotarod test, novel object location recognition task, and auditory fear conditioning..

Open Field Test. There were no significant differences between the genotypes for the distance travelled in the open field (*F < 1*; Fig. 1A). However, female mice travelled longer distances than male mice ($F_{(1,68)} = 10.13$; $p = 0.002$; $\eta_p^2 = 0.13$; Fig. 1A). The interaction between genotype and sex for this variable was not significant (*F < 1*; Fig. 1A). Regardless of genotypes or sex, all mice showed a strong place preference ($F_{(1,68)} = 2726.91$; $p < 0.001$; $\eta_p^2 = 0.976$; Fig. 1B, C), and p*ost-hoc* analyses revealed that they spent significantly more time in the corners than in the center of the open field ($t = 52.2$; $p_{(tukey)} < 0.001$). No other factors were significance (factor *genotype*: $F < 1$; factor *sex*: $F < 1$; factor *genotype* × *sex*: $F_{(1,68)} = 2.32$; $p = 0.132$).

Elevated Plus Maze. All animals showed a strong place preference ($F_{(2,140)} = 2423.59$; $p < 0.001$; $\eta_p^2 = 0.972$; Fig. 2A), and p*ost-hoc* analyses revealed that they spent more time in the closed than the open arm ($t = 48.69$; $p_{tukey} < 0.001$), or the center ($t = 57.42$; $p_{(tukey)} < 0.001$). No other effects were significant ($F < 1$). Regarding the number of entries into arms, we did not find significant differences between the genotypes ($F_{(1,70)} = 1.33$; $p = 0.252$; Fig. 2B); yet, a trend suggests that female mice made more entries than male mice ($F_{(1,70)} = 3.16$; $p = 0.08$; Fig. 2B). There was no interaction between sex and genotype ($F_{(1,70)} = 0.73$; $p = 0.395$; Fig. 2B). Thus, in these two tests that assess anxiety and locomotion, *Capn15* cKO mice showed a phenotype not different from the CRE- control animals.

Grooming. We did not detect significant differences between genotypes in the total time mice spent grooming (Kruskal-Wallis test; $p = 0.571$; Fig. 3A). However, *Capn15* cKO displayed significantly fewer bouts of grooming than the CRE- controls (Kruskal-Wallis test; $p = 0.05$; Fig. 3B). The average bout time did not differ between the two genotypes (Kruskal-Wallis test; $p = 0.16$; Fig. 3C). Male and female mice performed similarly in all behavioral parameters examined (Kruskal-Wallis test; for all comparisons, $p > 0.5$).

Marble Burying Task. We observed that *Capn15* cKO mice buried fewer marbles than the control mice (Kruskal-Wallis test; $p = 0.008$; Fig. 4A). There was no difference between the sexes (Kruskal-Wallis test; $p = 0.607$; Fig. 4A). *Capn15* cKO did not bury less marbles because they were less active than the control mice, as the distance travelled during this task was the same for both genotypes (Kruskal-Wallis test; $p = 0.943$; Fig. 4B). Female mice, however, showed stronger locomotor activity than males (Kruskal-Wallis test; $p = 0.029$; Fig. 4B), similar to findings in the open-field test (Fig. 1). Overall, *Capn15* KO mice did not exhibit increased anxiety, but presented with reduced repetitive behaviors compared to CRE- control animals.

Rotarod Test. The time mice spent on drums that rotated at a constant speed was not significantly different between the genotypes ($F_{(1,53)} = 2.42$; $p = 0.126$; Fig. 5A) or sexes ($F < 1$; Fig. 5A); the interaction between genotype and sex was not significant ($F < 1$; Fig. 5A). All animals stayed longer on the drums on the second compared to the first trial ($F_{(1,53)} = 12.84$; $p < 0.001$; $\eta_p^2 = 0.195$; Fig. 5A). During the second phase of the rotarod test, when rotation speed continuously increased during the trials, we also found that the time mice spent on the drum was significantly different between trials ($F_{(1,53)} = 6.06$; $p < 0.001$; $\eta_p^2 = 0.103$; Fig. 5B). *Post-hoc* tests showed that all animals increased the time they stayed on the drums between the first and last trial ($t = -4.104$; $p_{(tukey)} < 0.001$; Fig. 5B). Independent of genotype, all animals increased the time they spent on the accelerating rotarod between the first trial and the last trial ($F < 1$; Fig. 5B). However, the control CRE- mice remained on the drums significantly longer than the *Capn15* cKO mice ($F_{(1,53)} = 4.30$; $p = 0.043$; $\eta_p^2 = 0.075$; Fig. 5B). There were no significant differences between the sexes ($F < 1$), and the interaction of genotype and sex was not significant ($F < 1$). Taken together, these findings suggest that *Capn15* cKO mice present with similar motor skill learning ability as the control animals, but show an overall deficit in motor coordination when the task is more difficult (i.e., accelerating rotarod compared to constant speed).

Novel Object Location Recognition Test. Mice of both genotypes ($F_{(1,51)} = 1.59$; $p = 0.213$; Fig. 6A) and sexes ($F < 1$; Fig. 6A) expressed a similar preference for exploring the object moved to a novel location. Comparing the discrimination index against what would be the change alone (i.e., zero), we found that all groups preferred exploring the object at the novel location ($t_{(13)} = 7.35$; $p < 0.001$ for female Cre-; $t_{(13)} = 8.15$; $p < 0.001$ for female *Capn15* cKO; $t_{(13)} = 5.93$; $p < 0.001$ for male Cre-; $t_{(12)} = 7.18$; $p < 0.001$ for male *Capn15* cKO). The total time spent exploring objects during testing was similar between the two genotypes (Kruskal-Wallis

test; $p = 0.446$; Figure 6B) and two sexes (Kruskal-Wallis test; $p = 0.100$; Figure 6B). Furthermore, the total time spent exploring objects during training was not different between the two genotypes ($F < 1$; Figure 6C). Female mice showed a strong statistical trend to spend more time exploring objects than male mice ($F_{(1,51)} = 3.49$; $p = 0.067$; Figure 6C). These results suggest that *Capn15* cKO mice have normal spatial memory.

Auditory Fear Conditioning and Extinction. Both genotypes ($F < 1$) and sexes ($F < 1$) reduced freezing to the conditioned stimulus during the course of each extinction session ($F_{(5, 325)} = 67.40$, $p < 0.001$, $\eta_p^2 = 0.51$; Figure 7A, B), and froze less during the second compared to the first day of extinction ($F_{(1,65)} = 114.17$, $p < 0.001$, $\eta_p^2 = 0.64$; Figure 7A, B). Yet, the slope of the extinction curve was different between the two days ($F_{(5,325)} = 2.63$, $p < 0.02$, $\eta_p^2 = 0.04$). *Post-hoc* tests (data not shown) revealed that during the first day of extinction, mice significantly reduced freezing from one bin to the next, but this was not the case during the second day, when only compared to the first bin animals froze less to all other bins, with freezing being the same between the second and the fifth bin, to significantly drop again to the last bin.

To assess fear generalization, we analyzed freezing to the extinction context, i.e., pre-CS freezing, during the first extinction session. Freezing was the same for both genotypes ($F_{(1,44)} = 1.8$, $p = 0.19$, $\eta_p^2 = 0.04$; Figure 7C) and sexes ($F_{(1,44)} = 1.03$, $p = 0.32$, $\eta_p^2 = 0.02$; Figure 7C). Interestingly, we observed a significant genotype and sex interaction ($F_{(1,44)} = 10.14$; $p = 0.003$; $\eta_p^2 = 0.187$). *Post-hoc* tests showed that male control mice froze significantly more than male *Capn15* cKO mice ($t = 3.015$; $p_{\text{tukey}} = 0.021$) and more than female control mice ($t = 2.765$; $p_{(\text{tukey})} = 0.04$). These results suggest that auditory fear conditioning and extinction are unaffected in *Capn15* cKO mice. However, male *Capn15* cKOs mice are less prone to fear generalization, compared to male Cre- control animals.

We sought to determine whether the unexpected stronger fear generalization of *Capn15* cKO mice was moderated by the intensity of the unconditioned stimulus. In two follow-up experiments we therefore trained two groups of naïve mice in auditory fear conditioning (without assessing them with the test battery) -- one group received the same shock as the animals in the battery (i.e., 2 x 0.7 mA shock), another group received a stronger training protocol (4 x 1 mA). While all animals presented with stronger pre-CS freezing during the first extinction session ($F_{(1,63)} = 22.65$, $p < 0.001$, $\eta_p^2 = 0.26$; Figure 8A), we found that *Capn15* cKO mice froze significantly less than control animals ($F_{(1,63)} = 6.08$, $p = 0.016$, $\eta_p^2 = 0.09$; Figure 8A), independent of the shock intensity ($F_{(1,63)} = 1.93$, $p = 0.170$, $\eta_p^2 = 0.03$; Figure 8A). A strong statistical trend suggests that male mice froze more during the pre-CS period than female mice ($F_{(1,63)} = 3.86$, $p = 0.054$, $\eta_p^2 = 0.06$; Figure 8A). None of the remaining interactions was significant ($F < 1$).

All animals reduced freezing to the tone during each of the two extinction sessions ($F_{(5,295)} = 31.09$, $p < 0.001$, $\eta_p^2 = 0.35$; Figure 8B, C), and froze less overall during the second compared to the first session ($F_{(1,59)} = 45.08$, $p < 0.001$, $\eta_p^2 = 0.43$; Figure 8B, C). Extinction learning was, as before, not moderated by genotype ($F_{(1,59)} = 1.76$, $p = 0.189$, $\eta_p^2 = 0.03$; for all interaction terms containing genotype as a factor: $1 > F < 2.4$; Figure 8B). Overall, female mice froze less than male mice ($F_{(1,59)} = 5.07$, $p = 0.028$, $\eta_p^2 = 0.08$; Figure 8C), and animals froze more during extinction in the stronger shock protocol ($F_{(1,59)} = 16.39$, $p < 0.001$, $\eta_p^2 = 0.22$; Figure 8B, C). These effects, however, reflect that only male mice froze more to the stronger shock, which did not moderate freezing in female mice at all, while there were no differences between the sexes for the standard training protocol ($F_{(1,59)} = 7.52$, $p = 0.008$, $\eta_p^2 = 0.11$; Figure 8C; male standard vs male strong: $t = -4.76$, $p_{(Tukey)} < 0.001$; female standard vs female strong: t

< 1; male strong vs female strong: $t = 4.73$, $p_{(Tukey)} < 0.001$; male standard vs female standard: $t < 1$). Accordingly, the slopes of the extinction curves were different between sexes ($F_{(5,295)} = 3.21$, $p = 0.008$, $\eta_p^2 = 0.05$; Figure 8C), in that males froze more during the first pair of tones than female mice ($t = 4.29$, $p_{(Tukey)} = 0.004$). This pattern was moderated by extinction session ($F_{(5,295)} = 2.83$, $p < 0.016$, $\eta_p^2 = 0.05$; Figure 8C). First, the extinction curves were flatter for female mice on both days compared to the male animals, in that the females reduced their average freezing during the first extinction session from 41.9% to 20.8%, and post-hoc tests revealed that only the difference in freezing between the first and the last bin was statistically significant ($t = 4.66$, $p_{(Tukey)} = 0.004$). Male mice, on the other hand, reduced their freezing from 59.1% to 31.2%, freezing significantly less to the first pair of tones compared to the fourth ($t = 5.36$, $p_{(Tukey)} < 0.001$), fifth ($t = 6.43$, $p_{(Tukey)} < 0.001$), and last pair of tones ($t = 6.05$, $p_{(Tukey)} < 0.001$). Despite these differences, freezing to any given tone was not statistically significant between the sexes during the first extinction session. Regarding the second extinction session, female mice froze 25.8% to the first and 15.6% to the last pair of tones, with none of the freezing significantly different from each other. Male mice reduced their freezing from 46.9% to the first and 17.8% to the last pair of tones. Here, freezing was significantly different between the first and all other pair of tones ($4.09 <= t <= 5.85$, $0.001 >= p_{(Tukey)} <= 0.023$). Freezing was only significantly different between the sexes during the first pair of tone ($t = 4.24$, $p_{(Tukey)} = 0.004$).

The results suggest that *Capn15* cKOs are less prone to fear generalization, especially when the stimulations that induce fear generalization are strong. Furthermore, our findings indicate that female freeze less in our fear conditioning protocols, and are, apparently, less reactive to shock intensity than male animals.

4.6 Discussion

Assessing the effects of conditional KO of *Capn15* in adult male and female mice, we found a complex behavioral profile, with differences between control and cKO animals in the marble burying task, Rotarod, and auditory fear conditioning. In addition, we observed, independent of genotype, sex differences in the distance travelled during the marble burying task and the open field test, as well as in the extent of freezing expressed during extinction of auditory fear conditioning. These findings indicate that CAPN15 can contribute to behaviour in adult animals.

A common feature of loss of function of CAPN15 in humans is global neurodevelopmental delay, intellectual disability or a diagnosis of autism (Beaman et al., 2022; Marino et al., 2023; Mor-Shaked et al., 2021; Zha et al., 2020). It is not clear if this is due to the early loss of CAPN15 during development, or if CAPN15 is required for these behaviors in the adult, or both. Repetitive behavior is linked to human neurodevelopmental disorders and two behaviors in rodents are often examined in relationship to this, grooming and marble burying (Kalueff et al., 2016; Pasciuto et al., 2015). Many mutations and developmental insults that increase the risk of autism in humans lead to an increase in grooming behavior and marble burying in mice (Kalueff et al., 2016; Pasciuto et al., 2015). Overall, our results are not consistent with an autism-like phenotype when CAPN15 is removed in the adult, as our *Capn15* cKO mice show decreased marble burying and less bouts of grooming compared to the wild type animals, which is the opposite what is found in many rodent models of autism that express stereotypical or repetitive behaviors (Kalueff et al., 2016; Pasciuto et al., 2015). Aside from animal models of depression, there are few other genetic models that lead to decreases in marble

burying and grooming. On the other hand, increases in GABAergic tone, as seen after benzodiapene treatment, can decrease grooming and marble burying (Broekkamp, Rijk, Joly-Gelouin, & Lloyd, 1986). However, increased GABAergic tone is also linked to decreased anxiety as reflected in corresponding behavioral changes in the open field and elevated plus maze (Rosso et al., 2022), and we did not observe these in our *Capn15* cKO mice as there was no effect of genotype on either the time spent in corners in the open field nor on the time spent in the open arms in the elevated plus maze (Figs. 1, 2).

A significant difference between *Capn15* cKO and control mice emerged in the accelerating Rotarod test. Here, both genotypes increased their time spent on the rotating drums from trial to trial at the same rate, but the control animals stayed on longer in each trial than the cKO mice, which only in the last trial remained as long on the drums as the controls already in the first trial. This finding was rather unexpected because motor coordination is mainly linked to the cerebellum and striatum, two regions of the brain that generally do not express CRE in this transgenic strain (Sciolino et al., 2016; Sonner et al., 2005), although there is expression of CRE in a small subset of Purkinje cells (Farmer et al., 2016). We therefore suspect that *Capn15* cKO in the motor- and somatosensory cortex might contribute to this deficit. Recently, it has been show that a subset of hippocampal CA1 neurons are involved in learning of the Rotarod task, as their chemogenetic activation decreased animal performance without affecting behavior in the open field or novel object recognition learning (Brito et al., 2022). It would therefore be interesting to explore in future studies if this subset of neurons in CA1 is particularly affected by loss of CAPN15 in the adult animal.

While we did not observe any differences in auditory fear conditioning between the genotypes, we found that *Capn15* cKO mice showed weaker fear generalization to the testing context, i.e.,

less pre-CS freezing than the control animals, particularly in the strong shock group. In contextual fear conditioning, generalization effects normally appear weeks after training, probably due to memory reorganization process ("systems consolidation") that shifts memory expression away from recruiting mainly the hippocampus to invoking extra-hippocampal areas (Poulos et al., 2016; Wiltgen & Silva, 2007). Generalization effects seen after a single training trial also usually take several days to appear (Balogh & Wehner, 2003; Poulos et al., 2016; Wiltgen & Silva, 2007). Therefore, it is unlikely that decreased pre-CS freezing observed after 24 h in our cKO mice reflects a deceleration of fear generalization.

We can only speculate to explain this finding. Generalization of fear at 24 h increases with shock intensity (Baldi, Lorenzini, & Bucherelli, 2004; Fanselow, 1980) (Gazarini, Stern, & Bertoglio, 2023; Ghosh & Chattarji, 2015). It is possible that the loss of CAPN15 affects the differential sensing of the shock intensity required for this. An interesting alternative interpretation for the decrease in pre-CS freezing of the *Capn15* cKO arises from findings in *Aplysia*, in which the analogous SOL calpain critically contributes to non-associative plasticity. In *Aplysia* sensorimotor cocultures, long-term non-associative facilitation can be induced by the neurotransmitter serotonin, without presynaptic tetanus, through heterosynaptic facilitation (Hu et al., 2017b). Applied to our corresponding rodent model, pre-CS freezing during the auditory fear conditioning test may reflect non-associative responding, to a certain degree, in that the fear conditioning induced a non-specific (i.e., cue-generalized) fear response in any situation that remotely resembles the original training situation. This is conceptually different from contextual fear generalization, which requires more time to develop and involves complex interactions between various brain regions. Rather, we suggest that the conditioning itself can induce an increased fear-related reactivity, similar to non-associative sensitization in *Aplysia*, that will

manifest in any stressful situations, and this form of plasticity involves CAPN15 in rodents. Clearly, more research will be necessary to determine how CAPN15 affects fear conditioning in vertebrates.

While we did not find many behavioral differences between the genotypes, we often noted differences between the sexes. Female mice travelled longer distances in the open field (Fig. 1) and during marble burying (Fig. 4), showed a strong trend to express more entries in the elevated plus maze (Fig. 2), and a strong trend to spend more time examining objects in the novel object location task (Fig. 6). Indeed, it is typically found in rodent studies that female animals travel longer distances than males (Sestakova, Puzserova, Kluknavsky, & Bernatova, 2013), which can explain sex differences in various behavioral tasks. This does not, however, explain the decreased freezing in fear conditioning and decreased pre-CS freezing that we observed. Lower freezing in female rodents has been observed in other studies, and may be due to different behavioral responses to fear in females compared to males (Gruene, Flick, Stefano, Shea, & Shansky, 2015). In some transgenic animal models, increased activity in stressful situations is accompanied by less freezing after fear conditioning (Anstey et al., 2022). Another factor possibly contributing to behavioral sex differences is the biological sex of the experimenter. For example, a male experimenter induces more stress in rodents than a female one, and, depending on the task, this could affect the behavior of male and female rodents in different ways (Sorge et al., 2014). We only observed such differences, however, in fear conditioning, and not in other potentially stressful tasks, such as the elevated plus maze or behavior in the open field. Therefore, it is not clear how much of the sex difference in fear conditioning can be explained by an experimenter effect. An effect of conditional knockout of *Capn15* on pre-CS freezing following training with a 0.7 mA shock was only observed in male

mice, but this result was not replicated in the naïve animals, which might have been affected by the use of fewer animals. The interaction between sex and genotype was not found with the stronger shock protocol although the effect was larger in the male group (Fig. 8A). Whether this reflects a sex-specific effect of CAPN15 loss or a threshold effect due to the decreased pre-CS freezing seen in female compared to male mice will require further studies.

4.7 Conclusion

In conclusion, we report that the loss of CAPN15 in forebrain excitatory neurons in the adult alters certain behaviors, such as marble burying, rotarod and fear generalization in auditory fear conditioning. Complete loss of CAPN15 causes a neurodevelopmental disorder, and the fact that we do not observe a behavioral profile that consistently shows deficits in various cognitive domains, we believe that our conditional KO animal can only model parts of the pathology as CAPN15 seems to play a critical role during development, that is altered in the adult organism. Clearly, more experiments are required to understand the role of CAPN15 in behavior and to identify the underlying molecular mechanisms.

4.8 Acknowledgements

We thank Karim Nader for advice in the early stages of this project.

4.9 Funding sources

This work was supported by Canadian Institute of Health Researcproject grant 180274

4.10 Figures and legends

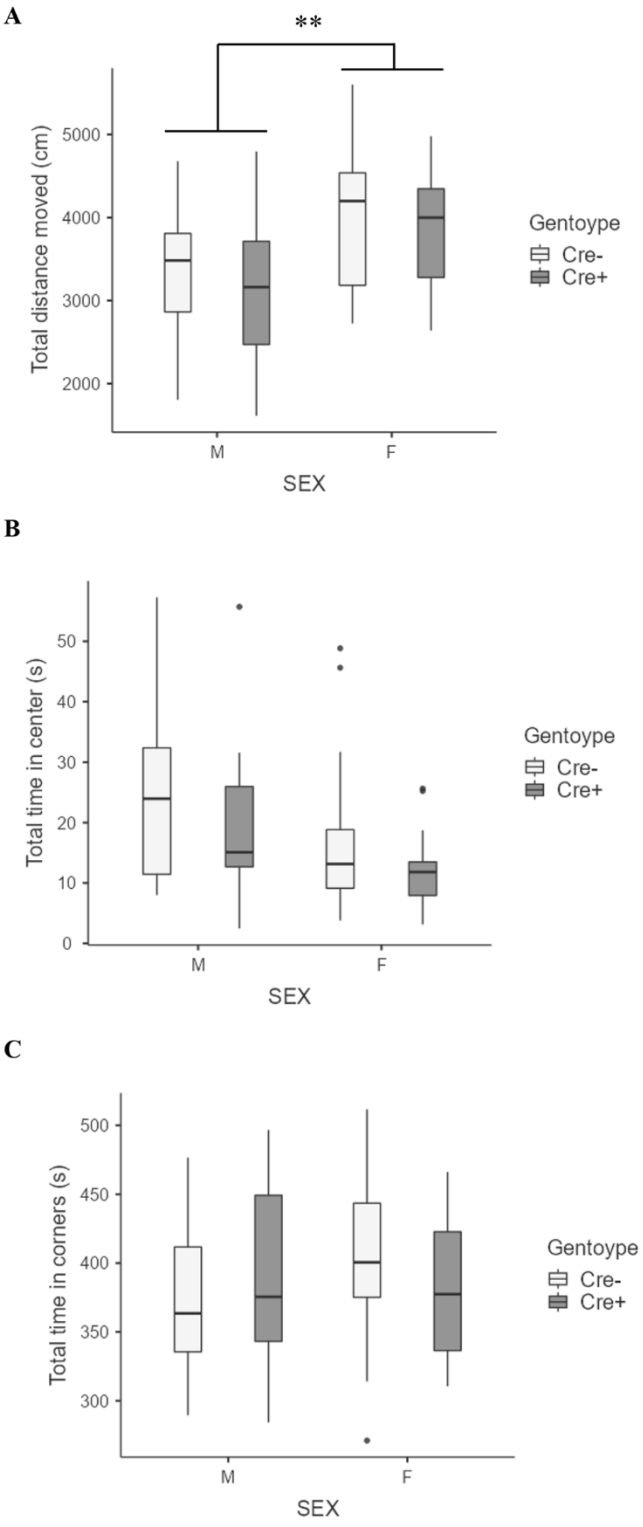

Figure 4.1. Female mice were more active than male mice.

(A) Box and whisker plots showing total distance moved during open field tests (number of cohorts = 4). Female mice moved significantly more than male mice did (ANOVA; $F_{(1,68)}$ = 10.1290; p = 0.002; η_p^2 = 0.130). No significant difference was observed between two genotypes (ANOVA; $F_{(1,68)}$ = 0.1597; p = 0.691). (B, C) Box and whisker plots showing time spent in corners vs. center during tests (number of cohorts = 4). Mice in all groups showed a strong place preference (Repeated measure of ANOVA; $F_{(1,68)}$ = 2726.9051; $p < 0.001$; η_p^2 = 0.976). n = 19 for male Cre-; n = 21 for female Cre-; n = 17 for male Cre+; n = 15 for female Cre+. Dots are data points outside the box and whiskers. **$p < 0.01$. One male Cre-and one male Cre+ were removed as outliers (Grubb's test).

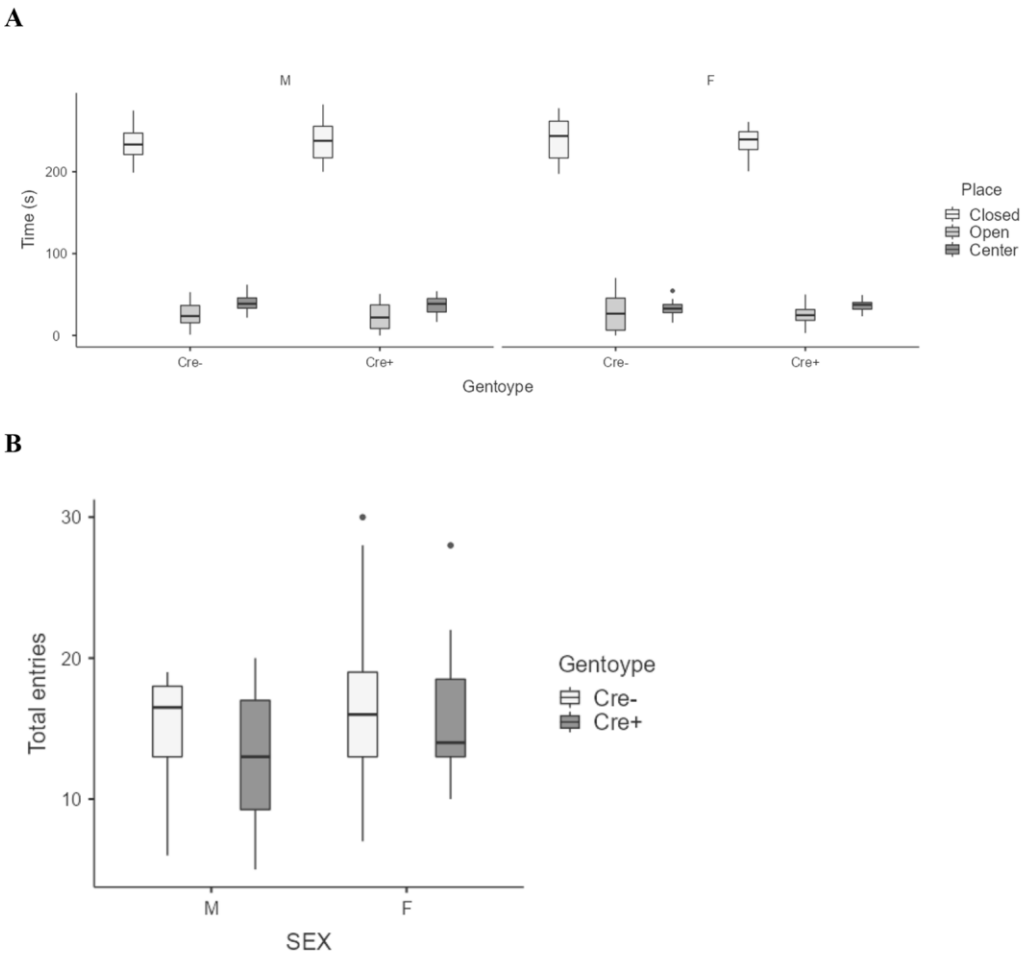

Figure 4.2. All mice preferred to explore closed arms than open arms or the center.

(A) Box and whisker plots showing how much time they spent in each arm during tests (number of cohorts = 4). All mice showed strong place preference (repeated measure of ANOVA, $F_{(2,140)} = 2423.592$; $p < 0.001$; $\eta_p^2 = 0.972$). (B) Mice in both genotypes made similar number of arm entries (ANOVA; $F_{(1,70)} = 1.334$; $p = 0.252$). We observed a not significant but strong trend in terms of sex, in which female mice made more arm entries than male mice did (ANOVA; $F_{(1,70)} = 3.161$; $p = 0.08$). $n = 20$ for male Cre-; $n = 21$ for female Cre-; $n = 18$ for male Cre+; $n = 15$ for female Cre+. Dots are data points outside the box and whiskers.

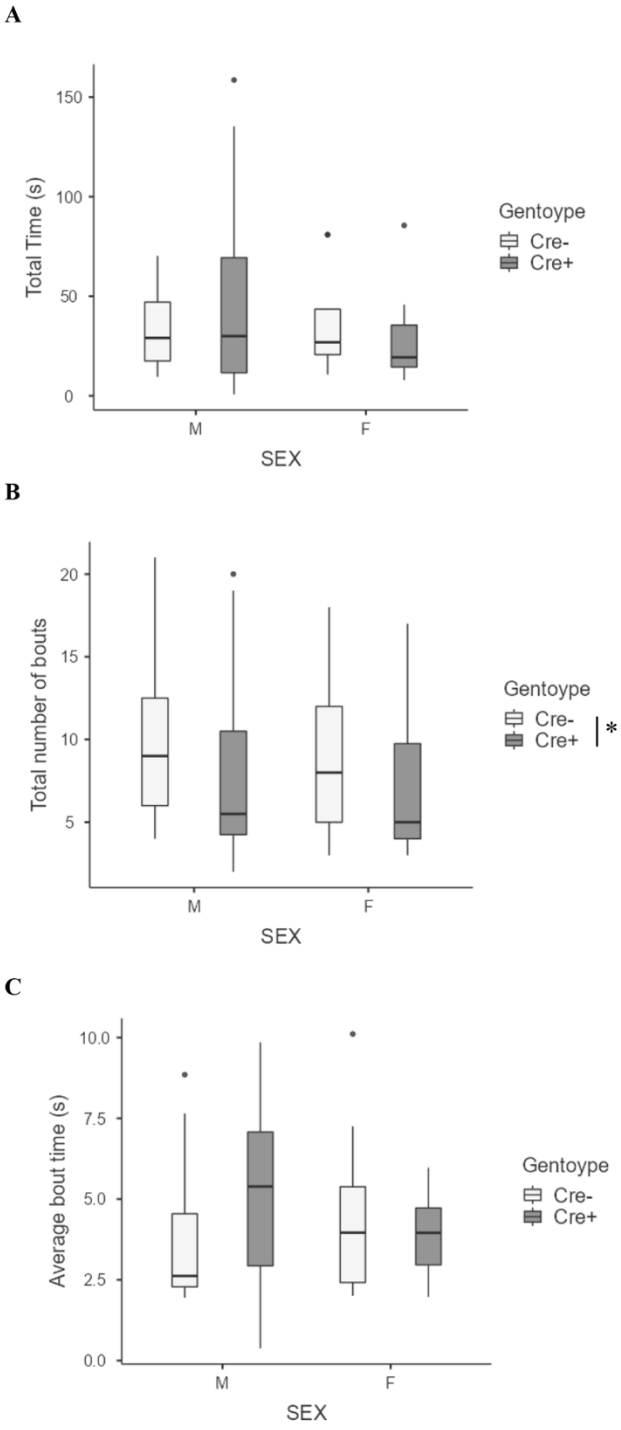

Figure 4.3. *Capn15* cKO mice performed fewer bouts.

(A) Box and whisker plots showing total time of grooming during the last 10 minutes of the recording (number of cohorts = 4). No significant difference was observed between two genotypes (Kruskal-Wallis non-parametric one-way ANOVA; p = 0.571) or sexes (Kruskal-Wallis non-parametric one-way ANOVA; p = 0.589). (B) Box and whisker plots showing total number of bouts during the last 10 minutes of the recording (number of cohorts = 4). *CAPN15* cKO mice performed significantly fewer bouts (Kruskal-Wallis non-parametric one-way ANOVA; p = 0.05). No significant difference was observed between two sexes (Kruskal-Wallis non-parametric one-way ANOVA; p = 0.526). (C) Box and whisker plots showing average bout time during the last 10 minutes of the recording (number of cohorts = 4). No significant difference was observed between two genotypes (Kruskal-Wallis non-parametric one-way ANOVA; p = 0.160) or sexes (Kruskal-Wallis non-parametric one-way ANOVA; p = 0.888). n = 19 for male Cre-; n = 21 for female Cre-; n = 18 for male Cre+; n = 14 for female Cre+. Dots are data points outside the box and whiskers. *$p < 0.05$. One male Cre- and one female Cre+ were removed as outliers (Grubb's test).

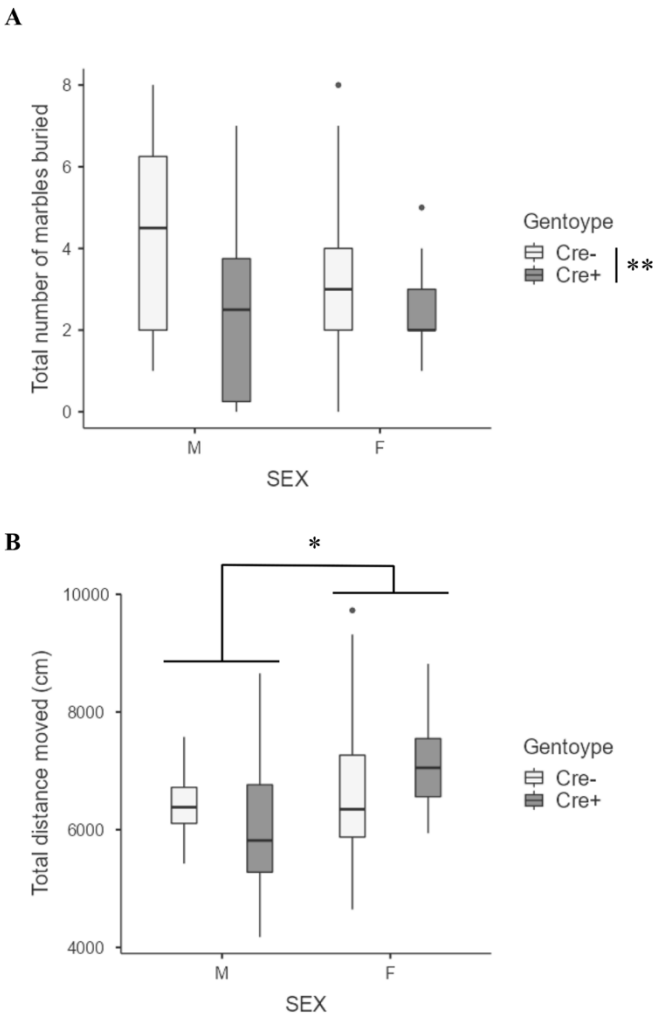

Figure 4.4. *Capn15* cKO bury significantly fewer marbles than the control.

(A) Box and whisker plots showing how many marbles are buried during tests (number of cohorts = 4). *CAPN15* cKO bury significantly fewer marbles than the control (Kruskal-Wallis non-parametric one-way ANOVA; $p = 0.008$). There is no significant difference in sex (Kruskal-Wallis non-parametric one-way ANOVA, $p = 0.607$). $n = 20$ for male Cre-; $n = 21$ for female Cre-; $n = 18$ for male Cre+; $n = 14$ for female Cre+. (B) Box and whisker plots showing distance total distance moved during tests (number of cohorts = 3). Female mice moved significantly more than male mice did (Kruskal-Wallis non-parametric one-way ANOVA; $p = 0.029$). There is

no significant difference between genotypes (Kruskal-Wallis non-parametric one-way ANOVA; $p = 0.956$). $n = 14$ for female Cre+; $n = 14$ for male Cre+; $n = 14$ for female Cre-; $n = 10$ for male Cre-. Dots are data points outside the box and whiskers. *$p < 0.05$, **$p < 0.01$. One female Cre+ was removed as an outlier (Grubb's test).

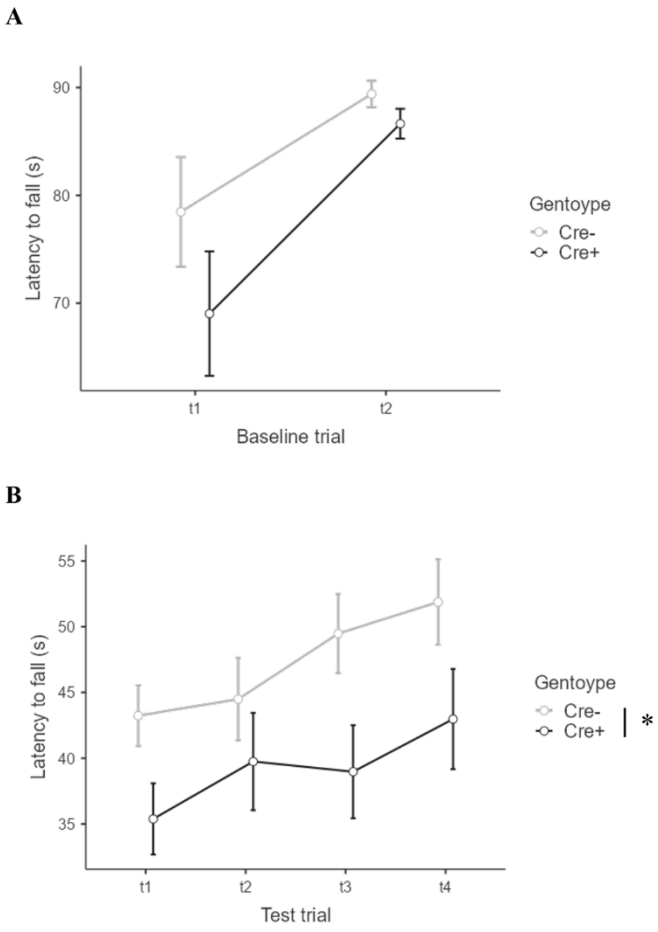

Figure 4.5. *Capn15* cKO performed poorly in accelerating rotarod training.

(A) Graph showing how long mice were able to stay on the rod without falling during baseline rotarod training (number of cohorts = 3). There is no significant difference in performance during training between two genotypes (repeated measure of ANOVA, $F_{(1,53)} = 2.4159$, $p = 0.126$) or two sexes (repeated measure of ANOVA, $F_{(1,53)} = 0.0453$, $p = 0.836$). Error bars represent SEM. (B) Graph showing how long mice were able to stay on the rod without falling during accelerating rotarod training (number of cohorts = 3). *Capn15* cKO performed poorly in general compared to Cre- control (repeated measure of ANOVA, $F_{(1,53)} = 4.2979$, p = 0.043; $\eta_p^2 = 0.075$). There is no difference in performance between two sexes (repeated measure of

ANOVA, $F_{(1,53)} = 0.0869$, p = 0.769). $n = 16$ for male Cre-; $n = 17$ for female Cre-; $n = 14$ for male Cre+; $n = 11$ for female Cre+. Error bars represent SEM. *$p < 0.05$.

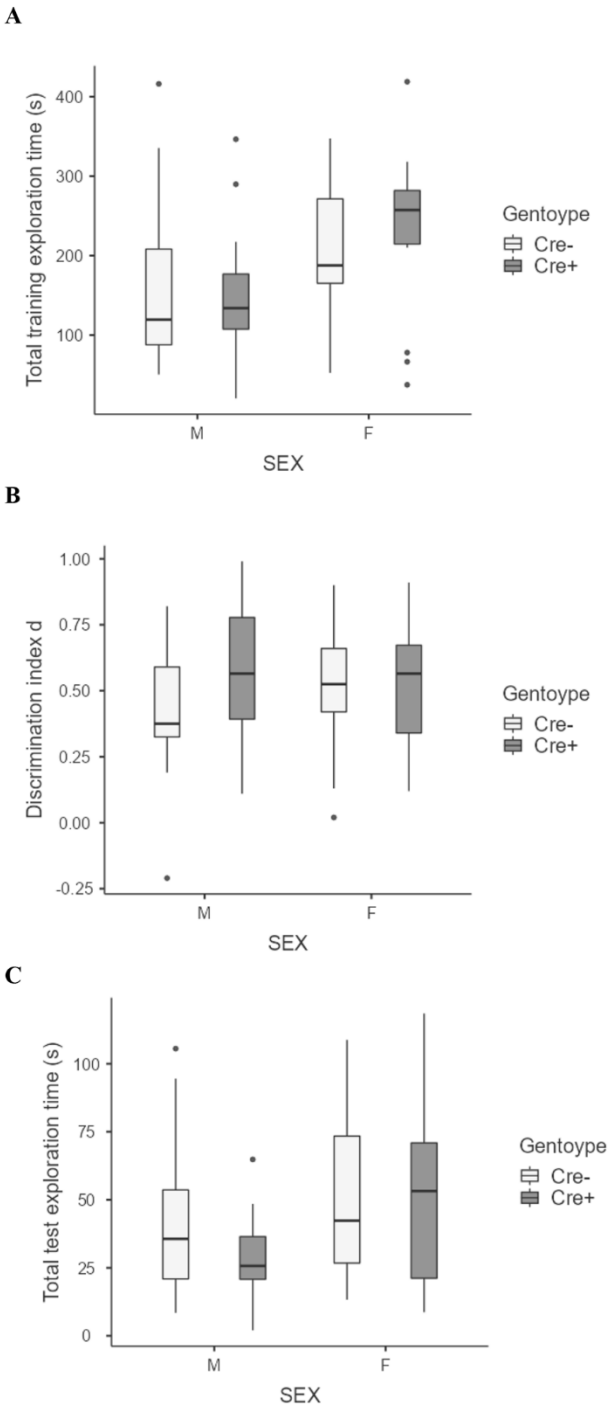

Figure 4.6. Mice in all groups showed similar level of preference to the object at novel location during object location test.

(A) Box and whisker plots showing how much time they spent exploring objects during training (number of cohorts = 4). Mice in all groups spent similar amount of time exploring objects during training as there is no significant difference between genotypes (ANOVA; $F_{(1,51)}$ = 0.2025; p = 0.655) or sexes (ANOVA; $F_{(1,51)}$ = 3.4919; p = 0.067). (B) Box and whisker plots showing the discrimination index between each group during test (number of cohorts = 4). Mice in all groups displayed similar level of preference to the object moved to the novel location as there was no significant difference between genotypes (ANOVA; $F_{(1,51)}$ = 1.589; p = 0.213) or sexes (ANOVA; $F_{(1,51)}$ = 0.135; p = 0.715). One sample t-tests showed that all groups exceeded the chance level of 0 ($p < 0.001$), expressing novelty preference. (C) Box and whisker plots showing how much time they spent exploring objects during test (number of cohorts = 4). Mice in all groups spent similar amount of time exploring objects during testing as there is no significant difference between genotypes (Kruskal-Wallis non-parametric one-way ANOVA test; p = 0.446) or sexes (Kruskal-Wallis non-parametric one-way ANOVA test; p = 0.100). n = 14 for male Cre-; n = 14 for female Cre-; n = 12 for male Cre+; n = 14 for female Cre+. Dots are data points outside the box and whiskers. Five male Cre-, 5 male Cre+, 7 female Cre- and 1 female Cre+ were removed because they spent less than 50 s exploring objects during training and less than 20 s exploring objects during the test. One male Cre- and one male Cre+ were removed as outliers (Grubb's test).

A

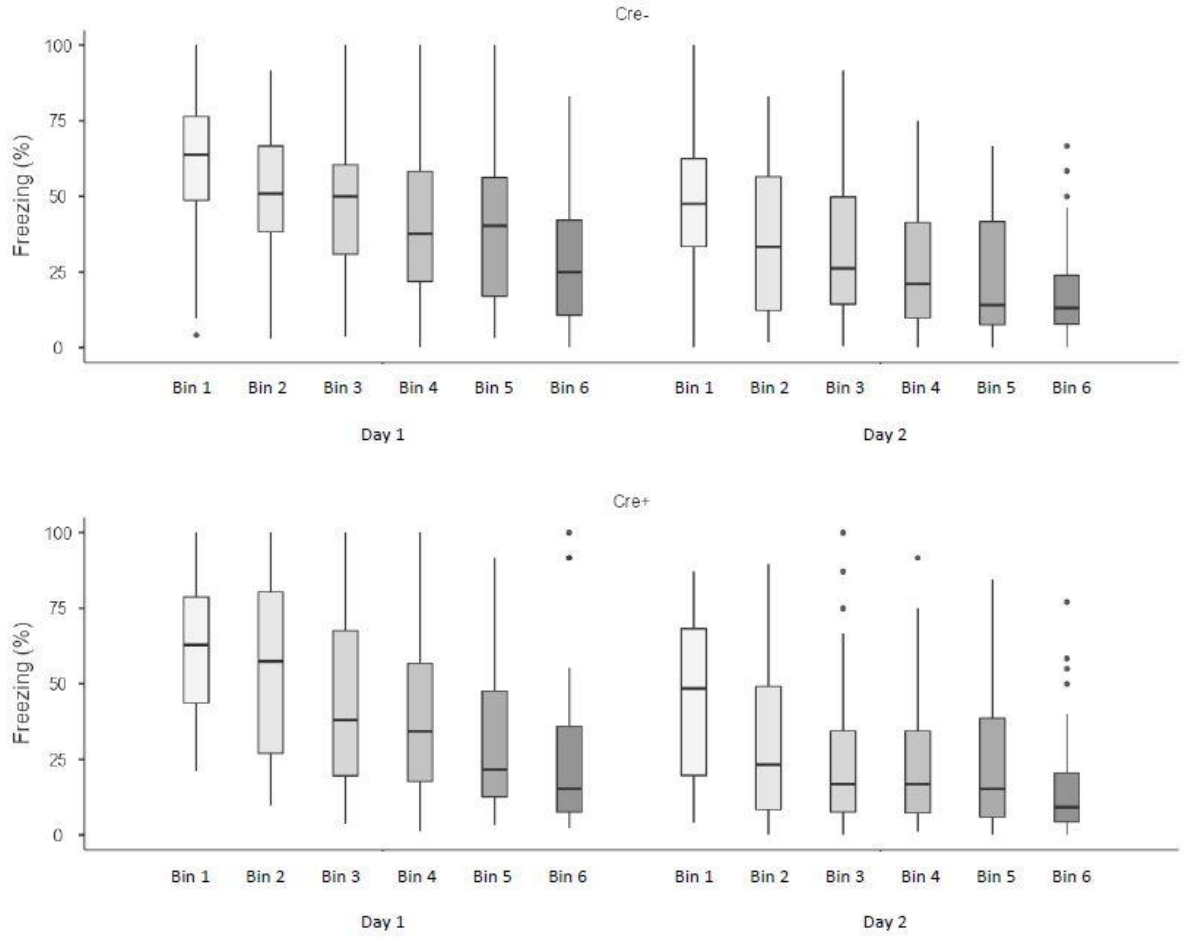
Cre-
Freezing (%)
100
75
50
25
0
Bin 1
Bin 2
Bin 3
Bin 4
Bin 5
Bin 6
Day 1
Day 2
Cre+
Freezing (%)
Bin 1
Bin 2
Bin 3
Bin 4
Bin 5
Bin 6
Day 1
Day 2

B

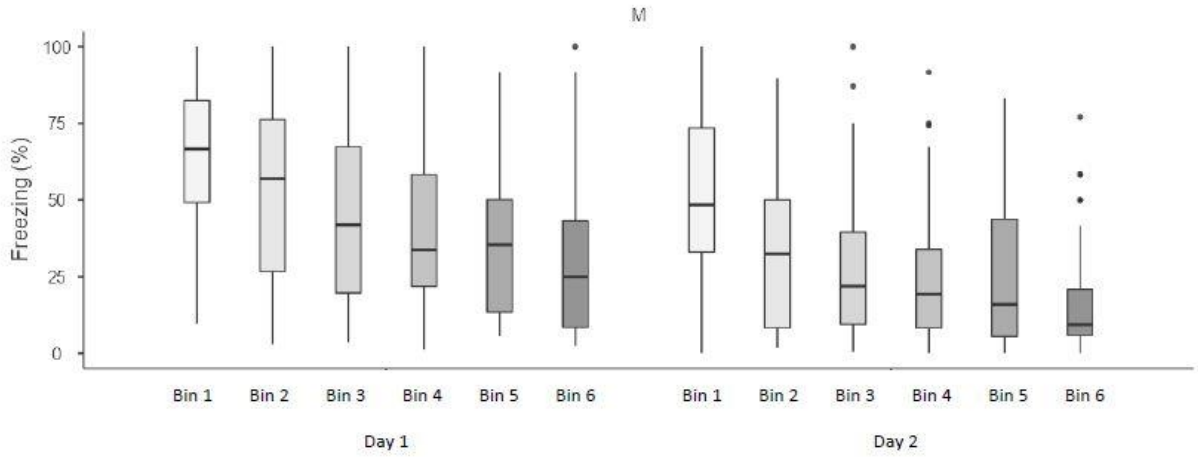
M
Freezing (%)
100
75
50
25
0
Bin 1
Bin 2
Bin 3
Bin 4
Bin 5
Bin 6
Day 1
Day 2

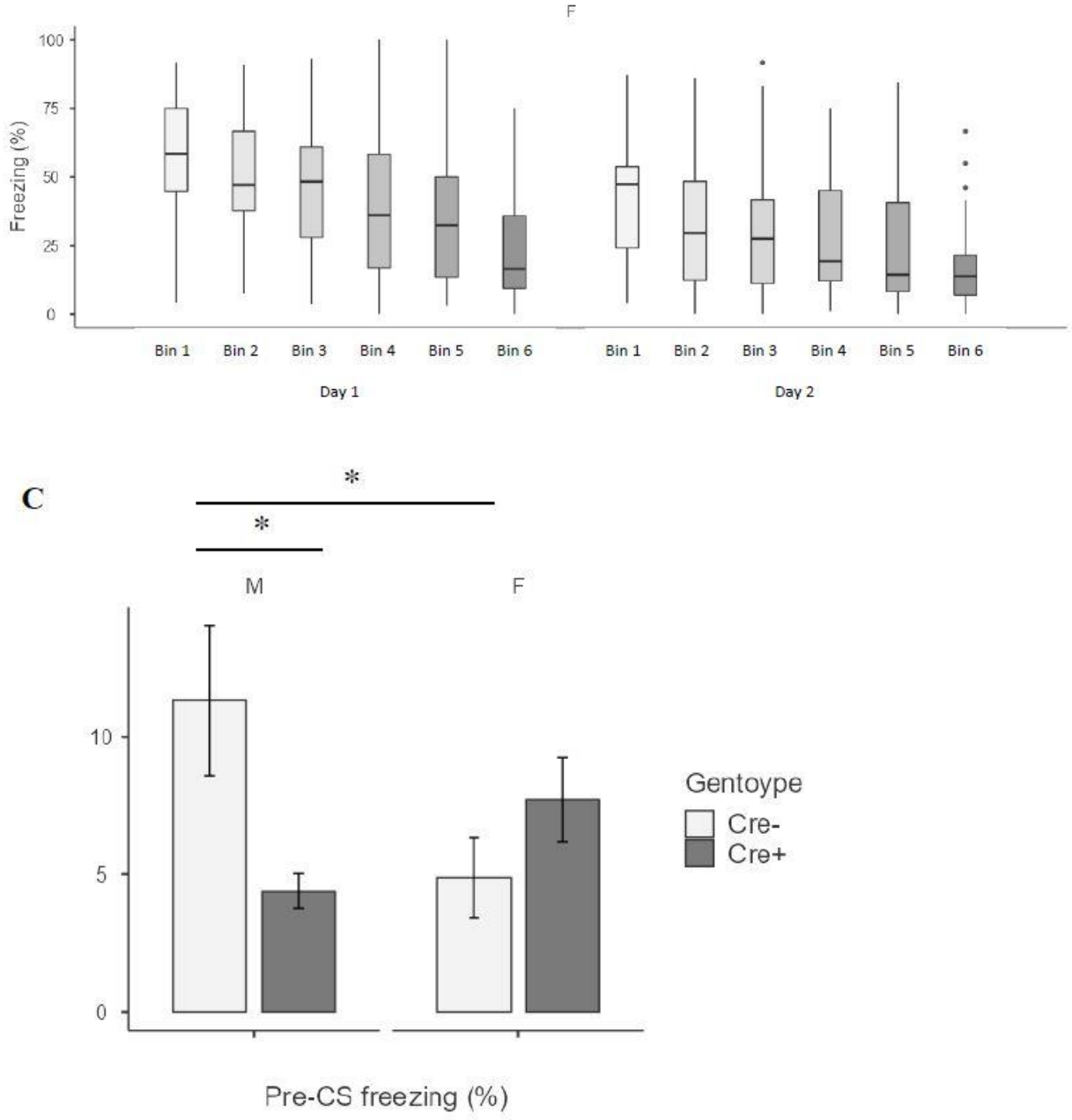

Figure 4.7. Quantification of auditory fear conditioning/extinction.

(A, B) Box and whisker plots showing quantification of freezing of mice in standard training group towards tones (number of cohorts = 4). A: difference between two genotypes; B: difference between two sexes. Mice of both genotypes and sexes froze at similar level (repeated

measure of ANOVA; $F < 1$). n = 18 for male Cre-; n = 20 for female Cre-; n = 18 for male Cre+; n = 13 for female Cre+. (C) Graph showing how much mice froze before the presentation of first tone in standard shock group (number of cohorts = 3). We detected a significant genotype and sex interaction (ANOVA, $F_{(1,44)} = 10.14$; $p = 0.003$; $\eta_p^2 = 0.187$), that male control mice froze significantly more than male *Capn15* cKO mice ($t = 3.015$; $p_{tukey} = 0.021$), and female control mice ($t = 2.765$; $p_{tukey} = 0.04$). Dots are data points outside the box and whiskers. 1 male Cre-, one female Cre- and 2 female Cre+ were removed due to excessive pre-CS freezing (>30%). One male Cre- was removed due to apparatus malfunction. *$p < 0.05$.

A

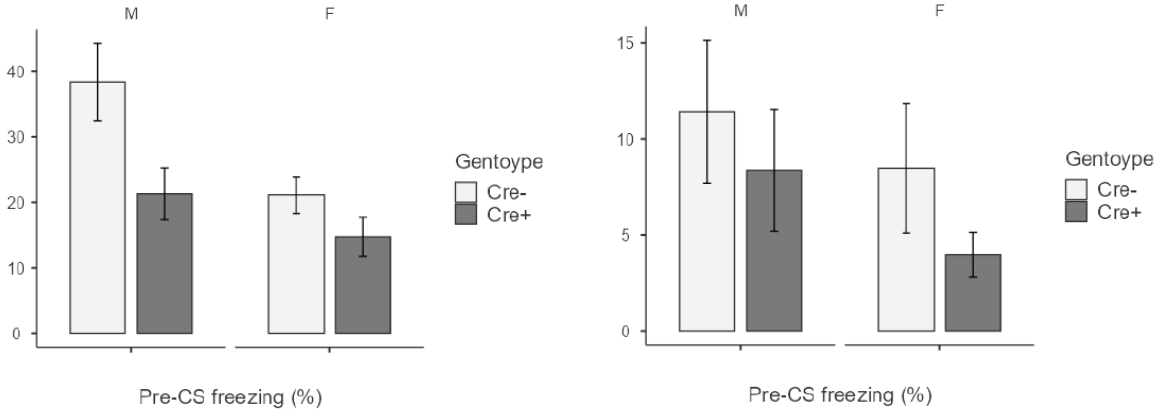
M
F
40
30
20
10
0
Gentoype
Cre-
Cre+
Pre-CS freezing (%)
M
F
15
10
5
0
Gentoype
Cre-
Cre+
Pre-CS freezing (%)

B

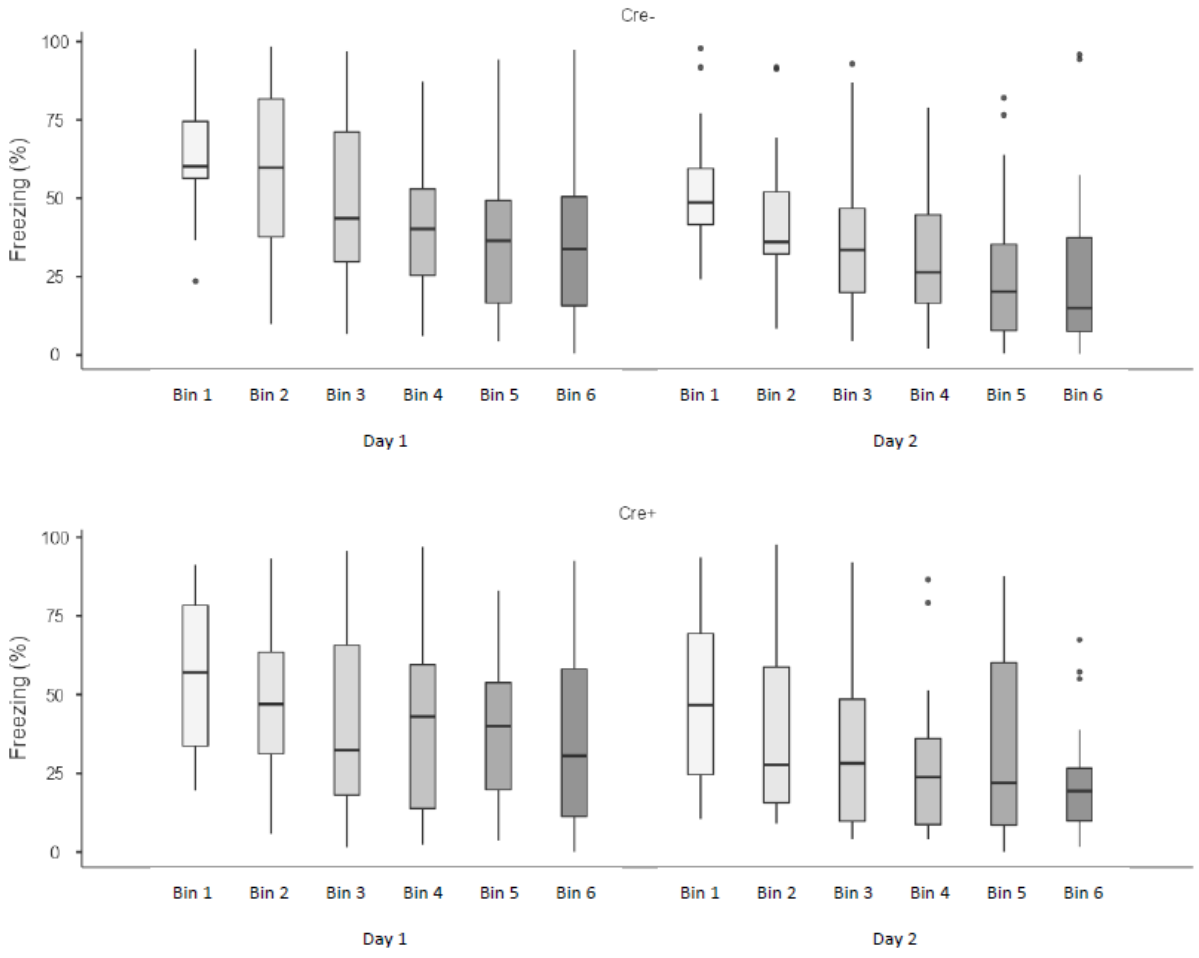
Cre-
Freezing (%)
100
75
50
25
0
Bin 1
Bin 2
Bin 3
Bin 4
Bin 5
Bin 6
Day 1
Day 2
Cre+
Freezing (%)
Day 1
Day 2

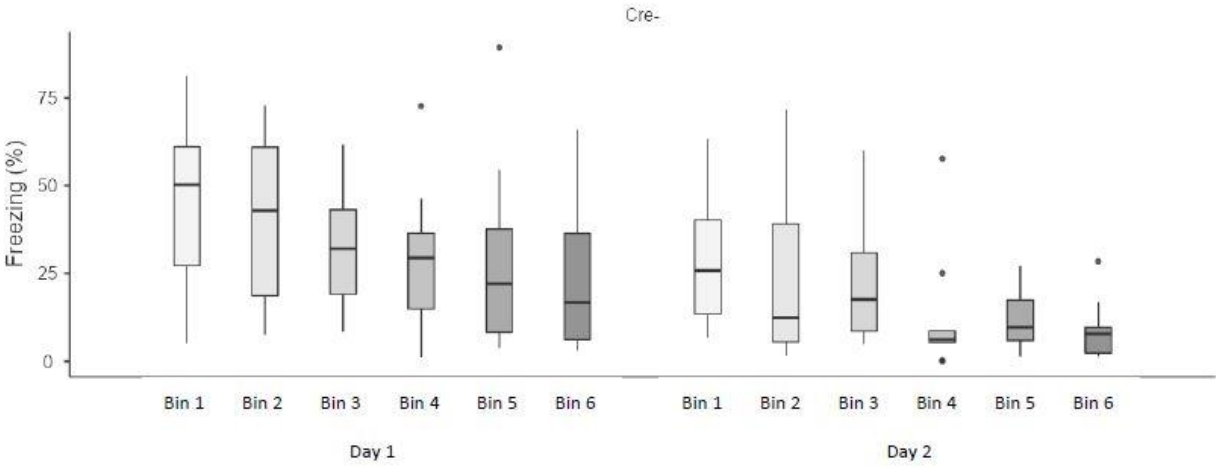
Cre-
Freezing (%)
75
50
25
0
Bin 1
Bin 2
Bin 3
Bin 4
Bin 5
Bin 6
Day 1
Day 2

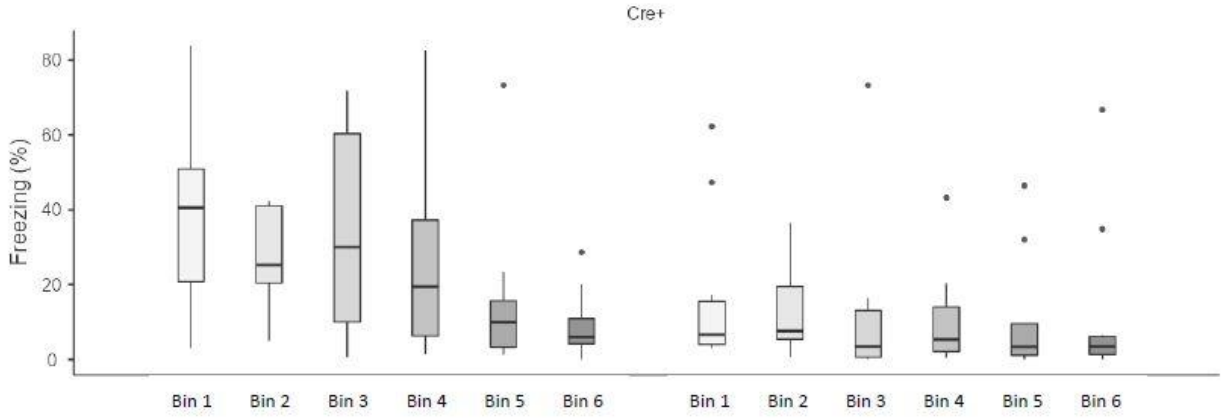
Cre+
Freezing (%)
80
60
40
20
0
Bin 1
Bin 2
Bin 3
Bin 4
Bin 5
Bin 6

C

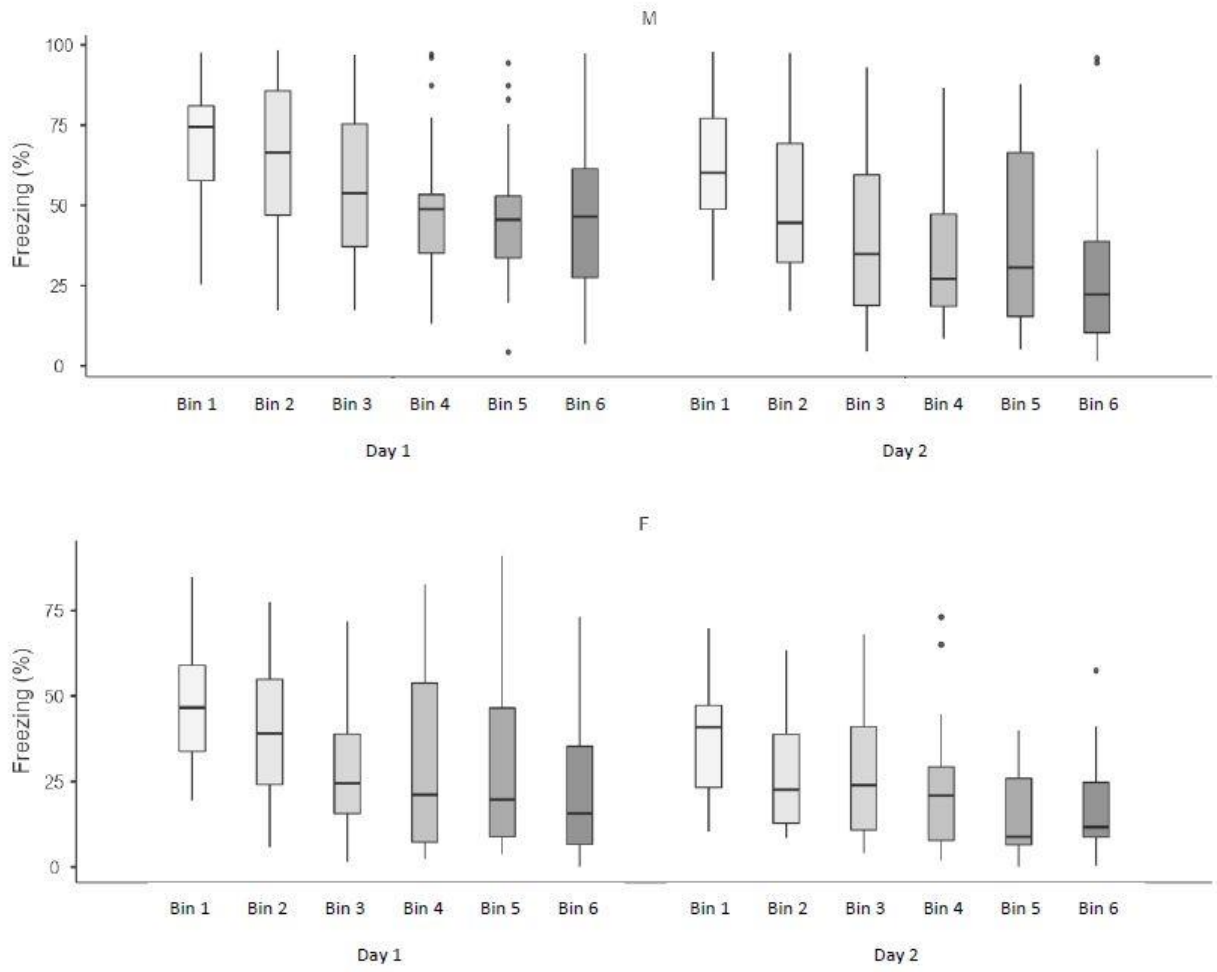
M
Freezing (%)
100
75
50
25
0
Bin 1
Bin 2
Bin 3
Bin 4
Bin 5
Bin 6
Day 1
Day 2
F
Freezing (%)
75
50
25
0
Bin 1
Bin 2
Bin 3
Bin 4
Bin 5
Bin 6
Day 1
Day 2

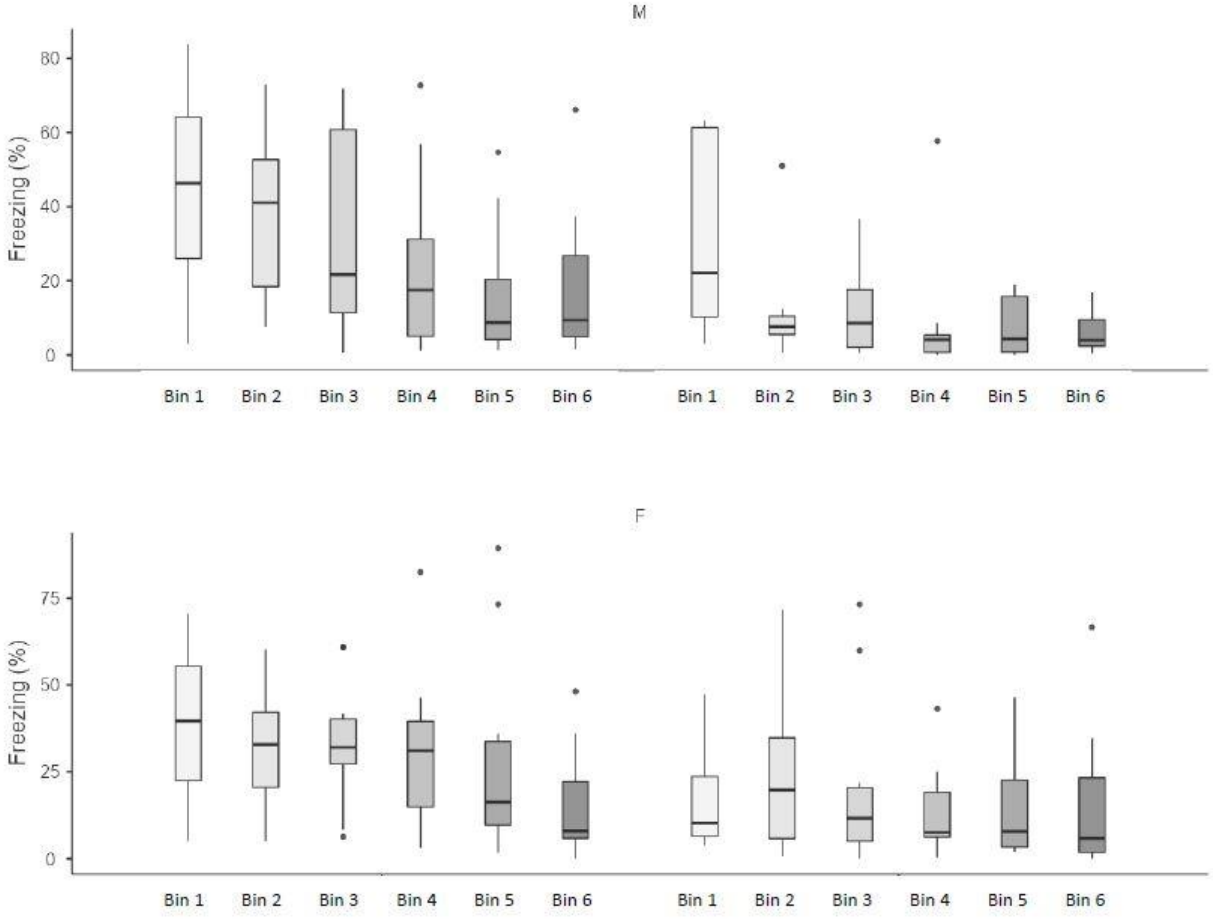

Figure 4.8. *Capn15* cKO mice showed less pre-CS freezing after training with stronger shocks. (A) Graph showing how much mice froze before the presentation of first tone in (left) strong shock group and (right) standard shock group (number of cohorts = 2). Mice in strong shock group froze significantly more than those in standard shock group (ANOVA; $F_{(1,63)}$ = 22.65; $p < 0.001$; $\eta_p^2 = 0.26$). *Capn15* cKO mice froze significantly less than the control mice (ANOVA; $F_{(1,63)} = 6.08$; $p = 0.016$; $\eta_p^2 = 0.09$). (B) Box and whisker plots showing quantification of freezing of mice between genotypes in (top) strong training group and (bottom) standard training group towards tones (number of cohorts = 2). Mice of both genotypes froze at similar level (repeated measure of ANOVA; $F_{(1,59)} = 1.76$; $p = 0.189$). (C) Box and whisker plots

showing quantification of freezing of mice between sexes in (top) strong training group and (bottom) standard training group towards tones (number of cohorts = 2). Female mice froze significantly less than male mice (repeated measure of ANOVA; $F_{(1,59)} = 5.07$; $p = 0.028$; $\eta_p^2 = 0.08$). Only male mice froze more to stronger shocks, but not female mice (repeated measure of ANOVA; $F_{(1,59)} = 7.52$, $p = 0.008$, $\eta_p^2 = 0.11$). Dots are data points outside the box and whiskers. For strong shock group, $n = 13$ for male Cre-; $n = 12$ for female Cre-; $n = 12$ for male Cre+; $n = 11$ for female Cre+. For standard shock group, $n = 6$ for male Cre-; $n = 6$ for female Cre-; $n = 5$ for male Cre+; $n = 6$ for female Cre+. One male Cre+ were removed due to excessive pre-CS freezing (>30%). Error bars represent SEM.

4.11 References

Anstey, N. J., Kapgal, V., Tiwari, S., Watson, T. C., Toft, A. K. H., Dando, O. R., . . . Kind, P. C. (2022). Imbalance of flight-freeze responses and their cellular correlates in the Nlgn3(-/y) rat model of autism. *Mol Autism, 13*(1), 34. doi: 10.1186/s13229-022-00511-8

Augereau, K., Migues, P. V., & Hardt, O. (2022). Infusing zeta inhibitory peptide into the perirhinal cortex of rats abolishes long-term object recognition memory without affecting novel object location recognition. *Front Behav Neurosci, 16*, 1007748. doi: 10.3389/fnbeh.2022.1007748

Baldi, E., Lorenzini, C. A., & Bucherelli, C. (2004). Footshock intensity and generalization in contextual and auditory-cued fear conditioning in the rat. *Neurobiol Learn Mem, 81*(3), 162-166. doi: 10.1016/j.nlm.2004.02.004

Balogh, S. A., & Wehner, J. M. (2003). Inbred mouse strain differences in the establishment of long-term fear memory. *Behav Brain Res, 140*(1-2), 97-106. doi: 10.1016/s0166-4328(02)00279-6

Beaman, M. M., Guidugli, L., Hammer, M., Barrows, C., Gregor, A., McDonald, M., . . . Cohen, J. L. (2022). Dandy Walker malformation in three unrelated families with biallelic variants in CAPN15 expands the phenotypic spectrum of oculogastrointestinal neurodevelopmental disorder. *Genetics in Medicine, 24*(3), S53-S54. doi: 10.1016/j.gim.2022.01.118

Brito, V., Montalban, E., Sancho-Balsells, A., Pupak, A., Flotta, F., Masana, M., . . . Giralt, A. (2022). Hippocampal Egr1-Dependent Neuronal Ensembles Negatively Regulate Motor Learning. *J Neurosci, 42*(27), 5346-5360. doi: 10.1523/JNEUROSCI.2258-21.2022

Broekkamp, C. L., Rijk, H. W., Joly-Gelouin, D., & Lloyd, K. L. (1986). Major tranquillizers can be distinguished from minor tranquillizers on the basis of effects on marble burying and swim-induced grooming in mice. *Eur J Pharmacol, 126*(3), 223-229. doi: 10.1016/0014-2999(86)90051-8

Delaney, S. J., Hayward, D. C., Barleben, F., Fischbach, K. F., & Miklos, G. L. (1991). Molecular cloning and analysis of small optic lobes, a structural brain gene of Drosophila melanogaster. *Proc Natl Acad Sci U S A, 88*(16), 7214-7218. doi: 10.1073/pnas.88.16.7214

Fanselow, M. S. (1980). Conditioned and unconditional components of post-shock freezing. *Pavlov J Biol Sci, 15*(4), 177-182. doi: 10.1007/BF03001163

Farmer, W. T., Abrahamsson, T., Chierzi, S., Lui, C., Zaelzer, C., Jones, E. V., . . . Murai, K. K. (2016). Neurons diversify astrocytes in the adult brain through sonic hedgehog signaling. *Science, 351*(6275), 849-854. doi: 10.1126/science.aab3103

Fischbach, K. F., & Heisenberg, M. (1981). Structural brain mutant of Drosophila melanogaster with reduced cell number in the medulla cortex and with normal optomotor yaw response. *Proc Natl Acad Sci U S A, 78*(2), 1105-1109. doi: 10.1073/pnas.78.2.1105

Gazarini, L., Stern, C. A. J., & Bertoglio, L. J. (2023). On making (and turning adaptive to) maladaptive aversive memories in laboratory rodents. *Neurosci Biobehav Rev, 147*, 105101. doi: 10.1016/j.neubiorev.2023.105101

Ghosh, S., & Chattarji, S. (2015). Neuronal encoding of the switch from specific to generalized fear. *Nat Neurosci, 18*(1), 112-120. doi: 10.1038/nn.3888

Gruene, T. M., Flick, K., Stefano, A., Shea, S. D., & Shansky, R. M. (2015). Sexually divergent expression of active and passive conditioned fear responses in rats. *Elife, 4*. doi: 10.7554/eLife.11352

Guroff, G. (1964). A Neutral, Calcium-Activated Proteinase from the Soluble Fraction of Rat Brain. *J Biol Chem, 239*, 149-155.

Hastings, M. H., Gong, K., Freibauer, A., Courchesne, C., Fan, X., & Sossin, W. S. (2017). Novel calpain families and novel mechanisms for calpain regulation in Aplysia. *PLoS One, 12*(10), e0186646. doi: 10.1371/journal.pone.0186646

Hu, J., Adler, K., Farah, C. A., Hastings, M. H., Sossin, W. S., & Schacher, S. (2017). Cell-Specific PKM Isoforms Contribute to the Maintenance of Different Forms of Persistent Long-Term Synaptic Plasticity. *J Neurosci, 37*(10), 2746-2763. doi: 10.1523/JNEUROSCI.2805-16.2017

Hu, J., Ferguson, L., Adler, K., Farah, C. A., Hastings, M. H., Sossin, W. S., & Schacher, S. (2017). Selective Erasure of Distinct Forms of Long-Term Synaptic Plasticity Underlying Different Forms of Memory in the Same Postsynaptic Neuron. *Curr Biol, 27*(13), 1888-1899 e1884. doi: 10.1016/j.cub.2017.05.081

jamovi. (2022). jamovi: The jamovi project. Retrieved from www.jjamovi.org

Kalueff, A. V., Stewart, A. M., Song, C., Berridge, K. C., Graybiel, A. M., & Fentress, J. C. (2016). Neurobiology of rodent self-grooming and its value for translational neuroscience. *Nat Rev Neurosci, 17*(1), 45-59. doi: 10.1038/nrn.2015.8

Kandel, E. R. (2001). The molecular biology of memory storage: a dialogue between genes and synapses. *Science, 294*(5544), 1030-1038. doi: 10.1126/science.1067020

Kandel, E. R., & Schwartz, J. H. (1982). Molecular biology of learning: modulation of transmitter release. *Science, 218*(4571), 433-443. doi: 10.1126/science.6289442

Marinesco, S., & Carew, T. J. (2002). Serotonin release evoked by tail nerve stimulation in the CNS of aplysia: characterization and relationship to heterosynaptic plasticity. *J Neurosci, 22*(6), 2299-2312. doi: 10.1523/JNEUROSCI.22-06-02299.2002

Marino, T. C., Leblanc, J., Pratte, A., Tardif, J., Thomas, M.-J., Fortin, C.-A., . . . Bouchard, L. (2023). Portrait of autosomal recessive diseases in the French-Canadian founder population of Saguenay-Lac-Saing-Jean. *American Journal of Human Genetics part A, 191*(5), 1145-1163. doi: https://doi.org/10.1002/ajmg.a.63147

Mor-Shaked, H., Salah, S., Yanovsky-Dagan, S., Meiner, V., Atawneh, O. M., Abu-Libdeh, B., . . . Harel, T. (2021). Biallelic deletion in a minimal CAPN15 intron in siblings with a recognizable syndrome of congenital malformations and developmental delay. *Clin Genet, 99*(4), 577-582. doi: 10.1111/cge.13920

Pasciuto, E., Borrie, S. C., Kanellopoulos, A. K., Santos, A. R., Cappuyns, E., D'Andrea, L., . . . Bagni, C. (2015). Autism Spectrum Disorders: Translating human deficits into mouse behavior. *Neurobiol Learn Mem, 124*, 71-87. doi: 10.1016/j.nlm.2015.07.013

Poulos, A. M., Mehta, N., Lu, B., Amir, D., Livingston, B., Santarelli, A., . . . Fanselow, M. S. (2016). Conditioning- and time-dependent increases in context fear and generalization. *Learn Mem, 23*(7), 379-385. doi: 10.1101/lm.041400.115

Rosso, M., Wirz, R., Loretan, A. V., Sutter, N. A., Pereira da Cunha, C. T., Jaric, I., . . . Voelkl, B. (2022). Reliability of common mouse behavioural tests of anxiety: A systematic review and meta-analysis on the effects of anxiolytics. *Neurosci Biobehav Rev, 143*, 104928. doi: 10.1016/j.neubiorev.2022.104928

Sciolino, N. R., Plummer, N. W., Chen, Y. W., Alexander, G. M., Robertson, S. D., Dudek, S. M., . . . Jensen, P. (2016). Recombinase-Dependent Mouse Lines for Chemogenetic

Activation of Genetically Defined Cell Types. *Cell Rep, 15*(11), 2563-2573. doi: 10.1016/j.celrep.2016.05.034

Sestakova, N., Puzserova, A., Kluknavsky, M., & Bernatova, I. (2013). Determination of motor activity and anxiety-related behaviour in rodents: methodological aspects and role of nitric oxide. *Interdiscip Toxicol, 6*(3), 126-135. doi: 10.2478/intox-2013-0020

Sonner, J. M., Cascio, M., Xing, Y., Fanselow, M. S., Kralic, J. E., Morrow, A. L., . . . Homanics, G. E. (2005). Alpha 1 subunit-containing GABA type A receptors in forebrain contribute to the effect of inhaled anesthetics on conditioned fear. *Mol Pharmacol, 68*(1), 61-68. doi: 10.1124/mol.104.009936

Sorge, R. E., Martin, L. J., Isbester, K. A., Sotocinal, S. G., Rosen, S., Tuttle, A. H., . . . Mogil, J. S. (2014). Olfactory exposure to males, including men, causes stress and related analgesia in rodents. *Nat Methods, 11*(6), 629-632. doi: 10.1038/nmeth.2935

Tsien, J. Z., Chen, D. F., Gerber, D., Tom, C., Mercer, E. H., Anderson, D. J., . . . Tonegawa, S. (1996). Subregion- and cell type-restricted gene knockout in mouse brain. *Cell, 87*(7), 1317-1326. doi: 10.1016/s0092-8674(00)81826-7

Wiebe, S., Nagpal, A., Truong, V. T., Park, J., Skalecka, A., He, A. J., . . . Sonenberg, N. (2019). Inhibitory interneurons mediate autism-associated behaviors via 4E-BP2. *Proc Natl Acad Sci U S A, 116*(36), 18060-18067. doi: 10.1073/pnas.1908126116

Wiltgen, B. J., & Silva, A. J. (2007). Memory for context becomes less specific with time. *Learn Mem, 14*(4), 313-317. doi: 10.1101/lm.430907

Zha, C., Farah, C. A., Fonov, V., Rudko, D. A., & Sossin, W. S. (2021). MRI of Capn15 Knockout Mice and Analysis of Capn 15 Distribution Reveal Possible Roles in Brain Development and Plasticity. *Neuroscience, 465*, 128-141. doi: 10.1016/j.neuroscience.2021.04.023

Zha, C., Farah, C. A., Holt, R. J., Ceroni, F., Al-Abdi, L., Thuriot, F., . . . Sossin, W. S. (2020). Biallelic variants in the small optic lobe calpain CAPN15 are associated with congenital eye anomalies, deafness and other neurodevelopmental deficits. *Hum Mol Genet, 29*(18), 3054-3063. doi: 10.1093/hmg/ddaa198

Zhao, S., Liang, Z., Demko, V., Wilson, R., Johansen, W., Olsen, O. A., & Shalchian-Tabrizi, K. (2012). Massive expansion of the calpain gene family in unicellular eukaryotes. *BMC Evol Biol, 12*, 193. doi: 10.1186/1471-2148-12-193

Chapter 5 - Discussion

5.1 Summary

The work in this thesis documents the phenotypes of *Capn15* KO and *CaMKII-Cre Capn15* cKO mice, which might function as a foundation for future research on CAPN15. In Chapter 2, we documented general phenotypes of *Capn15* KO mice. We found that *Capn15* KO mice are not born in a mendelian ratio and those that survived are usually accompanied by developmental eye anomalies such as microphthalmia, anophthalmia, and cataract. Human patients with homozygous or compound heterozygous variants in *CAPN15* also displayed microphthamlia/coloboma as well as other development-related phenotypes, suggesting a conserved role of CAPN15 in eye development as well as global development in mammals.

In Chapter 3, we demonstrated volumetric changes in the brain of *Capn15* KO mice and CAPN15 expression patterns in the adult brain. By using MRI, we showed that *Capn15* KO brains are around 12% smaller than the control. In addition, certain brain areas such as thalamus, CA1, CA2, and dentate gyrus of hippocampus are significantly smaller while other areas such as amygdala are bigger. By using histology, we showed that CAPN15 is expressed in brain regions that are heavily related to plasticity, such as hippocampus, amygdala, cortex as well as Purkinje cells. The expression profile of CAPN15 in adult brains does not correspond to the brain areas that are most affected by the loss of CAPN15 during development, suggesting that CAPN15 might serve different functions at different developmental stages. Unfortunately, it is still unclear why *Capn15 KO* brains are smaller, as neuronal density of CA1 pyramidal cells and cerebellar Purkinje cells is unchanged in the *Capn15 KO* group. This study also proved that *CaMKII-Cre Capn15* cKO mice do not have any signs of developmental deficits.

In Chapter 4, we demonstrated the behavioral characteristics of *CaMKII-Cre Capn15* cKO mice. Loss of CAPN15 in forebrain excitatory neurons alters certain behaviors, such as marble burying, rotarod, and fear generalization in auditory fear conditioning. We showed that *Capn15* cKO buried significantly fewer marbles, had poorer performance during accelerating rotarod test, and less fear generalization after auditory fear conditioning with strong shock intensity.

Taken together, we showed that CAPN15 is implicated not only in development, but also possibly in learning and memory. We for the first time demonstrated that *CAPN15* is a causative gene of congenital microphthalmia and/or coloboma eye disorders.

5.2 Implications

5.2.1 Involvement of CAPN15 in development supported by additional cases

Five patients reported in Chapter 2 all have homozygous or compound heterozygous missense variants in *CAPN15* and show relatively moderate phenotypes. Shortly after the publication, another two patients with a mutation in *CAPN15* were reported (Mor-Shaked et al., 2021). The two siblings have homozygous intronic deletion including a splice donor site of exon 12, resulting in skipping of exon 12 and premature termination due to frameshift. The mutation is likely to be a loss of function mutation as the two siblings showed more severe phenotypes with multiple congenital developmental anomalies. Beaman et al. reported six individuals from three unrelated families with frameshift mutations in *CAPN15*. Four patients also showed Dandy Walker malformation, characterized by malformations in cerebellum, including hypoplastic vermis, enlarged fourth ventricles, and torcular inversion (Beaman et al., 2023). Another three

patients from two unrelated families are reported by Bouchard and his colleagues. Interestingly, they share the same homozygous missense *CAPN15* variant with individuals 4 and 5 reported in Chapter 2 and all of them are from families from Saguenay-Lac-Saint-Jean region of Quebec, suggesting a founder effect in this population. The three patients showed similar eye anomalies, including coloboma, microphthalmia, corectopia, cataract, corneal opacities, and other congenital developmental deficits (Cruz Marino et al., 2023). Due to the discovery and more extensive diagnosis of new cases, novel symptoms that are not reported in Chapter 2 are gradually unveiled. The syndromic disorder due to disruption in *CAPN15* is later named oculogastrointestinal neurodevelopmental syndrome (OGIN syndrome; MIM 619318). Altogether, it clearly suggests that CAPN15 has an essential role in development, and our study has brought more spotlights to this protein.

5.2.2 Possible role of CAPN15 in development

Loss or disruption in *CAPN15* leads to multiple congenital developmental anomalies, including dysmorphic craniofacial features, ocular anomalies, hearing impairment, dental abnormalities, cardiac anomalies, genitourinary anomalies, and skeletal abnormalities. It also results in global developmental delay, seizures, microcephaly, cortical atrophy, ventricular dilation, and autism (Cruz Marino et al., 2023). Malformations of cerebellum are also discovered in some individuals (Beaman et al., 2023; Cruz Marino et al., 2023).

Cranial neural crest cells are the major cell type responsible for facial morphogenesis (Cordero et al., 2011). They migrate dorsal-laterally to pharyngeal arches and pouches and differentiate into facial cartilage, bones, cranial neurons, glia, connective tissue, thymic cells, teeth odontoblasts, and bones middle ear and jaws (Gilbert, 2000). Variations in gene expression

in cranial neural crest cells are responsible for common facial variations among individuals and disruption in transcriptional regulation in cranial neural crest cells can lead to craniofacial malformation (Naqvi et al., 2022). The cardiac neural crest cells are involved in early heart development, proper septation, and separation of the aorta and pulmonary artery (Waldo et al., 1998). Cardiac neural crest cells are also involved in thymus, thyroid, and parathyroid development, as suggested by cardiac neural crest cell ablation experiments in chick embryos (Bockman & Kirby, 1984; Kirby & Waldo, 1990). The presence of hypothyroidism, dental abnormalities, cardiac anomalies, and dysmorphic craniofacial features in patients with disruptions in *CAPN15* further suggest that CAPN15 is important to the proper functioning of neural crest cells.

Neurological manifestations in individuals with *CAPN15* variants include seizure, microcephaly, cortical atrophy, autism, and cerebellum malformation. Based on the presence of these symptoms and the absence of symptoms found in neuronal migration disorders such as lissencephaly or polymicrogyria, it is possible that mutations in *CAPN15* have more impact on processes that control the number of neurons present in the brain than neuronal migration. While the number of neurons in the brain can be affected by multiple factors, such as proliferative division of neuroepithelial cells, neurogenesis, and apoptosis, it is unclear which process CAPN15 is involved in. Although in *Drosophila*, small optic lobe due to loss of CAPN15 is caused by excessive degeneration of ganglion cells rather than impaired proliferation (Fischbach & Heisenberg, 1981), our immunostaining experiments using CASP3 as an apoptosis marker did not show any difference in E15 brain sections from WT and *CAPN15* KO mice (data not published). Interestingly, some cells that are destined to be eliminated do not necessarily undergo apoptosis and are CASP3-negative. In fact, binary cell death is observed in many intermediate

progenitor daughter cells that are destined for further proliferation (Mihalas & Hevner, 2018). Studies showed that many viable intermediate progenitor cells are phagocytosed by microglia without showing any signs of apoptosis (Cunningham et al., 2013). Based on X-gal staining of E18 brain showing that CAPN15 is expressed in subventricular zone, where intermediate progenitor cells reside, CAPN15 might regulate total neurogenic output through microglia-dependent phagocytosis of intermediate progenitor cells. Regardless, we cannot rule out the possibility that CAPN15 is involved in progenitor cell proliferation, as CAPN15 might acquire additional functions during evolution. Indeed, in E18 hippocampus, X-gal staining is observed in the neuroepithelial layer. This might suggest the expression of CAPN15 in neuroepithelial cells or radial glia cells and a role in proliferative symmetric division, or differentiation of those cells.

The phenotypes due to disruption of *CAPN15* in humans overlap with many other congenital anomaly disorders, such as CHARGE syndrome, mainly caused by mutation in *CHD7*, and CSS/NBS, caused by mutations in components of SWI/SNF complex. As mentioned in the introduction, SWI/SNF complex and CHD7 are chromatin regulators that are critical to gene expression in neural stem cells, neural crest cell development, and cerebellar development (Bajpai et al., 2010; Engelen et al., 2011; Feng et al., 2017; King & Klose, 2017; Lessard et al., 2007; Yu et al., 2013). Therefore, it is highly likely that a common pathway is disrupted in those disorders. It is possible that CAPN15 regulates and modifies the activity or binding preference of certain transcription factors downstream of those chromatin remodelers through proteolytic cleavage.

5.2.3 Unidentified β-gal puncta in adult mouse brains

One unresolved mystery in Chapter 3 is the identity of those X-gal puncta located in the molecular layer of dentate gyrus as well as stratum radiatum of CA1. A similar X-gal puncta pattern is observed in other studies (Shahapal et al., 2019). Unfortunately, this observation is not explained in the text. It is possible that those puncta represent diffused signals from the granule cells of dentate gyrus and pyramidal neurons in CA1, given that they do not necessarily colocalize to DAPI staining. While we have tried to determine their identity with multiple markers, the high background in immunostaining makes data interpretation rather difficult.

5.2.4 Non-associative memory in vertebrates

In Chapter 4, we found that after intense auditory fear conditioning, *Capn15* cKO mice showed reduced freezing to the safe context compared to the control, especially in male animals. It is not surprising that animals showed generalized fear towards an environment that is not associated with unconditioned stimulus in auditory fear conditioning. Therefore, it is interesting that *Capn15* cKO mice showed less pre-CS freezing than the *Cre*- control did. In fact, in *Aplysia*, SOL calpain is shown to be important to the induction of non-associative LTF. This however raised an interesting question: is the decrease in pre-CS freezing in *Capn15* cKOs and the lack of CAPN15 in cKO animals associated because the pre-CS freezing is actually a form of non-associative memory like sensitization? In *Aplysia* sensorimotor cocultures, non-associative long-term facilitation can be induced by a low dose of neurotransmitter serotonin without presynaptic tetanus through heterosynaptic facilitation (Hu, Ferguson, et al., 2017). It is possible that in our animals, non-associative memory, manifested as freezing during pre-CS, was induced by foot shocks in the training context, without the association of the safe context and the shocks.

In current literature, fear generalization is defined as the spread of fear from a traumatic conditioned stimulus to another similar stimulus and it is thought to be an associative process (Haddad et al., 2012; Lissek et al., 2008). In contrast, sensitization, the behavioral representation of non-associative plasticity in *Aplysia*, is able to induce fear of novel object that might not resemble the original fearful stimulus and is non-associative (Haddad et al., 2012; Lissek & van Meurs, 2015). On a cellular level, the key to determining whether the fear response is fear generalization or sensitization is to determine whether the presynaptic neuron of that particular synapse is firing or not during training. This can be particularly difficult as it may require real-time and precise recording of engram neurons during training. Therefore, without solid evidence, we cannot rule out the possibility of associative learning contributing to pre-CS freezing, as some of the factors between the two contexts are unchanged, such as scent and the context of some of the walls of the conditioning chamber. In fact, pre-CS freezing in *Capn15* cKO is not completely erased and is still more or less proportional to training intensity, suggesting an associative component in the process. However, we do not believe associative learning is the sole reason behind pre-CS freezing as changing the configuration of the floor is sufficient to induce discrimination (Huckleberry et al., 2016), and as mentioned in Chapter 4, the effect of fear generalization is more prominent at remote time points. Therefore, pre-CS freezing is probably a combination of both non-associative memory and associative fear generalization.

5.3 Future directions

Although this thesis provides many valuable insights about the function of CAPN15, the puzzle is still missing many critical pieces. Further research is definitely required to fully

understand the role of CAPN15 in development and in learning and memory. In this section, I will briefly talk about the missing pieces of the puzzle.

5.3.1 Further characterization of CAPN15 – putative substrates and mechanism of activation

The two important questions that are unanswered are ‘What are the substrates of CAPN15’ and ‘How is it activated’. Without knowing the substrate of CAPN15, it would be very hard to find the biological pathway it is involved in; without knowing the substrates of CAPN15, it would be very cumbersome to assay the catalytic activity of the protease in any indirect way, and therefore, impossible to determine how the disease variants of CAPN15 affects its catalytic activity. While many calpains show autolytic activity in vitro upon activation, affinity-purified SOL calpain failed to show any signs of activation or autolytic activity (Hastings et al., 2018). Therefore, it is critical to find the substrates and its mechanism of activation.

One way to look for putative substrates of CAPN15 is to compare the proteomics of WT mice and *Capn15* KO mice. Terminal amine isotopic labeling of substrates (TAILS) is a quantitative proteolytic method that can quantify the abundance of protein N-termini as well as neo-N-termini of protease cleavage products (Kleifeld et al., 2010; Kleifeld et al., 2011; Wang et al., 2021). In TAILS, the primary amine group from the most N-terminal amino acid and lysine side chain will be labeled with isotopic dimethyl group. Samples will then be digested by trypsin. A high molecular weight aldehyde reactive polymer will be added to the mixture to remove all N-terminally unlabeled peptides and will be removed through ultrafiltration. Finally, all N-terminally labeled peptides will be separated by liquid chromatography and analyzed by mass spectrometry. Given that WT and *Capn15* KO mice have different N-terminal proteomics, TAILS will be able to pick up the difference, which could be a putative substrate of CAPN15.

Development depends on a series of tightly regulated gene expression. Disruption of gene regulation during early development can lead to catastrophic outcomes. Based on facts that loss of CAPN15 results in developmental deficits in both mice and humans and calpains are known to regulate gene expression through their interactions with transcription factors, we speculate that CAPN15 might regulate transcription factor activity through proteolytic cleavage. Therefore, another way to look for putative substrates of CAPN15 is to compare RNA levels in WT and *Capn15* KO mice with RNA sequencing. Although RNA sequencing cannot directly find the substrates of CAPN15, it will show us what genes are transcribed differentially, possibly due to changes in transcriptional activity due to the loss of CAPN15. It is then possible to deduce transcriptional factors involved in the expression of those differentially expressed genes based on ChIP-sequencing data and transcription factor binding motif (Qin et al., 2020).

To study the mechanism of action of CAPN15, we can learn from studies done on other calpains: solve the crystal structure of CAPN15. Crystal structure of CAPN15 will possibly show us the interaction between different domains before and after activation; whether calcium or polyubiquitin can induce any conformational changes upon binding to facilitate activation. Interaction between residues in the protease domain will show us how the active site is held inactive before activation.

5.3.2 Further characterization of CAPN15 – function during early development

To study the role of CAPN15 in eye development, we should first determine where it is expressed during the early stage of eye development. Eye development starts as early as embryonic day 8 in mice. By the end of embryonic day 13, optic cups are formed and optic fissure is closed (Krueger & Morris, 2022; Pei & Rhodin, 1970). Although the pathological

mechanism of microphthalmia and anophthalmia is unclear, given the phenotype of *Capn15* KO mice (microphthalmia and anophthalmia) and human patients with CAPN15 variants (microphthalmia and coloboma), it is likely that CAPN15 is expressed as early as E8 during the formation of eye field. After that, histological sections of developing eyes from WT and *Capn15* KO should be made in order to compare their morphology. Although CAPN15 substrates are still elusive, understanding when and where CAPN15 is expressed will help us narrow the targets.

Similarly, to study the role of CAPN15 in brain development, we should first determine CAPN15 expression in developing brain during different developmental stages. While we have tried to determine CAPN15 expression during early development in E13 mouse embryos, sections are cut sagitally and the quality of images is not good enough. Coronal sections might serve better in this situation to investigate CAPN15 expression. Ideally, brain sections at different developmental time points (symmetric division of neuroepithelial cells, asymmetric division of radial glia cells, division of intermediate progenitor cells, neuronal migration) should be investigated and where CAPN15 is expressed should be documented. Based on its expression, we should be able to determine what developmental stages we should focus on. It would also be interesting to investigate the function of CAPN15 in the migration and differentiation of neural crest cells or neural crest-derived cells. Other than histology, another way to study CAPN15 function in brain development is to culture and study the development of neural progenitor cells or neural progenitor-derived cells from *CAPN15* KO mice. Likewise, using induced pluripotent stem cells from healthy and *CAPN15* variant individuals, we are able to understand the causality between genotypes and phenotypes, disease mechanism, and physiological function of CAPN15 (Zhou et al., 2023).

5.3.3 Different forms of plasticity governed by different PKC/PKM isoforms

In *Aplysia* sensorimotor cultures, associative LTF and non-associative LTF are governed by different PKM isoforms in the postsynaptic neurons (Hu, Adler, et al., 2017; Hu, Ferguson, et al., 2017). In order to investigate whether there are multiple forms of plasticity mediated by different sets of PKC/PKMs in vertebrates, we can bilaterally inject class/isoform-specific PKC/PKM inhibitors into lateral amygdala and determine how different inhibitors are going to affect the freezing behavior of wild type animals. For example, if a classical PKC inhibitor is injected into lateral amygdala, we would expect to see a reduction in pre-CS freezing as classical PKM in motor neurons is important to non-associative LTF in *Aplysia*. Likewise, injection of atypical PKC inhibitor would reduce freezing towards tone, and to a lesser extent, towards pre-CS, as atypical PKM in motor neurons is important to associative LTF in *Aplysia*.

5.3.4 Synaptic plasticity in the non-conditioned pathway

Experiments in *Aplysia* sensorimotor coculture showed that non-associative LTF can be induced through heterosynaptic facilitation. It would be interesting to determine whether this is also true in vertebrates. Experiments done by Dr. Cho's lab showed that after six pairs of tone shock pairings, mice will freeze to the paired tone (CS+) as well as another unpaired tone with a different frequency (CS-). After a few days of discriminative auditory fear conditioning training (CS+ tone with shock and CS- tone without shock), animals freeze only to CS+ but not CS-. They labeled neurons that are active towards either CS+ or CS- with ChR2-eYFP and showed that LTP is only induced in the CS+ pathway after discriminative fear learning, indicated by an increase in AMPA/NMDA ratio (Kim & Cho, 2017). However, it is unclear whether LTP exists in the CS- pathway before discriminative fear learning, when animals still freeze to CS-. In

contextual fear conditioning, they again demonstrated that LTP is observed only in the conditioned context (CTX+) pathway after training, in animals that are able to discriminate. However, if they take a group of mice that discriminate poorly (generalizers who freeze in both conditioned and unconditioned contexts) into account, they showed that AMPA/NMDA ratio in the unconditioned context (CTX-) pathway is positively correlated to the freezing score in CTX- (Kim & Cho, 2020). This likely suggests the presence of LTP in the CTX- pathway in animals that discriminate poorly. Hence, in their discriminative auditory fear conditioning experiments, it is likely that the freezing to CS- tone before discriminative training is probably accompanied by an increase in AMPA/NMDA ratio on the molecular level. Therefore, in order to determine whether LTP in the CTX- pathway can be induced through heterosynaptic facilitation, we will label neurons in ventral CA1 that are active in the CTX- with ChR2-eYFP, repeat the auditory fear conditioning experiments described in Chapter 4 using intense foot shock, and eventually measure AMPA/NMDA ratio in the postsynaptic neurons. If LTP is present, indicated by an increase in AMPA/NMDA ratio compared to no foot shock control or weak foot shock control, then we can determine whether the ratio is affected in *Capn15* cKO mice or in WT mice injected with different class/isoform-specific PKC/PKM inhibitors.

It would be more convincing if we could visualize heterosynaptic facilitation: presynaptic neurons from both hippocampus and auditory cortex innervating the same postsynaptic amygdala neuron. One way that might accomplish this is to use the dual-eGRASP strategy (Choi et al., 2021; Choi et al., 2018). Briefly, after virus injection, the presynaptic neuron will express the color-determining pre-eGRASP domain and the postsynaptic neuron will express the common post-eGRASP domain, on the membrane. The two domains will be reconstituted into function fluorescent protein in synaptic cleft. Specific labeling of neurons allocated to memory can be

done using the c-fos promoter-driven reverse tetracycline-controlled transactivator system. In order to visualize the connection, we can tag hippocampal neurons encoding safe context with yellow pre-eGRASP while tagging auditory cortex neurons encoding the tone with cyan pre-eGRASP. We will label postsynaptic neurons allocated to memory from amygdala with mCherry and post-eGRASP. If two presynaptic neurons converge onto the same postsynaptic neuron, we should be able to see both yellow and cyan puncta on the same red postsynaptic neuron. Then, we can compare the size of yellow spines to those from *Capn15* cKO mice.

5.4 Conclusion

The work in this thesis described the phenotypes of *Capn15* KO and *Capn15* cKO mice. We showed that CAPN15 is important to global development, as well as eye development in mice, which are validated by human patients with *CAPN15* variants. In addition, we showed significant volumetric changes in the brains of *Capn15* KO mice. We showed that *Capn15* cKO mice have altered marble burying behavior and poorer motor performance. Furthermore, they have reduced pre-CS freezing after auditory fear conditioning, which suggests that CAPN15 might play a role in fear generalization/non-associative memory.

PTSD is induced by maladaptive learning after a traumatic encounter. In fact, sensitization has been proposed to be associated with PTSD, as a non-associative component of maladaptive learning (Lissek & van Meurs, 2015). The work presented in this thesis and previous *Aplysia* studies suggest that removing CAPN15/SOL calpain might impair or even block non-associative plasticity. This is promising as it provides a candidate molecule that might

be required for the maladaptive memory in PTSD, and therefore, suggests a possibility to selectively erase maladaptive memories.

References

Ali, F., Hindley, C., McDowell, G., Deibler, R., Jones, A., Kirschner, M., Guillemot, F., & Philpott, A. (2011). Cell cycle-regulated multi-site phosphorylation of Neurogenin 2 coordinates cell cycling with differentiation during neurogenesis. *Development*, *138*(19), 4267-4277. https://doi.org/10.1242/dev.067900

Amini, M., Ma, C. L., Farazifard, R., Zhu, G. Q., Zhang, Y., Vanderluit, J., Zoltewicz, J. S., Hage, F., Savitt, J. M., Lagace, D. C., Slack, R. S., Beique, J. C., Baudry, M., Greer, P. A., Bergeron, R., & Park, D. S. (2013). Conditional Disruption of Calpain in the CNS Alters Dendrite Morphology, Impairs LTP, and Promotes Neuronal Survival following Injury. *Journal of Neuroscience*, *33*(13), 5773-5784. https://doi.org/10.1523/Jneurosci.4247-12.2013

Anderson, S. A., Eisenstat, D. D., Shi, L., & Rubenstein, J. L. R. (1997). Interneuron migration from basal forebrain to neocortex: Dependence on Dlx genes. *Science*, *278*(5337), 474-476. https://doi.org/10.1126/science.278.5337.474

Anthony, T. E., Klein, C., Fishell, G., & Heintz, N. (2004). Radial glia serve as neuronal progenitors in all regions of the central nervous system. *Neuron*, *41*(6), 881-890. https://doi.org/10.1016/S0896-6273(04)00140-0

Arthur, J. S. C., Elce, J. S., Hegadorn, C., Williams, K., & Greer, P. A. (2000). Disruption of the murine calpain small subunit gene, Capn4: Calpain is essential for embryonic development but not for cell growth and division. *Molecular and Cellular Biology*, *20*(12), 4474-4481. https://doi.org/10.1128/Mcb.20.12.4474-4481.2000

Azam, M., Andrabi, S. S., Sahr, K. E., Kamath, L., Kuliopulos, A., & Chishti, A. H. (2001). Disruption of the mouse mu-calpain gene reveals an essential role in platelet function. *Molecular and Cellular Biology*, *21*(6), 2213-2220. https://doi.org/10.1128/Mcb.21.6.2213-2220.2001

Bai, J. L., Ramos, R. L., Ackman, J. B., Thomas, A. M., Lee, R. V., & LoTurco, J. J. (2003). RNAi reveals doublecortin is required for radial migration in rat neocortex. *Nature Neuroscience*, *6*(12), 1277-1283. https://doi.org/10.1038/nn1153

Bailey, C. H., & Chen, M. (1988). Long-term sensitization in Aplysia increases the number of presynaptic contacts onto the identified gill motor neuron L7. *Proc Natl Acad Sci U S A*, *85*(23), 9356-9359. https://doi.org/10.1073/pnas.85.23.9356

Bajpai, R., Chen, D. A., Rada-Iglesias, A., Zhang, J. M., Xiong, Y. Q., Helms, J., Chang, C. P., Zhao, Y. M., Swigut, T., & Wysocka, J. (2010). CHD7 cooperates with PBAF to control multipotent neural crest formation. *Nature*, *463*(7283), 958-U135. https://doi.org/10.1038/nature08733

Barnes, T. M., & Hodgkin, J. (1996). The tra-3 sex determination gene of Caenorhabditis elegans encodes a member of the calpain regulatory protease family. *Embo Journal*, *15*(17), 4477-4484. https://doi.org/10.1002/j.1460-2075.1996.tb00825.x

Bartsch, D., Casadio, A., Karl, K. A., Serodio, P., & Kandel, E. R. (1998). CREB1 encodes a nuclear activator, a repressor, and a cytoplasmic modulator that form a regulatory unit critical for long-term facilitation. *Cell*, *95*(2), 211-223. https://doi.org/10.1016/S0092-8674(00)81752-3

Bassuk, A. G., Yeh, S., Wu, S., Martin, D. F., Tsang, S. H., Gakhar, L., & Mahajan, V. B. (2015). Structural Modeling of a Novel CAPN5 Mutation that Causes Uveitis and Neovascular Retinal Detachment. *Plos One*, *10*(4). https://doi.org/10.1371/journal.pone.0122352

Baumann, M., Beaver, E. M., Palomares-Bralo, M., Santos-Simarro, F., Holzer, P., Povysil, G., Muller, T., Valovka, T., & Janecke, A. R. (2020). Further delineation of putative ACTB loss-of-function variants: A 4-patient series. *Human Mutation*, *41*(4), 753-758. https://doi.org/10.1002/humu.23970

Beaman, M. M., Guidugli, L., Hammer, M., Barrows, C., Gregor, A., Lee, S., Deak, K. L., McDonald, M. T., Jensen, C., Zaki, M. S., Masri, A. T., Hobbs, C. A., Gleeson, J. G., & Cohen, J. L. (2023). Novel association of Dandy-Walker malformation with CAPN15 variants expands the phenotype of oculogastrointestinal neurodevelopmental syndrome. *Am J Med Genet A*. https://doi.org/10.1002/ajmg.a.63363

Bochner, R., Samuelov, L., Sarig, O., Li, Q. L., Adase, C. A., Isakov, O., Malchin, N., Vodo, D., Shayevitch, R., Peled, A., Yu, B. D., Fainberg, G., Warshauer, E., Adir, N., Erez, N., Gat, A., Gottlieb, Y., Rogers, T., Pavlovsky, M., . . . Sprecher, E. (2017). Calpain 12 Function Revealed through the Study of an Atypical Case of Autosomal Recessive Congenital Ichthyosis. *Journal of Investigative Dermatology*, *137*(2), 385-393. https://doi.org/10.1016/j.jid.2016.07.043

Bockman, D. E., & Kirby, M. L. (1984). Dependence of Thymus Development on Derivatives of the Neural Crest. *Science*, *223*(4635), 498-500. https://doi.org/DOI 10.1126/science.6606851

Bogershausen, N., & Wollnik, B. (2018). Mutational Landscapes and Phenotypic Spectrum of SWI/SNF-Related Intellectual Disability Disorders. *Frontiers in Molecular Neuroscience*, *11*. https://doi.org/10.3389/fnmol.2018.00252

Bonaglia, M. C., Giorda, R., Borgatti, R., Felisari, G., Gagliardi, C., Selicorni, A., & Zuffardi, O. (2001). Disruption of the ProSAP2 gene in a t(12;22)(q24.1;q13.3) is associated with the 22q13.3 deletion syndrome. *American Journal of Human Genetics*, *69*(2), 261-268. https://doi.org/10.1086/321293

Bonnefont, J., Tiberi, L., van den Ameele, J., Potier, D., Gaber, Z. B., Lin, X., Bilheu, A., Herpoel, A., Velez Bravo, F. D., Guillemot, F., Aerts, S., & Vanderhaeghen, P. (2019). Cortical Neurogenesis Requires Bcl6-Mediated Transcriptional Repression of Multiple Self-Renewal-Promoting Extrinsic Pathways. *Neuron*, *103*(6), 1096-1108 e1094. https://doi.org/10.1016/j.neuron.2019.06.027

Bougie, J. K., Lim, T., Farah, C. A., Manjunath, V., Nagakura, I., Ferraro, G. B., & Sossin, W. S. (2009). The atypical protein kinase C in Aplysia can form a protein kinase M by cleavage. *Journal of Neurochemistry*, *109*(4), 1129-1143. https://doi.org/10.1111/j.1471-4159.2009.06045.x

Bourgeron, T. (2015). From the genetic architecture to synaptic plasticity in autism spectrum disorder. *Nature Reviews Neuroscience*, *16*(9), 551-563. https://doi.org/10.1038/nrn3992

Breuss, M. W., Leca, I., Gstrein, T., Hansen, A. H., & Keays, D. A. (2017). Tubulins and brain development - The origins of functional specification. *Molecular and Cellular Neuroscience*, *84*, 58-67. https://doi.org/10.1016/j.mcn.2017.03.002

Briz, V., Hsu, Y. T., Li, Y., Lee, E., Bi, X., & Baudry, M. (2013). Calpain-2-mediated PTEN degradation contributes to BDNF-induced stimulation of dendritic protein synthesis. *J Neurosci*, *33*(10), 4317-4328. https://doi.org/10.1523/JNEUROSCI.4907-12.2013

Brown, K. N., Chen, S., Han, Z., Lu, C. H., Tan, X., Zhang, X. J., Ding, L. Y., Lopez-Cruz, A., Saur, D., Anderson, S. A., Huang, K., & Shi, S. H. (2011). Clonal Production and Organization of Inhibitory Interneurons in the Neocortex. *Science*, *334*(6055), 480-486. https://doi.org/10.1126/science.1208884

Brunelli, M., Castellucci, V., & Kandel, E. R. (1976). Synaptic facilitation and behavioral sensitization in Aplysia: possible role of serotonin and cyclic AMP. *Science*, *194*(4270), 1178-1181. https://doi.org/10.1126/science.186870

Busch, W. A., Suzuki, A., Stromer, M. H., & Goll, D. E. (1972). Ca2+-Specific Removal of Z Lines from Rabbit Skeletal-Muscle. *Journal of Cell Biology*, *52*(2), 367-&. https://doi.org/10.1083/jcb.52.2.367

Cai, D. C., Pearce, K., Chen, S. P., & Glanzman, D. L. (2011). Protein Kinase M Maintains Long-Term Sensitization and Long-Term Facilitation in Aplysia. *Journal of Neuroscience*, *31*(17), 6421-6431. https://doi.org/10.1523/Jneurosci.4744-10.2011

Campbell, R. L., & Davies, P. L. (2012). Structure-function relationships in calpains. *Biochemical Journal*, *447*, 335-351. https://doi.org/10.1042/Bj20120921

Carew, T. J., Walters, E. T., & Kandel, E. R. (1981). Classical conditioning in a simple withdrawal reflex in Aplysia californica. *J Neurosci*, *1*(12), 1426-1437. https://doi.org/10.1523/JNEUROSCI.01-12-01426.1981

Carson, R. P., Van Nielen, D. L., Winzenburger, P. A., & Ess, K. C. (2012). Neuronal and glia abnormalities in Tsc1-deficient forebrain and partial rescue by rapamycin. *Neurobiology of Disease*, *45*(1), 369-380. https://doi.org/10.1016/j.nbd.2011.08.024

Castellucci, V. F., Blumenfeld, H., Goelet, P., & Kandel, E. R. (1989). Inhibitor of protein synthesis blocks long-term behavioral sensitization in the isolated gill-withdrawal reflex of Aplysia. *J Neurobiol*, *20*(1), 1-9. https://doi.org/10.1002/neu.480200102

Castellucci, V. F., Kandel, E. R., Schwartz, J. H., Wilson, F. D., Nairn, A. C., & Greengard, P. (1980). Intracellular injection of t he catalytic subunit of cyclic AMP-dependent protein kinase simulates facilitation of transmitter release underlying behavioral sensitization in Aplysia. *Proc Natl Acad Sci U S A*, *77*(12), 7492-7496. https://doi.org/10.1073/pnas.77.12.7492

Chang, L., Blain, D., Bertuzzi, S., & Brooks, B. P. (2006). Uveal coloboma: clinical and basic science update. *Current Opinion in Ophthalmology*, *17*(5), 447-470. https://doi.org/10.1097/01.icu.0000243020.82380.f6

Chassaing, N., Causse, A., Vigouroux, A., Delahaye, A., Alessandri, J. L., Boespflug-Tanguy, O., Boute-Benejean, O., Dollfus, H., Duban-Bedu, B., Gilbert-Dussardier, B., Giuliano, F., Gonzales, M., Holder-Espinasse, M., Isidor, B., Jacquemont, M. L., Lacombe, D., Martin-Coignard, D., Mathieu-Dramard, M., Odent, S., . . . Calvas, P. (2014). Molecular findings and clinical data in a cohort of 150 patients with anophthalmia/microphthalmia. *Clinical Genetics*, *86*(4), 326-334. https://doi.org/10.1111/cge.12275

Chen, C. H., Chen, H. I., Liao, H. M., Chen, Y. J., Fang, J. S., Lee, K. F., & Gau, S. S. (2017). Clinical and molecular characterization of three genomic rearrangements at chromosome 22q13.3 associated with autism spectrum disorder. *Psychiatr Genet*, *27*(1), 23-33. https://doi.org/10.1097/YPG.0000000000000151

Chiang, C., Ying, L. T. T., Lee, E., Young, K. E., Corden, J. L., Westphal, H., & Beachy, P. A. (1996). Cyclopia and defective axial patterning in mice lacking Sonic hedgehog gene function. *Nature*, *383*(6599), 407-413. https://doi.org/10.1038/383407a0

Choi, D. I., Kim, J., Lee, H., Kim, J. I., Sung, Y., Choi, J. E., Venkat, S. J., Park, P., Jung, H., & Kaang, B. K. (2021). Synaptic correlates of associative fear memory in the lateral amygdala. *Neuron*, *109*(17), 2717-2726 e2713. https://doi.org/10.1016/j.neuron.2021.07.003

Choi, J. H., Sim, S. E., Kim, J. I., Choi, D. I., Oh, J., Ye, S., Lee, J., Kim, T., Ko, H. G., Lim, C. S., & Kaang, B. K. (2018). Interregional synaptic maps among engram cells underlie memory formation. *Science*, *360*(6387), 430-435. https://doi.org/10.1126/science.aas9204

Cloetta, D., Thomanetz, V., Baranek, C., Lustenberger, R. M., Lin, S., Oliveri, F., Atanasoski, S., & Ruegg, M. A. (2013). Inactivation of mTORC1 in the Developing Brain Causes Microcephaly and Affects Gliogenesis. *Journal of Neuroscience*, *33*(18), 7799-7810. https://doi.org/10.1523/Jneurosci.3294-12.2013

Cordero, D. R., Brugmann, S., Chu, Y. N., Bajpai, R., Jame, M., & Helms, J. A. (2011). Cranial Neural Crest Cells on the Move: Their Roles in Craniofacial Development. *American Journal of Medical Genetics Part A*, *155a*(2), 270-279. https://doi.org/10.1002/ajmg.a.33702

Crespo, J. A., Stockl, P., Ueberall, F., Jenny, M., Saria, A., & Zernig, G. (2012). Activation of PKCzeta and PKMzeta in the Nucleus Accumbens Core Is Necessary for the Retrieval, Consolidation and Reconsolidation of Drug Memory. *Plos One*, *7*(2). https://doi.org/10.1371/journal.pone.0030502

Cruz Marino, T., Leblanc, J., Pratte, A., Tardif, J., Thomas, M. J., Fortin, C. A., Girard, L., & Bouchard, L. (2023). Portrait of autosomal recessive diseases in the French-Canadian founder population of Saguenay-Lac-Saint-Jean. *Am J Med Genet A*, *191*(5), 1145-1163. https://doi.org/10.1002/ajmg.a.63147

Cunningham, C. L., Martinez-Cerdeno, V., & Noctor, S. C. (2013). Microglia regulate the number of neural precursor cells in the developing cerebral cortex. *J Neurosci*, *33*(10), 4216-4233. https://doi.org/10.1523/JNEUROSCI.3441-12.2013

Cuvertino, S., Stuart, H. M., Chandler, K. E., Roberts, N. A., Armstrong, R., Bernardini, L., Bhaskar, S., Callewaert, B., Clayton-Smith, J., Davalillo, C. H., Deshpande, C., Devriendt, K., Digilio, M. C., Dixit, A., Edwards, M., Friedman, J. M., Gonzalez-Meneses, A., Joss, S., Kerr, B., . . . Study, D. (2017). ACTB Loss-of-Function Mutations Result in a Pleiotropic Developmental Disorder. *American Journal of Human Genetics*, *101*(6), 1021-1033. https://doi.org/10.1016/j.ajhg.2017.11.006

Dear, T. N., Meier, N. T., Hunn, M., & Boehm, T. (2000). Gene structure, chromosomal localization, and expression pattern of Capn12, a new member of the calpain large subunit gene family. *Genomics*, *68*(2), 152-160. https://doi.org/10.1006/geno.2000.6289

Delaney, S. J., Hayward, D. C., Barleben, F., Fischbach, K. F., & Miklos, G. L. G. (1991). Molecular-Cloning and Analysis of Small Optic Lobes, a Structural Brain Gene of Drosophila-Melanogaster. *Proceedings of the National Academy of Sciences of the United States of America*, *88*(16), 7214-7218. https://doi.org/10.1073/pnas.88.16.7214

Delgado, R. N., Allen, D. E., Keefe, M. G., Leon, W. R. M., Ziffra, R. S., Crouch, E. E., Alvarez-Buylla, A., & Nowakowski, T. J. (2022). Individual human cortical progenitors can produce excitatory and inhibitory neurons. *Nature*, *601*(7893), 397-+. https://doi.org/10.1038/s41586-021-04230-7

Denison, S. H., Orejas, M., & Arst, H. N. (1995). Signaling of Ambient Ph in Aspergillus Involves a Cysteine Protease. *Journal of Biological Chemistry*, *270*(48), 28519-28522. https://doi.org/10.1074/jbc.270.48.28519

Derry, M. C., Yanagiya, A., Martineau, Y., & Sonenberg, N. (2006). Regulation of Poly(A)-binding Protein through PABP-interacting Proteins. *Regulatory Rnas*, *71*, 537-543. https://doi.org/10.1101/sqb.2006.71.061

Diez, E., Alvaro, J., Espeso, E. A., Rainbow, L., Suarez, T., Tilburn, J., Arst, H. N., & Penalva, M. A. (2002). Activation of the Aspergillus PacC zinc finger transcription factor requires two proteolytic steps. *Embo Journal*, *21*(6), 1350-1359. https://doi.org/10.1093/emboj/21.6.1350

Dong, Z. F., Han, H. L., Li, H. J., Bai, Y. R., Wang, W., Tu, M., Peng, V., Zhou, L. M., He, W. T., Wu, X. B., Tan, T., Liu, M. J., Wu, X. Y., Zhou, W. H., Jin, W. Y., Zhang, S., Sacktor, T. C., Li, T. Y., Song, W. H., & Wang, Y. T. (2015). Long-term potentiation decay and memory loss are mediated by AMPAR endocytosis. *Journal of Clinical Investigation*, *125*(1), 234-247. https://doi.org/10.1172/Jci77888

Durand, C. M., Betancur, C., Boeckers, T. M., Bockmann, J., Chaste, P., Fauchereau, F., Nygren, G., Rastam, M., Gillberg, I. C., Anckarsater, H., Sponheim, E., Goubran-Botros, H., Delorme, R., Chabane, N., Mouren-Simeoni, M. C., de Mas, P., Bieth, E., Roge, B., Heron, D., . . . Bourgeron, T. (2007). Mutations in the gene encoding the synaptic scaffolding protein SHANK3 are associated with autism spectrum disorders. *Nature Genetics*, *39*(1), 25-27. https://doi.org/10.1038/ng1933

Dutt, P., Arthur, J. S. C., Grochulski, P., Cygler, M., & Elce, J. S. (2000). Roles of individual EF-hands in the activation of m-calpain by calcium. *Biochemical Journal*, *348*, 37-43. https://doi.org/10.1042/0264-6021:3480037

Dutt, P., Croall, D. E., Arthur, J. S. C., De Veyra, T., Williams, K., Elce, J. S., & Greer, P. A. (2006). m-Calpain is required for preimplantation embryonic development in mice. *Bmc Developmental Biology*, *6*. https://doi.org/10.1186/1471-213x-6-3

Echelard, Y., Epstein, D. J., Stjacques, B., Shen, L., Mohler, J., Mcmahon, J. A., & Mcmahon, A. P. (1993). Sonic-Hedgehog, a Member of a Family of Putative Signaling Molecules, Is Implicated in the Regulation of Cns Polarity. *Cell*, *75*(7), 1417-1430. https://doi.org/10.1016/0092-8674(93)90627-3

Ehninger, D., & Silva, A. J. (2011). Rapamycin for treating Tuberous sclerosis and Autism spectrum disorders. *Trends Mol Med*, *17*(2), 78-87. https://doi.org/10.1016/j.molmed.2010.10.002

Engelen, E., Akinci, U., Bryne, J. C., Hou, J., Gontan, C., Moen, M., Szumska, D., Kockx, C., van IJcken, W., Dekkers, D. H. W., Demmers, J., Rijkers, E. J., Bhattacharya, S., Philipsen, S., Pevny, L. H., Grosveld, F. G., Rottier, R. J., Lenhard, B., & Poot, R. A. (2011). Sox2 cooperates with Chd7 to regulate genes that are mutated in human syndromes. *Nature Genetics*, *43*(6), 607-U153. https://doi.org/10.1038/ng.825

Errichiello, E., Mustafa, N., Vetro, A., Notarangelo, L. D., de Jonge, H., Rinaldi, B., Vergani, D., Giglio, S. R., Morbini, P., & Zuffardi, O. (2017). SMARCA4 inactivating mutations cause concomitant Coffin-Siris syndrome, microphthalmia and small-cell carcinoma of the ovary hypercalcaemic type. *J Pathol*, *243*(1), 9-15. https://doi.org/10.1002/path.4926

Espeso, E. A., Roncal, T., Diez, E., Rainbow, L., Bignell, E., Alvaro, J., Suarez, T., Denison, S. H., Tilburn, J., Arst, H. N., & Penalva, M. A. (2000). On how a transcription factor can avoid its proteolytic activation in the absence of signal transduction. *Embo Journal*, *19*(4), 719-728. https://doi.org/10.1093/emboj/19.4.719

Farah, C. A., Hastings, M. H., Dunn, T. W., Gong, K., Baker-Andresen, D., & Sossin, W. S. (2017). A PKM generated by calpain cleavage of a classical PKC is required for activity-

dependent intermediate-term facilitation in the presynaptic sensory neuron of Aplysia. *Learning & Memory*, *24*(1), 1-13. https://doi.org/10.1101/lm.043745.116

Farah, C. A., & Sossin, W. S. (2012). The Role of C2 Domains in PKC Signaling. *Calcium Signaling*, *740*, 663-683. https://doi.org/10.1007/978-94-007-2888-2_29

Feng, W. J., Kawauchi, D., Korkel-Qu, H., Deng, H., Serger, E., Sieber, L., Lieberman, J. A., Jimeno-Gonzalez, S., Lambo, S., Hanna, B. S., Harim, Y., Jansen, M., Neuerburg, A., Friesen, O., Zuckermann, M., Rajendran, V., Gronych, J., Ayrault, O., Korshunov, A., . . . Liu, H. K. (2017). Chd7 is indispensable for mammalian brain development through activation of a neuronal differentiation programme. *Nature Communications*, *8*. https://doi.org/ARTN 14758

10.1038/ncomms14758

Fischbach, K. F., & Heisenberg, M. (1981). Structural Brain Mutant of Drosophila-Melanogaster with Reduced Cell Number in the Medulla Cortex and with Normal Optomotor Yaw Response. *Proceedings of the National Academy of Sciences of the United States of America-Biological Sciences*, *78*(2), 1105-1109. https://doi.org/10.1073/pnas.78.2.1105

Frost, W. N., Castellucci, V. F., Hawkins, R. D., & Kandel, E. R. (1985). Mono-Synaptic Connections Made by the Sensory Neurons of the Gill-Withdrawal and Siphon-Withdrawal Reflex in Aplysia Participate in the Storage of Long-Term-Memory for Sensitization. *Proceedings of the National Academy of Sciences of the United States of America*, *82*(23), 8266-8269. https://doi.org/DOI 10.1073/pnas.82.23.8266

Futai, E., Kubo, T., Sorimachi, H., Suzuki, K., & Maeda, T. (2001). Molecular cloning of PalBH, a mammalian homologue of the Aspergillus atypical calpain PalB. *Biochimica Et Biophysica Acta-Gene Structure and Expression*, *1517*(2), 316-319. https://doi.org/10.1016/S0167-4781(00)00256-6

Gage, P. J., Hurd, E. A., & Martin, D. M. (2015). Mouse Models for the Dissection of CHD7 Functions in Eye Development and the Molecular Basis for Ocular Defects in CHARGE Syndrome. *Investigative Ophthalmology & Visual Science*, *56*(13), 7923-7930. https://doi.org/10.1167/iovs.15-18069

Gao, P., Postiglione, M. P., Krieger, T. G., Hernandez, L., Wang, C., Han, Z., Streicher, C., Papusheva, E., Insolera, R., Chugh, K., Kodish, O., Huang, K., Simons, B. D., Luo, L., Hippenmeyer, S., & Shi, S. H. (2014). Deterministic progenitor behavior and unitary production of neurons in the neocortex. *Cell*, *159*(4), 775-788. https://doi.org/10.1016/j.cell.2014.10.027

Geddes, J. W., Bondada, V., Croall, D. E., Rodgers, D. W., & Gal, J. (2023). Impaired activity and membrane association of most calpain-5 mutants causal for neovascular inflammatory vitreoretinopathy. *Biochim Biophys Acta Mol Basis Dis*, *1869*(6), 166747. https://doi.org/10.1016/j.bbadis.2023.166747

Gerth-Kahlert, C., Williamson, K., Ansari, M., Rainger, J. K., Hingst, V., Zimmermann, T., Tech, S., Guthoff, R. F., van Heyningen, V., & FitzPatrick, D. R. (2013). Clinical and mutation analysis of 51 probands with anophthalmia and/or severe microphthalmia from a single center. *Molecular Genetics & Genomic Medicine*, *1*(1), 15-31. https://doi.org/10.1002/mgg3.2

Gilbert, S. F. (2000). *Developmental biology* (6th ed.). Sinauer Associates.

Giovannini, M. G. (2006). The role of the extracellular signal-regulated kinase pathway in memory encoding. *Reviews in the Neurosciences*, *17*(6), 619-634. https://doi.org/10.1515/revneuro.2006.17.6.619

Goodman, J. V., & Bonni, A. (2019). Regulation of neuronal connectivity in the mammalian brain by chromatin remodeling. *Current Opinion in Neurobiology*, *59*, 59-68. https://doi.org/10.1016/j.conb.2019.04.010

Gregory-Evans, C. Y., Williams, M. J., Halford, S., & Gregory-Evans, K. (2004). Ocular coloboma: a reassessment in the age of molecular neuroscience. *Journal of Medical Genetics*, *41*(12), 881-891. https://doi.org/10.1136/jmg.2004.025494

Guroff, G. (1964). A Neutral, Calcium-Activated Proteinase from the Soluble Fraction of Rat Brain. *J Biol Chem*, *239*, 149-155.

Haddad, A. D. M., Pritchett, D., Lissek, S., & Lau, J. Y. F. (2012). Trait Anxiety and Fear Responses to Safety Cues: Stimulus Generalization or Sensitization? *Journal of Psychopathology and Behavioral Assessment*, *34*(3), 323-331. https://doi.org/10.1007/s10862-012-9284-7

Hardt, O., Migues, P. V., Hastings, M., Wong, J., & Nader, K. (2010). PKMzeta maintains 1-day- and 6-day-old long-term object location but not object identity memory in dorsal hippocampus. *Hippocampus*, *20*(6), 691-695. https://doi.org/10.1002/hipo.20708

Hastings, M. H., Gong, K., Freibauer, A., Courchesne, C., Fan, X. T., & Sossin, W. S. (2017). Novel calpain families and novel mechanisms for calpain regulation in Aplysia. *Plos One*, *12*(10). https://doi.org/10.1371/journal.pone.0186646

Hastings, M. H., Qiu, A., Zha, C. Y., Farah, C. A., Mahdid, Y., Ferguson, L., & Sossin, W. S. (2018). The zinc fingers of the small optic lobes calpain bind polyubiquitin. *Journal of Neurochemistry*, *146*(4), 429-445. https://doi.org/10.1111/jnc.14473

Hata, S., Abe, M., Suzuki, H., Kitamura, F., Toyama-Sorimachi, N., Abe, K., Sakimura, K., & Sorimachi, H. (2010). Calpain 8/nCL-2 and Calpain 9/nCL-4 Constitute an Active Protease Complex, G-Calpain, Involved in Gastric Mucosal Defense. *Plos Genetics*, *6*(7). https://doi.org/10.1371/journal.pgen.1001040

Hata, S., Kitamura, F., Yamaguchi, M., Shitara, H., Murakami, M., & Sorimachi, H. (2016). A Gastrointestinal Calpain Complex, G-calpain, Is a Heterodimer of CAPN8 and CAPN9 Calpain Isoforms, Which Play Catalytic and Regulatory Roles, Respectively. *Journal of Biological Chemistry*, *291*(53), 27313-27322. https://doi.org/10.1074/jbc.M116.763912

Heavner, W., & Pevny, L. (2012). Eye Development and Retinogenesis. *Cold Spring Harbor Perspectives in Biology*, *4*(12). https://doi.org/10.1101/cshperspect.a008391

Hentges, K. E., Sirry, B., Gingras, A. C., Sarbassov, D., Sonenberg, N., Sabatini, D., & Peterson, A. S. (2001). FRAP/mTOR is required for proliferation and patterning during embryonic development in the mouse. *Proceedings of the National Academy of Sciences of the United States of America*, *98*(24), 13796-13801. https://doi.org/10.1073/pnas.241184198

Hernandez, A. I., Blace, N., Crary, J. F., Serrano, P. A., Leitges, M., Libien, J. M., Weinstein, G., Tcherapanov, A., & Sacktor, T. C. (2003). Protein kinase M zeta synthesis from a brain mRNA encoding an independent protein kinase C zeta catalytic domain - Implications for the molecular mechanism of memory. *Journal of Biological Chemistry*, *278*(41), 40305-40316. https://doi.org/10.1074/jbc.M307065200

Hervas-Aguilar, A., Rodriguez, J. M., Tilburn, J., Arst, H. N., & Penalva, M. A. (2007). Evidence for the direct involvement of the proteasome in the proteolytic processing of the Aspergillus nidulans zinc finger transcription factor PacC. *Journal of Biological Chemistry*, *282*(48), 34735-34747. https://doi.org/10.1074/jbc.M706723200

Ho, L., Ronan, J. L., Wu, J., Staahl, B. T., Chen, L., Kuo, A., Lessard, J., Nesvizhskii, A. I., Ranish, J., & Crabtree, G. R. (2009). An embryonic stem cell chromatin remodeling

complex, esBAF, is essential for embryonic stem cell self-renewal and pluripotency. *Proceedings of the National Academy of Sciences of the United States of America*, *106*(13), 5181-5186. https://doi.org/10.1073/pnas.0812889106

Hu, J. Y., Adler, K., Farah, C. A., Hastings, M. H., Sossin, W. S., & Schacher, S. (2017). Cell-Specific PKM Isoforms Contribute to the Maintenance of Different Forms of Persistent Long- Term Synaptic Plasticity. *Journal of Neuroscience*, *37*(10), 2746-2763. https://doi.org/10.1523/Jneurosci.2805-16.2017

Hu, J. Y., Ferguson, L., Adler, K., Farah, C. A., Hastings, M. H., Sossin, W. S., & Schacher, S. (2017). Selective Erasure of Distinct Forms of Long-Term Synaptic Plasticity Underlying Different Forms of Memory in the Same Postsynaptic Neuron. *Current Biology*, *27*(13), 1888-+. https://doi.org/10.1016/j.cub.2017.05.081

Huckleberry, K. A., Ferguson, L. B., & Drew, M. R. (2016). Behavioral mechanisms of context fear generalization in mice. *Learn Mem*, *23*(12), 703-709. https://doi.org/10.1101/lm.042374.116

Hung, A. Y., Futai, K., Sala, C., Valtschanoff, J. G., Ryu, J., Woodworth, M. A., Kidd, F. L., Sung, C. C., Miyakawa, T., Bear, M. F., Weinberg, R. J., & Sheng, M. (2008). Smaller dendritic spines, weaker synaptic transmission, but enhanced spatial learning in mice lacking Shank1. *J Neurosci*, *28*(7), 1697-1708. https://doi.org/10.1523/JNEUROSCI.3032-07.2008

Inomata, M., Kasai, Y., Nakamura, M., & Kawashima, S. (1988). Activation Mechanism of Calcium-Activated Neutral Protease - Evidence for the Existence of Intramolecular and Intermolecular Autolyses. *Journal of Biological Chemistry*, *263*(36), 19783-19787.

Inoue, M., Kishimoto, A., Takai, Y., & Nishizuka, Y. (1977). Studies on a cyclic nucleotide-independent protein kinase and its proenzyme in mammalian tissues. II. Proenzyme and its activation by calcium-dependent protease from rat brain. *J Biol Chem*, *252*(21), 7610-7616.

Ishiura, S., Murofushi, H., Suzuki, K., & Imahori, K. (1978). Studies of a Calcium-Activated Neutral Protease from Chicken Skeletal-Muscle .1. Purification and Characterization. *Journal of Biochemistry*, *84*(1), 225-230. https://doi.org/10.1093/oxfordjournals.jbchem.a132111

Jaglin, X. H., Poirier, K., Saillour, Y., Buhler, E., Tian, G. L., Bahi-Buisson, N., Fallet-Bianco, C., Phan-Dinh-Tuy, F., Kong, X. P., Bomont, P., Castelnau-Ptakhine, L., Odent, S., Loget, P., Kossorotoff, M., Snoeck, I., Plessis, G., Parent, P., Beldjord, C., Cardoso, C., . . . Chelly, J. (2009). Mutations in the beta-tubulin gene TUBB2B result in asymmetrical polymicrogyria. *Nature Genetics*, *41*(6), 746-752. https://doi.org/10.1038/ng.380

Jongmans, M. C. J., Admiraal, R. J., van der Donk, K. P., Vissers, L. E. L. M., Baas, A. F., Kapusta, L., van Hagen, J. M., Donnai, D., de Ravel, T. J., Veltman, J. A., van Kessel, A. G., De Vries, B. B. A., Brunner, H. G., Hoefsloot, L. H., & van Ravenswaaij, C. M. A. (2006). CHARGE syndrome: the phenotypic spectrum of mutations in the CHD7 gene. *Journal of Medical Genetics*, *43*(4), 306-314. https://doi.org/10.1136/jmg.2005.036061

Kadoch, C., & Crabtree, G. R. (2015). Mammalian SWI/SNF chromatin remodeling complexes and cancer: Mechanistic insights gained from human genomics. *Science Advances*, *1*(5). https://doi.org/10.1126/sciadv.1500447

Kamei, M., Webb, G. C., Heydon, K., Hendry, I. A., Young, I. G., & Campbell, H. D. (2000). Solh, the mouse homologue of the Drosophila melanogaster small optic lobes gene:

Organization, chromosomal mapping, and localization of gene product to the olfactory bulb. *Genomics*, *64*(1), 82-89. https://doi.org/10.1006/geno.1999.6098

Kamei, M., Webb, G. C., Young, L. G., & Campbell, H. D. (1998). SOLH, a human homologue of the Drosophila melanogaster small optic lobes gene is a member of the calpain and zinc-finger gene families and maps to human chromosome 16p13.3 near CATM (Cataract with microphthalmia). *Genomics*, *51*(2), 197-206. https://doi.org/10.1006/geno.1998.5395

Kandel, E. R. (2001). The molecular biology of memory storage: a dialogue between genes and synapses. *Science*, *294*(5544), 1030-1038. https://doi.org/10.1126/science.1067020

Kandel, E. R., & Schwartz, J. H. (1982). Molecular-Biology of Learning - Modulation of Transmitter Release. *Science*, *218*(4571), 433-443. https://doi.org/10.1126/science.6289442

Karim, M. M., Svitkin, Y. V., Kahvejian, A., De Crescenzot, G., Costa-Mattioli, M., & Sonenberg, N. (2006). A mechanism of translational repression by competition of Paip2 with eIF4G for poly(A) binding protein (PABP) binding. *Proceedings of the National Academy of Sciences of the United States of America*, *103*(25), 9494-9499. https://doi.org/10.1073/pnas.0603701103

Keays, D. A., Tian, G., Poirier, K., Huang, G. J., Siebold, C., Cleak, J., Oliver, P. L., Fray, M., Harvey, R. J., Molnar, Z., Pinon, M. C., Dear, N., Valdar, W., Brown, S. D. M., Davies, K. E., Rawlins, J. N. P., Cowan, N. J., Nolan, P., Chelly, J., & Flint, J. (2007). Mutations in alpha-tubulin cause abnormal neuronal migration in mice and lissencephaly in humans. *Cell*, *128*(1), 45-57. https://doi.org/10.1016/j.cell.2006.12.017

Khoutorsky, A., Yanagiya, A., Gkogkas, C. G., Fabian, M. R., Prager-Khoutorsky, M., Cao, R. F., Gamache, K., Bouthiette, F., Parsyan, A., Sorge, R. E., Mogil, J. S., Nader, K., Lacaille, J. C., & Sonenberg, N. (2013). Control of Synaptic Plasticity and Memory via Suppression of Poly(A)-Binding Protein. *Neuron*, *78*(2), 298-311. https://doi.org/10.1016/j.neuron.2013.02.025

Kim, W. B., & Cho, J. H. (2017). Encoding of Discriminative Fear Memory by Input-Specific LTP in the Amygdala. *Neuron*, *95*(5), 1129-1146 e1125. https://doi.org/10.1016/j.neuron.2017.08.004

Kim, W. B., & Cho, J. H. (2020). Encoding of contextual fear memory in hippocampal-amygdala circuit. *Nature Communications*, *11*(1), 1382. https://doi.org/10.1038/s41467-020-15121-2

King, H. W., & Klose, R. J. (2017). The pioneer factor OCT4 requires the chromatin remodeller BRG1 to support gene regulatroy element funciton in mouse embryonic stem cells. *Elife*, *6*. https://doi.org/10.7554/eLife.22631

Kirby, M. L., & Waldo, K. L. (1990). Role of Neural Crest in Congenital Heart-Disease. *Circulation*, *82*(2), 332-340. https://doi.org/Doi 10.1161/01.Cir.82.2.332

Kishimoto, A., Kajikawa, N., Shiota, M., & Nishizuka, Y. (1983). Proteolytic Activation of Calcium-Activated, Phospholipid-Dependent Protein-Kinase by Calcium-Dependent Neutral Protease. *Journal of Biological Chemistry*, *258*(2), 1156-1164.

Kishimoto, A., Mikawa, K., Hashimoto, K., Yasuda, I., Tanaka, S., Tominaga, M., Kuroda, T., & Nishizuka, Y. (1989). Limited Proteolysis of Protein Kinase-C Subspecies by Calcium-Dependent Neutral Protease (Calpain). *Journal of Biological Chemistry*, *264*(7), 4088-4092.

Kleifeld, O., Doucet, A., auf dem Keller, U., Prudova, A., Schilling, O., Kainthan, R. K., Starr, A. E., Foster, L. J., Kizhakkedathu, J. N., & Overall, C. M. (2010). Isotopic labeling of terminal amines in complex samples identifies protein N-termini and protease cleavage products. *Nat Biotechnol*, *28*(3), 281-288. https://doi.org/10.1038/nbt.1611

Kleifeld, O., Doucet, A., Prudova, A., auf dem Keller, U., Gioia, M., Kizhakkedathu, J. N., & Overall, C. M. (2011). Identifying and quantifying proteolytic events and the natural N terminome by terminal amine isotopic labeling of substrates. *Nat Protoc*, *6*(10), 1578-1611. https://doi.org/10.1038/nprot.2011.382

Kottyan, L. C., Davis, B. P., Sherrill, J. D., Liu, K., Rochman, M., Kaufman, K., Weirauch, M. T., Vaughn, S., Lazaro, S., Rupert, A. M., Kohram, M., Stucke, E. M., Kemme, K. A., Magnusen, A., He, H., Dexheimer, P., Chehade, M., Wood, R. A., Pesek, R. D., . . . Rothenberg, M. E. (2014). Genome-wide association analysis of eosinophilic esophagitis provides insight into the tissue specificity of this allergic disease. *Nature Genetics*, *46*(8), 895-900. https://doi.org/10.1038/ng.3033

Krueger, L. A., & Morris, A. C. (2022). Eyes on CHARGE syndrome: Roles of CHD7 in ocular development. *Frontiers in Cell and Developmental Biology*, *10*. https://doi.org/10.3389/fcell.2022.994412

Kumar, R. A., Pilz, D. T., Babatz, T. D., Cushion, T. D., Harvey, K., Topf, M., Yates, L., Robb, S., Uyanik, G., Mancini, G. M. S., Rees, M. I., Harvey, R. J., & Dobyns, W. B. (2010). TUBA1A mutations cause wide spectrum lissencephaly (smooth brain) and suggest that multiple neuronal migration pathways converge on alpha tubulins. *Human Molecular Genetics*, *19*(14), 2817-2827. https://doi.org/10.1093/hmg/ddq182

Kuwabara, P. E., Okkema, P. G., & Kimble, J. (1998). Germ-line regulation of the Caenorhabditis elegans sex-determining gene tra-2. *Developmental Biology*, *204*(1), 251-262. https://doi.org/10.1006/dbio.1998.9062

Lacomme, M., Liaubet, L., Pituello, F., & Bel-Vialar, S. (2012). NEUROG2 Drives Cell Cycle Exit of Neuronal Precursors by Specifically Repressing a Subset of Cyclins Acting at the G(1) and S Phases of the Cell Cycle. *Molecular and Cellular Biology*, *32*(13), 2596-2607. https://doi.org/10.1128/Mcb.06745-11

Lahrouchi, N., George, A., Ratbi, I., Schneider, R., Elalaoui, S. C., Moosa, S., Bharti, S., Sharma, R., Abu-Asab, M., Onojafe, F., Adadi, N., Lodder, E. M., Laarabi, F. Z., Lamsyah, Y., Elorch, H., Chebbar, I., Postma, A. V., Lougaris, V., Plebani, A., . . . Sefiani, A. (2019). Homozygous frameshift mutations in FAT1 cause a syndrome characterized by colobomatous-microphthalmia, ptosis, nephropathy and syndactyly. *Nature Communications*, *10*. https://doi.org/10.1038/s41467-019-08547-w

Lalani, S. R., Safiullah, A. M., Fernbach, S. D., Harutyunyan, K. G., Thaller, C., Peterson, L. E., McPherson, J. D., Gibbs, R. A., White, L. D., Hefner, M., Davenport, S. L. H., Graham, J. M., Bacino, C. A., Glass, N. L., Towbin, J. A., Craigen, W. J., Neish, S. R., Lin, A. E., & Belmont, J. W. (2006). Spectrum of CHD7 mutations in 110 individuals with CHARGE syndrome and genotype-phenotype correlation. *American Journal of Human Genetics*, *78*(2), 303-314. https://doi.org/10.1086/500273

Lange, C., Huttner, W. B., & Calegari, F. (2009). Cdk4/cyclinD1 overexpression in neural stem cells shortens G1, delays neurogenesis, and promotes the generation and expansion of basal progenitors. *Cell Stem Cell*, *5*(3), 320-331. https://doi.org/10.1016/j.stem.2009.05.026

Lavdas, A. A., Grigoriou, M., Pachnis, V., & Parnavelas, J. G. (1999). The medial ganglionic eminence gives rise to a population of early neurons in the developing cerebral cortex. *Journal of Neuroscience*, *19*(18), 7881-7888. https://doi.org/10.1523/JNEUROSCI.19-18-07881.1999

Lee, A. M., Kanter, B. R., Wang, D., Lim, J. P., Zou, M. E., Qiu, C. C., McMahon, T., Dadgar, J., Fischbach-Weiss, S. C., & Messing, R. O. (2013). Prkcz null mice show normal learning and memory. *Nature*, *493*(7432), 416-U163. https://doi.org/10.1038/nature11803

Lee, D. Y. (2015). Roles of mTOR Signaling in Brain Development. *Exp Neurobiol*, *24*(3), 177-185. https://doi.org/10.5607/en.2015.24.3.177

Lee, J. H., Huynh, M., Silhavy, J. L., Kim, S., Dixon-Salazar, T., Heiberg, A., Scott, E., Bafna, V., Hill, K. J., Collazo, A., Funari, V., Russ, C., Gabriel, S. B., Mathern, G. W., & Gleeson, J. G. (2012). De novo somatic mutations in components of the PI3K-AKT3-mTOR pathway cause hemimegalencephaly. *Nature Genetics*, *44*(8), 941-945. https://doi.org/10.1038/ng.2329

Legendre, M., Abadie, V., Attie-Bitach, T., Philip, N., Busa, T., Bonneau, D., Colin, E., Dollfus, H., Lacombe, D., Toutain, A., Blesson, S., Julia, S., Martin-Coignard, D., Genevieve, D., Leheup, B., Odent, S., Jouk, P. S., Mercier, S., Faivre, L., . . . Gilbert-Dussardier, B. (2017). Phenotype and genotype analysis of a French cohort of 119 patients with CHARGE syndrome. *Am J Med Genet C Semin Med Genet*, *175*(4), 417-430. https://doi.org/10.1002/ajmg.c.31591

Lessard, J., Wu, J. I., Ranish, J. A., Wan, M., Winslow, M. M., Staahl, B. T., Wu, H., Aebersold, R., Graef, I. A., & Crabtree, G. R. (2007). An essential switch in subunit composition of a chromatin remodeling complex during neural development. *Neuron*, *55*(2), 201-215. https://doi.org/10.1016/j.neuron.2007.06.019

Lim, S., Bhinge, A., Alonso, S. B., Aksoy, I., Aprea, J., Cheok, C. F., Calegari, F., Stanton, L. W., & Kaldis, P. (2017). Cyclin-Dependent Kinase-Dependent Phosphorylation of Sox2 at Serine 39 Regulates Neurogenesis. *Molecular and Cellular Biology*, *37*(16). https://doi.org/10.1128/MCB.00201-17

Ling, D. S. F., Benardo, L. S., Serrano, P. A., Blace, N., Kelly, M. T., Crary, J. F., & Sacktor, T. C. (2002). Protein kinase M zeta is necessary and sufficient for LTP maintenance. *Nature Neuroscience*, *5*(4), 295-296. https://doi.org/10.1038/nn829

Lisman, J. (2012). Memory erasure by very high concentrations of ZIP may not be due to PKM-zeta. *Hippocampus*, *22*(3), 648-649. https://doi.org/10.1002/hipo.20980

Lissek, S., Biggs, A. L., Rabin, S. J., Cornwell, B. R., Alvarez, R. P., Pine, D. S., & Grillon, C. (2008). Generalization of conditioned fear-potentiated startle in humans: experimental validation and clinical relevance. *Behav Res Ther*, *46*(5), 678-687. https://doi.org/10.1016/j.brat.2008.02.005

Lissek, S., & van Meurs, B. (2015). Learning models of PTSD: Theoretical accounts and psychobiological evidence. *International Journal of Psychophysiology*, *98*(3), 594-605. https://doi.org/10.1016/j.ijpsycho.2014.11.006

Liu, C. J., Kang, N., Guo, Y. C., & Gong, P. (2021). Advances in Chromodomain Helicase DNA-Binding (CHD) Proteins Regulating Stem Cell Differentiation and Human Diseases. *Frontiers in Cell and Developmental Biology*, *9*. https://doi.org/10.3389/fcell.2021.710203

Liu, G. Y., & Sabatini, D. M. (2020). mTOR at the nexus of nutrition, growth, ageing and disease. *Nature Reviews Molecular Cell Biology*, *21*(4), 183-203. https://doi.org/10.1038/s41580-019-0199-y

Liu, I. S. C., Chen, J. D., Ploder, L., Vidgen, D., Vanderkooy, D., Kalnins, V. I., & Mcinnes, R. R. (1994). Developmental Expression of a Novel Murine Homeobox Gene (Chx10) - Evidence for Roles in Determination of the Neuroretina and Inner Nuclear Layer. *Neuron*, *13*(2), 377-393. https://doi.org/10.1016/0896-6273(94)90354-9

Liu, L., Michowski, W., Kolodziejczyk, A., & Sicinski, P. (2019). The cell cycle in stem cell proliferation, pluripotency and differentiation. *Nat Cell Biol*, *21*(9), 1060-1067. https://doi.org/10.1038/s41556-019-0384-4

Llorca, A., & Deogracias, R. (2022). Origin, Development, and Synaptogenesis of Cortical Interneurons. *Frontiers in Neuroscience*, *16*. https://doi.org/10.3389/fnins.2022.929469

Macdonald, R., Barth, K. A., Xu, Q. L., Holder, N., Mikkola, I., & Wilson, S. W. (1995). Midline Signaling Is Required for Pax Gene-Regulation and Patterning of the Eyes. *Development*, *121*(10), 3267-3278. https://doi.org/10.1242/dev.121.10.3267

Maemoto, Y., Kiso, S., Shibata, H., & Maki, M. (2013). Analysis of limited proteolytic activity of calpain-7 using non-physiological substrates in mammalian cells. *Febs Journal*, *280*(11), 2594-2607. https://doi.org/10.1111/febs.12243

Magri, L., Cambiaghi, M., Cominelli, M., Alfaro-Cervello, C., Cursi, M., Pala, M., Bulfone, A., Garcia-Verdugo, J. M., Leocani, L., Minicucci, F., Poliani, P. L., & Galli, R. (2011). Sustained Activation of mTOR Pathway in Embryonic Neural Stem Cells Leads to Development of Tuberous Sclerosis Complex-Associated Lesions. *Cell Stem Cell*, *9*(5), 447-462. https://doi.org/10.1016/j.stem.2011.09.008

Mahajan, V. B., Skeie, J. M., Bassuk, A. G., Fingert, J. H., Braun, T. A., Daggett, H. T., Folk, J. C., Sheffield, V. C., & Stone, E. M. (2012). Calpain-5 Mutations Cause Autoimmune Uveitis, Retinal Neovascularization, and Photoreceptor Degeneration. *Plos Genetics*, *8*(10). https://doi.org/10.1371/journal.pgen.1003001

Marinesco, S., & Carew, T. J. (2002). Serotonin release evoked by tail nerve stimulation in the CNS of Aplysia: Characterization and relationship to heterosynaptic plasticity. *Journal of Neuroscience*, *22*(6), 2299-2312. https://doi.org/10.1523/Jneurosci.22-06-02299.2002

Mehra, A., Gaudet, J., Heck, L., Kuwabara, P. E., & Spence, A. M. (1999). Negative regulation of male development in Caenorhabditis elegans by a protein-protein interaction between TRA-2A and FEM-3. *Genes & Development*, *13*(11), 1453-1463. https://doi.org/10.1101/gad.13.11.1453

Meyer, W. L., Krebs, E. G., & Fischer, E. H. (1964). Activation of Skeletal Muscle Phosphorylase B Kinase by Ca2plus. *Biochemistry*, *3*(8), 1033-&. https://doi.org/10.1021/bi00896a004

Mihalas, A. B., & Hevner, R. F. (2018). Clonal analysis reveals laminar fate multipotency and daughter cell apoptosis of mouse cortical intermediate progenitors. *Development*, *145*(17). https://doi.org/10.1242/dev.164335

Mills, A. A. (2017). The Chromodomain Helicase DNA-Binding Chromatin Remodelers: Family Traits that Protect from and Promote Cancer. *Cold Spring Harbor Perspectives in Medicine*, *7*(4). https://doi.org/10.1101/cshperspect.a026450

Mirzaa, G. M., Campbell, C. D., Solovieff, N., Goold, C., Jansen, L. A., Menon, S., Timms, A. E., Conti, V., Biag, J. D., Adams, C., Boyle, E. A., Collins, S., Ishak, G., Poliachik, S., Girisha, K. M., Yeung, K. S., Chung, B. H. Y., Rahikkala, E., Gunter, S. A., . . . Dobyns,

W. B. (2016). Association of MTOR Mutations With Developmental Brain Disorders, Including Megalencephaly, Focal Cortical Dysplasia, and Pigmentary Mosaicism. *JAMA Neurol*, *73*(7), 836-845. https://doi.org/10.1001/jamaneurol.2016.0363

Moldoveanu, T., Gehring, K., & Green, D. R. (2008). Concerted multi-pronged attack by calpastatin to occlude the catalytic cleft of heterodimeric calpains. *Nature*, *456*(7220), 404-U473. https://doi.org/10.1038/nature07353

Moldoveanu, T., Hosfield, C. M., Lim, D., Elce, J. S., Jia, Z. C., & Davies, P. L. (2002). A Ca2+ switch aligns the active site of calpain. *Cell*, *108*(5), 649-660. https://doi.org/10.1016/S0092-8674(02)00659-1

Moldoveanu, T., Jia, Z. C., & Davies, P. L. (2004). Calpain activation by cooperative Ca2+ binding at two non-EF-hand sites. *Journal of Biological Chemistry*, *279*(7), 6106-6114. https://doi.org/10.1074/jbc.M310460200

Montarolo, P. G., Goelet, P., Castellucci, V. F., Morgan, J., Kandel, E. R., & Schacher, S. (1986). A critical period for macromolecular synthesis in long-term heterosynaptic facilitation in Aplysia. *Science*, *234*(4781), 1249-1254. https://doi.org/10.1126/science.3775383

Mor-Shaked, H., Salah, S., Yanovsky-Dagan, S., Meiner, V., Atawneh, O. M., Abu-Libdeh, B., Elpeleg, O., & Harel, T. (2021). Biallelic deletion in a minimal CAPN15 intron in siblings with a recognizable syndrome of congenital malformations and developmental delay. *Clinical Genetics*, *99*(4), 577-582. https://doi.org/10.1111/cge.13920

Murachi, T., Tanaka, K., Hatanaka, M., & Murakami, T. (1980). Intracellular Ca2+-dependent protease (calpain) and its high-molecular-weight endogenous inhibitor (calpastatin). *Adv Enzyme Regul*, *19*, 407-424. https://doi.org/10.1016/0065-2571(81)90026-1

Murali, D., Yoshikawa, S., Corrigan, R. R., Plas, D. J., Crair, M. C., Oliver, G., Lyons, K. M., Mishina, Y., & Furuta, Y. (2005). Distinct developmental programs require different levels of Bmp signaling during mouse retinal development. *Development*, *132*(5), 913-923. https://doi.org/10.1242/dev.01673

Naisbitt, S., Kim, E., Tu, J. C., Xiao, B., Sala, C., Valtschanoff, J., Weinberg, R. J., Worley, P. F., & Sheng, M. (1999). Shank, a novel family of postsynaptic density proteins that binds to the NMDA receptor/PSD-95/GKAP complex and cortactin. *Neuron*, *23*(3), 569-582. https://doi.org/10.1016/s0896-6273(00)80809-0

Naqvi, S., Hoskens, H., Wilke, F., Weinberg, S. M., Shaffer, J. R., Walsh, S., Shriver, M. D., Wysocka, J., & Claes, P. (2022). Decoding the Human Face: Progress and Challenges in Understanding the Genetics of Craniofacial Morphology. *Annual Review of Genomics and Human Genetics*, *23*, 383-412. https://doi.org/10.1146/annurev-genom-120121-102607

Neale, B. M., Kou, Y., Liu, L., Ma'ayan, A., Samocha, K. E., Sabo, A., Lin, C. F., Stevens, C., Wang, L. S., Makarov, V., Polak, P., Yoon, S., Maguire, J., Crawford, E. L., Campbell, N. G., Geller, E. T., Valladares, O., Schafer, C., Liu, H., . . . Daly, M. J. (2012). Patterns and rates of exonic de novo mutations in autism spectrum disorders. *Nature*, *485*(7397), 242-U129. https://doi.org/10.1038/nature11011

Nguyen, M. T. T., & Arnheiter, H. (2000). Signaling and transcriptional regulation in early mammalian eye development: a link between FGF and MITF. *Development*, *127*(16), 3581-3591. https://doi.org/10.1242/dev.127.16.3581

Nie, K. L., Huang, J. T., Liu, L. Q., Lv, H. B., Chen, D. N., & Fan, W. (2022). Identification of a De Novo Heterozygous Missense ACTB Variant in Baraitser-Winter Cerebrofrontofacial Syndrome. *Frontiers in Genetics*, *13*. https://doi.org/10.3389/fgene.2022.828120

Nikolich, K., Ernst Strüngmann, F., Nikolich, K., Nikolich, K., Hyman, S. E., & Project, M. (2015). *Translational neuroscience : toward new therapies*. The MIT Press.

Nitarska, J., Smith, J. G., Sherlock, W. T., Hillege, M. M. G., Nott, A., Barshop, W. D., Vashisht, A. A., Wohlschlegel, J. A., Mitter, R., & Riccio, A. (2016). A Functional Switch of NuRD Chromatin Remodeling Complex Subunits Regulates Mouse Cortical Development. *Cell Reports*, *17*(6), 1683-1698. https://doi.org/10.1016/j.celrep.2016.10.022

Noctor, S. C., Flint, A. C., Weissman, T. A., Dammerman, R. S., & Kriegstein, A. R. (2001). Neurons derived from radial glial cells establish radial units in neocortex. *Nature*, *409*(6821), 714-720. https://doi.org/10.1038/35055553

Noctor, S. C., Flint, A. C., Weissman, T. A., Wong, W. S., Clinton, B. K., & Kriegstein, A. R. (2002). Dividing precursor cells of the embryonic cortical ventricular zone have morphological and molecular characteristics of radial glia. *J Neurosci*, *22*(8), 3161-3173. https://doi.org/10.1523/JNEUROSCI.22-08-03161.2002

Noctor, S. C., Martinez-Cerdeno, V., Ivic, L., & Kriegstein, A. R. (2004). Cortical neurons arise in symmetric and asymmetric division zones and migrate through specific phases. *Nature Neuroscience*, *7*(2), 136-144. https://doi.org/10.1038/nn1172

O'Roak, B. J., Vives, L., Fu, W. Q., Egertson, J. D., Stanaway, I. B., Phelps, I. G., Carvill, G., Kumar, A., Lee, C., Ankenman, K., Munson, J., Hiatt, J. B., Turner, E. H., Levy, R., O'Day, D. R., Krumm, N., Coe, B. P., Martin, B. K., Borenstein, E., . . . Shendure, J. (2012). Multiplex Targeted Sequencing Identifies Recurrently Mutated Genes in Autism Spectrum Disorders. *Science*, *338*(6114), 1619-1622. https://doi.org/10.1126/science.1227764

Oberst, P., Fievre, S., Baumann, N., Concetti, C., Bartolini, G., & Jabaudon, D. (2019). Temporal plasticity of apical progenitors in the developing mouse neocortex. *Nature*, *573*(7774), 370-374. https://doi.org/10.1038/s41586-019-1515-6

Ogawa, M., Miyata, T., Nakajima, K., Yagyu, K., Seike, M., Ikenaka, K., Yamamoto, H., & Mikoshiba, K. (1995). The Reeler Gene-Associated Antigen on Cajal-Retzius Neurons Is a Crucial Molecule for Laminar Organization of Cortical-Neurons. *Neuron*, *14*(5), 899-912. https://doi.org/10.1016/0896-6273(95)90329-1

Okamoto, N., Kubota, T., Nakamura, Y., Murakami, R., Nishikubo, T., Tanaka, I., Takahashi, Y., Hayashi, S., Imoto, I., Inazawa, J., Hosokai, N., Kohsaka, S., & Uchino, S. (2007). 22q13 Microduplication in two patients with common clinical manifestations: a recognizable syndrome? *Am J Med Genet A*, *143A*(23), 2804-2809. https://doi.org/10.1002/ajmg.a.31771

Ono, Y., & Sorimachi, H. (2012). Calpains - An elaborate proteolytic system. *Biochimica Et Biophysica Acta-Proteins and Proteomics*, *1824*(1), 224-236. https://doi.org/10.1016/j.bbapap.2011.08.005

Orourke, N. A., Sullivan, D. P., Kaznowski, C. E., Jacobs, A. A., & Mcconnell, S. K. (1995). Tangential Migration of Neurons in the Developing Cerebral-Cortex. *Development*, *121*(7), 2165-2176. https://doi.org/10.1242/dev.121.7.2165

Osako, Y., Maemoto, Y., Tanaka, R., Suzuki, H., Shibata, H., & Maki, M. (2010). Autolytic activity of human calpain 7 is enhanced by ESCRT-III-related protein IST1 through MIT-

MIM interaction. *Febs Journal*, *277*(21), 4412-4426. https://doi.org/10.1111/j.1742-4658.2010.07822.x

Pagon, R. A., Graham, J. M., Zonana, J., & Yong, S. L. (1981). Coloboma, Congenital Heart-Disease, and Choanal Atresia with Multiple Anomalies - Charge Association. *Journal of Pediatrics*, *99*(2), 223-227. https://doi.org/10.1016/S0022-3476(81)80454-4

Parenti, I., Rabaneda, L. G., Schoen, H., & Novarino, G. (2020). Neurodevelopmental Disorders: From Genetics to Functional Pathways. *Trends Neurosci*, *43*(8), 608-621. https://doi.org/10.1016/j.tins.2020.05.004

Patel, A., & Sowden, J. C. (2019). Genes and pathways in optic fissure closure. *Seminars in Cell & Developmental Biology*, *91*, 55-65. https://doi.org/10.1016/j.semcdb.2017.10.010

Peca, J., Feliciano, C., Ting, J. T., Wang, W., Wells, M. F., Venkatraman, T. N., Lascola, C. D., Fu, Z., & Feng, G. (2011). Shank3 mutant mice display autistic-like behaviours and striatal dysfunction. *Nature*, *472*(7344), 437-442. https://doi.org/10.1038/nature09965

Pei, Y. F., & Rhodin, J. A. (1970). The prenatal development of the mouse eye. *Anat Rec*, *168*(1), 105-125. https://doi.org/10.1002/ar.1091680109

Penalva, M. A., Tilburn, J., Bignell, E., & Arst, H. N. (2008). Ambient pH gene regulation in fungi: making connections. *Trends in Microbiology*, *16*(6), 291-300. https://doi.org/10.1016/j.tim.2008.03.006

Phelan, K., & McDermid, H. E. (2012). The 22q13.3 Deletion Syndrome (Phelan-McDermid Syndrome). *Molecular Syndromology*, *2*(3-5), 186-201. https://doi.org/10.1159/000334260

Piluso, G., Politano, L., Aurino, S., Fanin, M., Ricci, E., Ventriglia, V. M., Belsito, A., Totaro, A., Saccone, V., Topaloglu, H., Nascimbeni, A. C., Fulizio, L., Broccolini, A., Canki-Klain, N., Comi, L. I., Nigro, G., Angelini, C., & Nigro, V. (2005). Extensive scanning of the calpain-3 gene broadens the spectrum of LGMD2A phenotypes. *Journal of Medical Genetics*, *42*(9), 686-693. https://doi.org/10.1136/jmg.2004.028738

Plaisancie, J., Ceroni, F., Holt, R., Seco, C. Z., Calvas, P., Chassaing, N., & Ragge, N. K. (2019). Genetics of anophthalmia and microphthalmia. Part 1: Non-syndromic anophthalmia/microphthalmia. *Human Genetics*, *138*(8-9), 799-830. https://doi.org/10.1007/s00439-019-01977-y

Poirier, K., Keays, D. A., Francis, F., Saillour, Y., Bahi, N., Manouvrier, S., Fallet-Bianco, C., Pasquier, L., Toutain, A., Tuy, F. P. D., Bienvenu, T., Joriot, S., Odent, S., Ville, D., Desguerre, I., Goldenberg, A., Moutard, M. L., Fryns, J., Van Esch, H., . . . Chelly, J. (2007). Large spectrum of lissencephaly and pachygyria phenotypes resulting from de novo missense mutations in tubulin alpha 1A (TUBA1A). *Human Mutation*, *28*(11), 1055-1064. https://doi.org/10.1002/humu.20572

Qin, Q., Fan, J. Y., Zheng, R. B., Wan, C. X., Mei, S. L., Wu, Q., Sun, H. F., Brown, M., Zhang, J., Meyer, C. A., & Liu, X. S. (2020). Lisa: inferring transcriptional regulators through integrative modeling of public chromatin accessibility and ChIP-seq data. *Genome Biology*, *21*(1). https://doi.org/10.1186/s13059-020-1934-6

Rainger, J., Williamson, K. A., Soares, D. C., Truch, J., Kurian, D., Gillessen-Kaesbach, G., Seawright, A., Prendergast, J., Halachev, M., Wheeler, A., McTeir, L., Gill, A. C., van Heyningen, V., Davey, M. G., FitzPatrick, D. R., & Uk10k. (2017). A recurrent de novo mutation in ACTG1 causes isolated ocular coloboma. *Human Mutation*, *38*(8), 942-946. https://doi.org/10.1002/humu.23246

Randazzo, N. M., Shanks, M. E., Clouston, P., & MacLaren, R. E. (2019). Two Novel CAPN5 Variants Associated with Mild and Severe Autosomal Dominant Neovascular Inflammatory Vitreoretinopathy Phenotypes. *Ocular Immunology and Inflammation*, *27*(5), 693-698. https://doi.org/10.1080/09273948.2017.1370651

Ravulapalli, R., Diaz, B. G., Campbell, R. L., & Davies, P. L. (2005). Homodimerization of calpain 3 penta-EF-hand domain. *Biochemical Journal*, *388*, 585-591. https://doi.org/10.1042/Bj20041821

Reiner, O. (2013). LIS1 and DCX: Implications for Brain Development and Human Disease in Relation to Microtubules. *Scientifica*, *2013*. https://doi.org/10.1155/2013/393975

Richard, I., Broux, O., Allamand, V., Fougerousse, F., Chiannilkulchai, N., Bourg, N., Brenguier, L., Devaud, C., Pasturaud, P., Roudaut, C., Hillaire, D., Passosbueno, M. R., Zatz, M., Tischfield, J. A., Fardeau, M., Jackson, C. E., Cohen, D., & Beckmann, J. S. (1995). Mutations in the Proteolytic-Enzyme Calpain-3 Cause Limb-Girdle Muscular-Dystrophy Type-2a. *Cell*, *81*(1), 27-40. https://doi.org/10.1016/0092-8674(95)90368-2

Ronan, J. L., Wu, W., & Crabtree, G. R. (2013). From neural development to cognition: unexpected roles for chromatin. *Nature Reviews Genetics*, *14*(5), 347-359. https://doi.org/10.1038/nrg3413

Roussignol, G., Ango, F., Romorini, S., Tu, J. C., Sala, C., Worley, P. F., Bockaert, J., & Fagni, L. (2005). Shank expression is sufficient to induce functional dendritic spine synapses in aspiny neurons. *J Neurosci*, *25*(14), 3560-3570. https://doi.org/10.1523/JNEUROSCI.4354-04.2005

Sacktor, T. C., Osten, P., Valsamis, H., Jiang, X., Naik, M. U., & Sublette, E. (1993). Persistent activation of the zeta isoform of protein kinase C in the maintenance of long-term potentiation. *Proc Natl Acad Sci U S A*, *90*(18), 8342-8346. https://doi.org/10.1073/pnas.90.18.8342

Sala, C., Piech, V., Wilson, N. R., Passafaro, M., Liu, G., & Sheng, M. (2001). Regulation of dendritic spine morphology and synaptic function by Shank and Homer. *Neuron*, *31*(1), 115-130. https://doi.org/10.1016/s0896-6273(01)00339-7

Sandestig, A., Green, A., Jonasson, J., Vogt, H., Wahlstrom, J., Pepler, A., Ellnebo, K., Biskup, S., & Stefanova, M. (2018). Could Dissimilar Phenotypic Effects of ACTB Missense Mutations Reflect the Actin Conformational Change? Two Novel Mutations and Literature Review. *Molecular Syndromology*, *9*(5), 259-265. https://doi.org/10.1159/000492267

Santen, G. W., Aten, E., Vulto-van Silfhout, A. T., Pottinger, C., van Bon, B. W., van Minderhout, I. J., Snowdowne, R., van der Lans, C. A., Boogaard, M., Linssen, M. M., Vijfhuizen, L., van der Wielen, M. J., Vollebregt, M. J., Coffin-Siris, c., Breuning, M. H., Kriek, M., van Haeringen, A., den Dunnen, J. T., Hoischen, A., . . . van Belzen, M. J. (2013). Coffin-Siris syndrome and the BAF complex: genotype-phenotype study in 63 patients. *Human Mutation*, *34*(11), 1519-1528. https://doi.org/10.1002/humu.22394

Santen, G. W. E., Aten, E., Sun, Y., Almomani, R., Gilissen, C., Nielsen, M., Kant, S. G., Snoeck, I. N., Peeters, E. A. J., Hilhorst-Hofstee, Y., Wessels, M. W., den Hollander, N. S., Ruivenkamp, C. A. L., van Ommen, G. J. B., Breuning, M. H., den Dunnen, J. T., van Haeringen, A., & Kriek, M. (2012). Mutations in SWI/SNF chromatin remodeling complex gene ARID1B cause Coffin-Siris syndrome. *Nature Genetics*, *44*(4), 379-380. https://doi.org/10.1038/ng.2217

Saxton, R. A., & Sabatini, D. M. (2017). mTOR Signaling in Growth, Metabolism, and Disease. *Cell*, *168*(6), 960-976. https://doi.org/10.1016/j.cell.2017.02.004

Schmeisser, M. J., Ey, E., Wegener, S., Bockmann, J., Stempel, A. V., Kuebler, A., Janssen, A. L., Udvardi, P. T., Shiban, E., Spilker, C., Balschun, D., Skryabin, B. V., Dieck, S., Smalla, K. H., Montag, D., Leblond, C. S., Faure, P., Torquet, N., Le Sourd, A. M., . . . Boeckers, T. M. (2012). Autistic-like behaviours and hyperactivity in mice lacking ProSAP1/Shank2. *Nature*, *486*(7402), 256-260. https://doi.org/10.1038/nature11015

Sekiguchi, F., Tsurusaki, Y., Okamoto, N., Teik, K. W., Mizuno, S., Suzumura, H., Isidor, B., Ong, W. P., Haniffa, M., White, S. M., Matsuo, M., Saito, K., Phadke, S., Kosho, T., Yap, P., Goyal, M., Clarke, L. A., Sachdev, R., McGillivray, G., . . . Matsumoto, N. (2019). Genetic abnormalities in a large cohort of Coffin-Siris syndrome patients. *Journal of Human Genetics*, *64*(12), 1173-1186. https://doi.org/10.1038/s10038-019-0667-4

Serrano, P., Friedman, E. L., Kenney, J., Taubenfeld, S. M., Zimmerman, J. M., Hanna, J., Alberini, C., Kelley, A. E., Maren, S., Rudy, J. W., Yin, J. C. P., Sacktor, T. C., & Fenton, A. A. (2008). PKM zeta Maintains Spatial, Instrumental, and Classically Conditioned Long-Term Memories. *Plos Biology*, *6*(12), 2698-2706. https://doi.org/10.1371/journal.pbio.0060318

Serrano, P., Yao, Y. D., & Sacktor, T. C. (2005). Persistent phosphorylation by protein kinase M zeta maintains late-phase long-term potentiation. *Journal of Neuroscience*, *25*(8), 1979-1984. https://doi.org/10.1523/Jneurosci.5132-04.2005

Shahapal, A., Cho, E. B., Yong, H. J., Jeong, I., Kwak, H., Lee, J. K., Kim, W., Kim, B., Park, H. C., Lee, W. S., Kim, H., Hwang, J. I., & Seong, J. Y. (2019). FAM19A5 Expression During Embryogenesis and in the Adult Traumatic Brain of FAM19A5-LacZ Knock-in Mice. *Front Neurosci*, *13*, 917. https://doi.org/10.3389/fnins.2019.00917

Shema, R., Sacktor, T. C., & Dudai, Y. (2007). Rapid erasure of long-term memory associations in the cortex by an inhibitor of PKM zeta. *Science*, *317*(5840), 951-953. https://doi.org/10.1126/science.1144334

Shimizu, K., Phan, T., Mansuy, I. M., & Storm, D. R. (2007). Proteolytic degradation of SCOP in the hippocampus contributes to activation of MAP kinase and memory. *Cell*, *128*(6), 1219-1229. https://doi.org/10.1016/j.cell.2006.12.047

Siegelbaum, S. A., Camardo, J. S., & Kandel, E. R. (1982). Serotonin and cyclic AMP close single K+ channels in Aplysia sensory neurones. *Nature*, *299*(5882), 413-417. https://doi.org/10.1038/299413a0

Silbereis, J. C., Pochareddy, S., Zhu, Y., Li, M., & Sestan, N. (2016). The Cellular and Molecular Landscapes of the Developing Human Central Nervous System. *Neuron*, *89*(2), 248-268. https://doi.org/10.1016/j.neuron.2015.12.008

Silverman, J. L., Turner, S. M., Barkan, C. L., Tolu, S. S., Saxena, R., Hung, A. Y., Sheng, M., & Crawley, J. N. (2011). Sociability and motor functions in Shank1 mutant mice. *Brain Res*, *1380*, 120-137. https://doi.org/10.1016/j.brainres.2010.09.026

Sokol, S. B., & Kuwabara, P. E. (2000). Proteolysis in Caenorhabditis elegans sex determination: cleavage of TRA-2A by TRA-3. *Genes & Development*, *14*(8), 901-906.

Sorimachi, H., Hata, S., & Ono, Y. (2011). Calpain chronicle-an enzyme family under multidisciplinary characterization. *Proceedings of the Japan Academy Series B-Physical and Biological Sciences*, *87*(6), 287-327. https://doi.org/10.2183/pjab.87.287

Sossin, W. S. (2007). Isoform specificity of protein kinase Cs in synaptic plasticity. *Learning & Memory*, *14*(4), 236-246. https://doi.org/10.1101/lm.469707
Sossin, W. S. (2018). Memory Synapses Are Defined by Distinct Molecular Complexes: A Proposal. *Frontiers in Synaptic Neuroscience*, *10*. https://doi.org/10.3389/fnsyn.2018.00005
Sousa, S. B., Abdul-Rahman, O. A., Bottani, A., Cormier-Daire, V., Fryer, A., Gillessen-Kaesbach, G., Horn, D., Josifova, D., Kuechler, A., Lees, M., MacDermot, K., Magee, A., Morice-Picard, F., Rosser, E., Sarkar, A., Shannon, N., Stolte-Dijkstra, I., Verloes, A., Wakeling, E., . . . Hennekam, R. C. (2009). Nicolaides-Baraitser syndrome: Delineation of the phenotype. *Am J Med Genet A*, *149A*(8), 1628-1640. https://doi.org/10.1002/ajmg.a.32956
Spinozzi, S., Albini, S., Best, H., & Richard, I. (2021). Calpains for dummies: What you need to know about the calpain family. *Biochimica Et Biophysica Acta-Proteins and Proteomics*, *1869*(5). https://doi.org/10.1016/j.bbapap.2021.140616
Stiles, J., & Jernigan, T. L. (2010). The basics of brain development. *Neuropsychol Rev*, *20*(4), 327-348. https://doi.org/10.1007/s11065-010-9148-4
Suzuki, K. (1991). Nomenclature of Calcium Dependent Proteinase. *Biomedica Biochimica Acta*, *50*(4-6), 483-484.
Suzuki, K., Tsuji, S., Ishiura, S., Kimura, Y., Kubota, S., & Imahori, K. (1981). Autolysis of Calcium-Activated Neutral Protease of Chicken Skeletal-Muscle. *Journal of Biochemistry*, *90*(6), 1787-1793. https://doi.org/10.1093/oxfordjournals.jbchem.a133656
Takahashi, T., Nowakowski, R. S., & Caviness, V. S., Jr. (1995). The cell cycle of the pseudostratified ventricular epithelium of the embryonic murine cerebral wall. *J Neurosci*, *15*(9), 6046-6057. https://doi.org/10.1523/JNEUROSCI.15-09-06046.1995
Takai, Y., Yamamoto, M., Inoue, M., Kishimoto, A., & Nishizuka, Y. (1977). A proenzyme of cyclic nucleotide-independent protein kinase and its activation by calcium-dependent neutral protease from rat liver. *Biochem Biophys Res Commun*, *77*(2), 542-550. https://doi.org/10.1016/s0006-291x(77)80013-2
Taranova, O. V., Magness, S. T., Fagan, B. M., Wu, Y. Q., Surzenko, N., Hutton, S. R., & Pevny, L. H. (2006). SOX2 is a dose-dependent regulator of retinal neural progenitor competence. *Genes & Development*, *20*(9), 1187-1202. https://doi.org/10.1101/gad.1407906
Thomanetz, V., Angliker, N., Cloetta, D., Lustenberger, R. M., Schweighauser, M., Oliveri, F., Suzuki, N., & Ruegg, M. A. (2013). Ablation of the mTORC2 component rictor in brain or Purkinje cells affects size and neuron morphology. *Journal of Cell Biology*, *201*(2), 293-308. https://doi.org/10.1083/jcb.201205030
Tiberi, L., Vanderhaeghen, P., & van den Ameele, J. (2012). Cortical neurogenesis and morphogens: diversity of cues, sources and functions. *Curr Opin Cell Biol*, *24*(2), 269-276. https://doi.org/10.1016/j.ceb.2012.01.010
Tilburn, J., Sarkar, S., Widdick, D. A., Espeso, E. A., Orejas, M., Mungroo, J., Penalva, M. A., & Arst, H. N. (1995). The Aspergillus Pacc Zinc-Finger Transcription Factor Mediates Regulation of Both Acid-Expressed and Alkaline-Expressed Genes by Ambient Ph. *Embo Journal*, *14*(4), 779-790. https://doi.org/10.1002/j.1460-2075.1995.tb07056.x
Tsokas, P., Hsieh, C., Yao, Y., Lesburgueres, E., Wallace, E. J. C., Tcherepanov, A., Jothianandan, D., Hartley, B. R., Pan, L., Rivard, B., Farese, R. V., Sajan, M. P., Bergold, P. J., Hernandez, A. I., Cottrell, J. E., Shouval, H. Z., Fenton, A. A., & Sacktor, T. C.

(2016). Compensation for PKM zeta in long-term potentiation and spatial long-term memory in mutant mice. *Elife*, *5*. https://doi.org/10.7554/eLife.14846

Tsurusaki, Y., Okamoto, N., Ohashi, H., Kosho, T., Imai, Y., Hibi-Ko, Y., Kaname, T., Naritomi, K., Kawame, H., Wakui, K., Fukushima, Y., Homma, T., Kato, M., Hiraki, Y., Yamagata, T., Yano, S., Mizuno, S., Sakazume, S., Ishii, T., . . . Matsumoto, N. (2012). Mutations affecting components of the SWI/SNF complex cause Coffin-Siris syndrome. *Nature Genetics*, *44*(4), 376-378. https://doi.org/10.1038/ng.2219

Tu, J. C., Xiao, B., Naisbitt, S., Yuan, J. P., Petralia, R. S., Brakeman, P., Doan, A., Aakalu, V. K., Lanahan, A. A., Sheng, M., & Worley, P. F. (1999). Coupling of mGluR/Homer and PSD-95 complexes by the Shank family of postsynaptic density proteins. *Neuron*, *23*(3), 583-592. https://doi.org/10.1016/s0896-6273(00)80810-7

Van Houdt, J. K. J., Nowakowska, B. A., Sousa, S. B., van Schaik, B. D. C., Seuntjens, E., Avonce, N., Sifrim, A., Abdul-Rahman, O. A., van den Boogaard, M. J. H., Bottani, A., Castori, M., Cormier-Daire, V., Deardorff, M. A., Filges, I., Fryer, A., Fryns, J. P., Gana, S., Garavelli, L., Gillessen-Kaesbach, G., . . . Vermeesch, J. R. (2012). Heterozygous missense mutations in SMARCA2 cause Nicolaides-Baraitser syndrome. *Nature Genetics*, *44*(4), 445-U261. https://doi.org/10.1038/ng.1105

Van Nostrand, J. L., Brady, C. A., Jung, H. Y., Fuentes, D. R., Kozak, M. M., Johnson, T. M., Lin, C. Y., Lin, C. J., Swiderski, D. L., Vogel, H., Bernstein, J. A., Attie-Bitach, T., Chang, C. P., Wysocka, J., Martin, D. M., & Attardi, L. D. (2014). Inappropriate p53 activation during development induces features of CHARGE syndrome. *Nature*, *514*(7521), 228-+. https://doi.org/10.1038/nature13585

Vasistha, N. A., Garcia-Moreno, F., Arora, S., Cheung, A. F., Arnold, S. J., Robertson, E. J., & Molnar, Z. (2015). Cortical and Clonal Contribution of Tbr2 Expressing Progenitors in the Developing Mouse Brain. *Cereb Cortex*, *25*(10), 3290-3302. https://doi.org/10.1093/cercor/bhu125

Velez, G., Bassuk, A. G., Schaefer, K. A., Brooks, B., Gakhar, L., Mahajan, M., Kahn, P., Tsang, S. H., Ferguson, P. J., & Mahajan, V. B. (2018). A novel de novo CAPN5 mutation in a patient with inflammatory vitreoretinopathy, hearing loss, and developmental delay. *Cold Spring Harbor Molecular Case Studies*, *4*(3). https://doi.org/10.1101/mcs.a002519

Velez, G., Sun, Y. J., Khan, S., Yang, J., Herrmann, J., Chemudupati, T., MacLaren, R. E., Gakhar, L., Wakatsuki, S., Bassuk, A. G., & Mahajan, V. B. (2020). Structural Insights into the Unique Activation Mechanisms of a Non-classical Calpain and Its Disease-Causing Variants. *Cell Reports*, *30*(3), 881-+. https://doi.org/10.1016/j.celrep.2019.12.077

Vincent, O., Rainbow, L., Tilburn, J., Arst, H. N., & Penalva, M. A. (2003). YPXL/I is a protein interaction motif recognized by Aspergillus PalA and its human homologue, AIP1/Alix. *Molecular and Cellular Biology*, *23*(5), 1647-1655. https://doi.org/10.1128/Mcb.23.5.1647-1655.2003

Vissers, L. E. L. M., van Ravenswaaij, C. M. A., Admiraal, R., Hurst, J. A., de Vries, B. B. A., Janssen, I. M., van der Vliet, W. A., Huys, E. H. L. P. G., de Jong, P. J., Hamel, B. C. J., Schoenmakers, E. F. P. M., Brunner, H. G., Veltman, J. A., & van Kessel, A. G. (2004). Mutations in a new member of the chromodomain gene family cause CHARGE syndrome. *Nature Genetics*, *36*(9), 955-957. https://doi.org/10.1038/ng1407

Volk, L. J., Bachman, J. L., Johnson, R., Yu, Y., & Huganir, R. L. (2013). PKM-zeta is not required for hippocampal synaptic plasticity, learning and memory. *Nature*, *493*(7432), 420-423. https://doi.org/10.1038/nature11802

Voronina, V. A., Kozhemyakina, E. A., O'Kernick, C. M., Kahn, N. D., Wenger, S. L., Linberg, J. V., Schneider, A. S., & Mathers, P. H. (2004). Mutations in the human RAX homeobox gene in a patient with anophthalmia and sclerocornea. *Human Molecular Genetics*, *13*(3), 315-322. https://doi.org/10.1093/hmg/ddh025

Waghray, A., Wang, D. S., McKinsey, D., Hayes, R. L., & Wang, K. K. W. (2004). Molecular cloning and characterization of rat and human calpain-5. *Biochemical and Biophysical Research Communications*, *324*(1), 46-51. https://doi.org/10.1016/j.bbrc.2004.09.012

Wan, L., Liu, D., Xiao, W. B., Zhang, B. X., Yan, X. X., Luo, Z. H., & Xiao, B. (2022). Association of SHANK Family with Neuropsychiatric Disorders: An Update on Genetic and Animal Model Discoveries. *Cell Mol Neurobiol*, *42*(6), 1623-1643. https://doi.org/10.1007/s10571-021-01054-x

Wang, L., Main, K., Wang, H., Julien, O., & Dufour, A. (2021). Biochemical Tools for Tracking Proteolysis. *J Proteome Res*, *20*(12), 5264-5279. https://doi.org/10.1021/acs.jproteome.1c00289

Wang, S. L., Sheng, T., Ren, S. Q., Tian, T., & Lu, W. (2016). Distinct Roles of PKC iota/lambda and PKM zeta in the Initiation and Maintenance of Hippocampal Long-Term Potentiation and Memory. *Cell Reports*, *16*(7), 1954-1961. https://doi.org/10.1016/j.celrep.2016.07.030

Wang, S. P., & Kimble, J. (2001). The TRA-1 transcription factor binds TRA-2 to regulate sexual fates in Caenorhabditis elegans. *Embo Journal*, *20*(6), 1363-1372. https://doi.org/10.1093/emboj/20.6.1363

Wert, K. J., Bassuk, A. G., Wu, W. H., Gakhar, L., Coglan, D., Mahajan, M., Wu, S., Yang, J., Lin, C. S., Tsang, S. H., & Mahajan, V. B. (2015). CAPN5 mutation in hereditary uveitis: the R243L mutation increases calpain catalytic activity and triggers intraocular inflammation in a mouse model. *Human Molecular Genetics*, *24*(16), 4584-4598. https://doi.org/10.1093/hmg/ddv189

Wert, K. J., Koch, S. F., Velez, G., Hsu, C. W., Mahajan, M., Bassuk, A. G., Tsang, S. H., & Mahajan, V. B. (2019). CAPN5 genetic inactivation phenotype supports therapeutic inhibition trials. *Human Mutation*, *40*(12), 2377-2392. https://doi.org/10.1002/humu.23894

Westenskow, P., Piccolo, S., & Fuhrmann, S. (2009). beta-catenin controls differentiation of the retinal pigment epithelium in the mouse optic cup by regulating Mitf and Otx2 expression. *Development*, *136*(15), 2505-2510. https://doi.org/10.1242/dev.032136

Wolff, D., Endele, S., Azzarello-Burri, S., Hoyer, J., Zweier, M., Schanze, I., Schmitt, B., Rauch, A., Reis, A., & Zweier, C. (2011). In-Frame Deletion and Missense Mutations of the C-Terminal Helicase Domain of SMARCA2 in Three Patients with Nicolaides-Baraitser Syndrome. *Molecular Syndromology*, *2*(6), 237-244. https://doi.org/10.1159/000337323

Xu, W. J., & Mitchell, A. P. (2001). Yeast PalA/AIP1/Alix homolog Rim20p associates with a PEST-like region and is required for its proteolytic cleavage. *Journal of Bacteriology*, *183*(23), 6917-6923. https://doi.org/10.1128/Jb.183.23.6917-6923.2001

Yamada, M., Yoshida, Y., Mori, D., Takitoh, T., Kengaku, M., Umeshima, H., Takao, K., Miyakawa, T., Sato, M., Sorimachi, H., Wynshaw-Boris, A., & Hirotsune, S. (2009). Inhibition of calpain increases LIS1 expression and partially rescues in vivo phenotypes

in a mouse model of lissencephaly. *Nature Medicine*, *15*(10), 1202-U1132. https://doi.org/10.1038/nm.2023

Yang, M., Yang, S. L., Herrlinger, S., Liang, C., Dzieciatkowska, M., Hansen, K. C., Desai, R., Nagy, A., Niswander, L., Moss, E. G., & Chen, J. F. (2015). Lin28 promotes the proliferative capacity of neural progenitor cells in brain development. *Development*, *142*(9), 1616-1627. https://doi.org/10.1242/dev.120543

Yao, H., Hannum, D. F., Zhai, Y., Hill, S. F., Albanus, R. D., Lou, W., Skidmore, J. M., Sanchez, G., Saiakhova, A., Bielas, S. L., Scacheri, P., Ljungman, M., Parker, S. C. J., & Martin, D. M. (2020). CHD7 promotes neural progenitor differentiation in embryonic stem cells via altered chromatin accessibility and nascent gene expression. *Sci Rep*, *10*(1), 17445. https://doi.org/10.1038/s41598-020-74537-4

Yorikawa, C., Takaya, E., Osako, Y., Tanaka, R., Terasawa, Y., Hamakubo, T., Mochizuki, Y., Iwanari, H., Kodama, T., Maeda, T., Hitomi, K., Shibata, H., & Maki, M. (2008). Human calpain 7/PalBH associates with a subset of ESCRT-III-related proteins in its N-terminal region and partly localizes to endocytic membrane compartments. *Journal of Biochemistry*, *143*(6), 731-745. https://doi.org/10.1093/jb/mvn030

Yoshizawa, T., Sorimachi, H., Tomioka, S., Ishiura, S., & Suzuki, K. (1995). A Catalytic Subunit of Calpain Possesses Full Proteolytic Activity. *Febs Letters*, *358*(1), 101-103. https://doi.org/10.1016/0014-5793(94)01401-L

Yu, T., Meiners, L. C., Danielsen, K., Wong, M. T., Bowler, T., Reinberg, D., Scambler, P. J., van Ravenswaaij-Arts, C. M., & Basson, M. A. (2013). Deregulated FGF and homeotic gene expression underlies cerebellar vermis hypoplasia in CHARGE syndrome. *Elife*, *2*, e01305. https://doi.org/10.7554/eLife.01305

Zhou, Y., Song, H., & Ming, G. L. (2023). Genetics of human brain development. *Nature Reviews Genetics*. https://doi.org/10.1038/s41576-023-00626-5

Zimmerman, U. J. P., Boring, L., Pak, J. H., Mukerjee, N., & Wang, K. K. W. (2000). The calpain small subunit gene is essential: Its inactivation results in embryonic lethality. *Iubmb Life*, *50*(1), 63-68. https://doi.org/10.1080/15216540050176610

Zoghbi, H. Y., & Bear, M. F. (2012). Synaptic dysfunction in neurodevelopmental disorders associated with autism and intellectual disabilities. *Cold Spring Harb Perspect Biol*, *4*(3). https://doi.org/10.1101/cshperspect.a009886

Zuber, M. E., Gestri, G., Viczian, A. S., Barsacchi, G., & Harris, W. A. (2003). Specification of the vertebrate eye by a network of eye field transcription factors. *Development*, *130*(21), 5155-5167. https://doi.org/10.1242/dev.00723